

ATTACHMENT 27

**Browns Ferry Nuclear Plant (BFN)
Unit 1**

Technical Specifications (TS) Change 473

AREVA Fuel Transition

**Part 1: Previous NRC Requests for Additional Information Matrix and Text
(Non-Proprietary)**

**Part 2: ANP-2860P
Browns Ferry Unit 1 -- Summary of Response to Requests for Additional Information
(Non-Proprietary)**

**Part 3:
Response to Previous NRC Requests for Supplemental Information Regarding Utilization
of AREVA Fuel and Associated Analysis Methodologies
(Non-Proprietary)**

Part 1 contains the non-proprietary version of the matrix and text of previous NRC requests for additional information.

Part 2 contains the non-proprietary version of a summary report of previously issued NRC requests for additional information.

Part 3 contains the non-proprietary version of the Response to previous NRC Requests for Supplemental Information Regarding Utilization of AREVA Fuel and Associated Analysis Methodologies.

ATTACHMENT 27

PART 1

Previous NRC Requests for Additional Information Matrix and Text

(Non-proprietary Version)

The Table 1 matrix below provides the reference to the documents and associated sections/page in this submittal where previous NRC Requests for Additional Information, applicable to this License Amendment Request, have been addressed for Browns Ferry Nuclear Plant, Unit 1.

Table 1 Previous NRC Requests for Additional Information (RAIs) Matrix					
RAI Number (See Table 2 for RAI text)	Reference for RAI Transmittal to NRC	Section in ANP-2860	Section in ANP-2638	Page in ANP-2637	Section in ANP-2864
Brunswick Steam Electric Plant					
RAI-1	2	-	-	-	2.0
RAI-2	2	7.3	-	-	-
RAI-3	2	5.1	-	-	-
RAI-5	2	-	-	-	7.2.2
RAI-6	2	-	-	-	6.1
RAI-7	2	-	-	-	4.3
RAI-8	2	2.1	-	-	-
RAI-9	2	-	-	-	4.2, 5.0
RAI-10	2	7.1	-	-	-
RAI-11	2	6.7	-	-	-
Susquehanna Steam Electric Station					
Item 1	1	5.2	-	-	-
Item 2	1	6.7	-	-	-
Item 3	1	2.1	-	-	-
Item 4	1	-	App C.2	-	-
River Bend Station					
RAI-6.1	3	3.1 (Note 1)	-	-	-
RAI-6.2	3	3.1, 3.2 (Note 2)	-	-	-
RAI-6.3	3	6.1	-	-	-
RAI-6.4	3	6.2	-	-	-
RAI-6.5	3	6.2	-	-	-
RAI-6.6	3	6.3	-	-	-
RAI-6.7	3	7.2	-	-	-
RAI-6.8	3	7.2	-	-	-
RAI-6.9	3	-	6	-	-
RAI-6.10	3	-	6	-	-
RAI-6.11	3	6.4	-	-	-
RAI-6.12	3	7.3	-	-	-
RAI-6.13	3	-	-	-	5.0
RAI-6.14	3	4.1, 5.6	-	-	-

**Table 1
Previous NRC Requests for Additional Information (RAIs) Matrix**

RAI Number (See Table 2 for RAI text)	Reference for RAI Transmittal to NRC	Section in ANP-2860	Section in ANP-2638	Page in ANP-2637	Section in ANP-2864
RAI-6.15	3	4.2 (Note 3)	-	-	-
RAI-6.16	3	4.3	-	-	-
RAI-6.17	3	6.5 (Note 4)	-	-	-
RAI-6.18	3	6.6 (Note 5)	-	-	-
RAI-6.19	3	4.5	-	-	-
Browns Ferry Nuclear Plant					
SRXB-A.14	10	6.1	-	-	-
SRXB-A.15	10	-	All	-	-
SRXB-A.16	10	-	-	2-29	-
SRXB-A.22	10	-	-	-	2.0
SRXB-A.26	10	-	App C.2	-	-
SRXB-A.27	10,11	-	App C.3	-	-
SRXB-A.28	10	-	App C.3	-	-
SRXB-A.29	10	-	App C.3	-	-
SRXB-A.30	10,11	-	App C.2, C.3	-	-
SRXB-A.31	10	-	App C.2	-	-
SRXB-A.32	10	5.4	-	-	-
SRXB-A.33	10	7.4	-	-	-
SRXB-A.34	10,11,4	-	App C.1	-	-
SRXB-A.35	10,11	-	App B.1	-	-
SRXB-A.36	10	-	3	-	-
SRXB-A.37	10	7.5	-	-	-
SRXB-A.38	10	7.5	-	-	-
SRXB-A.39	10	7.5	-	-	-
SRXB-A.40	10	-	App C.1	-	-
SRXB-A.41	10	7.5	-	-	-
SRXB-A.42	10,4	-	5	-	-
SRXB-A.43	10	-	5	-	-
SRXB-A.44	10	-	5	-	-
SRXB-A.45	10	5.3	-	-	-
SRXB-A.46	10	-	6, 9	-	-
SRXB-A.47	10	-	4	-	-
SRXB-A.48	10	-	-	-	2.0
SRXB-87	9,5	7.3	-	-	-
SRXB-88	9,6	6.7	-	-	-
SRXB-89	9,5	2.1	-	-	-
SRXB-91	4	8.2	-	-	-
SRXB-92	7	4.4	-	-	-
SRXB-93	7	-	App B.1	-	-

**Table 1
Previous NRC Requests for Additional Information (RAIs) Matrix**

RAI Number (See Table 2 for RAI text)	Reference for RAI Transmittal to NRC	Section in ANP-2860	Section in ANP-2638	Page in ANP-2637	Section in ANP-2864
SRXB-94	4	8.3	-	-	-
SRXB-95	7	8.4	-	-	-
SRXB-96	7	8.5	-	-	-
SRXB-97	7	8.6	-	-	-
SRXB-98	4	3.3	-	-	-
SRXB-99	7	3.4	-	-	-
SRXB-100	7,4	3.5	-	-	-
SRXB-101	4	3.2, 6.8	-	-	-
SRXB-102	7	5.5	-	-	-
SRXB-103	7,4	4.3, 5.5	-	-	-
SRXB-104	7	5.5	-	-	-
SRXB-105	7,4	4.4	-	-	-
SRXB-106	7	4.5	-	-	-
SRXB-107	7,4	5.6	-	-	-
SRXB-108	7,4	4.4	-	-	-
SRXB-109	7,4	4.5	-	-	-
SRXB-110	7	6.9	-	-	-
SRXB-111	7	6.9	-	-	-
SRXB-112	7,4	3.2,6.5,6.9	-	-	-
SRXB-113	7	4.6 (Note 6)	-	-	-
SRXB-114	7	4.7	-	-	-
SRXB-115	7	6.6, 6.10	-	-	-
SRXB-116	7,4	4.1,4.2,4.8	-	-	-
SRXB-117	4	2.2	-	-	-
SRXB-118	4	6.7	-	-	-
SRXB-119	4	6.7	-	-	-
SRXB-120	4	6.7	-	-	-
SRXB-121	4	6.7	-	-	-
SRXB-122	4	6.7	-	-	-
SRXB-123	4	8.1	-	-	-
SRXB-124	4	8.1	-	-	-
SRXB-125	4	8.1	-	-	-
SRXB-126	4	8.1	-	-	-
SRXB-128	8	App A	-	-	-

Notes to Table 1

1. A discussion was held with the NRC (December 4, 2008) to clarify the intent of question RAI-6.1 for River Bend Station and the response to this question in Reference 3 reflects the discussion with the NRC rather than the detailed text of question RAI-6.1.
2. A discussion was held with the NRC (December 4, 2008) to clarify the intent of question RAI-6.2 for River Bend Station and the response to this question in Reference 3 reflects the discussion with the NRC rather than the detailed text of question RAI-6.2.
3. A discussion was held with the NRC (December 4, 2008) to clarify the intent of question RAI-6.15 for River Bend Station and the response to this question in Reference 3 reflects the discussion with the NRC rather than the detailed text of question RAI-6.15.
4. A discussion was held with the NRC (December 4, 2008) to clarify the intent of question RAI-6.17 for River Bend Station and the response to this question in Reference 3 reflects the discussion with the NRC rather than the detailed text of question RAI-6.17.
5. A discussion was held with the NRC (December 4, 2008) to clarify the intent of question RAI-6.18 for River Bend Station and the response to this question in Reference 3 reflects the discussion with the NRC rather than the detailed text of question RAI-6.18.
6. The original response to the original RAI discussed MELLLA+. However, TVA no longer has an interest in pursuing MELLLA+ licensing at this time.

References for Table 1

1. B.T. McKinney (PPL), Letter to NRC, "Supplement to Proposed License Amendment Numbers 285 for Unit 1 Operating License No. NPF-14 and 253 for Unit 2 License NPF-22 Constant Pressure Power Uprate," PLA -6306, November 30, 2007.
2. B. Waldrep (Progress Energy), Letter to NRC, "Brunswick Steam Electric Plant, Unit Nos. 1 and 2, Docket Nos. 50-325 and 50-324/License Nos. DPR-71 and DPR-62, Additional Information in Support for License Amendments Regarding Linear Heat Generation Rate and Core Operating Limits Report References for AREVA NP Fuel (NRC TAC Nos. MD4063 and MD4064)," January 24, 2008.
3. J. C. Roberts (Entergy), Letter to NRC, "License Amendment Request, Main Turbine Bypass System, River Bend Station, Unit 1 – Docket No. 50-458, License No. NPF-47," April 14, 2009.
4. TVA Letter, D. Langley to NRC, "Browns Ferry Nuclear Plant (BFN) – Units 2 and 3 – Technical Specifications (TS) Change TS-418 – Extended Power Uprate (EPU) – Supplemental Response to Request for Additional Information (RAI) Rounds 3 and 18 and Response to Round 20 Fuels Methods RAIs (TAC Nos. MD5263 and MD5264)," September 19, 2008.
5. TVA letter, D. Langley to NRC, "Browns Ferry Nuclear Plant (BFN) - Units 2 and 3 – Technical Specification (TS) Change TS-418 – Extended Power Uprate (EPU) – Supplemental Response to NRC Round 16 Request for Additional Information (RAI) – SRXB-87 and SRXB-89 (TAC Nos. MD5263 and MD5264)," May 1, 2008.
6. TVA letter, D. Langley to NRC, "Browns Ferry Nuclear Plant (BFN) - Units 2 and 3 – Technical Specification (TS) Change TS-418 – Extended Power Uprate (EPU) – Supplemental Response to NRC Round 16 Request for Additional Information (RAI) – SRXB-88 (TAC Nos. MD5263 and MD5264)," June 3, 2008,
7. TVA letter, J. Emens to NRC, "Browns Ferry Nuclear Plant (BFN) - Units 2 and 3 – Technical Specification (TS) Change TS-418 – Extended Power Uprate (EPU) – Partial Response to NRC Round 18 Request for Additional Information (RAI) (TAC Nos. MD5263 and MD5264)," August 15, 2008.
8. TVA Letter, M. Brandon to NRC, "Browns Ferry Nuclear Plant (BFN) – Units 2 and 3 – Technical Specifications (TS) Change TS-418 –Extended Power Uprate (EPU) – Response to Round 21 Request for Additional Information (RAI) on Channel Bow (TAC Nos. MD5263 and MD5264)," October 17, 2008.
9. TVA letter, S. Douglas to NRC, "Browns Ferry Nuclear Plant (BFN) – Units 1, 2, and 3 – Technical Specifications (TS) Change TS-418 and TS-431 – Extended Power Uprate (EPU) – Response to Round 16 Request For Additional Information (RAI) – SRXB-74/86 and SRXB-87 Through SRXB-90 (TAC Nos. MD5262, MD5263, and MD5264)," March 6, 2008.
10. TVA letter, W. Crouch to NRC, "Browns Ferry Nuclear Plant (BFN) – Units 2, and 3 – Response to NRC Round 3 Requests for Additional Information Related to Technical Specifications (TS) Change No. TS-418 – Request for Extended Power Uprate Operation (TAC NOS. MC3743 and MC3744)," March 7, 2006.
11. TVA letter, W. Crouch to NRC, "Browns Ferry, Units 2 and 3 – Supplemental Response to NRC Round 3 Request for Additional Information Related to Technical Specifications Change No. TS-418 – Extended Power Uprate Operation (EPU) (TAC Nos. MC3743 and MC3744)," May 11, 2006.

**Table 2
Previous NRC Requests for Additional Information (RAIs) Text**

RAI Number	Text
Brunswick Steam Electric Plant	
RAI-1	<p>General Based on the information provided for the license amendment (References I through 8), it appears that certain generic and specific analyses were performed for one BSEP unit and applied to both. With regard to those analyses intended to apply to both units, please provide a description of key differences in operation and system configuration between Units 1 and 2, and show that the analyses bound both units.</p> <p>For Unit 2 transition, the NRC requests that cycle specific analysis reports (i.e. thermal-hydraulic design, fuel cycle design, reload safety analysis) be provided for staff confirmation 3 months prior to startup from the first refueling outage that uses AREVA fuel.</p>
RAI-2	<p>Power Distribution Uncertainty During a recent review of a BWR extended power uprate and associated AREVA fuel methodologies, the adequacy of benchmark data associated with neutronic power prediction methods was questioned. The issue was resolved by increasing the power distribution uncertainties and propagating them into the SLMCPR calculation. Please discuss the applicability of this issue to BSEP and, if applicable, discuss the approach that will be taken to resolve it.</p>
RAI-3	<p>Void-Quality Correlation Please justify the application of the [] void-quality correlation to co-resident GE14 fuel.</p>
RAI-5	<p>ATWS Containment Please provide the suppression pool temperature and containment pressure limits (i.e. acceptance criteria) and the corresponding licensing values of record.</p>
RAI-6	<p>GE14 LOCA PCT Please justify the continued applicability of the GE14 licensing basis PCT and associated MAPLHGR limits for the projected mixed core operation with ATRIUM 10. Please confirm that no system modifications were made at BSEP that would invalidate the reactor system response assumed in the GE14 LOCA analysis of record.</p>
RAI-7	<p>Stability RAMONA5-FA code is used to calculate the critical power ratio response during core oscillations. While the RAMONA5-FA method has not been generically approved by staff, its application has been previously accepted on an application-specific basis. Please confirm that the RAMONA5-FA methodology has been applied to Brunswick in a manner consistent with previously accepted applications.</p>
RAI-8	<p>Bypass Boiling Please discuss the impact of bypass boiling on the OPRM setpoints, and whether bypass voiding was considered in the analyses for BSEP.</p>
RAI-9	<p>MCPR Part 21 Please discuss any impact of AREVA's October 8, 2007, Part 21 report regarding MCPR calculation to projected Brunswick Units 1 and 2 operation with ATRIUM-10 fuel and AREVA fuel methodologies.</p>

**Table 2
Previous NRC Requests for Additional Information (RAIs) Text**

RAI Number	Text
RAI-10	<p>Shutdown Margin</p> <p>Please describe qualitatively and quantitatively, the analysis procedure used to ensure that the shutdown margin is within the TS limit through out the transition cycles. In particular please address how the eigenvalue biases and uncertainties are determined and accounted for the first and second transition cycles.</p>
RAI-11	<p>Void-Quality Correlation</p> <p>During a recent review of a BWR extended power uprate and associated AREVA fuel methodologies, the staff questioned the void-quality correlation bias and uncertainties. The issue was addressed by performing a plant specific calculation to assess the impact of the uncertainties on the OLMCPR. Please discuss how the void-quality correlation bias and uncertainties are addressed for the projected Brunswick Units 1 and 2 operations.</p>
Susquehanna Steam Electric Station	
	<p>Based on topics discussed at the October 9 and November 14, 2007, ACRS subcommittee meetings and a teleconference held with the NRC staff on October 18, 2007, PPL is submitting the following information to assist the NRC staff in their review of the PPL Constant Pressure Power Uprate (CPPU).</p> <p>The information provided addresses:</p>
Item 1	Void Fraction Measurement
Item 2	Void Quality Correlation
Item 3	Bypass Voiding
Item 4	Power Distribution Uncertainties
River Bend Station	
RAI-6.1	<p>Verify that the upstream transient COTRANSA2 analysis: (1) includes the 110% integral thermal power multiplier, (2) biases all relevant input parameters to the limiting values allowable by TSs as appropriate, (3) biases non-TS controlled input parameters to the most conservative value based on their associated uncertainty, and (4) is representative of the limiting plant configuration allowable for equipment out-of-service in the TSs.</p>
RAI-6.2	<p>If COTRANSA2 or another one-dimensional code is used to determine the transient reactor power, please describe how appropriate axial planar average fuel rod parameters are determined for the analysis. This discussion should address: gap conductance, thermal conductivity, pellet size, and heat capacity. Justify that these parameters are acceptably accurate or conservative. Demonstrate that the conservatism in the COTRANSA2 analysis is sufficient to bound any bias in the transient peak heat flux calculation as a result of known [] for ATRIUM-10 fuel.</p>
RAI-6.3	<p>For the transient analysis, is the thermal power assumed to be 102% of the licensed thermal power at the initiation of the transient?</p>
RAI-6.4	<p>Specify the code that is used to determine the transient LHGR limit relative to the 1% plastic strain criterion and fuel centerline melt criterion if this code is not RODEX2.</p>

**Table 2
Previous NRC Requests for Additional Information (RAIs) Text**

RAI Number	Text
RAI-6.5	During cycle operations, please describe what surveillances or checks are performed by the licensee to ensure that actual plant operations are within the bounds of the COLR analysis in terms of meeting the 1% plastic strain and fuel centerline melt criteria.
RAI-6.6	Verify that conformance with the operating limit MLHGR is performed accounting for channel bow. If not, justify why not.
RAI-6.7	Verify that conformance with the operating limit MLHGR is performed accounting for LPRM rod power biases. If not, justify why not.
RAI-6.8	Verify that conformance with the operating limit MLHGR is performed accounting for PLFR fission gas plena. If not, justify why not.
RAI-6.9	Clarify if the relevant rod power histories used in the thermal mechanical analysis come from calculated off-line or [] power histories. Justify the approach used.
RAI-6.10	Verify that the power shapes used in the thermal-mechanical calculations of the operating limit and transient limit are conservative for the plant-specific application. If these shapes are different from the shapes reported in BAW-10247(P)(A), justify why they are different.
RAI-6.11	The NRC staff is aware that the transient analysis is performed using off-line simulations. For the COLR analysis, verify that the steady state off-line cycle analysis used to determine the EOC axial power shape is conservative relative to the operational flexibility allowed by the flow control window along the licensed thermal power line (LTPL) of the approved operating domain.
RAI-6.12	The staff is aware that the transient analysis is performed using off-line simulations. Verify that the steady state off-line cycle tracking analysis is sufficiently detailed to meet the uncertainty requirements imposed on CASMO-4/MICROBURN-B2, in the SER for EMF-2158(P)(A), which References Tables 2.1 and 2.2 in the LTR. The response should provide operational data to verify the accuracy of the offline analysis against plant-specific axial, radial, and nodal TIP data.
RAI-6.13	Specify the code that is used to determine the transient LHGR during simulated FWCF events if this code is not XCOBRA-T.
RAI-6.14	Describe any differences between the XN-NF-84-105(P)(A) licensing topical report description of XCOBRA-T and the current standard production code version that supports the use of this methodology for modern fuel designs such as ATRIUM-10, the response should address axial geometry changes and modern fuel spacers.
RAI-6.15	Describe how gamma smearing, decay heat, and direct energy deposition are treated in XCOBRA-T. Provide justification for any assumptions in the analysis. If historical (non-ATRIUM-10 or non-cycle loading specific) parameters are used to model the event, justify the use of these values.
RAI-6.16	If XCOBRA-T or another one-dimensional code is used to perform the FWCF event analysis, justify the appropriateness of the assumption to hold the radial power shape constant. This justification should consider the sensitivity of the local sub-bundle radial pin power distribution to the instantaneous void fraction.
RAI-6.17	If XCOBRA-T or another one-dimensional code is used to determine the transient hot rod heat flux, please describe how appropriate fuel rod parameters are determined for the analysis. This discussion should address the following: gap conductance, thermal conductivity, pellet size, and heat capacity. Justify that these parameters are acceptably accurate or conservative.
RAI-6.18	If XCOBRA-T or another three-equation thermal hydraulic code is used to perform the FWCF event analysis, please justify the appropriateness of utilizing the []. In particular, pressurization in the FWCF may result in significant changes to the fluid saturation temperature. The code treats these

**Table 2
Previous NRC Requests for Additional Information (RAIs) Text**

RAI Number	Text
	<p>temperature changes as [] and may result in changes in the cladding heat flux that are nonphysical relative to the expected behavior based on a more detailed two fluid representation of the liquid film and vapor fields. Provide detailed transient analyses to demonstrate that the predicted transient peak heat flux is accurately calculated or conservative relative to the limitations in the thermal hydraulic model.</p>
RAI-6.19	<p>If XCOBRA-T is the code used to perform the transient LHGR analysis, confirm that the thermal hydraulic conditions simulated during the FWCF event do not exceed the application range of the critical heat flux correlation. If these bounds are exceeded the staff is aware that XCOBRA-T []. If the bounds are exceeded provide justification of the application of the analysis to demonstrate acceptable thermal-mechanical performance.</p>
Browns Ferry Nuclear Plant	
SRXB-A.14	<p>Section 1.2.1 of Enclosure 5, EMF-2982(P), Browns Ferry Units 2 and 3 Safety Analysis Report for Extended Power Uprate ATRIUM™-10 Fuel Supplement, Revision 0, or the FUSAR, states:</p> <p style="padding-left: 40px;">For most of the EPU analyses, the 2 percent power factor discussed in Regulatory Guide 1.49 is accounted for in the analysis methods. Three exceptions are ASME over pressurization, loss of feedwater (LOFW) flow, and LOCA analyses.</p> <p>However page 3-1, of Section 3.2 states that "[t]he events were analyzed at 102 percent of EPU rated thermal power. . . ." for the overpressure protection analysis. Discuss whether an exception was taken for the overpressure analysis.</p> <p>Explain in detail why exceptions are taken from the RG 1.49 position of 2-percent power factor for the LOFW and LOCA analyses.</p>
SRXB-A.15	<p>Table 1.3 of Section 1.2 of the June 6, 2005, submittal lists all the nuclear steam system codes used for the EPU request. Section 1.2.2 indicates that the Unit 1 application of these codes complies with the limitations, restrictions, and conditions specified in the applicable NRC safety evaluation (SE) report that approved each code, with exceptions as noted in Table 1-3.</p> <p>Provide a review of the fuel vendor's analytical methods and code systems (neutronic, LOCA, transient and accidents, etc.) used to perform the safety analyses supporting the Units 2 and 3 application and provide the following information to confirm that:</p> <ol style="list-style-type: none"> a) The steady state and transient neutronic and thermal-hydraulic analytical methods and code systems used to perform the safety analyses supporting the EPU conditions are being applied within the NRC-approved applicability ranges; b) For the EPU conditions, the calculational and measurement uncertainties applied to the thermal limits analyses are valid for the predicted neutronic and thermal hydraulic core and fuel conditions; and c) That the assessment database and the assessed uncertainty of models used in all licensing codes that interface with or are used to simulate the response of Units 2 and 3 during steady state, transient, or accident conditions remain valid and applicable for the EPU conditions.

Table 2
Previous NRC Requests for Additional Information (RAIs) Text

RAI Number	Text
SRXB-A.16	Section 2.1 of the FUSAR states that "[t]he NRC-approved exposure limits are not exceeded in the ATRIUM-10 equilibrium core design used in the EPU evaluations." Specify the NRC-approved exposure limits for ATRIUM-10 fuel.
SRXB-A.22	<p>The BFN Units 2 and 3 submittal is the first application of Framatome methods for the transient and accident analysis for EPU. Consistent with Appendix E of Licensing Topical Report, NEDC-32424P-A, Generic Guidelines for General Electric Boiling Water Reactor Extended Power Uprate, or ELTR1 provide a justification for the use of Framatome transient and accident analyses methods for EPU application. List all transients and accidents analyzed in support of EPU for Sections 2.8.5.1 to 2.8.5.6 of Matrix-8 in RS-01. In addition, explain how the limiting transients were selected and discuss in detail how each transient/accident in Sections 2.8.5 to 2.8.5.6 is dispositioned. Specifically:</p> <ul style="list-style-type: none"> a) Confirm that the scenario and sequence of event described in UFSAR is still valid for EPU; b) Identify the supporting analysis for the event, evaluation model used for the analysis, and identify the topical report which describes the event; c) Specify whether the disposition is based on a generic analysis or the current analysis in the UFSAR, or plant-specific equilibrium analysis or the reload analysis, and d) Describe how the acceptance criteria is met.
SRXB-A.26	Demonstrate quantitatively and qualitatively, that the Lattice/Depletion code systems' is capable of predicting the power peaking distribution at the upper part of the high powered bundles for operation under high void fractions. For example, show that the requirements in Chapter 4 of EMF-2158(P)-A, "Siemens Power Corporation Methodology for Boiling Water Reactors: Evaluation and Validation of CASMO-4/MICROBURN-B2," can still be met for EPU core designs.
SRXB-A.27	Demonstrate quantitatively and qualitatively, that the current uncertainties and biases established in the benchmarkings and presented in Table 9.8 and 9.9 of EMF-2158(P)-A remain valid for the neutronic and thermal-hydraulic conditions predicted for the EPU operation. Specifically, demonstrate the uncertainties and biases used in your reactivity coefficients (e.g., void coefficient) are applicable or remain valid for the neutronic and thermal-hydraulic conditions expected for EPU operation.
SRXB-A.28	Demonstrate quantitatively and qualitatively, that the fuel isotopic validations and testing performed in EMF-2158(P)-A remain applicable for prolonged operation under high void conditions for the fuel lattice designs that would be used for the expected EPU core designs.
SRXB-A.29	Demonstrate qualitatively and quantitatively that the Framatome-ANP neutronic methodology experience base is applicable to EPU conditions at BFN.
SRXB-A.30	Demonstrate that the Framatome-ANP neutronic methodology prediction capability for current fuel designs operated under the current operating strategies and core conditions. Prediction comparison should be made to gamma scans and traversing incore probe (TIP) core follow data. This demonstration applies to any recent fuel, such as the ATRIUM-9 and ATRIUM-10, in particular for first cycle and second cycle fuel. (Refer to Framatome Handout for August 4, 2005, Meeting; ADAMS Accession No. ML052370230.)
SRXB-A.31	The first three bullets of slide No. 63 of the CASMO-4/MICROBURN-B2 Methodology, of the August 4, 2005, presentation, alluded to the average value of the Correlation Coefficient (CC) for the Quad Cities cycles 2 and 4. These values were determined for

**Table 2
Previous NRC Requests for Additional Information (RAIs) Text**

RAI Number	Text
	the 8X8 bundle design. Provide quantitative and qualitative technical justification for the use of 8X8 CC to 10X10 bundle design, specifically, demonstrate that the correlation coefficients are independent of fuel bundle design.
SRXB-A.32	<p>The radial peaking factors (RPF) uncertainty presented on slide No. 35 of the Safety Analysis, of the August 4 presentation, point to the conclusion that the safety limit minimum critical power ratio (SLMCPR) is not very sensitive to small increases in RPF uncertainty. Provide quantitative and qualitative technical justification in support of this conclusion. Specifically:</p> <p>a) Provide statistical information (number of histories, number of bundle or rods, etc.) supporting the 0.0055 value; and</p> <p>b) Address whether the SLMCPR value of 1.0855 is rounded up to 1.09 as the final TS Value.</p>
SRXB-A.33	Provide qualitative and quantitative description of the gamma scanning process. Specifically address whether the data is obtained via gamma scanning, transformed mathematically and or chemically into providing isotopic burnup/depletion information.
SRXB-A.34	Describe qualitatively the cross-section reconstruction process incorporated in CASMO-4 and MICROBURN-B2. The response should reflect the information provided in the slides (1-35) of the August 4 presentations, including high void fraction effects and accuracy. Provide flow chart(s), road map(s) and any other means to demonstrate the process, starting from the gathered raw void fraction data, how that data is used by CASMO-4 to generate the required cross-sections. In addition, briefly describe the development of the void fraction correlation and associated uncertainties.
SRXB-A.35	Provide qualitative description of the void data base and the associated correlation. Specifically, describe the uncertainty associated with the data gathering, identifying the uncertainties currently applied to the void fraction correlation and justify its applicability for EPU conditions.
SRXB-A.36	Demonstrate that the database used to establish the two phase pressure drop for the fuel designs used for the EPU include predicted EPU channel and fuel assembly design conditions. Specifically, demonstrate that current normal power pertinent two-phase flow/pressure drop ranges are still applicable to EPU anticipated ranges of operations.
SRXB-A.37	Describe that the methods used in the licensing codes to model the bypass water (e.g., core simulator, steady state and transient codes, LOCA codes).
SRXB-A.38	State the bypass voiding criteria (if any) or specification that applies to the TIP and the LPRM.
SRXB-A.39	Demonstrate that the capability of the licensing code systems, including the core simulator, to determine the potential for bypass voiding.
SRXB-A.40	Provide an evaluation and discussion of the lattice/depletion code (CASMO-4) capability to generate the cross-section with voiding in the in-channel water rods and bypass.
SRXB-A.41	Evaluate EPU core neutronic and thermal-hydraulic conditions and state if for EPU core designs and operating conditions, if bypass voiding can occur during steady state or transient events. Consider operation at all limiting statepoints in the maximum extended load line limit analysis (MELLLA) domain.
SRXB-A.42	In August 30, 2004, General Electric Nuclear Energy (GENE) issued a 10 CFR Part 21 report (ADAMS ML042720293), stating that using limiting control rod blade patterns developed for less than rated flow at rated power conditions could sometimes yield more limiting bundle-by-bundle MCPR distributions and/or more limiting bundle axial power shapes than using limiting control rod patterns developed for rated flow/rated power in the SLMCPR calculation. The affected plants submitted amendment requests increasing

**Table 2
Previous NRC Requests for Additional Information (RAIs) Text**

RAI Number	Text
	<p>their SLMCPR value. The staff understands that Framatome did not issue a Part 21 reporting on the SLMCPR methodology that addresses the calculation of the SLMCPR at minimum core flow and off-rated conditions similar to GENE's Part 21 report.</p> <p>Reference the applicable sections of the ANF-524P-A SLMCPR methodology that specify the requirement to calculate the SLMCPR at the worst case conditions for minimum core flow conditions for rated power. Demonstrate that the SLMCPR is calculated at different statepoints of the licensed operating domain, including the minimum core flow statepoint and that the calculation is performed for different exposure points.</p>
SRXB-A.43	<p>Discuss or reference the applicable sections/chapters of ANF-524P-A that addresses what rod patterns are assumed in performing the nonrated flow SLMCPR calculations. State how it is established that the rod patterns assumed in the SLMCPR calculations for rated power, flow, and minimum core flow conditions, would reasonably bound the planned rod pattern that Units 2 and 3 would operate under EPU conditions.</p>
SRXB-A.44	<p>For implementation of Average Power Range Monitor, Rod Block Monitor, Technical Specifications Improvement Program (ARTS)/MELLLA using Framatome methods, show that Units 2 and 3 can operate at all statepoints, including the minimum core flow statepoint, without violating their SLMCPR in the event of an abnormal operating occurrence. The minimum core flow statepoint SLMCPR calculations should demonstrate that Units 2 and 3 can operate at the minimum flow statepoint with some margin.</p>
SRXB-A.45	<p>Regarding SAFLIM2 calculations, slides 27 - 31, please provide qualitative description of this process, including the termination of the process if the EPSBTR Criterion is satisfied.</p>
SRXB-A.46	<p>Describe the process for establishing the design limit curves for the linear heat generation rate (LHGR) and the maximum average planar LHGR (MAPLHGR). In addition, discuss what impact (if any) high void fractions have on this process.</p>
SRXB-A.47	<p>The Siemens Power Corporation- B (SPCB) CHF correlation was approved by the NRC staff to be applicable over specified ranges of mass flow, pressure, and inlet subcooling. Discuss whether the utilization of the SPCB Correlation to EPU take the Correlation beyond its approved applicable ranges?</p>
SRXB-A.48	<p>Table 1-3 of the FUSAR, lists computer codes used for EPU transient analyses. Please clarify which code was used for the over-pressure protection analysis, and was the code approved by the NRC specifically for this transient.</p>
SRXB-87	<p>To address the adequacy of benchmark data associated with neutronic power prediction methods, the staff understands that the issue was addressed by the fuel vendor by increasing the power distribution uncertainties and propagating them into the safety limit minimum critical power ratio calculation. Provide the following additional information:</p> <ol style="list-style-type: none"> <li data-bbox="421 1549 1483 1612">a. Discuss the applicability of this approach to projected Units 2 and 3 operations using ATRIUM-10 fuel and AREVA methodologies. <li data-bbox="421 1633 1483 1717">b. Justify the use of the local and radial power distribution uncertainties based on Quad Cities gamma scans in light of the harder neutron spectrum present in EPU cores.

Table 2
Previous NRC Requests for Additional Information (RAIs) Text

RAI Number	Text
SRXB-88	<p>To address the adequacy of void-quality correlation bias and uncertainties, the staff understands that a plant specific calculation can be performed to assess the impact of the uncertainties on the operating limit minimum critical power ratio (OLMCPR). Provide the following additional information:</p> <ol style="list-style-type: none"> a. Discuss how the void-quality correlation bias and uncertainties are addressed for the projected Units 2 and 3 operation at EPU conditions. b. Determine the net impact on the OLMCPR from a bias in the void-quality correlation within the uncertainty range based on full-scale-test data.
SRXB-89	<p>To address the effect of bypass boiling on the stability oscillation power range monitor (OPRM) setpoints, a setpoint setdown was performed. Provide the following additional information:</p> <ol style="list-style-type: none"> a. Discuss how the bypass boiling effect is addressed for Units 2 and 3 OPRM setpoints. b. Determine a method for conservatively accounting for the effect of bypass void formation on OPRM and average power range monitor sensitivity.
SRXB-91	<p>In Enclosure 1 of the letter dated March 7, 2006, Tennessee Valley Authority (TVA) provides information in support of the use of the Ohkawa-Lahey void quality correlation against ATRIUM-10 test data in response to SRXB-A.35. The Ohkawa-Lahey void quality correlation appears to under-predict the void fraction for the majority of the thermodynamic qualities tested at 6.9 Megapascal (MPa). The void reactivity coefficient is sensitive to the instantaneous void fraction, generally becoming more negative with increasing void fraction.</p> <p>Provide a quantitative determination of the impact of the bias in the void fraction in COTRANSA2 on ATWS overpressure analysis results for the bottom head peak pressure. This should include a comparison of the impact of the void bias to the margin between the peak calculated pressure and the American Society of Mechanical Engineers Boiler & Pressure Vessel Code (ASME) acceptance criterion of 1500 pounds per square inch gage.</p> <p>In addition, address how known biases are taken into account for future cycle specific calculations and for bundle designs other than ATRIUM-10.</p> <p><u>Clarifications provided by the NRC following a meeting on August 7, 2008</u></p> <p>Address the void bias for both the anticipated transient without scram (ATWS) overpressure as well as ASME overpressure.</p>
SRXB-92	<p>Subcooled boiling is a phenomenon that can have a significant impact on the efficacy of a code system to accurately predict the axial power shape and bundle flow (by impacting the two phase pressure losses). Using a subset of the KATHY data, provide a similar comparison for the XCOBRA-T Levy subcooled void model as provided for the Ohkawa-Lahey correlation in response to NRC-RAI-SRXB-A.35.</p>
SRXB-93	<p>Provide justification for the application of the Ohkawa-Lahey void-quality correlation to pressures above 6.9 MPa.</p>
SRXB-94	<p>The initial steam flow rate at extended power uprate (EPU) conditions is higher than at pre-EPU conditions, and the transient power pulse is expected to be higher during the pressurization. The suppression pool temperature for Units 2 and 3 is based on an analysis for GE14 fuel. Provide a discussion on the means used to confirm that the</p>

**Table 2
Previous NRC Requests for Additional Information (RAIs) Text**

RAI Number	Text
	results of the GE 14 analysis are bounding for ATRIUM-10 fuel. This justification should contain qualitative discussion regarding the impact of the differences in nuclear characteristics and should consider the timing and nature of the transient power response during pressurization, relief, and boration.
SRXB-95	Provide details regarding the bypass flow during the ATWS overpressure transient as predicted by COTRANSA2. In particular determine if the bypass flow is downward during any portion of the transient. Justify the applicability of these results given any inherent constraints in the COTRANSA2 code.
SRXB-96	Provide a plot of the total safety relief valve (SRV) flow during ATWS overpressurization for EPU and pre-EPU conditions.
SRXB-97	Condition 2 of the safety evaluation dated May 23, 1990, approving Advanced Nuclear Fuels (ANF) 913(P)(A), COTRANSA2: A Computer Program for Boiling Water Reactor Transient Analyses, August 1990 requires consideration of time step. Provide details regarding the nodalization of the steam line and time step used for ATWS overpressure analysis. Specifically provide results of sensitivity studies to verify that the node size and time steps are sufficient to preclude numerical errors in the calculation of the pressure wave propagation to the reactor core from the main steam isolation valves.
SRXB-98	It appears that COTRANSA2 has two centrifugal pump models, the first pump model neglects the inertia and the second pump model is based on homologous input. Identify which model option is used. If the second model option is used, verify that it is used to model the dual recirculation pump trip during ATWS evaluations. Verify that the homologous input for the recirculation pumps for the Unit 2 analyses have been benchmarked against operational data at Unit 2.
SRXB-99	The description of the steam line model in ANF-913(P)(A) does not provide descriptive details of the SRV model. Provide a description similar to Section 2.3.4 in ANF-913(P)(A) describing these models. In the description address the use of calculated pressures in modeling the SRV lift. When apportioning flow from a steam line node between an SRV and the downstream node, discuss how the SRV flow is calculated.
SRXB-100	Section 2.1 of ANF-913(P)(A) states that cross sections are interpolated based on both controlled and uncontrolled states at [] void fraction. These void cases appear to not be consistent with the void cases used to develop cross section response surfaces for MICROBURN-B2 [], explain this discrepancy.
SRXB-101	<p>The Doppler coefficient is stated to be dependent on the broadening of the fast group cross section and to be a function of fuel temperature.</p> <ul style="list-style-type: none"> • MICROBURN-B2 calculates the nodal fuel temperature based on quadratic fitting function. Provide this function. Discuss how the initial nodal fuel temperature is calculated. Provide a comparison of the quadratic function predicted nodal fuel temperature to results predicted using a more sophisticated thermal rod conduction model and heat transfer coefficient, such as XCOBRA-T. • Expand on the discussion provided in ANF-913(P)(A) and describe what combination of calculations is performed to determine the reactivity contribution from Doppler for ATWS overpressure analysis, for example, specify if a lattice calculation is performed to determine a coefficient relating microscopic cross sections to average fuel temperature. • Discuss whether the rod temperatures in Section 2.1.3 of ANF-913(P)(A) are calculated based on a nodal average rod or for each rod in the node. Clarify how

**Table 2
Previous NRC Requests for Additional Information (RAIs) Text**

RAI Number	Text
	<p>the transient nodal average fuel temperature is calculated.</p> <ul style="list-style-type: none"> Provide a description of any differences between the COTRANSA2 thermal conduction models, including material properties, and the RODEX2 models. Discuss whether the RODEX2 code was used to develop input for COTRANSA2 similar to XCOBRA-T.
SRXB-102	<p>In the response to SRXB-87 contained in the letter dated March 6, 2008, as supplemented in the letter dated May 1, 2008, TVA provided a sensitivity analysis to quantify the impact on the safety limit minimum critical power ratio (SLMCPR) of a potential increase in pin power peaking uncertainty at the harder spectrum EPU conditions.</p> <p>XCOBRA-T is used to determine the transient effect on the critical power ratio (CPR). To calculate the critical heat flux ratio XCOBRA-T requires S-factors. The S-factor accounts for lattice peaking and bundle geometry effects. Describe how the additive constants and lattice calculations are used to determine the S-factors for use by XCOBRA-T. In particular, address whether the analyses are performed for local peaking using XFYRE, CASMO-4, or MICROBURN-B2.</p>
SRXB-103	<p>Provide the relationship of the term F_{eff} to the S-factor. If axial integration is required to determine the S-factors, specify how this is performed. Address whether the S-factors are sensitive to the bundle void distribution. Describe how the S-factors are determined for conditions typical (or bounding) for operation at EPU conditions.</p>
SRXB-104	<p>Describe how S-factors are determined for part length rods.</p>
SRXB-105	<p>Verify that the Unit 2 transient analyses were performed using input options for closure relationships that are consistent with the NRC approval of XCOBRA-T. This includes specifying the Levy subcooled boiling model, the Martinelli-Nelson two phase friction multipliers, the two phase component loss multiplier, the wall viscosity model, and thermodynamic properties from the ASME steam tables.</p>
SRXB-106	<p>At EPU conditions, the core steam flow rate is increased. The pressure response to events such as turbine trip and load rejection is expected to be exacerbated at EPU conditions relative to pre-EPU conditions.</p> <p>The NRC staff notes that the SPCB critical power correlation for ATRIUM-10 fuel is not qualified above []. In the analysis of the pressurization transients, address whether the pressure exceed [] in the reactor core. Similarly compare the analysis conditions for those parameters listed in Condition 3 of the safety evaluation July 3, 2000, for EMF-2209(P)(A), SPCB Critical Power Correlation.</p>
SRXB-107	<p>Address how the wall friction and component loss coefficients were determined for Unit 2. Address whether these parameters were input in the analysis to account for friction. Provide these parameters and the technical basis for their selection. Relative to pre-EPU conditions, channel flow tends to redistribute at EPU conditions as there are fewer low resistance bundles in the core. Address whether the friction parameters were selected to be consistent with this expected trend.</p>
SRXB-108	<p>At EPU conditions there are a higher number of higher powered bundles. It is possible, and likely, for large axial sections of these bundles to be in an annular flow regime. Calculating pressure losses near bundle features such as fuel spacers can be important in the prediction of critical heat flux, which tends to occur below fuel spacers where the liquid film is typically thinnest.</p> <p>On page 25 of Exxon Nuclear Company's XN-NF-84-105(P)(A), XCOBRA-T.- A</p>

**Table 2
Previous NRC Requests for Additional Information (RAIs) Text**

RAI Number	Text
	Computer Code for BWR Transient Thermal-Hydraulic Core Analysis, it is stated that "[t]his [Martinelli-Nelson] formulation was developed for horizontal flow, but is reasonably accurate for vertical flow where both phasic flow rates are high enough to ensure turbulent co-current flow." Justify why the Martinelli-Nelson two phase friction multipliers are applicable in annular flow regimes.
SRXB-109	Section 3.3 of the Technical Evaluation Report attached to the NRC's safety evaluation approving XN-NF-84-105(P)(A) states that critical power calculations may be inaccurate if the inlet flow is negative or if the inlet quality is above zero. Verify that for the transient analyses that the bundle inlet flow is positive and that the inlet qualities are less than zero.
SRXB-110	Transient cladding heat flux during transients will be a function of the heat hold-up in the fuel pins during AOOs. Identify all changes that have been made to the fuel rod thermal conduction models since the NRC's review and approval of RODEX2. Provide a comparison of the XCOBRA-T fuel rod models to those approved to the NRC during review of EMF-85-74(P), RODEX2A (BWR) Fuel Rod Thermal Mechanical Evaluation Model, or RODEX2A. Also, provide a comparison of these models to those in BAW-10247(P), Realistic Thermal-Mechanical Fuel Rod Methodology for Boiling Water Reactors, or RODEX4.
SRXB-111	If different historical models are preserved in XCOBRA-T relative to RODEX2A, justify the use of XCOBRA-T to model transients for fuel above the previously established burnup limits for RODEX2.
SRXB-112	<p>Some models may have been updated to conservatively bound experimental data collected subsequent to the NRC review and approval of RODEX2. The staff notes that certain assumptions may be conservative in the assessment of linear heat generation rate limits that may not be conservative when evaluating transient heat flux during AOO simulation due to the competing effects of reactivity feedback and heat flux flow mismatch. If a model is "conservatively bounding" in RODEX2, and translated to XCOBRA-T, provide a discussion of the performance of the model for thermal margin transient calculations</p> <p><u>Clarifications provided by the NRC following a meeting on August 7, 2008</u></p> <p>The draft response for SRXB-112 deals with changes to the RODEX2 code in its first part, but requests additional information regarding the use of conservative assumptions in the abnormal operating occurrence (AOO) transient response. The discussion regarding the conservatism of the gap properties should be addressed in the response to the second part of RAI 112. See the second and third sentences:</p> <p style="padding-left: 40px;">The staff notes that certain assumptions may be conservative in the assessment of linear heat generation rate limits that may not be conservative when evaluating transient heat flux during AOO simulation due to the competing effects of reactivity feedback and heat flux/flow mismatch. If a model is "conservatively bounding" in RODEX2, and translated to XCOBRA-T, provide a discussion of the performance of the model for thermal margin transient calculations</p> <p>Summary of staff concern:</p> <p>The NRC staff considered the coupling of the neutron flux and fluid conditions for AOO transient evaluations for both a reduced thermal time constant and an increased thermal time constant. When the time constant is over predicted, the fluid response to changing neutron power is lagged. A pressurization transient, therefore, would result in an</p>

Table 2
Previous NRC Requests for Additional Information (RAIs) Text

RAI Number	Text
	<p>increase in the reactor power that is not impeded by subsequent rapid void formation due to hold up of the heat flux in the pellet. An over prediction of the time constant will tend to increase the fission power for such a transient. However, the same effect of holding the heat up in the fuel pellet has the dual effect of reducing the cladding heat flux response; therefore, the ultimate effect on the transient critical power ratio (CPR) is a combination of the conservative prediction of peak neutron flux with the non-conservative prediction of the transient cladding heat flux.</p> <p>For the case where the time constant is under predicted the inverse is true, the gross reactor power increase due to pressurization is limited due to more rapid void formation in response to the increasing neutron flux, but this is countered by a prediction of higher cladding surface heat flux relative to the pin power throughout the transient.</p> <p>The input assumptions regarding the gas gap may increase or decrease the thermal resistance, and similarly, an increase or decrease in the thermal resistance does not have a clear impact on the transient predicted CPR due to competing effects in the cladding heat flux and void reactivity.</p>
SRXB-113	<p>At EPU conditions a core contains a higher number of higher powered bundles. At these conditions the heat transfer may be driven by phenomena such as liquid entrainment and redeposition. The XCOBRA-T heat transfer is predicted according to Dittus-Boelter and Thom heat transfer correlations for forced convection and nucleate boiling, respectively. The NRC is aware that AREVA has temperature data from full scale critical power tests. Provide qualification of the heat transfer correlations to predict fuel rod surface temperatures for test conditions representative of higher powered bundles at flow rates similar to EPU conditions for ATRIUM-10 [i.e. ~5 – ~8 megawatts thermal]. Particularly, provide the relevant qualification data near the top of the bundle where liquid entrainment and droplet redeposition is expected to have an impact on heat transfer.</p>
SRXB-114	<p>XCOBRA-T accepts input from COTRANSA2 to capture the transient variation in power during AOOs. EPU cores are high energy cores and may have a higher peak hot excess reactivity, resulting in changes in SCRAM worth relative to pre-EPU conditions. Provide a more detailed description of how effects such as transient variation in axial power shape during SCRAM are captured in XCOBRA-T. Address whether detailed nodal power histories translated from COTRANSA2 to XCOBRA-T.</p>
SRXB-115	<p>At EPU conditions a larger number of bundles are operated a high power levels. It is expected, therefore, for more bundles to be near their thermal limits at the onset of a transient. Describe how the Unit 2 radial channel nodalization was evaluated. Address whether the potentially limiting bundles were grouped with non-limiting bundles. Provide the radial bundle power distribution (as predicted by MICROBURN-B2) and radial channel group assignments (in XCOBRA-T) for the initial conditions for the limiting transient analysis. Also, compare the COTRANSA2 radial grouping with the XCOBRA-T grouping. Provide justification that the resolution is sufficient to model the transient behavior in all potentially limiting bundles.</p> <p><u>Clarifications provided by the NRC following a meeting on August 7, 2008</u></p> <p>The appropriateness of the XCOBRA-T nodalization for transient LHGR analysis should be explicitly addressed.</p>
SRXB-116	<p>Address whether XCOBRA-T was used to demonstrate acceptable fuel rod thermal mechanical performance during transients. If XCOBRA-T is not used for this purpose, address how acceptable thermal mechanical performance is demonstrated during</p>

Table 2
Previous NRC Requests for Additional Information (RAIs) Text

RAI Number	Text
	<p>transients. If the method is not consistent with the models in RODEX2 or later NRC-approved thermal mechanical code, justify the approach.</p> <p><u>Clarifications provided by the NRC following a meeting on August 7, 2008</u></p> <p>Aside from describing the method for normalization of the transient LHGR to the initial LHGR, provide some additional minor clarifications:</p> <ol style="list-style-type: none"> (1) The decay heat contribution will remain essentially static during the transient, address whether the normalization capture the varying rod decay heat sources; (2) Specify the source of the decay heat constants (i.e. ANS standard); (3) The rod power distribution is flattened due to gamma smearing of the thermal power, address how these gamma smeared power fractions are calculated; and (4) Address how the direct moderator heat is accounted for. <p>The response should also provide a detailed description of the rod heat flux calculation for bundles with part length fuel rods, and address the code change as well as items 1-4 for each region (fully rodded, plena region, above plena region).</p>
SRXB-117	<p>Enclosure 4 of the letter dated June 25, 2004, references NEDO-32047-A. In particular it is noted that operation at EPU conditions is generally achieved by flattening radial core power. As a result of this flattening the second harmonic eigenvalue separation is likely to be greatly reduced. Therefore, under non-isolation ATWS conditions it is expected that the core will be more susceptible to regional mode oscillations that at pre-EPU conditions.</p> <p>Given the information provided in the NRC's contractors' technical evaluation report attached to the safety evaluation approving NEDO-32047-A dated February 5, 1994, Appendix C: "Consequences of Out-of-Phase Instability Mode Not Proven More Favorable than In-Phase Mode." Provide an evaluation of the likelihood of a regional mode oscillation to develop under non-isolation ATWS conditions. It is acceptable to evaluate the regional and core wide mode decay ratios for these conditions for an equilibrium ATRIUM-10 Unit 2 core using STAIF to respond to this request for additional information (RAI). Based on the available analyses, determine if such an oscillation at BFN would result in a significant increase in the fuel damage relative to the results in NEDO-32047-A.</p> <p>The analyses in NEDO-32047-A were performed for General Electric (GE) fuel. The analyses are generally applicable for pre-EPU core designs since hydraulic stability of the fuel products has improved or at least remained the same. Provide a comparison of the channel stability characteristics of ATRIUM-10 to GE 8x8 fuel. If ATRIUM-10 is less stable than GE 8x8 fuel, consider any impact on the projected consequences of a non-isolation ATWS instability event.</p>
SRXB-118	<p>In the supplemental response to RAI SRXB-88, TVA provided the results of sensitivity analyses to evaluate the impact of void fraction uncertainty on the calculated delta-critical power ratio (DCPR) and the safety limit minimum critical power (SLMCPR). In the void fraction reduction case, the DCPR is apparently unaffected and is accompanied by an increase in SLMCPR.</p> <p>If the void fraction were reduced throughout the core by a fixed bias, the result would be to redistribute the reactor power according to the change in reactivity associated with the</p>

Table 2
Previous NRC Requests for Additional Information (RAIs) Text

RAI Number	Text
	<p>void perturbation. Since those bundles with the higher bundle average void fractions will have a greater reactivity response, a reduction in the void fraction will tend to increase, slightly, the power in those bundles with a higher bundle average void fraction relative to the bundles that had a lower void content prior to the perturbation. The bundles with a higher bundle average void fraction are the high powered bundles. Therefore, a fixed reduction in void fraction will increase the radial power peaking factor. The increased radial power peaking factor for a given steady state power level would result in fewer rods entering boiling transition as a result of a transient initiated from this state.</p> <p>When this effect is considered, it is the equivalent of increasing the radial power peaking and reducing the SLMCPR since fewer rods are at the limiting end of the pin power statistical distribution. In effect, the span of pin powers to account for the 0.1 percent of highest powered pins increases. Results of the TVA sensitivity analysis demonstrate the opposite trend. It is expected that the imposition of a fixed void fraction reduction would result in a lower SLMCPR. Explain this discrepancy.</p>
SRXB-119	<p>Continuing with the void fraction reduction case, the decrease in void fraction would simultaneously result in a redistribution of the axial power. Since those higher void nodes would have a greater reactivity response than low void nodes, the axial power distribution would shift upwards in the core. The upward shift in the axial power distribution has the effect of increasing the reactor adjoint in the upper portions of the core. As pressurization transients are typically limiting, the impact of an upward shift in axial power on the transient power prediction should be considered. The upward shift in reactor adjoint directly affects the core void reactivity coefficient and tends to increase the sensitivity of the core reactivity to a pressure wave, since the back pressure wave is dissipated by void collapse in the upper parts of the core. Therefore, the core wide transient power would be increased relative to the base case, which appears to result in an increase in the DCPR.</p> <p>The results of the TVA sensitivity analysis do not demonstrate this trend. Address why imposing a fixed void fraction reduction does not result in a higher DCPR.</p>
SRXB-120	<p>The void increase cases exhibited opposite trends relative to the void reduction cases. The staff found that the void reduction cases were not consistent with the staffs expectations. Provide information similar to the information requested in SRXB-1 18 and 119 for the fixed increase in void fraction sensitivity analyses.</p> <p>For each case in Study 1 provide:</p> <ul style="list-style-type: none"> • The limiting bundle: core location, initial radial peaking factor and axial power shape • Plots of the perturbed axial and radial core power shape • Plots of transient limiting bundle peak rod heat flux and mass flow rate • Plots of transient critical CPR • A comparison of the predicted power pulse heights and widths
SRXB-121	<p>It should be noted that the increase in the operating limit CPR (OLMCPR) for the increased void fraction cases is substantial relative to the base case. The Study 1 increase in OLMCPR is 0.014 and the Study 2 increase in OLMCPR is 0.027.</p> <p>In response to RAI SRXB-88, TVA stated that COTRANSA2 includes a 110 percent multiplier on integral thermal power as a conservative assumption. However, XN-NF-80-19(P)(A) Exxon Nuclear Methodology for Boiling Water Reactors, THERMEX: Thermal Limits Methodology Summary Description Section 4.4 states: "In developing the</p>

**Table 2
Previous NRC Requests for Additional Information (RAIs) Text**

RAI Number	Text
	<p>methodology for the COTRANSA code Exxon Nuclear addressed uncertainties in the code through the integral power variable. The revised methodology uses a more conservative deterministic bounding value (+10 percent) for the integral power uncertainty." TVA's evaluation of the 110 percent conservatism found that the OLMCPR margin afforded by the conservatism is [].</p> <p>While analysis of pre-EPU reactor conditions, such as the Peach Bottom turbine trip tests, indicate that the 110 percent multiplier is adequate. The response to RAI SRXB-88 appears to indicate that at EPU conditions, that the integral thermal power response to a 5 percent uncertainty in void fraction may not be bounded by the conservatism afforded by the 110 percent multiplier. This is evidenced by an increase in the OLMCPR in Study 2 that exceeds the conservatism afforded by the total 110 percent multiplier.</p> <p>It should be noted that the intent of the 110 percent multiplier is to conservatively bound all uncertainties, including uncertainties in other important variables such as flow and friction factors.</p> <p>Given that the OLMCPR increase exceeds the 110 percent multiplier margin, provide a demonstration that the integrated effect of all conservatisms in COTRANSA2 for Unit 2 at EPU conditions is adequate. This demonstration may be provided by qualification against relevant operating plant transient data to ensure conservatism of the methodology for EPU or near-EPU conditions or by comparison against a rigorous statistical treatment of all uncertainties or by some alternative quantitative and applicable means.</p>
SRXB-122	The modified correlations are based on constant slip models. Provide a discussion regarding the treatment of subcooled boiling. This discussion should address void fraction continuity at the boiling boundary. Describe any impact on the transient analyses arising from SCRAM reactivity worth if significant differences are expected based on treatment of subcooled boiling.
SRXB-123	Discuss what allows the code to continue its evaluation of the ATWS transient without terminating.
SRXB-124	Discuss how the core coolability under 10 CFR 50.46 is evaluated for this event.
SRXB-125	Assuming that the pressure is out of bounds, address how does the code conservatively predicts the fuel temperature.
SRXB-126	If a fuel rod is predicted in dryout, address how the heat transfer is modeled.
SRXB-128	<p>Provide a discussion of the impact of channel bow on the critical power performance for Units 2 and 3 at EPU conditions. This discussion should include the following:</p> <p><u>SRXB-128.a</u> The effect of the EPU neutron spectrum on channel -bow mechanisms,</p> <p><u>SRXB-128.b</u> The appropriateness of the channel bow statistics,</p> <p><u>SRXB-128.c</u> Characterization of the susceptibility of Units 2 and 3 to abnormal channel bow,</p> <p><u>SRXB-128.d</u> Any channel bow monitoring methods, address inward and outward bow,</p> <p><u>SRXB-128.e</u> Any conservatism in the treatment of channel bow in the safety analysis in regard to</p>

Table 2
Previous NRC Requests for Additional Information (RAIs) Text

RAI Number	Text
	thermal margin. <u>SRXB-128.f</u> The measures taken in regard to Service Information Letter 320, and <u>SRXB-128.g</u> Any future plans to manage greater than expected bow based on the monitoring.

ATTACHMENT 27

PART 2

ANP-2860NP

**Browns Ferry Unit 1 – Summary of Response to Requests for Additional
Information**

(Non-proprietary Version)

An AREVA and Siemens company

ANP-2860NP
Revision 2

Browns Ferry Unit 1 – Summary of
Responses to Request for
Additional Information

October 2009



AREVA NP Inc.

ANP-2860NP
Revision 2

**Browns Ferry Unit 1 - Summary of
Responses to Request for
Additional Information**

skm

AREVA NP Inc.

ANP-2860NP
Revision 2

Copyright © 2009

AREVA NP Inc.
All Rights Reserved

Nature of Changes

Item	Page	Description and Justification
1.	9-1	Updated reference 3.

Contents

	Page
1.0 Introduction	1-1
2.0 Stability.....	2-1
2.1 OPRM.....	2-1
2.2 ATWS	2-10
2.2.1 Analytical Considerations	2-11
2.2.2 Description of the Reduced Order Model	2-13
2.2.3 Results	2-14
2.2.4 Conclusions.....	2-15
3.0 COTRANSA2	3-1
3.1 Conservatism	3-1
3.2 Thermal-Mechanical Model	3-2
3.3 Pump Model	3-3
3.4 SRV Model	3-3
3.5 Cross Sections	3-4
4.0 XCOBRA-T.....	4-1
4.1 Axial Geometry Changes	4-1
4.2 Power	4-3
4.3 Radial Pin Power Shape	4-4
4.4 Default Models	4-5
4.5 Bounds Checking	4-6
4.6 Heat Transfer Correlations	4-7
4.7 Axial Power Shape	4-7
4.8 Thermal Mechanical Performance.....	4-8
4.8.1 Thermal Mechanical Performance for GE14 Fuel.....	4-9
5.0 Thermal Hydraulic.....	5-1
5.1 Void Quality Applicability	5-1
5.2 ATRIUM-10 Void Fraction Measurement	5-1
5.2.1 Facility Description	5-2
5.2.2 Data Collection	5-2
5.2.3 Facility Calibration	5-3
5.2.4 Measurement Technique.....	5-3
5.2.5 Conclusion.....	5-3
5.3 SLMCPR Calculation Process.....	5-4
5.4 Safety Limit and Radial Peaking Factor Uncertainty	5-5
5.5 SPCB.....	5-6
5.6 Loss Coefficients	5-7
5.6.1 Spacer Pressure Drop Testing	5-7
5.6.2 Preliminary ATRIUM-10 Spacer Loss Coefficients.....	5-8
5.6.3 PHTF ATRIUM-10 Based Spacer Loss Coefficients.....	5-9

5.6.4	Loss Coefficients for GE14 Fuel.....	5-10
6.0	Transients and Accidents.....	6-1
6.1	Initial Core Power.....	6-1
6.2	LHGR Limit.....	6-1
6.3	Channel Bow Impact on Thermal-Mechanical Limits.....	6-2
6.4	Axial Power Shapes.....	6-3
6.5	Fuel Rod Parameters.....	6-3
6.6	Transient Hot Channel Analyses.....	6-4
6.7	Void Quality Correlation Uncertainties.....	6-5
6.7.1	Assessment of the Void-Quality Correlation.....	6-7
6.7.2	Biasing of the Void-Quality Correlation.....	6-8
6.7.3	Additional Sensitivity Analysis for SLMCPR.....	6-11
6.7.4	Impact on MICROBURN-B2 Accuracy.....	6-12
6.7.5	Void-Quality Correlation Uncertainty Summary.....	6-14
6.8	Doppler Effect on Cross Sections.....	6-16
6.9	Fuel Rod Model Changes.....	6-20
6.9.1	Comparison of RODEX2 to RODEX4.....	6-21
6.10	Nodalization.....	6-21
7.0	Neutronics.....	7-1
7.1	Shutdown Margin.....	7-1
7.2	Monitoring.....	7-3
7.3	Power Distribution Uncertainty.....	7-3
7.3.1	Radial Bundle Power Uncertainty.....	7-3
7.3.2	Local Power Uncertainty.....	7-9
7.4	Gamma Scans.....	7-9
7.5	Bypass Modeling.....	7-11
8.0	ATWS.....	8-1
8.1	ATWS General.....	8-1
8.2	Void Quality Correlation Bias.....	8-1
8.3	ATWS Containment Heatup.....	8-3
8.4	Bypass Flow.....	8-5
8.5	Safety Relief Value Flow.....	8-5
8.6	Time Steps.....	8-5
9.0	References.....	9-1
Appendix A	Channel Bow.....	A-1

Tables

	Page
Table 2-1 Bypass Voiding.....	2-17
Table 2-2 Detector Sensitivities.....	2-17
Table 2-3 LPRM Reading.....	2-18
Table 2-4 LPRM Detector to OPRM Cell Assignments for Channel 1.....	2-19
Table 2-5 LPRM Detector to OPRM Cell Assignments for Channel 2.....	2-20
Table 2-6 LPRM Detector to OPRM Cell Assignments for Channel 3.....	2-21
Table 2-7 PRM Detector to OPRM Cell Assignments for Channel 4.....	2-22
Table 2-8 Percent Change in OPRM Sensitivities.....	2-23
Table 2-9 Percent Change in OPRM Sensitivities.....	2-24
Table 3-1 Gap Conductance Study.....	3-13
Table 4-1 Deposited Heat Study.....	4-10
Table 4-2 Bounds Checking.....	4-10
Table 5-1 Hydraulic Characteristics of ATRIUM-10 Fuel Assemblies.....	5-11
Table 6-1 Gap Conductance Study.....	6-23
Table 6-2 Void Sensitivity Results.....	6-23
Table 6-3 Power Pulse.....	6-24
Table 6-4 Limiting Bundle Data.....	6-25
Table 6-5 Radial Bundle Power Distribution As Predicted by MICROBURN-B2 for the Limiting Transient Analysis.....	6-26
Table 6-6 Limiting Assemblies Analyzed in the Unit 3 Cycle 14 Limiting Transient Analysis.....	6-27
Table 8-1 Energy Release to Suppression Pool.....	8-6
Table 8-2 ATWS Time Step Study.....	8-6

Figures

	<u>Page</u>
Figure 2-1	Histogram of the Relative Change in the OPRM signals for 10% D level and 5% C level LPRM Signal Reduction.....2-25
Figure 2-2	Histogram of the Relative Change in the OPRM signals for 20% D level and 10% C level LPRM Signal Reduction.....2-26
Figure 2-3	Relative Change in the OPRM signals Versus Absolute Oscillation Magnitude for 10% D level and 5% C level LPRM Signal Reduction2-27
Figure 2-4	Relative Change in the OPRM signals Versus Absolute Oscillation Magnitude for 20% D level and 10% C level LPRM Signal Reduction2-28
Figure 2-5	Bypass Power Source Function Representing a Growing Oscillation.....2-29
Figure 2-6	Bypass Void Fraction at Detector Levels C and D2-30
Figure 2-7	[] With and Without the Effect of Bypass Voiding2-31
Figure 2-8	[] With and Without the Effect of Bypass Voiding.....2-32
Figure 2-9	[].....2-33
Figure 2-10	Relative Power for Case 1 Base Global Oscillation.....2-34
Figure 2-11	Relative Power for Case 2 Base Regional Oscillation.....2-35
Figure 2-12	Relative Power for Case 3 Global Oscillation.....2-35
Figure 2-13	Relative Power for Case 4 Regional Oscillation.....2-36
Figure 2-14	Relative Power for Case 5 Regional Oscillation With Decreased Subcriticality2-36
Figure 2-15	Relative Power for Case 6 Mitigated Global Oscillation2-37
Figure 2-16	Relative Power for Case 7 Mitigated Regional Oscillation2-37
Figure 2-17	Relative Power for Case 8 Late-Mitigated Global Oscillation2-38
Figure 2-18	Relative Power for Case 9 Late-Mitigated Regional Oscillation2-38
Figure 2-19	Inlet Mass Flow Rate for Case 1 Base Global Oscillation2-39
Figure 2-20	Inlet Mass Flow Rate for Case 2 Base Regional Oscillation2-39
Figure 2-21	Inlet Mass Flow Rate for Case 3 Global Oscillation2-40
Figure 2-22	Inlet Mass Flow Rate for Case 4 Regional Oscillation.....2-40

Figures

	<u>Page</u>
Figure 2-23 Inlet Mass Flow Rate for Case 5 Regional Oscillation With Decreased Subcriticality	2-41
Figure 2-24 Inlet Mass Flow Rate for Case 6 Mitigated Global Oscillation.....	2-41
Figure 2-25 Inlet Mass Flow Rate for Case 7 Mitigated Regional Oscillation	2-42
Figure 2-26 Inlet Mass Flow Rate for Case 8 Late-Mitigated Global Oscillation.....	2-42
Figure 2-27 Inlet Mass Flow Rate for Case 9 Late-Mitigated Regional Oscillation.....	2-43
Figure 2-28 Exit Void Fraction for Case 1 Base Global Oscillation.....	2-43
Figure 2-29 Exit Void Fraction for Case 2 Base Regional Oscillation.....	2-44
Figure 2-30 Exit Void Fraction for Case 3 Global Oscillation.....	2-44
Figure 2-31 Exit Void Fraction for Case 4 Regional Oscillation	2-45
Figure 2-32 Exit Void Fraction for Case 5 Regional Oscillation With Decreased Subcriticality	2-45
Figure 2-33 Exit Void Fraction for Case 6 Mitigated Global Oscillation	2-46
Figure 2-34 Exit Void Fraction for Case 7 Mitigated Regional Oscillation	2-46
Figure 2-35 Exit Void Fraction for Case 8 Late-Mitigated Regional Oscillation	2-47
Figure 2-36 Exit Void Fraction for Case 9 Late-Mitigated Regional Oscillation	2-47
Figure 2-37 Void Fraction in Selected Nodes for Case 1 Base Global Oscillation.....	2-48
Figure 2-38 Void Fraction in Selected Nodes for Case 2 Base Regional Oscillation.....	2-48
Figure 2-39 Void Fraction in Selected Nodes for Case 3 Global Oscillation.....	2-49
Figure 2-40 Void Fraction in Selected Nodes for Case 4 Regional Oscillation.....	2-49
Figure 2-41 Void Fraction in Selected Nodes for Case 5 Regional Oscillation With Decreased Subcriticality.....	2-50
Figure 3-1 Comparison of Scram Bank Worth for []	3-14
Figure 5-1 Geometry.....	5-12
Figure 5-2 Void Fraction Correlation Comparison to FRIGG and ATRIUM-10 Test Data.....	5-13
Figure 5-3 General Void Quality Correlation Behavior.....	5-14
Figure 5-4 Test Facility	5-15

Figures

		<u>Page</u>
Figure 5-5	Count Rate Plots	5-16
Figure 5-6	ATRIUM-10 Bundle Pressure Drop [].....	5-17
Figure 5-7	ATRIUM-10 Bundle Pressure Drop [].....	5-18
Figure 5-8	ATRIUM-10 Lower Region Spacer Pressure Drop Using PHTF Loss Coefficients []	5-19
Figure 5-9	ATRIUM-10 Transition Region Spacer Pressure Drop Using PHTF Loss Coefficients []	5-20
Figure 5-10	ATRIUM-10 Upper Region Spacer Pressure Drop Using PHTF Loss Coefficient []	5-21
Figure 5-11	Viewgraph From May 4, 1995 Presentation to NRC Regarding ATRIUM-10 Fuel	5-22
Figure 5-12	Viewgraph From May 4, 1995 Presentation to NRC Regarding ATRIUM-10 Fuel	5-22
Figure 6-1	SLMCPR Radial Power Distribution High-Powered Assemblies Depleted Voids	6-28
Figure 6-2	SLMCPR Radial Power Distribution High-Powered Assemblies Instantaneous Voids	6-28
Figure 6-3	SLMCPR Radial Power Distribution Low-Powered Assemblies Instantaneous Voids	6-29
Figure 6-4	Void Fraction Correlation Comparison to FRIGG and ATRIUM-10 Test Data	6-30
Figure 6-5	Modified Void Fraction Correlation Comparison to ATRIUM-10 Test Data	6-31
Figure 6-6	[] Void Fraction Results Comparison to ATRIUM-10 Test Data	6-32
Figure 6-7	Initial Axial Power Shape - Depleted Voids	6-33
Figure 6-8	Initial Radial Power Distribution From Transient Analyses - Depleted Voids	6-33
Figure 6-9	Heat Flux Vs. Time 25% x/L - Depleted Voids	6-34
Figure 6-10	Heat Flux Vs. Time 50% x/L - Depleted Voids	6-34
Figure 6-11	Heat Flux Vs. Time 75% x/L - Depleted Voids	6-35
Figure 6-12	Mass Flow Vs. Time 0% x/L - Depleted Voids	6-35
Figure 6-13	Mass Flow Vs. Time 25% x/L - Depleted Voids	6-36

Figures

	<u>Page</u>
Figure 6-14 Mass Flow Vs. Time 50% x/L - Depleted Voids.....	6-36
Figure 6-15 Mass Flow Vs. Time 75% x/L - Depleted Voids.....	6-37
Figure 6-16 Mass Flow Vs. Time 100% x/L - Depleted Voids.....	6-37
Figure 6-17 CPR Vs. Time Depleted Voids	6-38
Figure 6-18 RODEX Evolution of the Doppler Effective Fuel Temperature for SPC Fuel at Constant Power.....	6-39
Figure 6-19 RODEX Evolution of the Doppler Effective Fuel Temperature for SPC Fuel Vs. LHGR and Burnup	6-40
Figure 6-20 MICROBURN-B2 Correlation Evolution of the Doppler Effective Fuel Temperature for SPC Fuel Vs. LHGR and Burnup.....	6-41
Figure 6-21 BFN 2D TIP Statistic Comparison for Variations of the Void Quality Correlation.....	6-42
Figure 6-22 BFN 3D TIP Statistic Comparison for Variations of the Void Quality Correlation.....	6-42
Figure 6-23 BFN Core Average Axial TIP Comparison at 9026 MWd/MTU for Variations of the Void Quality Correlation.....	6-43
Figure 6-24 BFN Core Average Axial TIP Comparison at 1755 MWd/MTU for Variations of the Void Quality Correlation.....	6-43
Figure 6-25 BFN Core Average Axial TIP Comparison at 9197 MWd/MTU for Variations of the Void Quality Correlation.....	6-44
Figure 6-26 BFN Core Average Axial TIP Comparison at 1340 MWd/MTU for Variations of the Void Quality Correlation.....	6-44
Figure 6-27 A BWR/4 at EPU 2D TIP Statistic Comparison for Variations of the Void Quality Correlation	6-45
Figure 6-28 A BWR/4 at EPU 3D TIP Statistic Comparison for Variations of the Void Quality Correlation	6-45
Figure 6-29 A BWR/4 at EPU Core Average Axial TIP Comparison at 2127 MWd/MTU for Variations of the Void Quality	6-46
Figure 6-30 A BWR/4 at EPU Core Average Axial TIP Comparison at 10621 MWd/MTU for Variations of the Void Quality	6-46
Figure 6-31 A BWR/4 at EPU Core Average Axial TIP Comparison at 18459 MWd/MTU for Variations of the Void Quality	6-47
Figure 6-32 A BWR/4 at EPU Core Average Axial TIP Comparison at 2054 MWd/MTU for Variations of the Void Quality	6-47

Figures

	<u>Page</u>
Figure 6-33 Pump Speed.....	6-48
Figure 6-34 Core Power	6-48
Figure 6-35 Reactor Pressure	6-49
Figure 6-36 ATRIUM-10 LHGR Limit.....	6-50
Figure 6-37 ATRIUM-10 Void Data.....	6-51
Figure 7-1 Browns Ferry Cold Criticals.....	7-14
Figure 7-2 BFN $\delta T'_{ij}$ Gamma TIP Response vs. Cycle Number	7-15
Figure 7-3 FN $\delta T'_{ij}$ Gamma TIP Response vs. Power/Flow Ratio	7-15
Figure 7-4 BFN $\delta T'_{ij}$ Gamma TIP Response vs. Core Average Void Fraction.....	7-16
Figure 7-5 BFN $\delta T'_{ij}$ Gamma TIP Response vs. Core Power	7-16
Figure 7-6 Hypothetical MICROBURN-B2 Multi-Channel Average Bypass Void Distribution	7-17
Figure 8-1 SRV Flow During ATWS Overpressurization	8-7

1.0 Introduction

The purpose of this report is to respond to a request contained in the NRC meeting minutes "Summary of March 16, 2009, Meeting with the Tennessee Valley Authority Regarding Proposed Fuel Transition Amendment (TAC No. ME0438), dated June 3, 2009. The request was to provide information to support a Browns Ferry Unit 1 future license amendment request similar to the information provided in response to previous requests for additional information for reactors other than Browns Ferry Unit 1. The information requested in the meeting minutes is provided in either this document, ANP-2638 Revision 2, ANP-2637 Revision 2, or in a reload report. A primary topic of the previous NRC meetings was how AREVA NP handles the co-resident GE14 fuel in a mixed core. Additional information on AREVA NP methodology for mixed cores is provided in Appendix A of ANP-2638 Revision 2.

Except for core loading, all three Browns Ferry Units (1, 2 and 3) are essentially the same since the core operational conditions, modeled geometry, safety system performance and ECCS parameters are identical. A review of geometry between Units 1, 2 and 3 determined the only significant difference was the recirculation piping for Unit 3 (Unit 3 has undergone a recirculation header and riser replacement). The differences in recirculation piping for Unit 3 does not result in any modifications to recirculation piping model used in the analyses (the simplifications of the recirculation piping model does not distinguish the differences). The significant difference between the units is the core loading and corresponding core design. The impact of the differences in core design between units and cycles is addressed in the cycle specific reload report for each unit.

Browns Ferry Units 2 and 3 have already transitioned from GE14 fuel to ATRIUM-10 fuel. The methodology used to assess previous Unit 2 and Unit 3 cycles with or without EPU is the same for Unit 1. Many of the previous requests for additional information on AREVA NP methodology were for Browns Ferry Units 2 and 3; since the methodology has not changed, those previous responses remain applicable for Unit 1.

2.0 Stability

2.1 OPRM

Bypass voiding is not considered in OPRM setpoint analyses. Consideration of bypass voiding is not necessary due to the expected impact discussed below, as well as the overall conservatism of the approved Reference 39 methodology. Examples of conservatism in the Reference 39 methodology approved for application include:

- The reactor is assumed to be operating at the OLMCPR prior to the stability event
- A conservative Δ CPR response (limiting time in cycle) is assumed following a pump trip
- Equilibrium feedwater temperature for off-rated conditions is assumed to be instantaneously achieved following a pump trip
- The statistical analysis selects the hot channel oscillation magnitude value at the 95% probability, 95% confidence level

In addition the SLMCPR protected by the OPRM setpoints also reflects a conservative bundle power uncertainty due to the use of gamma TIPs.

AREVA NP has performed an assessment of the potential impact of bypass boiling on the effectiveness of the Option III Long Term Stability solution to provide reactor protection under oscillatory conditions. This assessment included evaluations of both the steady-state and transient bypass void fractions expected for operation at the intersection of the maximum extended load line limit analysis (MELLLA) rod line and natural recirculation flow.

The assessment of bypass boiling phenomena on the OPRM system is insensitive to the actual core design and therefore applies to the Browns Ferry Unit 1 transitions cycles.

Steady-State Evaluation

BWR core operation at high power and natural circulation may not result in sufficient core pressure drop to support upward bypass flow against the weight of a column of liquid water of the active core height. Boiling in the bypass is thus expected to balance the pressure drop, where direct bypass flow heating is provided by gamma radiation and neutron slowing down. Significant voiding in the bypass flow may occur at the upper elevation of the bypass channel

where the level D detectors are located, and to a lesser extent at level C detectors. The LPRM detector signals are proportional to the thermal neutron flux, and thus the bypass voiding around a detector causes a local decrease in the thermal neutron flux and will result in a reduction of the signal-to-power ratio, i.e. the sensitivity of the detector is reduced resulting in a calibration error. The methodology to account for this calibration error is based on the following calculations:

- a. Bypass flow and void fraction distribution under natural circulation conditions are determined using the core simulator MICROBURN-B2. A [

]

- b. The detector calibration error is determined as function of the bypass void fraction by performing calculations at several exposure points using the lattice code CASMO4.

Using the steps (a) and (b) above, the calibration error is determined at levels C and D detectors given the calculated bypass void distribution.

Expected Bypass Void Fractions and LPRM Calibration Errors

The expected void fraction in the bypass for MELLLA operation at both the original licensed thermal power (OLTP) and EPU is the same since the corresponding core power of the MELLLA operating line at natural circulation is unchanged. No voiding was calculated at levels A and B. The maximum and average bypass void fraction at levels C and D are given in Table 2-1 for different exposure points for the run back to natural circulation flow along the MELLLA line.

The calibration error relative to the signal is proportional to the void fraction in the bypass channel at the elevation where the detector is located. Other effects such as exposure of the bundles surrounding the detector were found to be small. The corresponding detector sensitivities to the bypass voiding in Table 2-1 are given in Table 2-2.

Assessment of Impact of Steady-State Bypass Boiling on OPRM Signals

Oscillatory LPRM signals are constructed for each detector using

$$LPRM(t) = LPRM(0) \cdot \zeta_i \cdot (1 + 0.1 \sin(2\pi \cdot f \cdot t - \theta_i))$$

Where:

$LPRM(t)$ Time dependent LPRM signal

$LPRM(0)$ Initial value of the LPRM signal

ζ_i LPRM sensitivity factor due to bypass boiling corresponding to the detector level

θ_i LPRM axial phase shift relative to level A. This will be set to 20 degrees for the B level, 40 degrees for the C level, and 60 degrees for the D level LPRMs.

f Oscillation frequency, set equal to 0.5 Hz

In this calculation example, the LPRM readings prior to oscillation inception assuming no change in their sensitivity due to bypass boiling are given in Table 2-3.

Representative LPRM assignments for the four OPRM trip channels are given in Table 2-4 through Table 2-7.

The generated OPRM signals with and without the effect of bypass boiling are calculated and compared for two sets of detector sensitivity reductions. In the first set, the levels C and D detector sensitivities are reduced to 95% and 90% respectively, which bounds the case specific examples determined above. In the second set, the levels C and D detector sensitivities are reduced to 90% and 80%, respectively. The second set is provided to demonstrate the extreme insensitivity of the bypass boiling on the OPRM relative signals.

The percentage change in OPRM sensitivities for the first set (C level sensitivity = 95%, D level sensitivity = 90%) is given in Table 2-8.

The percentage change in OPRM sensitivities for the second set (C level sensitivity = 90%, D level sensitivity = 80%) is given in Table 2-9 for the same OPRM configuration.

The corresponding statistics for the change in sensitivity is shown graphically in Figure 2-1 and Figure 2-2 for the first and second set, respectively. It is clear that there is a trend to [] not [] sensitivity of most OPRM signals due to the improved signal coherence when the contribution of the upper level LPRM detectors with [] . The few OPRMs where the sensitivity is slightly [] .

The OPRM detector sensitivities as function of the absolute oscillation magnitude are displayed in Figure 2-3 and Figure 2-4 for the two calculation sets respectively. These figures show that there is a majority of OPRMs with large absolute signal value (lower noise-to-signal ratio) where the sensitivity is either [] by the bypass voiding. Thus, it is concluded that the OPRM relative signal for the purpose of comparison with the amplitude setpoint [] possibility of some detectors being out-of-service.

First Principle Interpretation of the Results

The effect of bypass boiling on the relative OPRM signal for which numerical results are presented above can be interpreted analytically. []

]

[

1

[

]

Transient evaluation

The dynamic effect of bypass voiding is addressed in two ways. The first is a qualitative discussion from first principles and the second is through a simulation of a realistic bypass channel subjected to oscillating power input under conditions representing natural circulation.

First Principles Discussion:

[

] would lead to a net signal damping requiring assessment of a compensating penalty, a calculation example is presented next.

Numerical Example of Bypass Voiding with Oscillating Power

The calculation of a bypass voiding oscillation was performed by integrating a system of differential equations representing two-phase flow mass, momentum, and energy balance formulated similar to RAMONA5-FA. While the balance differential equations are identical to RAMONA5-FA, the boundary conditions and closing relations are simplified to suit the bypass calculation. These differences are:

[

] A bottom-peaked axial power shape typical of BWR operation at natural circulation is specified where a fraction of the energy generation in the fuel assembly is deposited directly in the bypass flow.

The power is specified as a source function driving the bypass channel thermal-hydraulics. The power source in the presented example, as shown in Figure 2-5, is specified as initially constant at [

]

The selected power and flow conditions result in calculated steady-state void fraction at the elevation of the level D detector of [] and [] at the C level detectors. This is slightly higher than expected values under typical natural circulation conditions at the MELLLA

boundary. Detailed MICROBURN-B2 studies, using a [] have shown that the maximum local bypass void fraction at the D level detectors is approximately [] and approximately [] at the C level detectors at the MELLA boundary at natural circulation. The power and flow conditions used in this case were chosen to provide a conservative representation of the void profile that would exist at natural circulation.

As shown in Figure 2-6, the level C and level D void fractions start to oscillate when the power source starts to oscillate and the magnitude of the void oscillations []

]

An example OPRM signal is composed of four LPRM detectors at levels A, B, C, and D. Assuming no bypass boiling effect on the calculated signal, an OPRM time trace is obtained. The effect of the bypass voiding on the reduction of the LPRM detector response is conservatively taken as []

[]. The effect of bypass boiling at levels C and D on the contribution of the corresponding detectors is used to construct a second OPRM signal, which is shown in Figure 2-7 to be lower than the first signal constructed without accounting for the bypass boiling. []

The absolute OPRM signals, with and without the bypass boiling effect, []

]

[

]

It is concluded that the steady state and dynamic effects of bypass boiling on lowering the sensitivity of individual LPRM detectors cause [

] OPRM signals used for comparison with the OPRM amplitude setpoint.

2.2 ATWS

The pre-EPU stability analysis for Browns Ferry indicates that the global mode is dominant over the regional (out-of-phase) mode where relatively large subcritical reactivity values are calculated with STAIF. For EPU cores with flatter radial power distributions, the calculated subcritical reactivity values are noticeably lower in comparison. The resulting regional decay ratios calculated for the EPU core are larger than the corresponding global mode decay ratio in a minority of cases, which warrants the examination of the effect of regional mode oscillations dominating postulated ATWS instability events.

The task of evaluating the impact of large regional versus global mode oscillations is first addressed below from an analytical point of view and calculations are presented using a reduced order model. The calculations will also address the effects of the parameters of interest, namely the subcritical reactivity due to core radial power flattening for EPU, increase in void-reactivity coefficient due to increasing the fresh fuel batch size, and fuel geometry effects (part-length rods and reduced pin conduction time constant for an ATRIUM-10 compared with an 8x8 fuel bundle). These effects will be demonstrated to result in equivalent consequences of a postulated ATWS event relative to the results in NEDO-32047-A (Reference 38).

Furthermore, the mitigation of the ATWS instability by reducing the core inlet subcooling, as a consequence of water level reduction by operator action (Reference 36), will be demonstrated to be as effective in suppressing regional mode oscillations as for global mode oscillations.

2.2.1 Analytical Considerations

Unstable global mode oscillations grow exponentially at a fixed rate (decay ratio) from a small perturbation. As the oscillation magnitude increases, nonlinear effects become important. The average power level drifts to higher values as a consequence of the nonlinearity of the neutron kinetics, which results in a negative reactivity feedback due to the increase of void fraction. The negative reactivity superimposed on the oscillating reactivity results in damping the neutron kinetics (References 18, 34, and 35). [

[

]

The regional mode oscillations are well understood in the linear limit where the power oscillation is attributed to the excitation of the first azimuthal harmonic mode of the neutron flux.

Compared with the fundamental flux mode excitation associated with the global oscillation, the subcritical reactivity of the first azimuthal eigenfunction contributes a damping effect on the neutron kinetics feedback. The hydraulic response is less damped compared to the global mode case due to bypassing the damping effects of the recirculation loop. The regional mode oscillations may become the preferred oscillation mode for large-orificed cores (hydraulic destabilization) and for small radial buckling (large core diameter and radial power distribution that is relatively flat or ring-of-fire with relatively low power in the center).

[

1

[

]

2.2.2 Description of the Reduced Order Model

The phenomenological description of large power oscillations in the global and regional modes is supported by the results of a reduced order model, which is used here to simulate large global and regional mode oscillations. [

]

[

]

[

]

The reduced order model allows fast and robust simulation of both the global and regional modes and helps to resolve issues that were not apparent at the time NEDO-32047-A (Reference 38) was issued. Most importantly, it helps to explore and provide insight into the differences between the global and regional mode oscillations and their common ultimate limiting mechanism.

2.2.3 Results

The results of several cases performed with the reduced order model are presented. All of these calculations represent unstable oscillations growing to large magnitudes with parameter variations to address the issues of global versus regional and the effect of EPU core loading with fuel design differing from the fuel type used in NEDO-32047-A (Reference 38). These cases are:

[

]

[

]

2.2.4 Conclusions

- Large regional mode oscillations have [] effects compared with global mode.
- ATRIUM-10 bundle design differences from an older 8x8 []
- EPU effects (lower subcritical reactivity and higher void reactivity coefficient) []

- [

]

Table 2-1 Bypass Voiding



Table 2-2 Detector Sensitivities



Table 2-3 LPRM Reading

LPRM	Level A	Level B	Level C	Level D
16-57	26.37	28.32	29.09	24.65
24-57	64.03	53.17	44.13	32.08
32-57	69.89	57.57	47.34	34.32
40-57	42.74	40.17	38.17	30.47
08-49	37.78	39.3	36.5	27.99
16-49	96.5	77.71	65.45	42.14
24-49	76.16	62.74	56.2	48.9
32-49	61.47	53.95	50.54	49.23
40-49	92	72.65	64.02	45.11
48-49	87.81	70.76	56.86	35.73
08-41	97.29	74.41	62.82	39.62
16-41	79.99	67	59.89	41.65
24-41	83.05	67.81	60.35	46.85
32-41	97.05	75.28	64.6	50.11
40-41	73.31	62.6	55.99	41.35
48-41	94.03	74.3	66.86	44.63
56-41	45.32	41.9	40.38	30.93
08-33	100.35	77.89	68.99	44.41
16-33	92.09	75.62	68.3	48.75
24-33	84.96	70.98	57.77	41.37
32-33	74.29	66.16	54.13	38.86
40-33	96.89	77.54	65.5	46.61
48-33	84.13	70.12	67.35	47.76
56-33	75.56	60.62	52.02	34.95
08-25	97.51	73.85	64.73	41.92
16-25	80.06	66.78	59.86	41.82
24-25	102.72	80.13	65.75	47.55
32-25	99.58	78.48	65.45	48.01
40-25	71.67	62.57	54.33	40.17
48-25	94.74	74.89	68.87	46.72
56-25	69.53	56.18	48.15	32.89
08-17	78.68	64.51	54.83	36.41
16-17	91.52	74.9	66.8	45.41
24-17	75.77	62.92	56.31	51.1
23-17	71.94	61.07	54.63	52.01
40-17	91.4	72.36	65.36	48.06
48-17	97.39	77.76	66.32	42.03
56-17	26.78	29.05	30.16	24.94
16-09	77.8	63.62	53.44	36.28
24-09	89.89	68.81	58.4	41.34
32-09	93.78	70.8	60.1	43.51
40-09	93.19	71.79	59.09	39.26
48-09	37.2	38.68	35.97	27.95

Table 2-4 LPRM Detector to OPRM Cell Assignments for Channel 1

Cell ID#	LPRM #1	LPRM #2	LPRM #3	LPRM #4
1	16-57B	24-57C	24-49C	16-49B
2	24-57C	32-57D	32-49D	24-49C
3	32-57D	40-57A	40-49A	32-49D
4	08-49A	16-49B	16-41D	08-41C
5	16-49B	24-49C	24-41A	16-41D
6	24-49C	32-49D	32-41B	24-41A
7	32-49D	40-49A	40-41C	32-41B
8	40-49A	48-49B	48-41D	40-41C
9	08-41C	16-41D	16-33D	08-33C
10	16-41D	24-41A	24-33A	16-33D
11	24-41A	32-41B	32-33B	24-33A
12	32-41B	40-41C	40-33C	32-33B
13	40-41C	48-41D	48-33D	40-33C
14	48-41D	56-41A	56-33A	48-33D
15	08-33C	16-33D	16-25B	08-25A
16	16-33D	24-33A	24-25C	16-25B
17	24-33A	32-33B	32-25D	24-25C
18	32-33B	40-33C	40-25A	32-25D
19	40-33C	48-33D	48-25B	40-25A
20	48-33D	56-33A	56-25C	48-25B
21	08-25A	16-25B	16-17B	08-17A
22	16-25B	24-25C	24-17C	16-17B
23	24-25C	32-25D	32-17D	24-17C
24	32-25D	40-25A	40-17A	32-17D
25	40-25A	48-25B	48-17B	40-17A
26	48-25B	56-25C	56-17C	48-17B
27	16-17B	24-17C	24-09A	16-09D
28	24-17C	32-17D	32-09B	24-09A
29	32-17D	40-17A	40-09C	32-09B
30	40-17A	48-17B	48-09D	40-09C

Table 2-5 LPRM Detector to OPRM Cell Assignments for Channel 2

Cell ID#	LPRM #1	LPRM #2	LPRM #3	LPRM #4
1	16-57C	24-57A	24-49D	16-49D
2	24-57A	32-57A	32-49B	24-49D
3	32-57A	40-57C	40-49B	32-49B
4	08-49B	16-49D	16-41A	08-41A
5	16-49D	24-49D	24-41C	16-41A
6	24-49D	32-49B	32-41C	24-41C
7	32-49B	40-49B	40-41A	32-41C
8	40-49B	48-49D	48-41A	40-41A
9	08-41A	16-41A	16-33B	08-33D
10	16-41A	24-41C	24-33B	16-33B
11	24-41C	32-41C	32-33D	24-33B
12	32-41C	40-41A	40-33D	32-33D
13	40-41A	48-41A	48-33B	40-33D
14	48-41A	56-41C	56-33B	48-33B
15	08-33D	16-33B	16-25C	08-25C
16	16-33B	24-33B	24-25A	16-25C
17	24-33B	32-33D	32-25A	24-25A
18	32-33D	40-33D	40-25C	32-25A
19	40-33D	48-33B	48-25C	40-25C
20	48-33B	56-33B	56-25A	48-25C
21	08-25C	16-25C	16-17D	08-17B
22	16-25C	24-25A	24-17D	16-17D
23	24-25A	32-25A	32-17B	24-17D
24	32-25A	40-25C	40-17B	32-17B
25	40-25C	48-25C	48-17D	40-17B
26	48-25C	56-25A	56-17D	48-17D
27	16-17D	24-17D	24-09C	16-09A
28	24-17D	32-17B	32-09C	24-09C
29	32-17B	40-17B	40-09A	32-09C
30	40-17B	48-17D	48-09A	40-09A

Table 2-6 LPRM Detector to OPRM Cell Assignments for Channel 3

Cell ID#	LPRM #1	LPRM #2	LPRM #3	LPRM #4
1	16-57D	24-57B	24-49A	16-49A
2	24-57B	32-57B	32-49C	24-49A
3	32-57B	40-57D	40-49C	32-49C
4	08-49C	16-49A	16-41B	08-41B
5	16-49A	24-49A	24-41D	16-41B
6	24-49A	32-49C	32-41D	24-41D
7	32-49C	40-49C	40-41B	32-41D
8	40-49C	48-49A	48-41B	40-41B
9	08-41B	16-41B	16-33C	08-33A
10	16-41B	24-41D	24-33C	16-33C
11	24-41D	32-41D	32-33A	24-33C
12	32-41D	40-41B	40-33A	32-33A
13	40-41B	48-41B	48-33C	40-33A
14	48-41B	56-41D	56-33C	48-33C
15	08-33A	16-33C	16-25D	08-25D
16	16-33C	24-33C	24-25B	16-25D
17	24-33C	32-33A	32-25B	24-25B
18	32-33A	40-33A	40-25D	32-25B
19	40-33A	48-33C	48-25D	40-25D
20	48-33C	56-33C	56-25B	48-25D
21	08-25D	16-25D	16-17A	08-17C
22	16-25D	24-25B	24-17A	16-17A
23	24-25B	32-25B	32-17C	24-17A
24	32-25B	40-25D	40-17C	32-17C
25	40-25D	48-25D	48-17A	40-17C
26	48-25D	56-25B	56-17A	48-17A
27	16-17A	24-17A	24-09D	16-09B
28	24-17A	32-17C	32-09D	24-09D
29	32-17C	40-17C	40-09B	32-09D
30	40-17C	48-17A	48-09B	40-09B

Table 2-7 LPRM Detector to OPRM Cell Assignments for Channel 4

Cell ID#	LPRM #1	LPRM #2	LPRM #3	LPRM #4
1	16-57A	24-57D	24-49B	16-49C
2	24-57D	32-57C	32-49A	24-49B
3	32-57C	40-57B	40-49D	32-49A
4	08-49D	16-49C	16-41C	08-41D
5	16-49C	24-49B	24-41B	16-41C
6	24-49B	32-49A	32-41A	24-41B
7	32-49A	40-49D	40-41D	32-41A
8	40-49D	48-49C	48-41C	40-41D
9	08-41D	16-41C	16-33A	08-33B
10	16-41C	24-41B	24-33D	16-33A
11	24-41B	32-41A	32-33C	24-33D
12	32-41A	40-41D	40-33B	32-33C
13	40-41D	48-41C	48-33A	40-33B
14	48-41C	56-41B	56-33D	48-33A
15	08-33B	16-33A	16-25A	08-25B
16	16-33A	24-33D	24-25D	16-25A
17	24-33D	32-33C	32-25C	24-25D
18	32-33C	40-33B	40-25B	32-25C
19	40-33B	48-33A	48-25A	40-25B
20	48-33A	56-33D	56-25D	48-25A
21	08-25B	16-25A	16-17C	08-17D
22	16-25A	24-25D	24-17B	16-17C
23	24-25D	32-25C	32-17A	24-17B
24	32-25C	40-25B	40-17D	32-17A
25	40-25B	48-25A	48-17C	40-17D
26	48-25A	56-25D	56-17B	48-17C
27	16-17C	24-17B	24-09B	16-09C
28	24-17B	32-17A	32-09A	24-09B
29	32-17A	40-17D	40-09D	32-09A
30	40-17D	48-17C	48-09C	40-09D

Table 2-8 Percent Change in OPRM Sensitivities

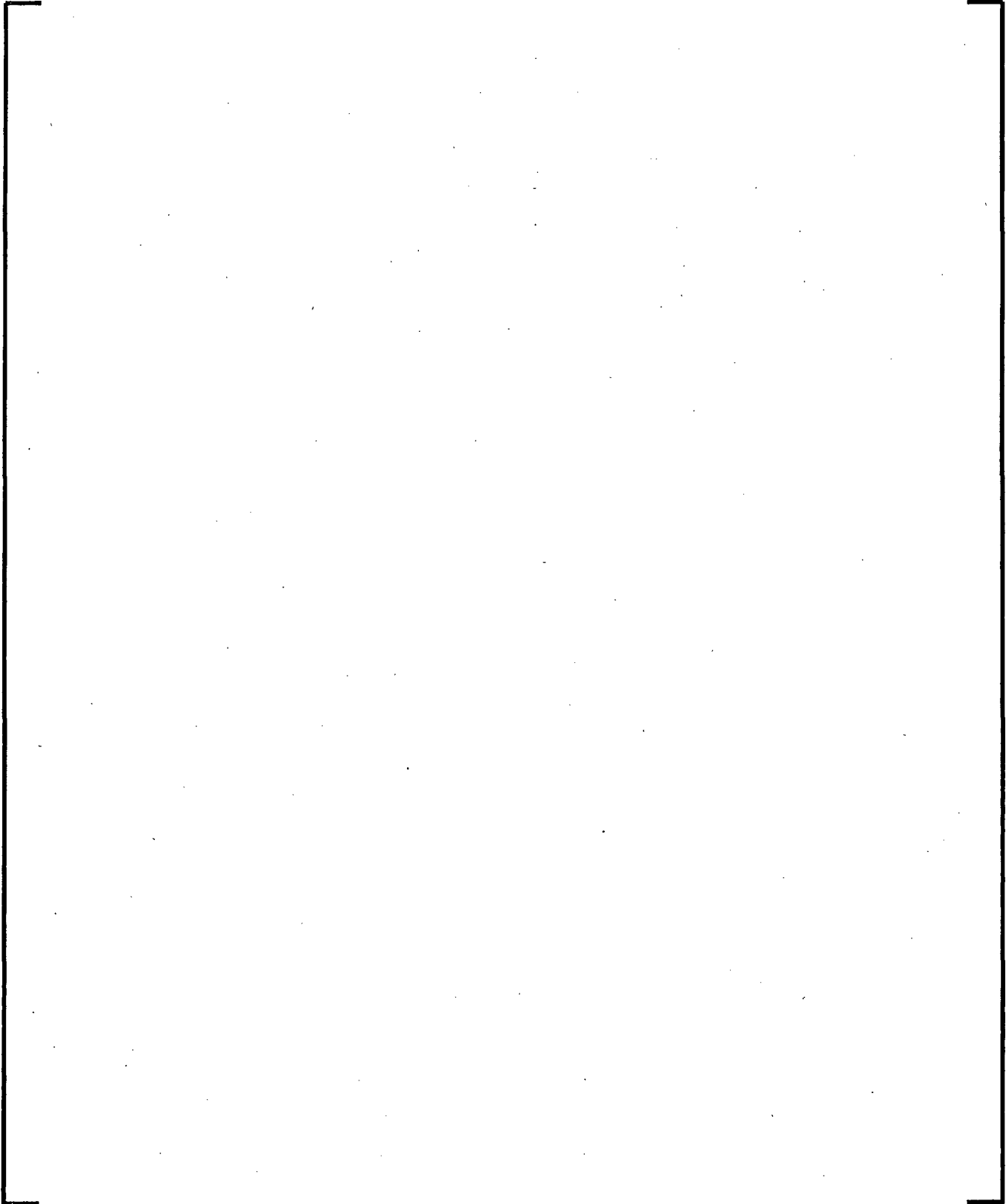
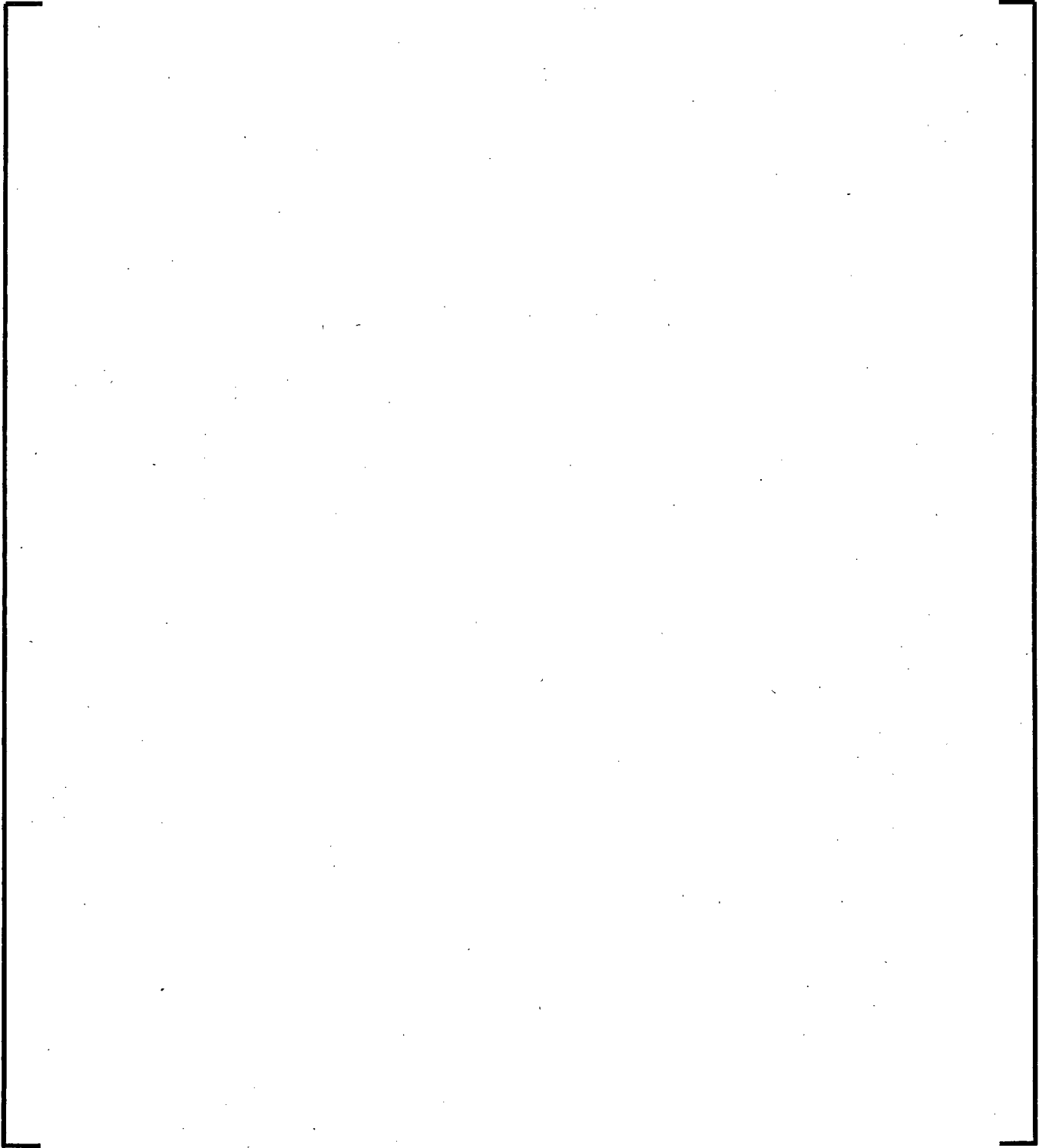


Table 2-9 Percent Change in OPRM Sensitivities





**Figure 2-1 Histogram of the Relative Change in the OPRM signals
for 10% D level and 5% C level LPRM Signal Reduction**



**Figure 2-2 Histogram of the Relative Change in the OPRM signals
for 20% D level and 10% C level LPRM Signal Reduction**

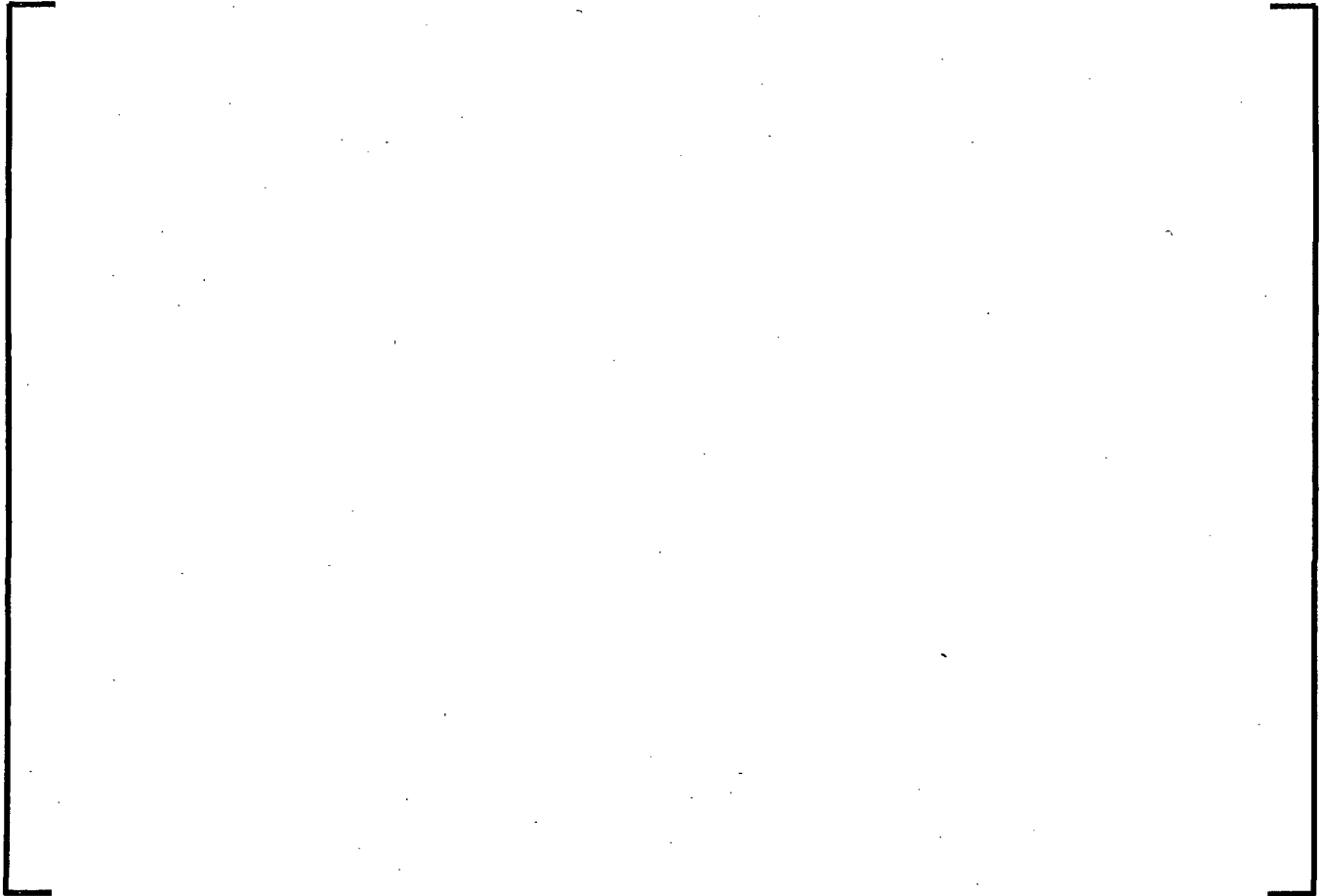


**Figure 2-3 Relative Change in the OPRM signals Versus Absolute
Oscillation Magnitude for 10% D level and 5% C level LPRM Signal
Reduction**



**Figure 2-4 Relative Change in the OPRM signals Versus Absolute
Oscillation Magnitude for 20% D level and 10% C level LPRM
Signal Reduction**



Figure 2-5 Bypass Power Source Function Representing a Growing Oscillation



Figure 2-6 Bypass Void Fraction at Detector Levels C and D

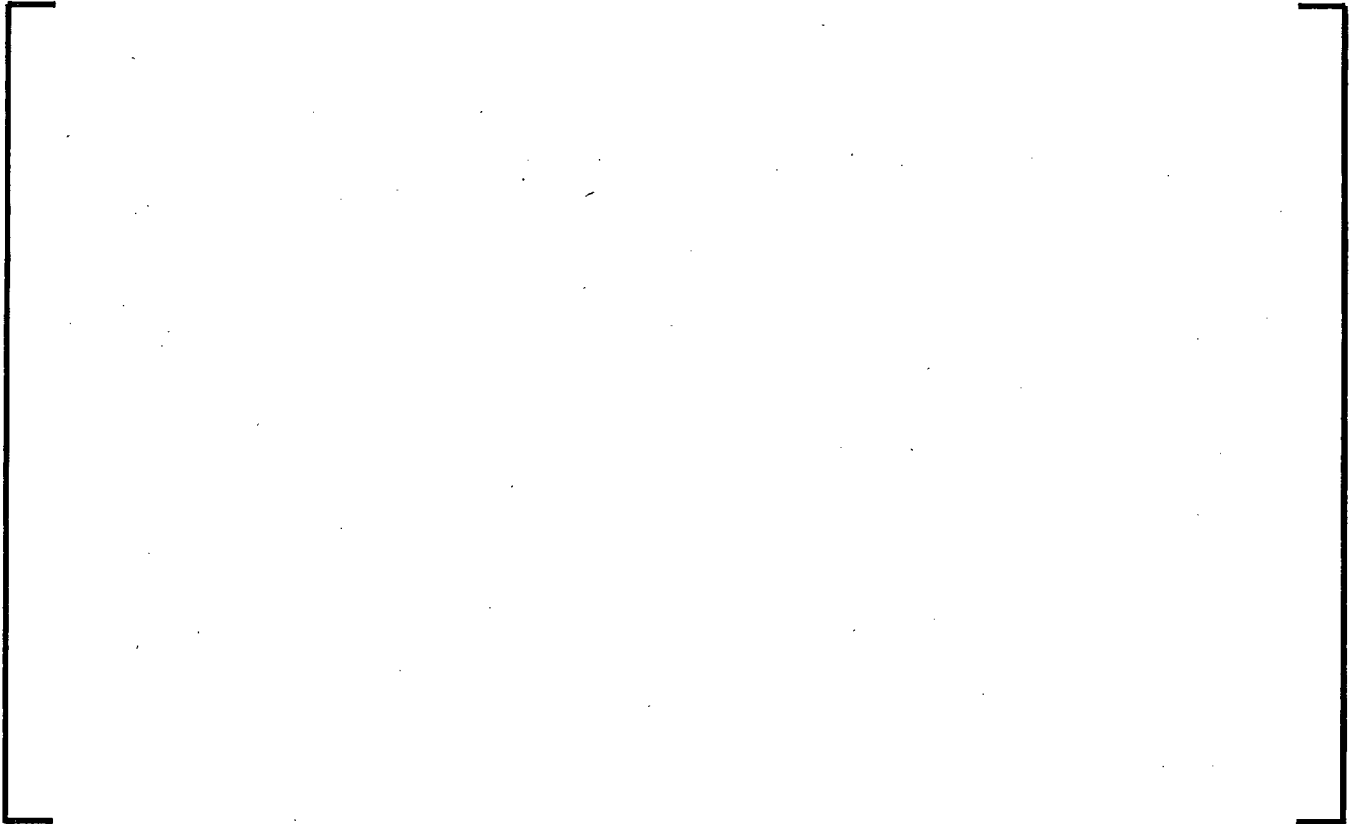


Figure 2-7 [
With and Without the Effect of Bypass Voiding]



Figure 2-8 []
With and Without the Effect of Bypass Voiding



Figure 2-9 [

]



Figure 2-10 Relative Power for Case 1 Base Global Oscillation



Figure 2-11 Relative Power for Case 2 Base Regional Oscillation



Figure 2-12 Relative Power for Case 3 Global Oscillation



Figure 2-13 Relative Power for Case 4 Regional Oscillation



Figure 2-14 Relative Power for Case 5 Regional Oscillation With Decreased Subcriticality



Figure 2-15 Relative Power for Case 6 Mitigated Global Oscillation



Figure 2-16 Relative Power for Case 7 Mitigated Regional Oscillation



Figure 2-17 Relative Power for Case 8 Late-Mitigated Global Oscillation



Figure 2-18 Relative Power for Case 9 Late-Mitigated Regional Oscillation



Figure 2-19 Inlet Mass Flow Rate for Case 1 Base Global Oscillation



Figure 2-20 Inlet Mass Flow Rate for Case 2 Base Regional Oscillation



Figure 2-21 Inlet Mass Flow Rate for Case 3 Global Oscillation



Figure 2-22 Inlet Mass Flow Rate for Case 4 Regional Oscillation



**Figure 2-23 Inlet Mass Flow Rate for Case 5 Regional Oscillation
With Decreased Subcriticality**



Figure 2-24 Inlet Mass Flow Rate for Case 6 Mitigated Global Oscillation



Figure 2-25 Inlet Mass Flow Rate for Case 7 Mitigated Regional Oscillation



Figure 2-26 Inlet Mass Flow Rate for Case 8 Late-Mitigated Global Oscillation



Figure 2-27 Inlet Mass Flow Rate for Case 9 Late-Mitigated Regional Oscillation



Figure 2-28 Exit Void Fraction for Case 1 Base Global Oscillation



Figure 2-29 Exit Void Fraction for Case 2 Base Regional Oscillation



Figure 2-30 Exit Void Fraction for Case 3 Global Oscillation



Figure 2-31 Exit Void Fraction for Case 4 Regional Oscillation



**Figure 2-32 Exit Void Fraction for Case 5 Regional Oscillation With
Decreased Subcriticality**



Figure 2-33 Exit Void Fraction for Case 6 Mitigated Global Oscillation



Figure 2-34 Exit Void Fraction for Case 7 Mitigated Regional Oscillation



Figure 2-35 Exit Void Fraction for Case 8 Late-Mitigated Regional Oscillation



Figure 2-36 Exit Void Fraction for Case 9 Late-Mitigated Regional Oscillation



Figure 2-37 Void Fraction in Selected Nodes for Case 1 Base Global Oscillation



**Figure 2-38 Void Fraction in Selected Nodes for Case 2
Base Regional Oscillation**

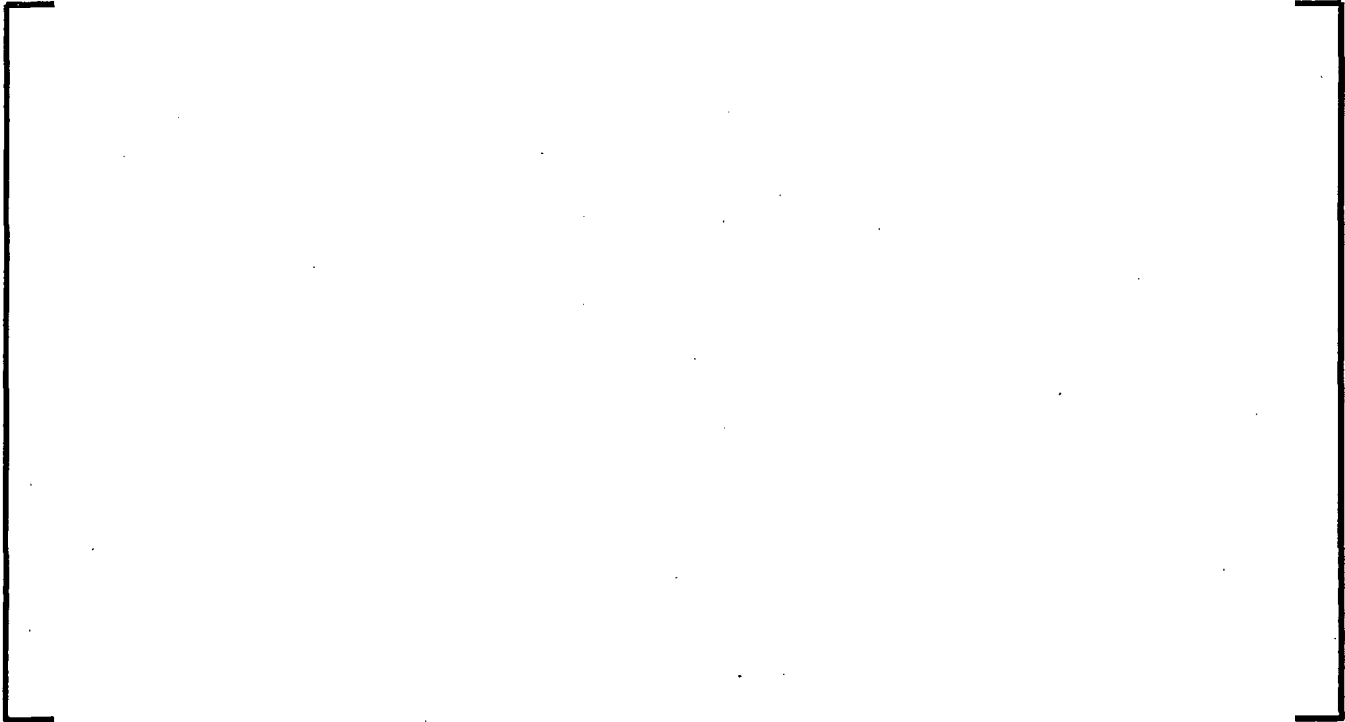


Figure 2-39 Void Fraction in Selected Nodes for Case 3 Global Oscillation



Figure 2-40 Void Fraction in Selected Nodes for Case 4 Regional Oscillation



**Figure 2-41 Void Fraction in Selected Nodes for Case 5
Regional Oscillation With Decreased Subcriticality**

3.0 COTRANSA2

3.1 Conservatism

Integral power is a parameter obtainable from test measurements that is directly related to Δ CPR and provides a means to assess code uncertainty by increasing heat flux during the duration of the event. The COTRANSA transient analysis methodology was a predecessor to the COTRANSA2 methodology. The integral power figure of merit was introduced with the COTRANSA methodology as a way to assess (not account for) code uncertainty impact on Δ CPR. From COTRANSA analyses of the Peach Bottom turbine trip tests, the mean of the predicted to measured integral power was 99.7% with a standard deviation of 8.1%. AREVA NP (Exxon Nuclear at the time) initially proposed to treat integral power as a statistical parameter. However, following discussions with the NRC, it was agreed to apply a deterministic 110% integral power multiplier (penalty) on COTRANSA calculations for licensing analyses. That increase was sufficient to make the COTRANSA predicted to measure integral power conservative for all of the Peach Bottom turbine trip tests.

COTRANSA2 (Reference 23) was developed and approved as a replacement for COTRANSA in the AREVA NP thermal limits methodology (Reference 19). Initially it was not planned to use the 110% integral power multiplier with the COTRANSA2 methodology. COTRANSA2 predictions of integral power were conservative for all Peach Bottom turbine trip tests. The minimum conservatism was [] and the mean of the predicted to measured integral power was []. The comparisons to the Peach Bottom turbine trip tests demonstrated that the 110% integral power multiplier was not needed for COTRANSA2. However, because the thermal limits methodology that was approved independently of COTRANSA2 included discussion of the 110% integral power multiplier, the use of the multiplier was retained for COTRANSA2 licensing calculations. With the 110% multiplier, the COTRANSA2 predicted to measured mean integral power is [] for the Peach Bottom turbine trip tests. Applying a [] integral power multiplier provides an OLMCPR conservatism of []. The 110% integral power multiplier is just one part of the conservatism in the COTRANSA2 methodology and application process that covers methodology uncertainties.

The 110% integral thermal power multiplier is applied to the output of COTRANSA2 that is used as the input to XCOBRA-T; therefore, the 110% integral power multiplier is included in the transient analyses. Important input parameters are biased in a conservative direction in licensing calculations. For Technical Specification (TS) controlled input parameters, the biasing is either the limiting value allowable by TS, or an analytical limit that is beyond the limiting value allowable by TS. If a particular equipment out-of-service is applicable to a particular transient event, the transient analysis is performed with the limiting plant configuration for the allowable equipment out-of-service.

3.2 *Thermal-Mechanical Model*

The RODEX2 computer code provides initial input information relative to core average fuel-to-cladding gap heat transfer coefficients for the COTRANSA2 computer code. As such, RODEX2 uses steady-state heat conduction models. The heat conduction model employed by COTRANSA2 includes transient terms.

The fuel thermal conductivity correlations used by COTRANSA2 are equivalent to the RODEX2 models.

COTRANSA2 computes a fuel temperature for each axial plane in the core. Based on the assumption of a core composition primarily consisting of uranium dioxide, COTRANSA2 does not account for gadolinium in the fuel thermal conductivity calculation.

Heat capacities of fuel components (uranium dioxide, gadolinium, and cladding) are not required for the RODEX2 steady-state calculations but are used in the COTRANSA2 transient calculations.

The fuel pellet-to-cladding gap heat transfer coefficient used in COTRANSA2 is the product of a RODEX2 calculation.

A gap conductance sensitivity study was performed for the load rejection with no bypass (LRNB) transient event for a BWR. The purpose of the sensitivity study was to show the Δ CPR trend for changes in gap conductance for COTRANSA2 versus XCOBRA-T. The gap conductance change considered was []. The results are provided in Table 3-1. As seen from the results, an increase in COTRANSA2 core average gap conductance results in a

decrease in ΔCPR ; whereas an increase in XCOBRA-T hot channel gap conductance results in an increase in ΔCPR . A decrease in gap conductance shows the opposite trend. The XCOBRA-T ATRIUM-10 hot channel model is slightly more sensitive to the change in gap conductance than the COTRANSA2 ATRIUM™-10* average core model. When both COTRANSA2 and XCOBRA-T gap conductance are changed by an equivalent amount, the net impact is no significant change in ΔCPR .

3.3 *Pump Model*

A pump model based on homologous input is used in COTRANSA2. This pump model is used to model the dual RPT during ATWS evaluations. The homologous curves are from the pump manufacturer. The pump speed and flow are initialized from operational plant data. Frictional torque and pump inertia are tuned to model the plant coastdown rate.

3.4 *SRV Model*

The safety and relief valves (SRVs) are modeled as a single mass sink from the steam line node where they are located. SRVs with the same setpoint are modeled as a combined valve in COTRANSA2. The net flow is the sum of the flow of each valve in parallel. Multiple SRVs are used in COTRANSA2 to represent banks of SRVs with different setpoints.

The SRVs are opened to relieve pressure when calculated pressure in the steam line node containing the valves reaches the opening setpoint pressure. The valve position is based on time since the valve setpoint was exceeded, the valve opening delay, and the valve stroke time.

* ATRIUM is a trademark of AREVA NP.

Full open valve flow (W) is calculated as:



The COTRANSA2 input for [] is adjusted to account for the total pressure loss in the SRV branch from the main steam line to the SRV.

3.5 *Cross Sections*

The original COTRAN cross section tables used piece-wise linear interpolation of cross section tables at [] void fraction. With the introduction of MICROBURN-B the 1-D cross section table produced by the core simulator and used by COTRANSA2 was changed to be a [

[]. This extension of the cross section interpolation was briefly described in RAI Response 1 of ANF-913(P)(A) Volume 1 Supplement 4.

Specifically, the cross section table in COTRANSA2 now contains [

[

] For limiting events, the nodal void fractions typically change by 0.03 to 0.10 before the power response is dominated by the scram bank insertion. In this formulation, the cross sections used by COTRANSA2 are much more representative of the actual radial conditions in the core than if the cross sections are generated assuming all of the nodes in the plane are at [] percent void fraction.

The MICROBURN-B code used [] void fraction libraries from CASMO-3 and used [] to generate the nodal cross sections for the specific nodal operating history and instantaneous void fraction. MICROBURN-B2 uses [] void fraction libraries from CASMO-4 and uses [] to generate the nodal cross sections for the specific nodal operating history and instantaneous void fraction. In either case, it is the instantaneous cross sections for each node in the plane that are collapsed to planar average values to produce the cross sections used by the 1-D flux solution in COTRANSA2. In this formulation, the migration from MICROBURN-B to MICROBURN-B2 did not change the cross section representation between the core simulator and COTRANSA2.

In order to produce the COTRAN neutronic parameters, a series of MICROBURN-B2 calculations are performed. These successive calculations are:

- (1) Nominal initial conditions

[

]

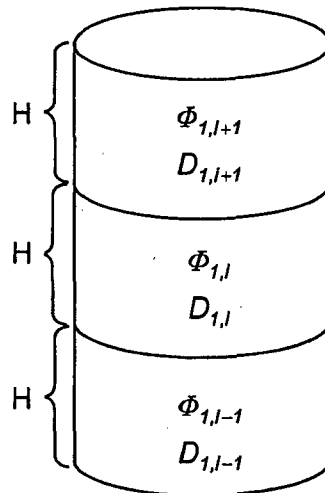
[

]

The 1½ energy group diffusion equation in steady-state can be written as

$$\nabla \cdot D_1 \nabla \Phi_1 - \left(\Sigma_{a1} + \frac{\Sigma_{1-2}}{\Sigma_{a2}} \cdot \Sigma_{a2} \right) \Phi_1 + \frac{\left(\nu \Sigma_{f1} + \frac{\Sigma_{1-2}}{\Sigma_{a2}} \cdot \nu \Sigma_{f2} \right) \Phi_1}{k_{eff}} = 0$$

The first term is a leakage. This equation is integrated over the cylindrical node depicted in the following figure.

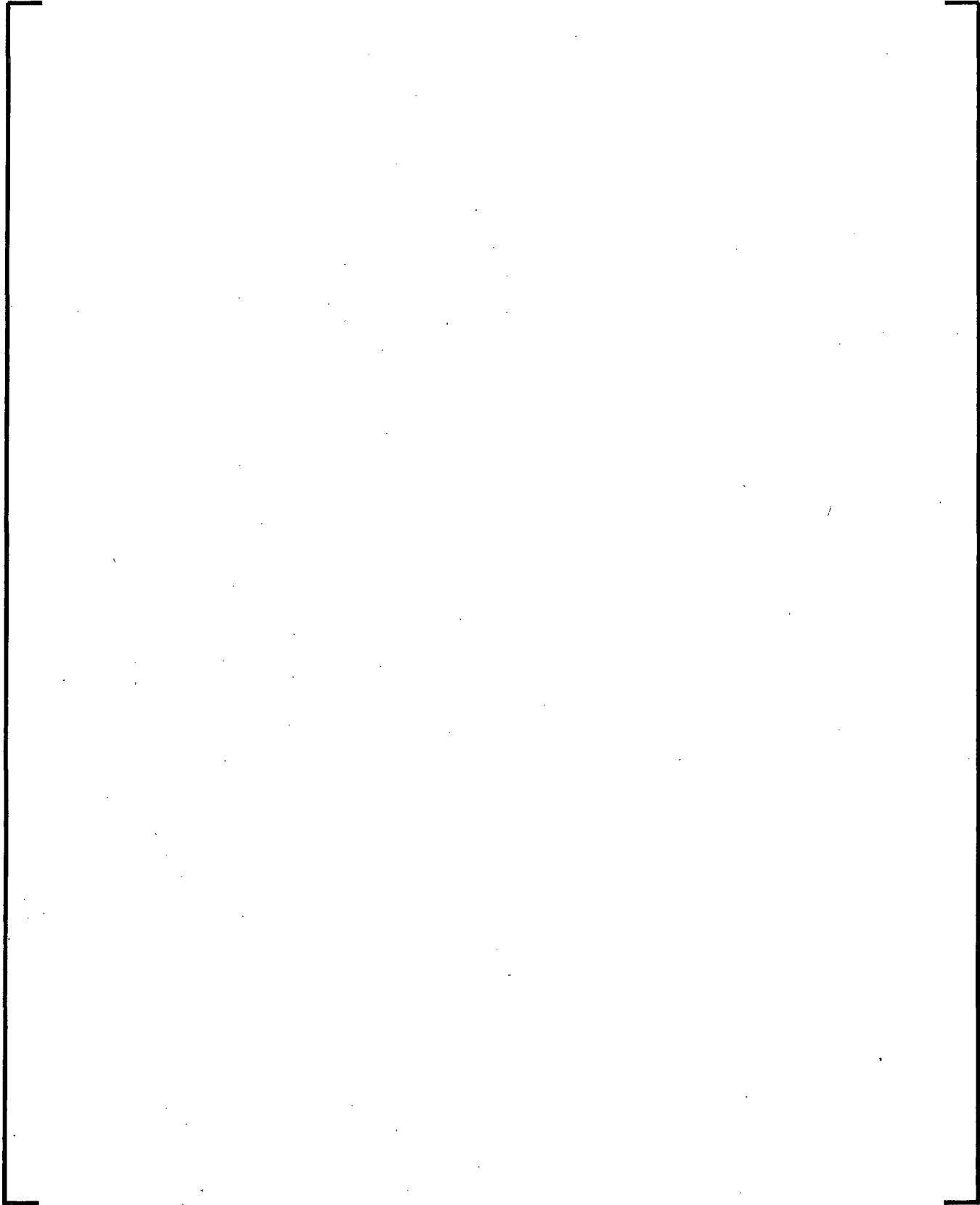


The leakage term is approximated as:

$$- \sum_{j=1}^3 \frac{2D_{1,i}D_{1,j}(\Phi_{1,i} - \Phi_{1,j})}{(D_{1,i} + D_{1,j})} \frac{A}{HV}$$

where

- $D_{1,i}$ = D for plane of interest
- $D_{1,j}$ = D for the nodes adjacent to the plane of interest
- $\Phi_{1,i}$ = flux in the plane of interest
- $\Phi_{1,j}$ = flux in the regions adjacent to the plane of interest
- A = surface area between nodes i and j
- H = distance between nodes i and nodes j
- V = node volume





[

]

[

]

I

1

[

]

These final one-group cross section and leakage parameters are used in a new 1-dimensional flux solution and the axial power distribution is updated for the next thermal hydraulic solution. Iterations between the 1-dimensional flux solution and the thermal hydraulic solution are repeated until converged results are obtained for core power, power distribution, temperature distribution, and density distribution.

Table 3-1 Gap Conductance Study

Gap Conductance Condition	$\Delta(\Delta\text{CPR})$
<i>Increase in Gap Conductance</i>	
Core average []	-0.011
Hot channel []	+0.012
Core average and hot channel []	0.000
<i>Decrease in Gap Conductance</i>	
Core average []	+0.015
Hot channel []	-0.016
Core average and hot channel []	-0.001



Figure 3-1 Comparison of Scram Bank Worth for
[]

4.0 XCOBRA-T

4.1 Axial Geometry Changes

XCOBRA-T calculates the fuel rod surface heat flux using a fuel rod heat conduction model, the power generated in the fuel rod, and the fluid conditions at the surface of the rod. The power generated in the fuel rod is described in Reference 20 Section 2.5.5. The power generated in each axial section of a fuel rod is calculated using Equation 2.130 from Reference 20. Although Reference 20 states that Equation 2.130 is calculated for each axial node, the equation itself does not denote which variables are axially dependent. Because the equation is for each axial node, the variables for heat generation rate, axial peaking factor, and number of rods are axial dependent. At the time Reference 20 was prepared, the number of rods at each axial plane was a constant for the fuel designs being supplied. For the ATRIUM-10 fuel design with part-length fuel rods (PLFRs), the number of rods became axial dependent and the code was modified to make application of Equation 2.130 correct and consistent with the NRC-approved Reference 20. For application to current fuel designs, a better definition of the variable N_r in Equation 2.130 would be "number of *heated* rods per assembly *at the axial plane*" (*italic indicates added text*).

For bundles with part-length fuel rods (PLFRs), the rod heat flux calculation begins by computing the time-dependent heat flux generation rate at each axial section in the fuel rod. The updated equation, corresponding to Equation 2.130 of Reference 20 is:

$$q''(t) = \frac{P(t)}{\pi D_{rod,i}} \frac{1}{LN_a N_{ri}} (f_f + f_c) F_{ri} F_{li} F_a$$

where

$P(t)$	=	transient reactor power
f_f	=	fraction of power produced in the fuel
f_c	=	fraction of power produced in the cladding
N_a	=	total number of assemblies in the core
N_{ri}	=	total number of heated rods for type i assembly at the axial plane
F_{ri}	=	radial peaking factor of type i assembly
F_{li}	=	local peaking factor of type i assembly

- F_a = axial peaking factor at the axial plane
 $D_{rod,i}$ = fuel rod diameter of type i assembly
 L = axial heated length

This equation differs from that in Reference 20 by replacing the initial reactor power in the denominator with π . In addition, the variable definitions have been modified to identify that the total number of heated rods is dependent on both the assembly type and axial elevation and the definition of L has been corrected to the axial heated length of the assembly. This equation is substituted into equations 2.129a and 2.129b in Section 2.5.5 of Reference 20 to define the volumetric heat deposition rate for the fuel pellet and cladding, respectively. This volumetric heat deposition rate is used in the right-hand side of equation 2.85 of Reference 20 to iteratively solve the transient heat conduction equation and the hydraulic conservation equations for the new time step temperatures and surface heat flux. The heat flux is introduced into the channel energy equation (2.2 of Reference 20) through the term q' . This linear heat deposition rate is a summation of the energy added by direct energy deposition and surface heat flux:

$$q'(t) = \left\{ \frac{P(t)}{N_a L} f_{cool} F_{ri} F_a + H_{surf} \cdot (T_{NodesT} - T_{fluid}) \cdot \pi \cdot D_{rod,i} \cdot N_{ri} \right\} N_i$$

where

- f_{cool} = fraction of power produced in the coolant
 H_{surf} = film heat transfer coefficient at the axial plane
 T_{NodesT} = cladding surface temperature at the axial plane
 T_{fluid} = fluid temperature at the axial plane
 N_i = number of fuel assemblies in channel i

In addition to axially varying number of heated rods, proper modeling of PLFRs also requires axial variations in the active flow area, the heated perimeter, and the wetted perimeter and these parameters are now defined as axially dependent quantities in AREVA NP methods. Consequently, all references to these parameters or parameters derived from the basic geometry data in the approved topical reports should be interpreted as being axially dependent variables. The pressure drop due to the area expansion at the end of the PLFRs (or anywhere

in the active flow path) is modeled using the specific volume for momentum as expressed in Equations 2.78 and 2.79 of Reference 20. For current designs, area contractions occur in the single phase region, but the coding was generalized to address area contractions in the two-phase region based on a solution of the two-phase Bernoulli equation.

4.2 **Power**

The decay heat is calculated by COTRANSA2 and is included in the total core power versus time provided as a boundary condition to XCOBRA-T. The decay heat model used in COTRANSA2 is a curve fit (11 groups) to the 1973 ANS standard decay heat model. The COTRANSA2 core power boundary condition includes the decay heat contribution based on the core average power density. The decay heat power remains essentially constant during the transient. Therefore, the decay heat during the transient is primarily a function of initial power density. Application of power peaking factors (axial, radial, local) to the COTRANSA2 average power properly accounts for local decay heat in the XCOBRA-T hot channel analysis.

Gamma smearing does not affect the XCOBRA-T hot channel calculation. The hot channel calculation models an average fuel rod (the average is not affected by flattening of the distribution). The calculation process for determining the peak transient LHGR is equivalent [] and is not dependent of the actual rod local peaking factor.

The total core power calculated by COTRANSA2 is distributed between the fuel rod, the active channel coolant, and the core bypass coolant. The fraction deposited in each component is based on fuel type specific calculations performed with the CASMO computer code. For XCOBRA-T, generic power fractions were used for Browns Ferry that approximate the values calculated by CASMO.

An XCOBRA-T deposited power fraction sensitivity study was performed for a BWR for the LRNB transient event. The purpose of the sensitivity study was to show the impact on Δ CPR from using generic ATRIUM-10 power fractions versus case-specific power fractions. The case-specific power fractions are used in COTRANSA2 and are obtained from CASMO-4/MICROBURN-B2. AREVA NP is in the process of automating the transfer of the case-specific power fractions into XCOBRA-T such that the generic values will no longer be used. Also,

[] The power that would have been deposited [] . A review of an ATRIUM-10 power deposition study showed that the [] . A study was performed by taking [] . The results are provided in Table 4-1. The study shows no significant change in ΔCPR . [] This study demonstrates that the ATRIUM-10 generic power fractions in XCOBRA-T are adequate. The GE14 fuel for Browns Ferry Unit 1 is handled in a similar manner as the ATRIUM-10 fuel; therefore, generic power fractions are also adequate for the GE14 in XCOBRA-T.

4.3 *Radial Pin Power Shape*

The local sub-bundle radial pin power is accounted for in the SPCB critical power correlation in the form of F_{eff} . Evaluations were performed to assess the impact on ΔCPR for a change in F_{eff} resulting from the variation in the lattice void fraction during a pressurization event for a BWR.

MICROBURN-B2 analyses were performed using the nominal void correlation and an adjusted void correlation to assess the change in F_{eff} as void changes. The MICROBURN-B2 cases were run to reflect an instantaneous change in core average void fraction of +0.05. For the limiting MCPR bundle in the core, the changes in void, local peaking factor (LPF), and F_{eff} were:

$\Delta\text{void} = +0.0441$ (node 24)
 $\Delta\text{void} = +0.0456$ (node 23)
 $\Delta\text{LPF} = -0.0026$ (node 24)
 $\Delta\text{LPF} = -0.0030$ (node 23)
 $\Delta F_{\text{eff}} = 0.0000$ (assembly)

For other potentially limiting bundles (10% highest powered bundles) in the core, the change in F_{eff} was between -0.0002 and +0.0011 for a +0.05 core average Δvoid . In general, an increase in void fraction resulted in an increase in F_{eff} for high power, low exposure (end of first cycle) assemblies and a decrease in F_{eff} for low power, high exposure assemblies.

A decrease in F_{eff} during the transient will improve the CPR during the transient and result in a reduced Δ CPR. The converse is true for an increase in F_{eff} during the transient. The sensitivity of MCPR to F_{eff} is about 2 to 1; therefore, the sensitivity of Δ CPR is about twice the ΔF_{eff} during the transient. The change in Δ CPR would be between 0.000 and +0.002 for a +0.05 core average Δ void.

During a pressurization event, the core void will initially decrease followed by an increase in core void. Therefore, the effect of the change in void on fuel rod peaking factors (and F_{eff}) will tend to be offset during the transient.

The assessment above for the impact of a void change on ΔF_{eff} and Δ (Δ CPR) is based on assuming the nuclear power is instantly converted to surface heat flux. Because the time of MCPR (~1.25 sec) is less than the fuel rod thermal time constant (~ 5 sec), the actual impact on F_{eff} and Δ CPR from the void change will be much less. Likewise, the time of the peak heat flux (~0.8 second) is less than the fuel rod thermal time constant. At the boiling transition plane, there is an insignificant change in void until after the time of peak power. Because the increase in void and the corresponding increase in F_{eff} occur close to the time of MCPR, the slight change in rod power will not significantly change the rod heat flux at the time of MCPR. Therefore, the effect on Δ CPR will be much less than estimated based on the MICROBURN-B2 analyses.

In summary, the above results show that the effect of the variation in void fraction during a transient on the F_{eff} has an insignificant effect on Δ CPR.

4.4 **Default Models**

The Browns Ferry EPU transient analyses used the default models of XCOBRA-T. The default models include Levy subcooled boiling model, the Martinelli-Nelson two phase friction multipliers, the two phase component loss multiplier, and the heated wall viscosity correction model. [

] as discussed with the NRC on May 4, 1995 (Reference 26).

Thermo-dynamic properties from the ASME steam tables were used. The code provides a message if the default models are not used. Per AREVA's licensing analyses requirements, use of default models is required.

The Martinelli-Nelson two phase friction multiplier has been confirmed to be applicable in the annular flow regime by verifying the AREVA NP hydraulic models against two-phase full-scale heated bundle tests in the KATHY test facility in Karlstein, Germany. The range of assembly conditions at EPU are bounded by the tested two-phase flow conditions. Many of the tested conditions are in the annular flow regime.

The Levy subcooled boiling model does not directly predict void fraction in subcooled boiling. Instead, the model predicts a critical subcooling that defines the onset of boiling. The critical subcooling is used in conjunction with a profile fit model to determine the local flow quality that accounts for the presence of subcooled boiling. The local flow quality is then used in the Ohkawa-Lahey correlation to predict the void fraction in subcooled boiling.

4.5 **Bounds Checking**

Bounds checking is provided in the XCOBRA-T coding to ensure the conditions provided to the SPCB correlation are within the correlation limits as specified in Table 1.1 of Reference 30. Should any of the condition limits be violated, the behavior will be as specified in Section 2.6 of Reference 30. In the specific case where the pressure limit is exceeded, XCOBRA-T will write an appropriate error message and terminate the calculation as specified in Section 2.6.3 of Reference 30.

With respect to the remaining parameters, the behavior for transient calculations is summarized in Table 4-2.

The out-of-bounds corrections affect the [] used in the evaluation of the transient LHGR. Therefore, the corrections do not impact the evaluation of the thermal-mechanical performance.

The critical power calculations for Browns Ferry fuel are made with the SPCB critical power correlation. Equivalent correlation bounds are specified in terms of []. The range of applicability of these parameters is sufficiently broad to cover the ranges of conditions encountered during the licensing calculations. Correlation bounds checking is incorporated in the XCOBRA-T critical power calculations. The bounds checking routine does not allow a calculation outside the range of applicability of these parameters.

The transient code, XCOBRA-T, evaluates Reynolds number for each node for each step of the calculation. If the flow becomes negative at any node, the code stops the calculation.

4.6 *Heat Transfer Correlations*

The thermocouples used for measuring temperature data in full scale critical power tests are

[

] measure heat transfer coefficients associated with pre-CHF heat transfer in the range of mass and heat fluxes associated with BWRs. As a result, no relevant qualification studies of the Dittus-Boelter and Thom heat transfer correlations can be performed from the test data.

As noted in Reference 25, fully developed nucleate boiling is relatively insensitive to flow rate and quality. However, "boiling suppression" may occur in high quality annular flow that provides very high heat transfer coefficients, resulting in decreasing wall temperature as the heat flux increases.

Extracted heat transfer information from experiments in a tube for a range of pressure, flow, and quality that is relevant to BWRs is reported in Reference 32. This reference shows the relative insensitivity of heat transfer coefficient to flow rate and quality and that boiling suppression does not become significant until quality reaches approximately 0.47, which is well above the range of interest to BWRs. [

] Therefore, it is concluded that liquid entrainment and droplet redeposition does not have an impact on boiling heat transfer for flow conditions that are applicable to an operating BWR at EPU.

4.7 *Axial Power Shape*

The initial axial power shape is determined from the COTRANSA2 calculation based on the cross section data for the core exposure considered in the analysis. The cross section data is obtained from the MICROBURN-B2 computer code. The MICROBURN-B2 calculations used to generate cross section data for COTRANSA2 licensing calculations are performed assuming that all control rods are fully withdrawn. Assuming all control rods are fully withdrawn results in

a significant conservatism in calculated scram reactivity for exposure conditions with some control rods partially inserted.

During pressurization transients, the axial power shape shifts due to the void collapse in the top of core (void reactivity), the core flow increase in the bottom of core (void reactivity), and control rod insertion in the bottom of the core (scram reactivity). The coupled 1-D neutronic and thermal-hydraulic core model in COTRANSA2 determines a [] including the impact of void collapse and scram. This [] is used in XCOBRA-T. The assembly []

[] and the assembly radial peaking factor input to XCOBRA-T.

The change in axial nodal power, []

[] results in a change in fuel rod surface heat flux and the energy transferred to the coolant at each axial node. Both COTRANSA2 and XCOBRA-T have fuel rod heat transfer models that determine the fuel rod surface heat flux based on the nodal power history and the coolant conditions at each axial node.

Both COTRANSA2 and XCOBRA-T have thermal-hydraulic models that are used to calculate the flow at each axial node in the core and the hot channel during the pressurization transient. The energy equation captures the effect of changes in fuel rod surface heat flux on coolant conditions. The mass and momentum equations, with applicable correlations, are used to determine the local coolant flow rate during the pressurization transient. During the initial phase of the pressurization transient, these models predict a decrease in flow near the top of the core and an increase in flow near the bottom of the core. Note, although the flow decreases in the upper portion of the hot assembly, the assembly flow does not stagnate during the pressurization phase of an AOO or ATWS. Local fluid conditions (enthalpy and flow) calculated from the thermal-hydraulic model are used to determine local dryout conditions.

4.8 ***Thermal Mechanical Performance***

XCOBRA-T was used to demonstrate acceptable fuel rod thermal-mechanical performance during transients (AOOs). The fuel rod models in XCOBRA-T are consistent with RODEX2 and the fuel rod gap conductance values input to XCOBRA-T are obtained from RODEX2 analyses.

The gap conductance includes the effect of pellet geometry changes (densification, swelling, etc.). The XCOBRA-T analyses are performed to ensure that fuel rod thermal mechanical limits established with RODEX2 are not exceeded during AOOs.

An average fuel rod (local rod peaking = 1.0) is modeled in the XCOBRA-T hot channel analysis. The assembly axial nodal power history in the XCOBRA-T analysis is based on the COTRANSA2 calculated core axial nodal power history and the assembly radial peaking factor. The power generated in each axial segment of the bundle average fuel rod is the assembly axial nodal power divided by the number of heated fuel rods in the axial node. Generally, the initial peak axial fuel rod LHGR in the XCOBRA-T hot channel analysis is less than the maximum allowed steady state LHGR. [

]

4.8.1 Thermal Mechanical Performance for GE14 Fuel

Fuel assembly thermal mechanical limits for both AREVA NP and co-resident fuel are verified and monitored for each mixed core designed by AREVA NP. The thermal mechanical limits established by the co-resident fuel vendor continue to be applicable for mixed (transition) cores. The thermal mechanical limits (steady-state and transient) for the co-resident fuel are provided to AREVA NP by the utility. AREVA NP performs design and licensing analyses to demonstrate that the core design meets steady-state limits and that transient limits are not exceeded during anticipated operational occurrences.

For fast pressurization transients and co-resident GE14 fuel AREVA NP provides transient COTRANSA2/XCOBRA-T surface heat flux benchmark data to the utility. The utility in turn develops corresponding surface heat flux limits and appropriate LHGRFAC values from the COTRANSA2/XCOBRA-T response based on GNF thermal-mechanical analyses. A sufficient number of cases are benchmarked such that a conservative correlation is developed. The process ensures compliance with GNF's thermal-mechanical licensing limits for transient analyses of the co-resident fuel performed with COTRANSA2/XCOBRA-T.

Table 4-1 Deposited Heat Study

Condition	Fuel Heat	Cladding Heat	Moderator Heat	Bypass Heat	$\Delta(\Delta\text{CPR})$
Generic power fractions	[]	[]	[]	[]	NA
Case-specific power fractions	[]	[]	[]	[]	-0.0004
Case-specific power fractions []	[]	[]	[]	[]	+0.0008

Table 4-2 Bounds Checking



5.0 Thermal Hydraulic

5.1 Void Quality Applicability

The [] void-quality correlation has been qualified by AREVA NP against both the FRIGG void measurements and ATRIUM-10 measurements. The cross-sectional views of these two test channels are illustrated in Figure 5-1 along with the geometry of the GE14 fuel design. Despite the significantly different geometrical configurations (between FRIGG and ATRIUM-10), the behavior of the [] calculations when compared to the measured data is remarkably similar as illustrated in Figure 5-2. This similarity of results indicates that the [] void-quality correlation is applicable to a range of geometries larger than the differences between ATRIUM-10 and GE14 and thus is equally applicable to the GE14 fuel design in the BF1 Cycle 9 mixed core configuration.

The void correlation [] has been validated against measured ATRIUM-10 void fractions up to void fractions of []. The comparison shows that the standard deviation between calculated and measured values is [].

[

]

5.2 ATRIUM-10 Void Fraction Measurement

[

]

[

]

5.2.1 Facility Description

[

]

5.2.2 Data Collection

[

]

[

]

5.2.3 Facility Calibration

[

]

5.2.4 Measurement Technique

[

]

5.2.5 Conclusion

[

]

5.3 *SLMCPR Calculation Process*

[

]

[

]

5.4 ***Safety Limit and Radial Peaking Factor Uncertainty***

The AREVA NP SLMCPR methodology is used to determine what TS SLMCPR value is required to meet the regulatory acceptance criterion ($< 0.1\%$ of the rods in the core in BT). The first step in the calculation procedure is to select a value for SLMCPR to two decimal places (usually the current TS SLMCPR). The SAFLIM2 computer code is then used to calculate the number of rods in BT for the selected SLMCPR (i.e., SLMCPR is an input, not a calculated result). If the calculated rods in BT is $< 0.1\%$, the selected SLMCPR is supported. If the acceptance criterion is not met, the SLMCPR is increased by 0.01 and the SAFLIM2 calculation is performed again. This iteration is continued until the acceptance criterion is met for the input SLMCPR.

To investigate the effect of the radial peaking factor uncertainty on SLMCPR two analyses were performed. In the first analysis, a SLMCPR of 1.08 and the base RPF uncertainty [] were input to SAFLIM2. The number of BT rods was calculated to be 60 from this analysis. The second analysis was the final case in a series of SAFLIM2 analyses using the increased RPF uncertainty [] and performed by iterating on the input value of SLMCPR. Different values for the SLMCPR input were used until the number of BT rods calculated by SAFLIM2

was the same as the base case (60 rods). A SLMCPR input value of 1.0855 resulted in 60 rods in BT when the increased RPF uncertainty was input. The difference in SLMCPR input for the two cases that resulted in the same number of BT rods is a measure of the sensitivity to the increased RPF uncertainty.

The only input parameters changed between the two SAFLIM2 analyses were the SLMCPR and the RPF uncertainty. For each analysis, 1000 Monte Carlo trials were performed. To minimize statistical variations in the sensitivity study, the same random number seed was used and all bundles were analyzed for both analyses. As discussed above, 60 rods were calculated to be in BT in both analyses.

The sensitivity study discussed above was performed to quantify the sensitivity of SLMCPR to an increase in RPF uncertainty and did not follow the standard approach used in SLMCPR licensing analyses. In standard licensing calculations, the SLMCPR is not input at a precision greater than the hundredths decimal place. As a result, the increased RPF uncertainty would result in either no change or a 0.01 increase in SLMCPR licensing analyses depending on how close the case was to the acceptance criterion prior to the increase in RPF uncertainty. This process is equivalent to rounding up to the next highest hundredths decimal place.

5.5 SPCB

The critical power ratio (CPR) correlation used in MICROBURN-B2, SAFLIM2, RELAX, XCOBRA, and XCOBRA-T is the SPCB CPR correlation, documented in the approved Topical Report EMF-2209 Revision 2, *SPCB Critical Power Correlation*, September 2003. The SPCB CPR correlation uses F-effective (FEFF) values to account for rod local peaking, rod location and bundle geometry effects. The FEFF parameter is described in detail in Section 2.3 of Reference 30 and is composed of two parts. [

] The additive constants are determined from the experimental data. The FEFF values are not based on the lattice calculations from XFYRE or CASMO-4, they are determined based on the local peaking factors from [] from the MICROBURN-B2 calculations.

The FEFF values are not based on []. The FEFF values are computed for [] determined and used with SPCB.

The FEFF values are computed [] of the part-length rods. FEFF is [] for the vacant array locations above the top of the part-length rods.

5.6 **Loss Coefficients**

Wall friction and component loss coefficients were determined for Browns Ferry based on single-phase testing of a prototypic ATRIUM-10 fuel assembly in the Portable Hydraulic Test Facility (PHTF). Prototypical fuel rods, spacer grids, flow channel, upper tie plate, and lower tie plate were used in the testing. A description of the PHTF facility and an overview of the process for determining the component loss coefficients are described in Reference 29.

5.6.1 Spacer Pressure Drop Testing

The PHTF is used by AREVA NP to obtain single phase loss coefficients for the spacers. The friction factor correlation is based on previous tests performed in PHTF that remain applicable for current fuel designs (rods and channel have a consistent surface condition). The pressure drops across the spacers are measured in PHTF for each new fuel design. PHTF has pressure taps just upstream of the spacers so that the flow will be fully developed. The component of pressure drop due to friction is calculated and subtracted from the total measured pressure drop. The remaining pressure drop is due to the spacer and is used to determine the spacer pressure loss coefficient.

The wall friction and component loss coefficients determined from the PHTF and utilized in Browns Ferry are provided in Table 5-1. The values are valid in pre-EPU and EPU conditions and account for friction. The values have been selected because they are representative of the hydraulic characteristics of actual ATRIUM-10 fuel assemblies loaded into the reactor.

Distribution of channel flow is explicitly accounted for in analyses at pre-EPU and EPU conditions by analyzing the flow distribution in the channels given the wall friction and component loss coefficients of each hydraulic channel, plus representative axial and radial

power distributions for the plant conditions being analyzed. Therefore, friction parameters inherently account for the expected trend whereby channel flow redistributes at EPU conditions relative to pre-EPU conditions.

5.6.2 Preliminary ATRIUM-10 Spacer Loss Coefficients

Development of the ATRIUM-10 fuel design took place in Germany. Because PHTF pressure drop testing was not complete, single phase pressure drop data for the ATRIUM-10 was obtained from the German development effort. For the use in preliminary ATRIUM-10 design assessments, the German data was used to develop single phase spacer pressure loss coefficients appropriate for use with Richland hydraulic models. Analyses using these single phase losses resulted in an under prediction of the pressure drop data as shown in Figure 5-6. The spacer loss coefficients (K) used to generate the results presented in Figure 5-6 are of the form

$$K = A + B Re^C$$

where A, B, and C are constants and Re is the Reynolds number based on local fluid conditions and geometry.

Until PHTF data was available for the ATRIUM-10 design, a means of adjusting the German-based pressure loss coefficients to better predict the pressure drop data using Richland methods was developed. [

Figure 5-7. The spacer loss coefficients (K) used to generate the results presented in Figure 5-7 are of the form

$$[\quad]$$

where [] for the ATRIUM-10 design.

Further development of ATRIUM-10 spacer loss coefficients was subsequently performed based on PHTF ATRIUM-10 pressure drop data.

5.6.3 PHTF ATRIUM-10 Based Spacer Loss Coefficients

The ATRIUM-10 PHTF tests form the basis for the single phase loss coefficients currently used for design and licensing analyses supporting U.S. BWRs. PHTF data was reduced to determine single phase losses for the spacers in the lower (fully-rodded) region of the bundle, the spacer in the transition (end of part-length rods) region of the bundle, and the spacers in the upper (partially-rodded) region of the bundle.

Assessments of the predicted pressure drop relative to measured two-phase pressure drop data confirmed the applicability of the [] for use with spacer pressure loss coefficients based on PHTF data. Results of analyses for each region of the bundle (lower, transition, upper) when using the PHTF spacer loss coefficients [] are shown in Figure 5-8, Figure 5-9, and Figure 5-10.

On May 4, 1995, a meeting was held with the NRC to describe the ATRIUM-10 design and the application of the approved AREVA NP methodology for the design. Two view graphs extracted from those presented at the meeting are provided in Figure 5-11 and Figure 5-12. A summary of the May 4, 1995 meeting was provided to the NRC in Reference 26.

The XCOBRA-T two phase pressure drop models implemented in the 1-dimensional hydraulic model of the COTRANSA2 code, the local (spacer grid) pressure losses are automatically adjusted to preserve the core pressure drop predicted by the more detailed 3-dimensional hydraulic representation in MICROBURN-B2. The XCOBRA-T initial flow rate is defined by a hydraulic demand curve predicted by XCOBRA, which defines the relationship between assembly power and the initial flow rate and accounts for the lack of a core bypass model in XCOBRA-T.

The orifice loss coefficient is automatically adjusted in XCOBRA-T to preserve the COTRANSA2 (and MICROBURN-B2) initial core pressure drop and the initial flow rate defined by the hydraulic demand curve. Therefore, adjustments made to the local (spacer grid) pressure losses in COTRANSA2 appear in the adjustments to the orifice loss coefficient in XCOBRA-T.

5.6.4 Loss Coefficients for GE14 Fuel

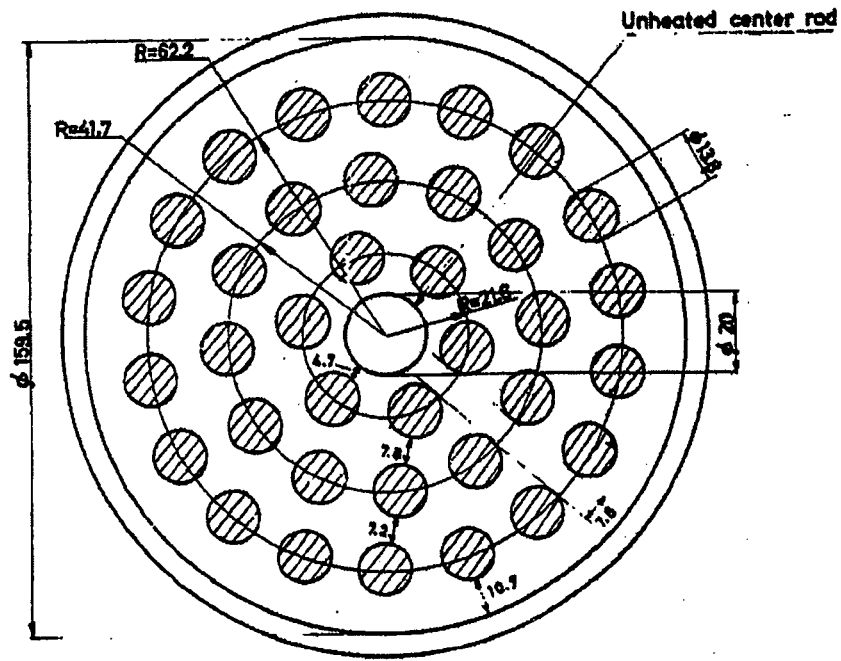
The GE14 fuel is hydraulically characterized in the same manner as the ATRIUM-10, i.e., a GE14 fuel assembly was tested in the PHTF. In addition to PHTF test data, TVA provided thermal-hydraulic data for the GE14 to assist in the characterization. Characterization of the ATRIUM-10 and GE14 is presented in the Thermal-Hydraulic design report.

**Table 5-1 Hydraulic Characteristics
of ATRIUM-10 Fuel Assemblies**

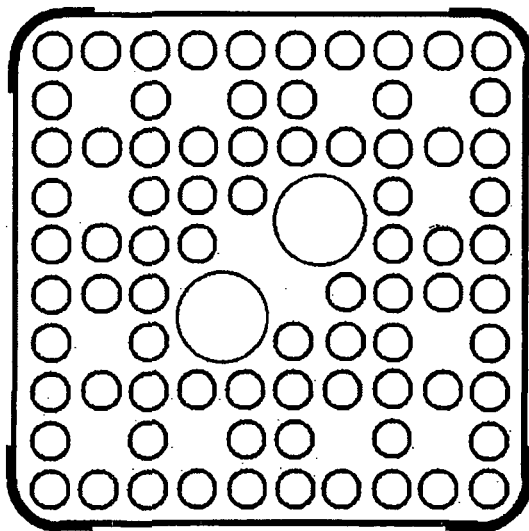


* Loss coefficients are referenced to the adjacent assembly bare rod flow area.

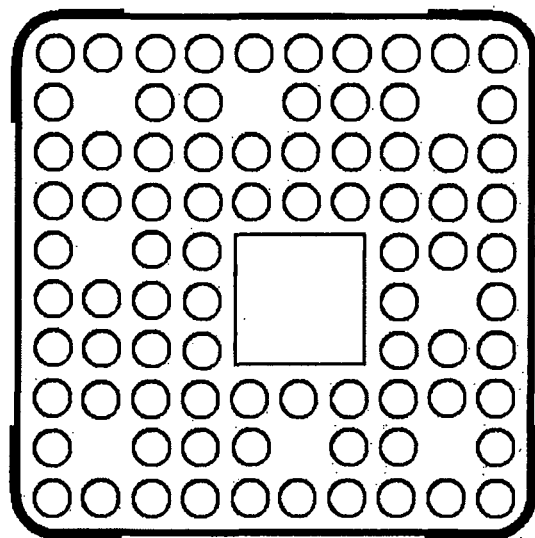
† Although there are 8 spacers, the losses associated with the bottom spacer are combined with the orifice/LTP model, so that only 7 spacers are explicitly modeled for ATRIUM-10.



FRIGG Test Cross Section



GE14



ATRIUM-10

Figure 5-1 Geometry



**Figure 5-2 Void Fraction Correlation
Comparison to FRIGG and ATRIUM-10 Test Data**



Figure 5-3 General Void Quality Correlation Behavior



Figure 5-4 Test Facility



Figure 5-5 Count Rate Plots



Figure 5-6 ATRIUM-10 Bundle Pressure Drop
[]



Figure 5-7 ATRIUM-10 Bundle Pressure Drop
[]



**Figure 5-8 ATRIUM-10 Lower Region Spacer Pressure Drop
Using PHTF Loss Coefficients**
[]



**Figure 5-9 ATRIUM-10 Transition Region Spacer Pressure Drop
Using PHTF Loss Coefficients**
[]



**Figure 5-10 ATRIUM-10 Upper Region Spacer Pressure Drop
Using PHTF Loss Coefficient**
[]



**Figure 5-11 Viewgraph From May 4, 1995 Presentation to NRC
Regarding ATRIUM-10 Fuel**



**Figure 5-12 Viewgraph From May 4, 1995 Presentation to NRC
Regarding ATRIUM-10 Fuel**

6.0 Transients and Accidents

6.1 Initial Core Power

AREVA NP uses two different approaches used to account for the 2 percent power factor in the analyses. Most of the analyses are performed at 100% power level and the impact of the two percent power factor is accounted for either statistically or through the inherent conservatism of the methodology. For three of the analyses, (ASME over-pressurization, loss of feedwater flow, and LOCA-ECCS analyses) the effects of the power uncertainty are not directly included in the methodology used for the analyses; therefore, these analyses are performed at 102% EPU power to account for the power uncertainty.

6.2 LHGR Limit

RODEX2A (Reference 27) is used to evaluate the fuel centerline temperature. RODEX2 in conjunction with the RAMPEX code (Reference 15) are used to evaluate cladding transient strain. The methodology for evaluating the cladding transient strain criterion and the fuel centerline melt criterion is described in Reference 27. Further clarification is contained in the TER for Reference 27 with regard to the cladding strain and fuel melt methods.

The core monitoring system is available during plant operations to monitor core performance parameters like MLHGR. The system models MLHGR explicitly, and the 24 hour surveillance requirement ensures that the result is routinely checked. Since the MLHGR is explicitly monitored during core operations, there are no additional surveillances or checks required to ensure that operations are within the bounds of the COLR analysis.

Regarding the fuel centerline melt criteria, the licensing analyses are performed to ensure the criteria will not be exceeded. For example, the flow run-up excursion analyses are performed employing all conservative assumptions with regard to the starting point on the power/flow map, i.e. the analyses are performed starting from a rod line that results in the most conservative result. Given the conservative bounding nature of the analyses, no further surveillances or checks are required.

6.3 Channel Bow Impact on Thermal-Mechanical Limits

The approach to account for channel bow in the mechanical limits methodology is described in the Item 13 response in Supplement 2 of Reference 24. The response is applicable to the ATRIUM-10 design since the local peaking and LHGR limits continue to provide margin to 1% strain and fuel centerline melt.

The 1% plastic strain limit, the fuel centerline melt limit, the LHGR at BOL, the degree of anticipated bow, and the LPF (local peaking factor) impact of that bow for the ATRIUM-10 design are described below for comparison to the values previously provided in Reference 24 for the 8x8 and 9x9 designs.

The respective typical LHGRs at fuel centerline melt and 1% cladding strain for the ATRIUM-10 design are [] kW/ft and [] kW/ft. The [] value is for a [] that is assumed to be at the allowed concentration of []. To provide an estimate of the LHGR at fuel centerline melt and at 1% cladding strain, it is necessary to extrapolate the results from existing analyses since the current analyses do not go high enough in power to reach either design limit. Note that the LHGRs at fuel melt and 1% strain in Reference 24 were likely obtained in the same way since the approved codes and methods used have not changed. For centerline melt, the fuel temperature []. A similar estimate is done for 1% cladding strain.

A typical ATRIUM-10 BOL LHGR limit is [] kW/ft. Figure 6-36 shows a typical LHGR limit for the ATRIUM-10 fuel. Note that the limit is now specified as a function of pellet exposure while previous limits are based on an assembly planar exposure.

A conservative value to use for the degree of anticipated bow for the ATRIUM-10 design is [] mils. This value is conservative for two reasons. First, the [] mils, when combined with bulge, is sufficient to result in contact with the control rod. Thus, higher values would be detectable in operation. Second, the [] mils is conservative because of the manner (described below) in which the bow value is applied in calculating the impact on the LPF.

A maximum change in lattice limiting LPF of [] is calculated to occur for a UO₂ rod located on the periphery of the fuel assembly lattice. The maximum change in LPF for a gadolinia rod is

[]. To calculate the increase in the LPF for a given amount of bow, a CASMO-4 colorset 4-bundle calculation was performed. Fuel channels on the three assemblies in the same control cell as the assembly of interest are bowed inward and outward (two cases) by a conservative amount and the channel on the assembly of interest is likewise bowed inward and outward by a conservative amount that is a function of lattice burnup. The change in LPF for each rod in the lattice is calculated. Note that a [] -mil change is assumed in the size of each of the four water gaps surrounding the assembly of interest.

Based on the information summarized above, the conclusion provided in the Item 13 response in Supplement 2 of Reference 24 for 8x8 and 9x9 fuel designs continues to apply for 10x10 fuel.

6.4 *Axial Power Shapes*

The transients are analyzed based on an assumed aggressive burn of the core at lower flow than is projected to be the case during actual plant operations. This provides a conservative margin to cover differences between the cycle step-out projection and actual plant operations. AREVA NP provides guidance for the reactor engineers in the form of a licensing basis axial power shape that the reactor engineers use to monitor actual operations. The reactor engineer's project actual operations to the end of cycle all rods out condition and compare the resulting axial power shape with that which is the basis of the licensing analyses, confirming compliance with the requirement.

6.5 *Fuel Rod Parameters*

For the pressurization transients, gap properties from RODEX2 are used to model the core average gap conductance in COTRANSA2 and the hot channel gap conductance in XCOBRA-T. The core average gap conductance in the system model is not the same as the gap conductance of the hot channel. The gap conductance of the system model is based on the average of all fuel in the core; whereas the hot channel gap conductance is based on a limiting assembly. The gap conductance is a function of exposure.

The COTRANSA2 system model includes the neutronic feedback from a change in the thermal time constant. [

]

[] The XCOBRA-T hot channel model uses the boundary conditions from COTRANSA2. A higher hot channel gap conductance in XCOBRA-T is conservative for pressurization events since higher values increase the heat flux and coolant quality, and thereby decrease the margin to boiling transition. These trends have been confirmed with AREVA NP sensitivity calculations.

For fuel rods early in life, the gap is not closed. AREVA NP applies the following conservatism for gap conductance for fuel rods with significant open gaps: [

]

A gap conductance sensitivity study was performed for the 100% power/105% flow BFN load rejection with no bypass (LRNB) transient event from Reference 31. The purpose of the sensitivity study was to show the Δ CPR trend for changes in gap conductance for COTRANSA2 versus XCOBRA-T. The gap conductance change considered was []. The results are provided in Table 6-1. As seen from the results, an increase in COTRANSA2 core average gap conductance results in a decrease in Δ CPR; whereas an increase in XCOBRA-T gap hot channel conductance results in an increase in Δ CPR. A decrease in gap conductance shows the opposite trend. The XCOBRA-T ATRIUM-10 hot channel model is slightly more sensitive to the change in gap conductance than the COTRANSA2 ATRIUM-10 average core model. When both COTRANSA2 and XCOBRA-T gap conductance are changed by an equivalent amount, the net impact is no significant change in Δ CPR.

6.6 *Transient Hot Channel Analyses*

The XCOBRA-T hot channel analysis is used to determine the peak LHGR during the transient. The XCOBRA-T hot channel analysis determines the assembly radial peaking factor that results in dryout during the transient. The peak axial LHGR in the fuel assembly during the transient is also calculated in this analysis. However, because the maximum allowed steady state LHGR may be higher than the initial LHGR used in the XCOBRA-T hot channel analysis, the peak transient LHGR may be higher than calculated in the XCOBRA-T analysis. The peak LHGR for the transient is determined []

[

] If necessary, the steady state LHGR limit is adjusted to ensure that the peak transient LHGR remains below the transient LHGR limit established from RODEX2 analyses. Exceeding the transient LHGR limit does not necessarily mean that fuel centerline melt or 1% cladding strain occurred. Particularly for fast pressurization transients, significant margin to fuel centerline melt and 1% cladding strain may exist.

Except for post-dryout conditions, which are not experienced for XCOBRA-T analyses, the thermal resistance of the fluid surrounding the cladding is much less than the resistance of the cladding, gap and pellet. A detailed two-fluid representation of the liquid film and vapor fields may determine a different fluid thermal resistance; however, the magnitude of the difference in the fluid resistance will not be significant relative to the total resistance and would not result in a significant impact on the cladding heat flux. Therefore, the limitations of the fluid model in XCOBRA-T would not impact the evaluations of the transient peak LHGR.

For the pressurization transients, gap properties from RODEX2 are used to model the core average gap conductance in COTRANSA2 and the hot channel gap conductance in XCOBRA-T. The core average gap conductance in the system model is not the same as the gap conductance of the hot channel. The gap conductance of the system model is based on the average of all fuel in the core; whereas the hot channel gap conductance is based on a limiting assembly. The gap conductance is a function of exposure.

6.7 Void Quality Correlation Uncertainties

The AREVA NP analysis methods and the correlations used by the methods are applicable for both pre-EPU and EPU conditions. The approach for addressing void-quality correlation bias and uncertainty remains unchanged and is applicable for BFN EPU operation.

The OLMCPR is determined based on the safety limit MCPR (SLMCPR) methodology and the transient analysis (Δ CPR) methodology. Void-quality correlation uncertainty is not a direct input to either of these methodologies; however, the impact of void-correlation uncertainty is inherently incorporated in both methodologies as discussed below.

The SLMCPR methodology explicitly considers important uncertainties in the Monte Carlo calculations performed to determine the number of rods in boiling transition. One of the uncertainties considered in the SLMCPR methodology is the bundle power uncertainty. This uncertainty is determined through comparison of calculated to measured core power distributions. Any miscalculation of void conditions will increase the error between the calculated and measured power distributions and be reflected in the bundle power uncertainty. Therefore, void-quality correlation uncertainty is an inherent component of the bundle power uncertainty used in the SLMCPR methodology.

The transient analysis methodology is not a statistical methodology and uncertainties are not directly input to the analyses. The transient analysis methodology is a deterministic, bounding approach that contains sufficient conservatism to offset uncertainties in individual phenomena. Conservatism is incorporated in the methodology in two ways: (1) computer code models are developed to produce conservative results on an integral basis relative to benchmark tests, and (2) important input parameters are biased in a conservative direction in licensing calculations.

The transient analysis methodology results in predicted power increases that are bounding relative to benchmark tests. In addition, for licensing calculations a 110% multiplier is applied to the calculated integral power to provide additional conservatism to offset uncertainties in the transient analysis methodology. Therefore, uncertainty in the void-quality correlation is inherently incorporated in the transient analysis methodology.

Based on the above discussions, the impact of void-quality correlation uncertainty is inherently incorporated in the analytical methods used to determine the OLMCPR. Biasing of important input parameters in licensing calculations provides additional conservatism in establishing the OLMCPR. No additional adjustments to the OLMCPR are required to address void-quality correlation uncertainty.

6.7.1 Assessment of the Void-Quality Correlation

In response to ACRS questions on the impact of uncertainties in the void-quality correlation, a sensitivity study was performed for an uprated BWR to assess the impact on licensing limits of biasing the current correlation towards the extreme of the ATRIUM-10 correlation data.

[

]

	Reference Depletion	Ohkawa-Lahey Depletion	Change
Limiting ΔCPR	[]	[]	[]
Licensing ΔCPR (2 significant digits)	[]	[]	[]

[

]

The same approach, substituting the Ohkawa-Lahey correlation in the cycle depletion, was also applied to a BFN plant specific calculation for a proposed EPU core design with the Ohkawa-Lahey alternate void-quality correlation. The BFN calculation demonstrated that the change in the SLMCPR (0.0017) and in the Δ CPR (0.0001) were small and did not impact the OLMCPR.

6.7.2 Biasing of the Void-Quality Correlation

While the previous studies provide evidence that the OLMCPR is not sensitive to reasonable changes in the void-quality correlation, additional studies were performed to determine the sensitivity to biases approaching the upper and lower extremes of the data comparisons.

Two additional studies were performed to assess the void-quality correlation. The first study propagated a change in the void-quality correlation to the calculation of the OLMCPR. The second study assessed the impact of only a change in the void reactivity coefficient in the transient response.

For the first study, the transient Δ CPR impact was determined by propagating void-quality biases through three main computer codes: MICROBURN-B2, COTRANSA2, and XCOBRA-T.

The [] correlation in MICROBURN-B2 was modified to correct the mean to match the measured ATRIUM-10 void fraction data. The modified [] correlation parameters were then modified to generate two bounding correlations for the ATRIUM-10 of ± 0.05 void. The results of this modified correlation are presented in Figure 6-5.

COTRANSA2 does not have the [] correlation. To avoid additional time needed to incorporate the [] correlation or modify the Ohkawa-Lahey correlation, the modified [] correlations in MICROBURN-B2 were approximated in COTRANSA2 with []. Figure 6-6 shows a comparison of the [] ratio results compared to the ATRIUM-10 test data. This approach created equivalent void fractions as the [] correlation modifications.

Like COTRANSA2, XCOBRA-T does not have the [] correlation. Unlike COTRANSA2, XCOBRA-T does not have [

]. For the other void scenarios, no correction was done in XCOBRA-T. Not modifying the void-quality correlation for the other void scenarios results in a very small difference in Δ CPR.

The second study assessed the impact of only a change in the void reactivity coefficient by increasing [] in COTRANSA2 by the ratio of the void reactivities (+0.05 Case/Reference Case) computed by MICROBURN-B2.

The transient response was assessed with a BFN plant specific calculation performed for a proposed EPU core design. The impact of the change in the void correlations was also captured in the burn history of the fuel. The SLMCPR response was also assessed with the new input corresponding to the three different void scenarios. The results are provided in Table 6-2.

As previously stated, the sensitivity study are based on depleting the fuel with the change in the void correlations (the results are not for an instantaneous change in the void correlations). Selected data comparisons are provided as follows:

- The limiting bundle: core location and initial radial peaking factor (Table 6-4).
- Initial axial power shape (Reference case) (Figure 6-7).
- Plots of the perturbed axial power shapes (initial conditions) (Figure 6-7).

- Plots of the perturbed radial core power shapes (initial conditions) (Figure 6-8).
- Plots of transient limiting bundle peak rod heat flux at axial heights of (x/L) 25%, 50%, and 75% (Figure 6-9 to Figure 6-11).
- Plots of transient limiting bundle mass flow rate at axial heights of (x/L) 0%, 25%, 50%, 75% and 100% (Figure 6-12 to Figure 6-16).
- Plots of transient critical power ratio (CPR) (Figure 6-17).
- A comparison of the predicted power pulse heights and widths (Table 6-3).

The thermal hydraulic methodology incorporates the effects of subcooled boiling through use of the Levy model. The Levy model predicts a critical subcooling that defines the onset of boiling. The critical subcooling is used with a profile fit model to determine the total flow quality that accounts for the presence of subcooled boiling. The total flow quality is used with the void-quality correlation to determine the void fraction. This void fraction explicitly includes the effects of subcooled boiling. Application of the Levy model results in a continuous void fraction distribution at the boiling boundary.

The major influence that the void-quality models have on scram reactivity worth is through the predicted axial power shape. The void-quality models used for ATRIUM-10 fuel result in a very good prediction of the axial power shape.

As seen in the results, modifying the void-quality correlations to correct the mean to match the measured ATRIUM-10 void fraction data results in a very small increase in Δ CPR, a very small decrease in SLMCPR, and a very small increase in OLMCPR for this study; therefore, the impact of the correlation bias is insignificant.

The +0.05 void scenarios show an increase in the OLMCPR; however, as mentioned previously, the transient analysis methodology is a deterministic, bounding approach that contains sufficient conservatism to offset uncertainties in individual phenomena. Conservatism is incorporated in the models to bound results on an integral basis relative to benchmark tests. For licensing calculations, important input parameters are biased in a conservative direction. In addition, the licensing calculations include a 110% multiplier to the calculated integral power to provide additional conservatism to offset uncertainties in the transient analysis methodology (which includes the void-quality correlation). Even with an extreme bias in the void correlation of +0.05,

the conservatism introduced by the 110% multiplier is alone sufficient to offset the increase in results in the first study. The conservatism of the 110% multiplier was []. These calculations demonstrate that the overall methodology has sufficient conservatism to account for both the bias and the uncertainty in the void-quality correlation.

To provide a more accurate assessment of the impact of a +0.05 void bias, AREVA NP would need to re-evaluate the Peach Bottom transient benchmarks; it is likely that the +0.05 void scenario would show overconservatism in the benchmarks. Likewise, the pressure drop correlations and core monitoring predictions of power will likely show a bias relative to measured data. Correcting the models to new benchmarks and measured data would further reduce the OLMCPR sensitivity.

6.7.3 Additional Sensitivity Analysis for SLMCPR

It should be noted that the sensitivity analyses presented in the Section 6.7.2 response were not based on "fixed" void fraction changes. Rather, the analyses were based on modifications to the void-quality correlation that resulted in a new nominal fit and offsets that were on average ± 0.05 void. The information included the impact of the fuel depleted with the changes in the void-quality correlation. The difference in depletion changes the sensitivity of void fraction modifications considerably due to the feedback of modified power distributions on exposure distribution.

For Section 6.7.2, the change in the void-quality correlation was imposed over all fuel in the core from beginning of life. No changes were made to the fuel loading and rod patterns. The result of this was that a reduction in void resulted in more assemblies at higher power. The radial peaking factors of the high-powered assemblies that contributed to rods in boiling transition were slightly more "flat" and resulted in a slightly higher SLMCPR. Figure 6-1 shows the slight differences in radial distributions.

The sensitivity analysis of Section 6.7.2 was repeated for an instantaneous change in voids. For an instantaneous change in voids, the SLMCPR trends were the same as in Section 6.7.2; however, the change is small for both depleted and instantaneous void change, i.e., an SLMCPR change of -0.003 for +0.05 voids and $+0.002$ for -0.05 voids. The sensitivity can be explained by the small radial power distribution shifts in Figure 6-2 and Figure 6-3. It is

concluded that the radial distribution is not significantly changed for the SLMCPR analysis; therefore, the impact of the prescribed void-quality correlation changes is insignificant on SLMCPR.

It is very difficult to identify the expected direction of the radial power distribution change due to a modification of the void-quality correlation. In addition to the void coefficient dependency on void fraction there is an even stronger dependency of the void coefficient on exposure. For the limiting case of SLMCPR the highest radial powers come from a range of assembly exposures. The importance of void changes in different assemblies of different exposures cannot be analyzed with simplified models and isolated trends.

Independent of the trend, the analyses demonstrate insignificant impacts on SLMCPR.

6.7.4 Impact on MICROBURN-B2 Accuracy

As discussed in Section 6.7.2 the [] correlation in MICROBURN-B2 was modified to adjust the mean to match the measured ATRIUM-10 void fraction data for both high and low void fractions. The modified [] correlation was then further modified to generate two bounding correlations for the ATRIUM-10 data of ± 0.05 mean void. The results of the modified correlations were shown in Figure 6-5 and were used in Sensitivity Study 1 and Study 2.

The sensitivity studies described in Section 6.7.2 are somewhat artificial and only capture the sensitivity of portions of the methodology to void correlation uncertainty. Study 2 is especially artificial in that the results of the study only reflect the increase in core void reactivity coefficient. Study 2 does not reflect that a different change in void fraction would occur for a given pressure change with the modified void correlation. Study 1 included this effect and resulted in a smaller effect on the operating limit MCPR (OLMCPR). Other effects of using a different void correlation uncertainty are not incorporated into the Study 1 (e.g., pressure drop correlation coefficients would be different). These sensitivity studies are not complete assessments of the impact of void correlation uncertainty on OLMCPR.

It should be noted that a ± 0.05 perturbation of the void correlation used in the Section 6.7.2 sensitivity studies is substantial. For example, the +0.05 void scenario is equivalent to a []. The

measure of void correlation uncertainty used in the sensitivity analyses was somewhat arbitrarily defined as a value that would bound the ATRIUM-10 test data. In a BWR, the core power and power distribution are tightly coupled with the void fraction and a large error in predicted core void fraction would have a significant effect on the predicted power distribution measurements obtained from operating reactors. If the error in void fraction was as large as assumed in the Section 6.7.2 sensitivity studies, the effect would be observed in comparisons of predicted to measured power distributions obtained from operating reactors.

Additional calculations were performed [

[

]

These results confirm the conclusion stated above that the increased void variation of +0.05 is not realistic.

6.7.5 Void-Quality Correlation Uncertainty Summary

Integral power is a parameter obtainable from test measurements that is directly related to Δ CPR and provides a means to assess code uncertainty. The COTRANSA transient analysis methodology was a predecessor to the COTRANSA2 methodology. The integral power figure of merit was introduced with the COTRANSA methodology as a way to assess (not account for) code uncertainty impact on Δ CPR. From COTRANSA analyses of the Peach Bottom turbine trip tests, the mean of the predicted to measured integral power was 99.7% with a standard deviation of 8.1%. AREVA NP (Exxon Nuclear at the time) initially proposed to treat integral power as a statistical parameter. However, following discussions with the NRC, it was agreed to apply a deterministic 110% integral power multiplier (penalty) on COTRANSA calculations for licensing analyses. That increase was sufficient to make the COTRANSA predicted to measured integral power conservative for all of the Peach Bottom turbine trip tests.

COTRANSA2 is not a statistical methodology and uncertainties are not directly input to the analyses. The methodology is a deterministic bounding approach that contains sufficient conservatism to offset uncertainties in individual phenomena. Conservatism is incorporated in the methodology in two ways: (1) computer code models are developed to produce conservative results on an integral basis relative to benchmark tests, and (2) important input parameters are biased in a conservative direction in licensing calculations. Justification that the integrated effect of all the conservatisms in COTRANSA2 licensing analyses is adequate for EPU operation is provided below.

The COTRANSA2 methodology results in predicted power increases that are bounding ([] on average) relative to Peach Bottom benchmark tests. In addition, for licensing calculations a 110% multiplier is applied to the calculated integral power to provide additional conservatism.

This approach adds significant conservatism to the calculated OLMCPR as discussed previously.

Biasing of important input parameters in licensing calculations provides additional conservatism in establishing the OLMCPR. The Peach Bottom turbine trips were performed assuming the measured performance of important input parameters such as control rod scram speed and turbine valve closing times. For licensing calculations, these (and other) parameters are biased in a conservative bounding direction. These conservative assumptions are not combined statistically; assuming all parameters are bounding at the same time produces very conservative results.

Assessments such as the Peach Bottom tests indicate that the integrated effect of all the conservatism in COTRANSA2 is adequate for non-EPU reactor conditions (as stated in the RAI). To demonstrate that the impact of the change in void-quality correlations is similar for EPU and non-EPU conditions, the Section 6.7.2 sensitivity analyses (Study 1) were repeated for BFN without EPU. The change in Δ CPR relative to the reference cases for EPU and non-EPU are shown in the table below:

$\Delta(\Delta$ CPR)		
Case	EPU	Non-EPU
+0.05 void	+0.016	+0.024
-0.05 void	-0.001	-0.007

Based on these results for EPU and non-EPU conditions, it is concluded that EPU conditions do not increase the sensitivity to a change in the void correlation.

As discussed previously, the core axial power distribution is tightly coupled with the void fraction. A large error in predicted void fraction would have a significant effect on the predicted axial power distribution measurements obtained from operating reactors. The very good comparisons between predicted and measured axial power distributions obtained from operating reactors indicates that the void distribution within the core is being predicted well.

Minimal plant transient data at EPU conditions is available to benchmark transient analysis methodologies. However, at the request of the NRC, a COTRANSA2 analysis was performed for a recent event that occurred at a BWR/4 approved for EPU operation. The event involved a reduction in pump speed in one of the recirculation loops followed by a sudden increase in the pump speed approximately 40 seconds later. The event did not pose a challenge to the fuel; however, the event did result in a significant change in core void fraction. Because of the tight coupling between core void fraction and core power, a comparison of the predicted to measured core power response during the event is a good way to assess the accuracy of the void correlation. For this analysis, a best estimate approach was used and event specific licensing conservatisms were not applied (e.g., measured data used as boundary conditions, realistic control system parameters, best estimate core neutronics data). The recirculation pump speed versus time from the plant data was used as a boundary condition for the analysis (Figure 6-33). The COTRANSA2 analysis predicted the core power and reactor pressure response very well (Figure 6-34 and Figure 6-35). The very good agreement for the predicted core power reached following the pump runback and the following pump runup indicates a good prediction of the core void fraction during the event.

Based on the above discussions, the impact of void correlation uncertainty is inherently incorporated in the analytical methods used to determine the OLMCPR. No additional adjustments to the OLMCPR are required to address void correlation uncertainty.

Since both the impact of a void correlation bias and the conservatism of the overall methodology (110% integral power multiplier) are expected to scale with the cycle specific transient response, the conservatism of the overall methodology is equally applicable to the Browns Ferry Unit 1 transition cycles.

6.8 *Doppler Effect on Cross Sections*

[

]

[

]



1

1

[

]

[

]

6.9 **Fuel Rod Model Changes**

NRC approval of the RODEX2 computer code is found in the Safety Evaluation Report associated with Reference 15.

NRC approval of a modification to the RODEX2 fission gas release model for application to BWRs is found in Reference 16. RODEX2A is acceptable for mechanical analyses. However, RODEX2 remains the approved model for LOCA and transient analysis methodologies. As described in the Technical Evaluation Report associated with Reference 16, the RODEX2A code is based on the RODEX2 code with modifications only to the fission gas release model while the thermal and mechanical portions remain identical to the RODEX2 code.

The limitation on the []
with NRC approval of Reference 17.

Use of RODEX2 for BWR applications (including LOCA and transient thermal-hydraulic analysis methodologies) to [] was acknowledged by the NRC in the Safety Evaluation Report Clarification associated with Reference 27.

Extension of RODEX2A burnup limit was approved in Reference 27. The Safety Evaluation Report for this document suggests that the RODEX2A code was "improved" relative to prior approvals. However, no changes were actually made to the code, only the benchmarking was extended to higher rod-average burnup. This point is made in Section 1.0 of the report.

With the exception of the changes associated with increasing the concentration of gadolinium that was approved in Reference 17, no changes (other than error corrections) have been made to the originally approved RODEX2 and RODEX2A models. Reproducibility of the RODEX2

and RODEX2A results relative to the results originally submitted to the NRC in References 15 and 16 were confirmed as recently as 2001 as described in Reference 28.

Since no updates have been made to RODEX2 or RODEX2A since the approval of XCOBRA-T, the fuel rod thermal conduction models approved for XCOBRA-T in Reference 20 are unchanged.

6.9.1 Comparison of RODEX2 to RODEX4

RODEX4 was submitted for review for use in thermal-mechanical calculations only and not for use in LOCA or transient applications. RODEX4 performs a best estimate calculation with both steady-state and transient temperature solution capability. All the RODEX4 fuel thermal-mechanical properties [

] All the Zircaloy thermal-mechanical properties used in RODEX4, [] RODEX4 properties are further described in the RODEX4 theory manual [] .

No RODEX2 models have been updated subsequent to the NRC review and approval of RODEX2, except those associated with the NRC approved update to the [] (Reference 17). For instance, the NRC Safety Evaluation approving RODEX2 for [] for PWR applications in Reference 22 identified that no models were changed relative to original approval in Reference 15. Instead, only additional comparisons were made to demonstrate the applicability of the code to [] . Note, the same RODEX2 code version is used for both PWR and BWR applications.

Reproducibility of the RODEX2 results relative to the results originally submitted to the NRC in Reference 15 was confirmed as recently as 2001 as described in Reference 28.

6.10 ***Nodalization***

The Browns Ferry radial channel nodalization was evaluated as follows:

- Each bundle is uniquely modeled hydraulically and neutronically in MICROBURN-B2 to establish input to the transient calculation at the desired state point. The limiting assemblies are identified from the MICROBURN-B2 results prior to running the transient.

Table 6-5 provides the predicted radial power distribution for the limiting transient analysis of a recent EPU calculation for Unit 3 Cycle 14 (this is the same unit and cycle that is the basis for other RAI sensitivity studies).

- The fuel assemblies in the core are collapsed to 1-D hydraulically and neutronically in COTRANSA2 analyses.
- With the exception of the most limiting assembly in each group of hydraulically equivalent assemblies, hydraulically equivalent assemblies are collapsed into their respective groups in the XCOBRA analyses. Multiple calculations are then performed on the power of the most limiting assembly to determine its relationship between assembly power and the inlet flow rate. Because assembly flow is very nearly linear with assembly power, there is no sensitivity to the amount of grouping in the XCOBRA analyses when determining the relationship between assembly power and the inlet flow rate.
- Individual limiting assemblies are analyzed in the XCOBRA-T Delta-CPR calculations, there is no grouping. The limiting assemblies are identified by having the [] for each unique fuel type. In situations where different assemblies of the same type (e.g., ATRIUM-10) are being considered as limiting, the F-effective defining the fuel type is the limiting F-effective of the different assemblies. The initial flow rate in each calculation is consistent with the relationship between assembly power and the flow rate calculated by XCOBRA. The transient hydraulic response in XCOBRA-T is driven by the lower-to-upper plenum pressure response predicted by COTRANSA2. Table 6-6 identifies the limiting assemblies for which Delta-CPR was analyzed by XCOBRA-T in the Unit 3 Cycle 14 limiting transient analysis. Note, only one assembly is listed because this cycle is an all-ATRIUM-10 core. Table 6-6 also provides the radial peaking factor for the limiting assembly from the MICROBURN-B2 analysis as well as the converged radial peaking factor from the XCOBRA-T analysis that was determined to result in dryout during the transient.

In summary, the above discussion shows that the transient analysis methodology has sufficient resolution to model the transient behavior in all potentially limiting bundles, and is justified for use in analyzing the limiting transient analyses at EPU conditions.

Table 6-1 Gap Conductance Study

Increase in Gap Conductance	
Gap conductance condition	$\Delta(\Delta\text{CPR})$
Core average []	-0.011
Hot channel []	+0.012
Core average and hot channel []	0.000
Decrease in Gap Conductance	
Gap conductance condition	$\Delta(\Delta\text{CPR})$
Core average []	+0.015
Hot channel []	-0.016
Core average and hot channel []	-0.001

Table 6-2 Void Sensitivity Results

Parameter	Reference Calculation	Study 1 Modified V-Q (0.0)	Study 1 Modified V-Q (+0.05)	Study 1 Modified V-Q (-0.05)	Study 2 Modified V-Q (+0.05)
ΔCPR	0.305	0.307	0.321	0.305	0.332
SLMCPR	1.09	1.09	1.09	1.09	1.09
ΔSLMCPR	NA	-0.001	-0.002	+0.002	0.000
OLMCPR	1.395	1.396	1.409	1.397	1.422

Table 6-3 Power Pulse

Void	Pulse Width (sec)	Pulse Height (% rated)
Reference	0.53	318
Modified	0.56	330
Modified +0.05	0.58	328
Modified -0.05	0.54	330

Table 6-4 Limiting Bundle Data

	Reference Calculation	Study 1 Modified V-Q (-0.05)	Study 1 Modified V-Q (0.0)	Study 1 Modified V-Q (+0.05)
Location in Core I,J	23,24	21,22	23,24	37,24
MB2 initial radial peaking factor	1.314	1.295	1.329	1.346
XCT converged initial peaking factor radial ^{**}	[]	[]	[]	[]

REGIONS

IR: 1 3 5 7 9 11 13 15 17 19 21 23 25 27 29 31 33 35 37 39 41 43 45 47 49 51 53 55 57 59

JR: BFA

60				1	2	3	4	5	6	7	8	9	10	11	12	13	14														
58				15	16	17	18	19	20	21	22	23	24	25	26	27	28	29	30												
56				31	32	33	34	35	36	37	38	39	40	41	42	43	44	45	46	47	48	49	50								
54				51	52	53	54	55	56	57	58	59	60	61	62	63	64	65	66	67	68	69	70								
52				71	72	73	74	75	76	77	78	79	80	81	82	83	84	85	86	87	88	89	90	91	92						
50				93	94	95	96	97	98	99	100	101	102	103	104	105	106	107	108	109	110	111	112	113	114	115	116	117	118		
48				119	120	121	122	123	124	125	126	127	128	129	130	131	132	133	134	135	136	137	138	139	140	141	142	143	144		
46				145	146	147	148	149	150	151	152	153	154	155	156	157	158	159	160	161	162	163	164	165	166	167	168	169	170	171	172
44	173	174	175	176	177	178	179	180	181	182	183	184	185	186	187	188	189	190	191	192	193	194	195	196	197	198	199	200	201	202	
42	203	204	205	206	207	208	209	210	211	212	213	214	215	216	217	218	219	220	221	222	223	224	225	226	227	228	229	230	231	232	
40	233	234	235	236	237	238	239	240	241	242	243	244	245	246	247	248	249	250	251	252	253	254	255	256	257	258	259	260	261	262	
38	263	264	265	266	267	268	269	270	271	272	273	274	275	276	277	278	279	280	281	282	283	284	285	286	287	288	289	290	291	292	
36	293	294	295	296	297	298	299	300	301	302	303	304	305	306	307	308	309	310	311	312	313	314	315	316	317	318	319	320	321	322	
34	323	324	325	326	327	328	329	330	331	332	333	334	335	336	337	338	339	340	341	342	343	344	345	346	347	348	349	350	351	352	
32	353	354	355	356	357	358	359	360	361	362	363	364	365	366	367	368	369	370	371	372	373	374	375	376	377	378	379	380	381	382	
30	383	384	385	386	387	388	389	390	391	392	393	394	395	396	397	398	399	400	401	402	403	404	405	406	407	408	409	410	411	412	
28	413	414	415	416	417	418	419	420	421	422	423	424	425	426	427	428	429	430	431	432	433	434	435	436	437	438	439	440	441	442	
26	443	444	445	446	447	448	449	450	451	452	453	454	455	456	457	458	459	460	461	462	463	464	465	466	467	468	469	470	471	472	
24	473	474	475	476	477	478	479	480	481	482	483	484	485	486	487	488	489	490	491	492	493	494	495	496	497	498	499	500	501	502	
22	503	504	505	506	507	508	509	510	511	512	513	514	515	516	517	518	519	520	521	522	523	524	525	526	527	528	529	530	531	532	
20	533	534	535	536	537	538	539	540	541	542	543	544	545	546	547	548	549	550	551	552	553	554	555	556	557	558	559	560	561	562	
18	563	564	565	566	567	568	569	570	571	572	573	574	575	576	577	578	579	580	581	582	583	584	585	586	587	588	589	590	591	592	
16	593	594	595	596	597	598	599	600	601	602	603	604	605	606	607	608	609	610	611	612	613	614	615	616	617	618	619	620			
14	621	622	623	624	625	626	627	628	629	630	631	632	633	634	635	636	637	638	639	640	641	642	643	644	645	646					
12	647	648	649	650	651	652	653	654	655	656	657	658	659	660	661	662	663	664	665	666	667	668	669	670	671	672					
10	673	674	675	676	677	678	679	680	681	682	683	684	685	686	687	688	689	690	691	692	693	694									
8	695	696	697	698	699	700	701	702	703	704	705	706	707	708	709	710	711	712	713	714											
6	715	716	717	718	719	720	721	722	723	724	725	726	727	728	729	730	731	732	733	734											
4	735	736	737	738	739	740	741	742	743	744	745	746	747	748	749	750															
2	751	752	753	754	755	756	757	758	759	760	761	762	763	764																	

IR: 1 3 5 7 9 11 13 15 17 19 21 23 25 27 29 31 33 35 37 39 41 43 45 47 49 51 53 55 57 59

** The XCOBRA-T radial that results in a [] during the transient event.

**Table 6-6 Limiting Assemblies
Analyzed in the Unit 3 Cycle 14
Limiting Transient Analysis**

Limiting Bundle Information	
Initial MCPR	1.5905
Location in Core I,J	23,24
MB2 radial power	1.3138
XCT converged radial	1.5465

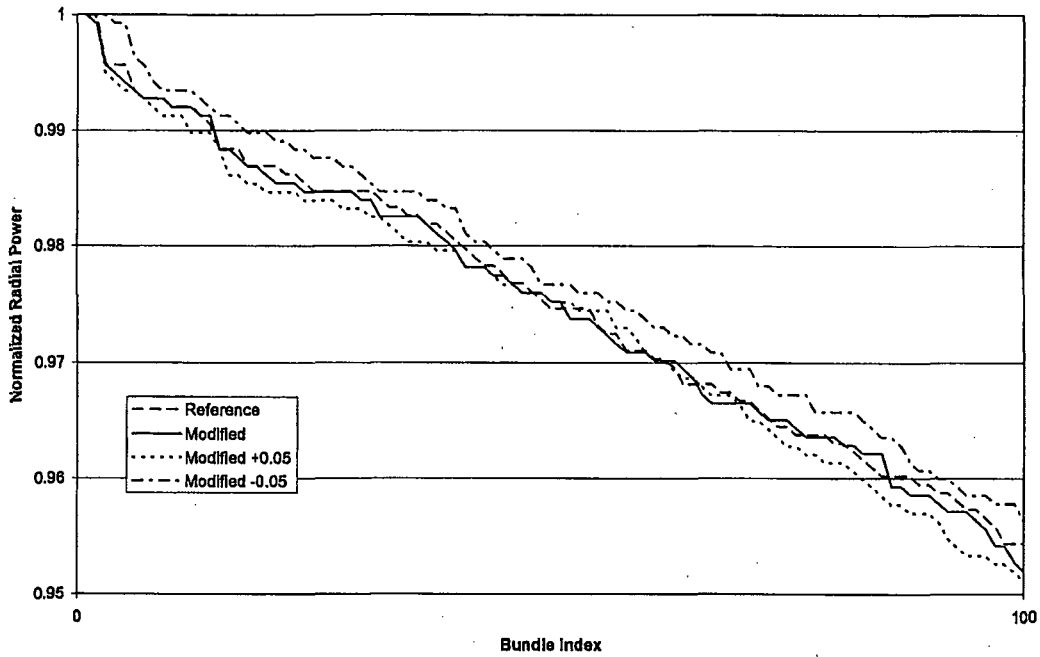


Figure 6-1 SLMCPR Radial Power Distribution High-Powered Assemblies Depleted Voids

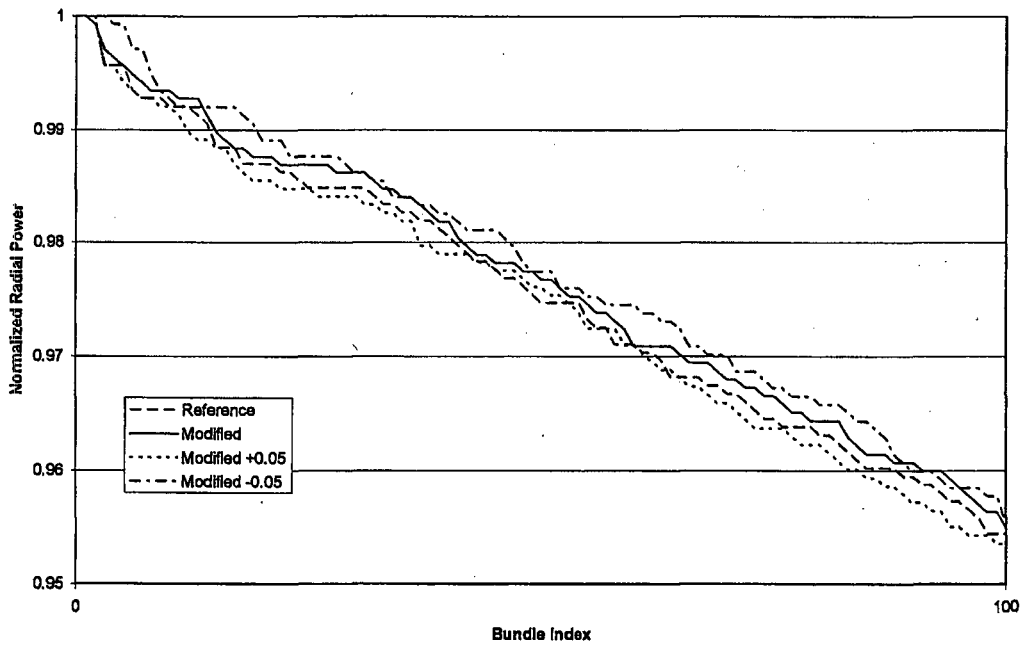


Figure 6-2 SLMCPR Radial Power Distribution High-Powered Assemblies Instantaneous Voids

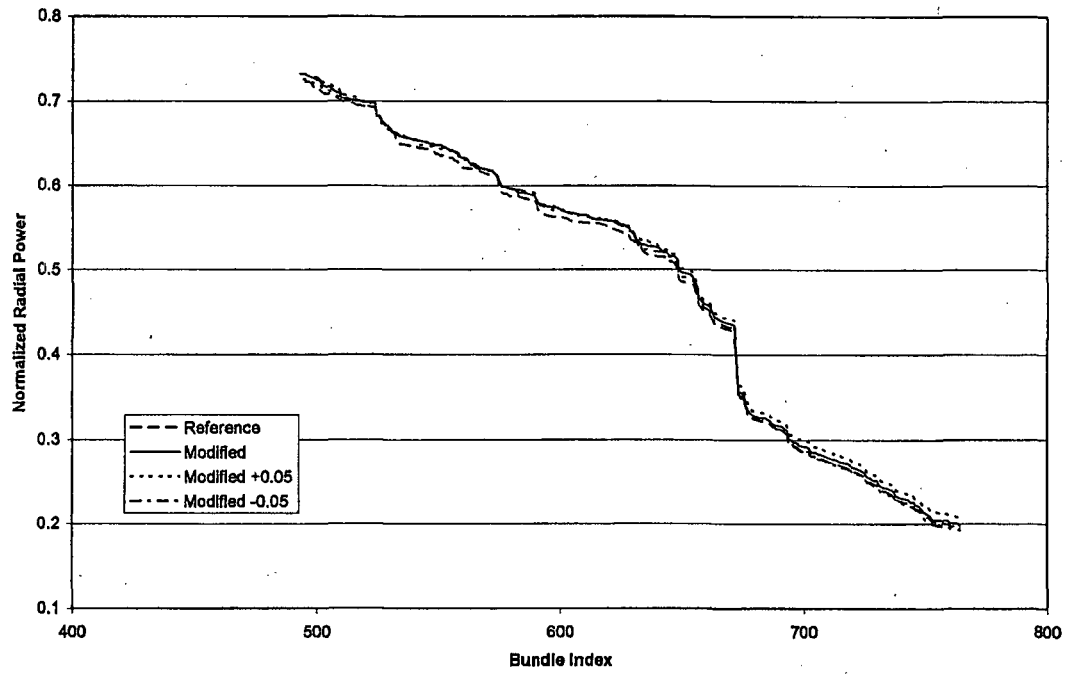


Figure 6-3 SLMCPR Radial Power Distribution Low-Powered Assemblies Instantaneous Voids



**Figure 6-4 Void Fraction Correlation
Comparison to FRIGG and ATRIUM-10 Test Data**



**Figure 6-5 Modified Void Fraction Correlation
Comparison to ATRIUM-10 Test Data**

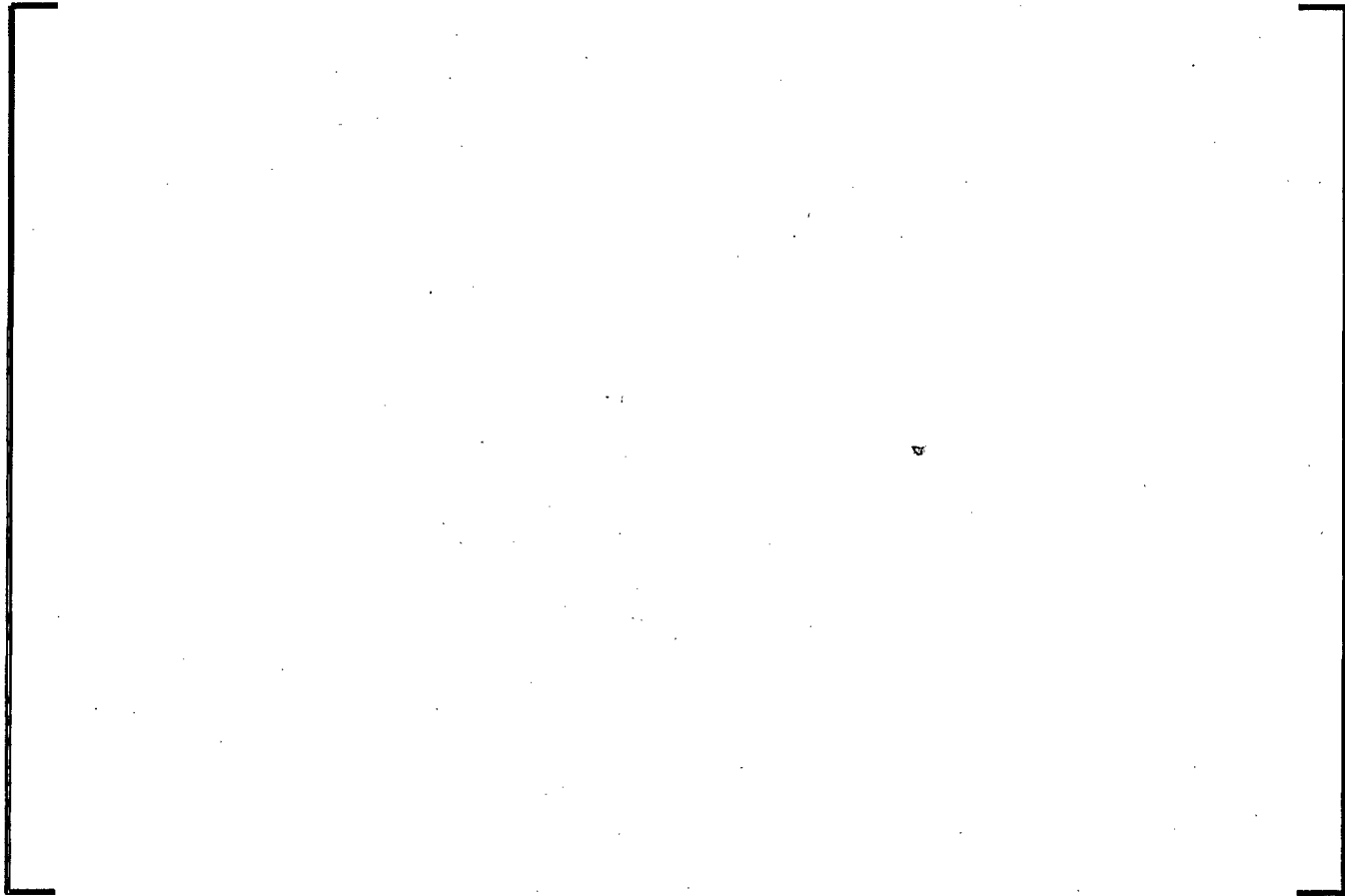


**Figure 6-6 [] Void Fraction Results
Comparison to ATRIUM-10 Test Data**

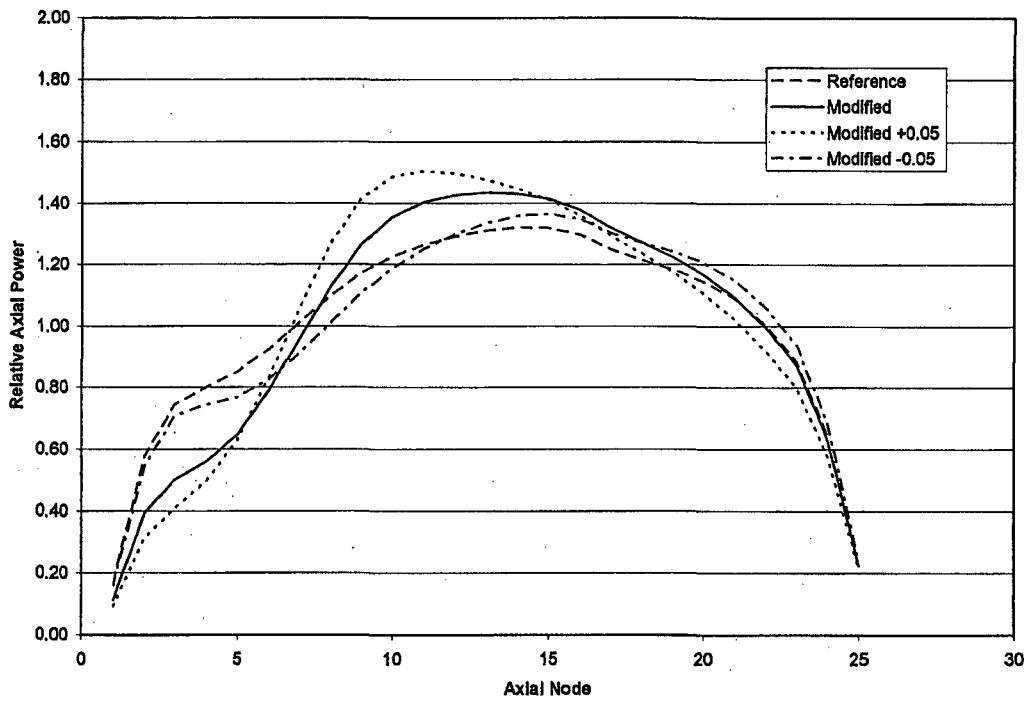


Figure 6-7 Initial Axial Power Shape - Depleted Voids

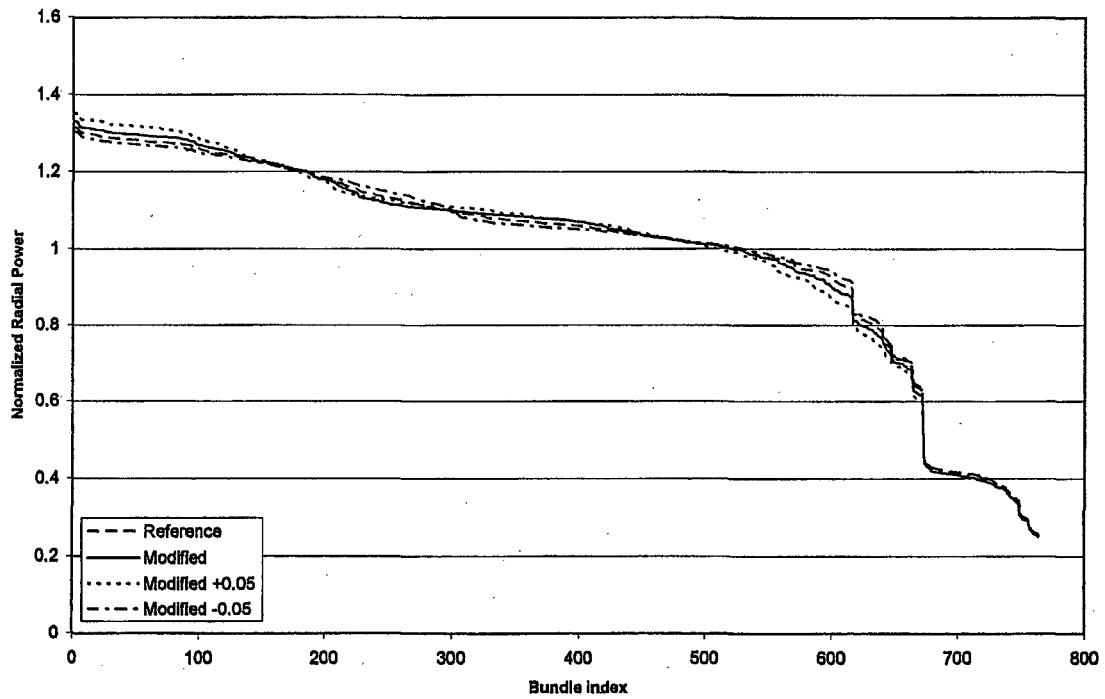


Figure 6-8 Initial Radial Power Distribution From Transient Analyses - Depleted Voids

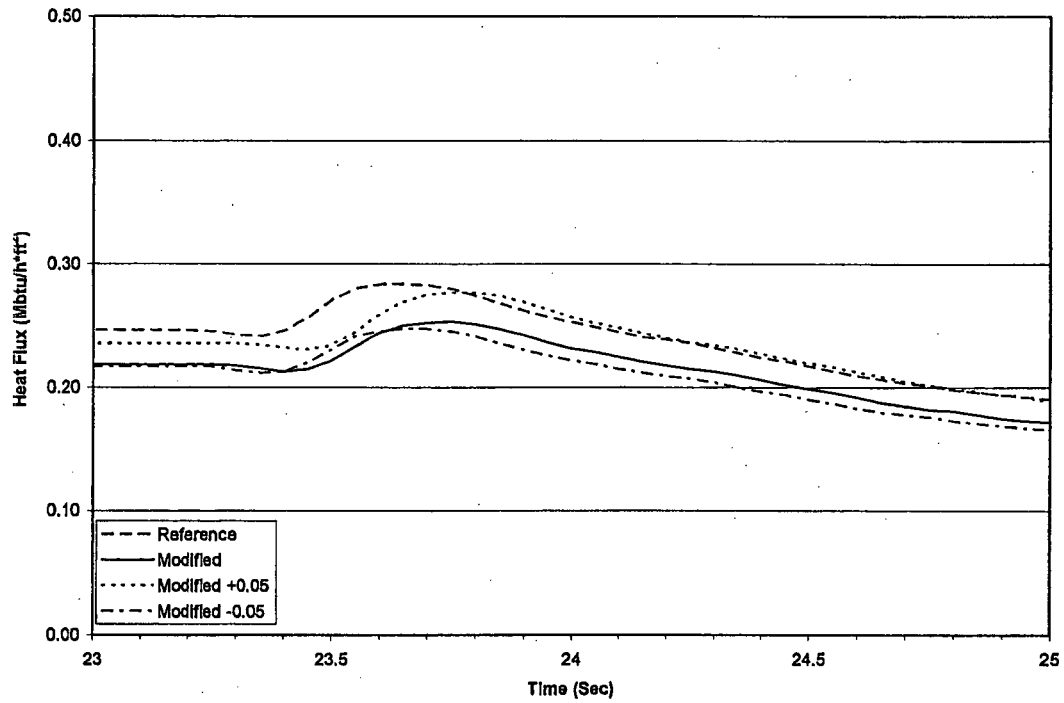


Figure 6-9 Heat Flux Vs. Time 25% x/L - Depleted Voids

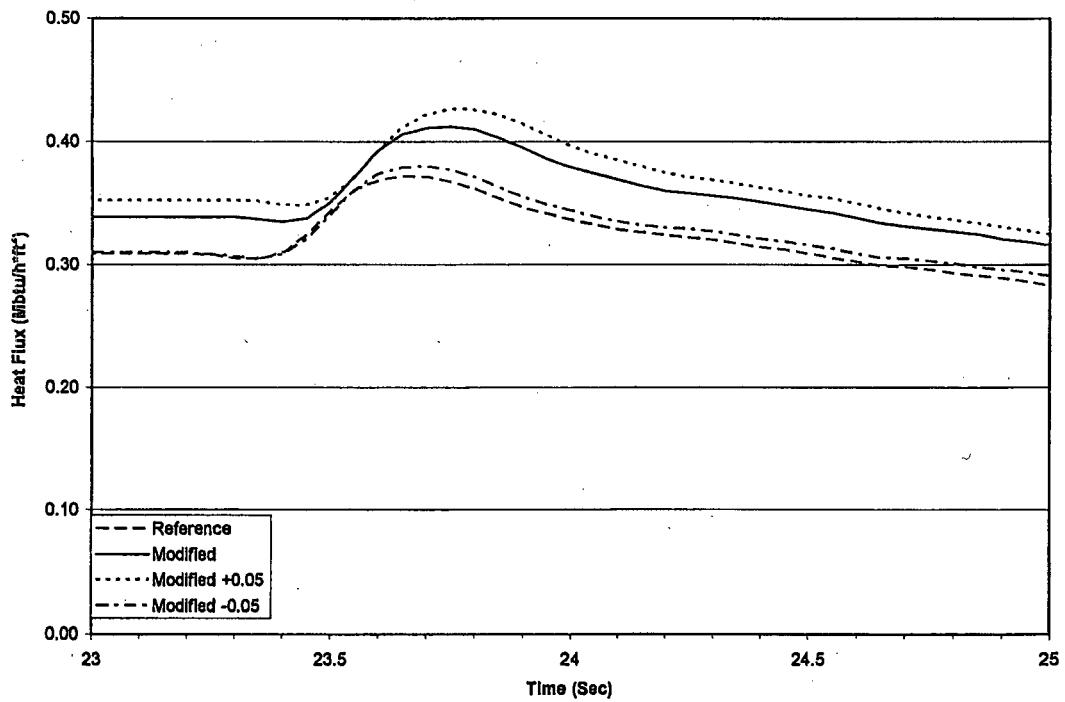


Figure 6-10 Heat Flux Vs. Time 50% x/L - Depleted Voids

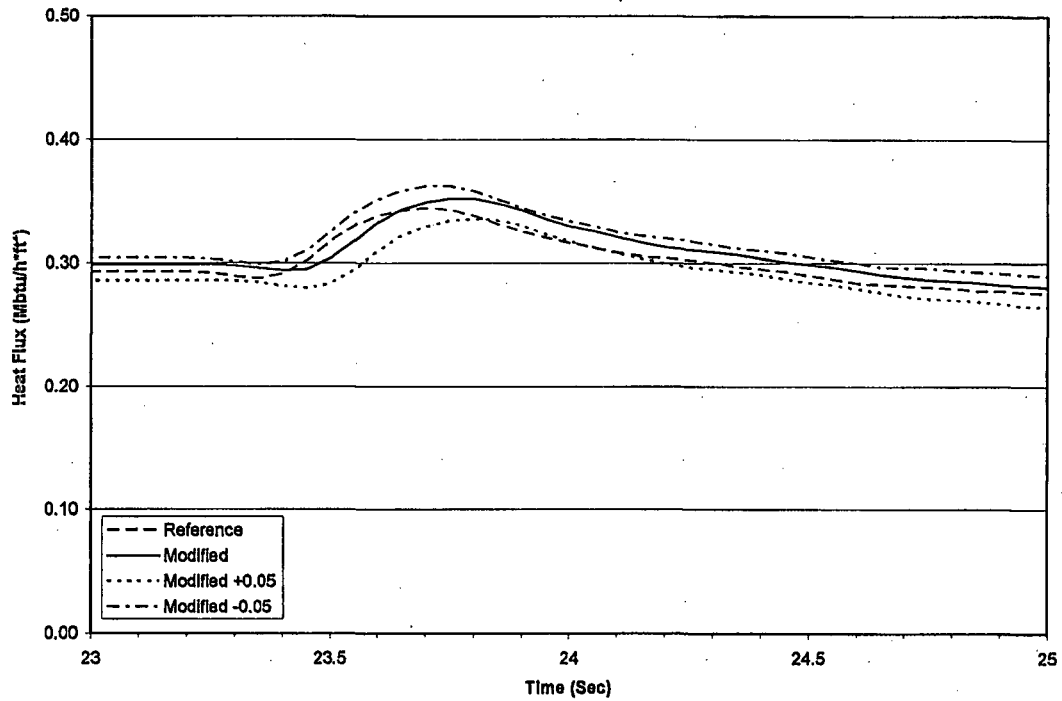


Figure 6-11 Heat Flux Vs. Time 75% x/L - Depleted Voids

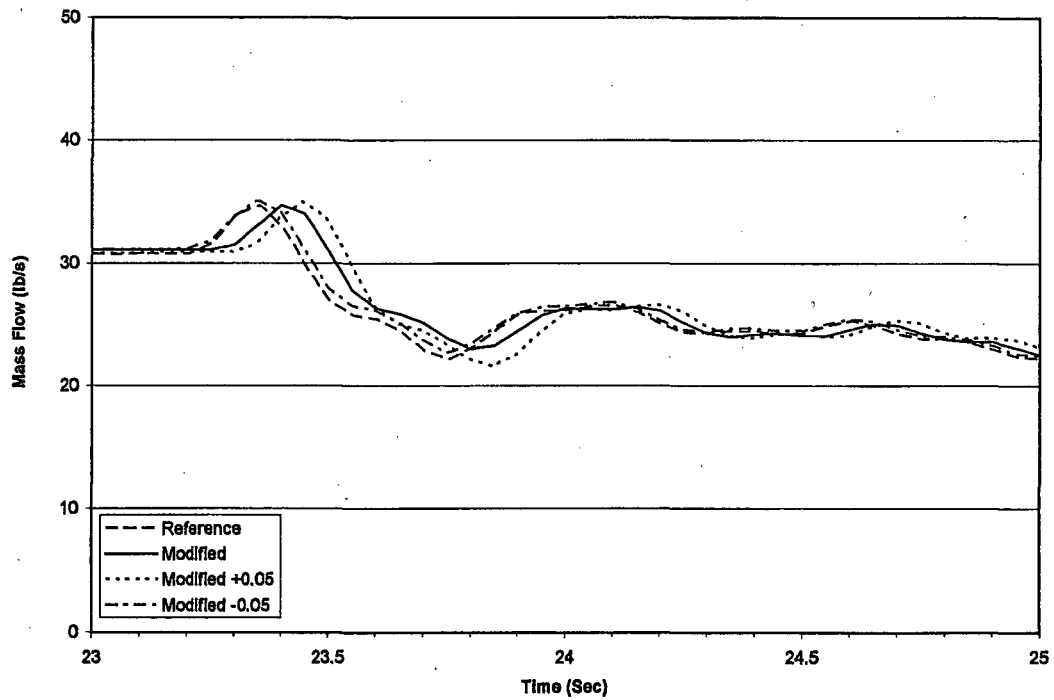


Figure 6-12 Mass Flow Vs. Time 0% x/L - Depleted Voids

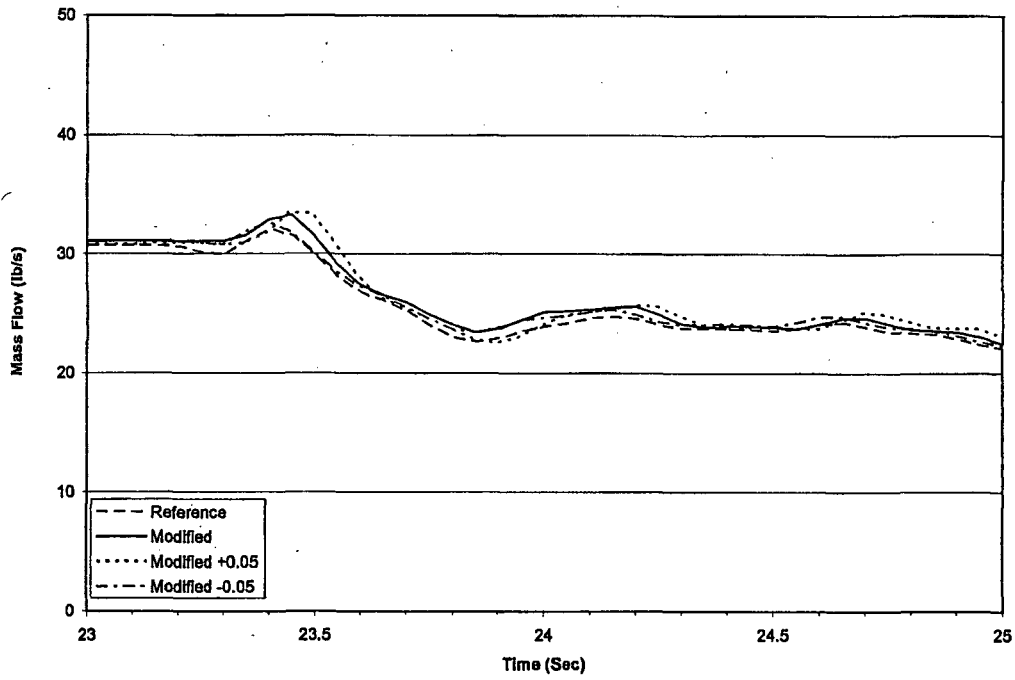


Figure 6-13 Mass Flow Vs. Time 25% x/L - Depleted Voids

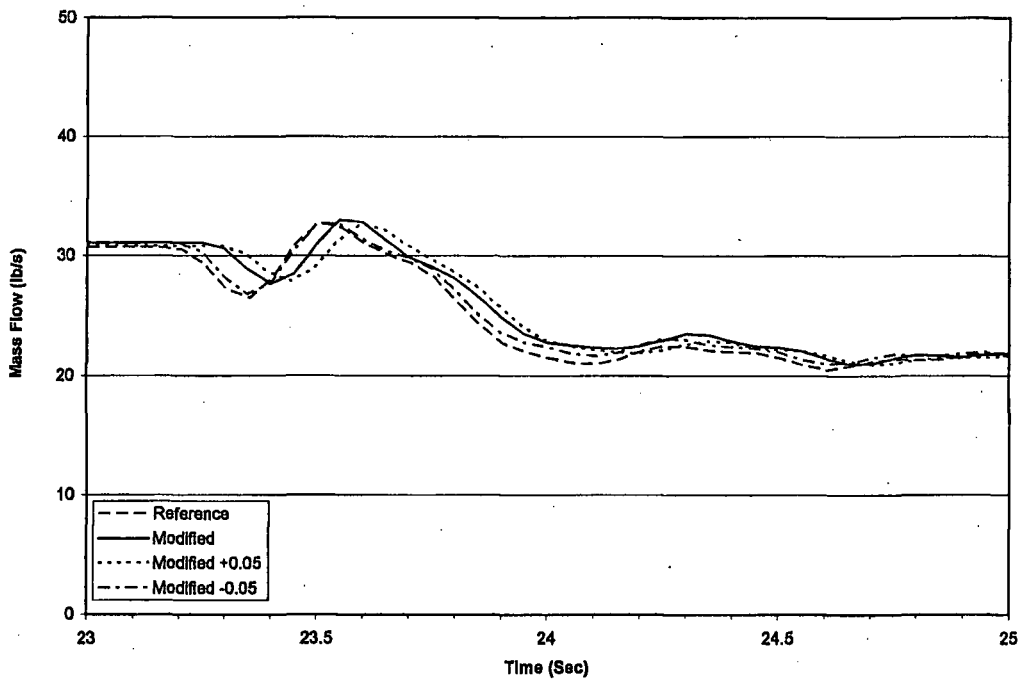


Figure 6-14 Mass Flow Vs. Time 50% x/L - Depleted Voids

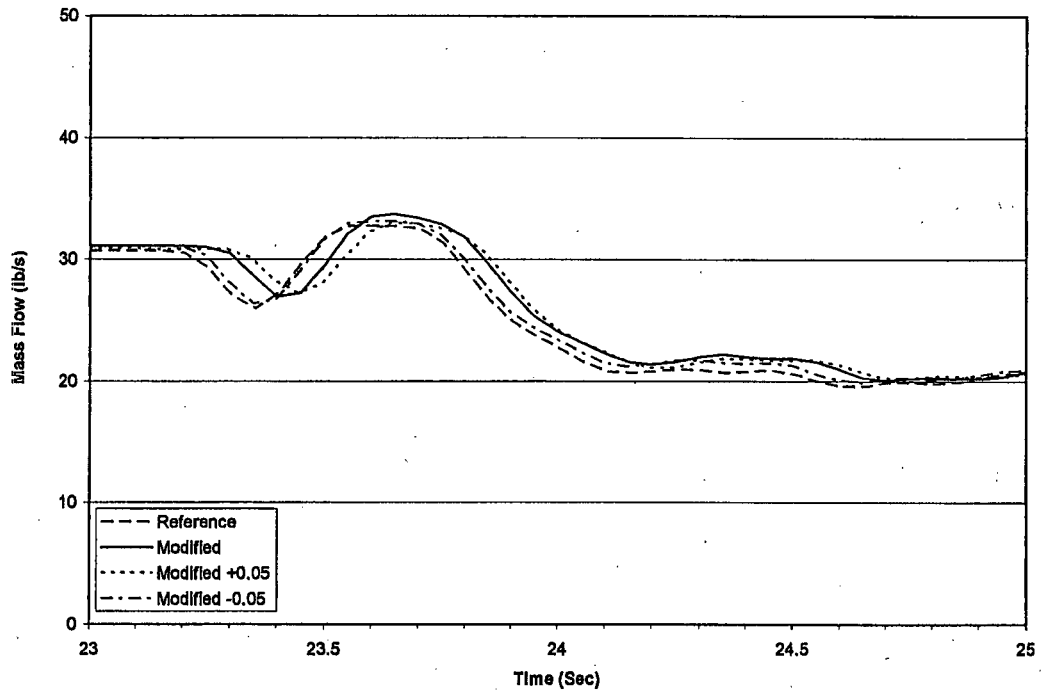


Figure 6-15 Mass Flow Vs. Time 75% x/L - Depleted Voids

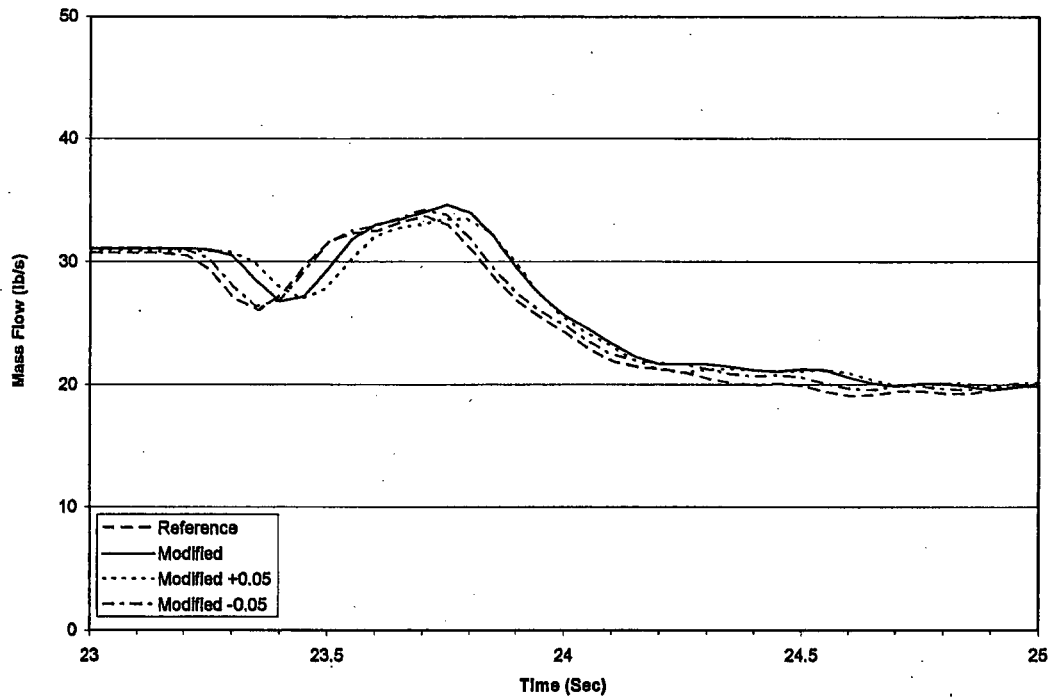
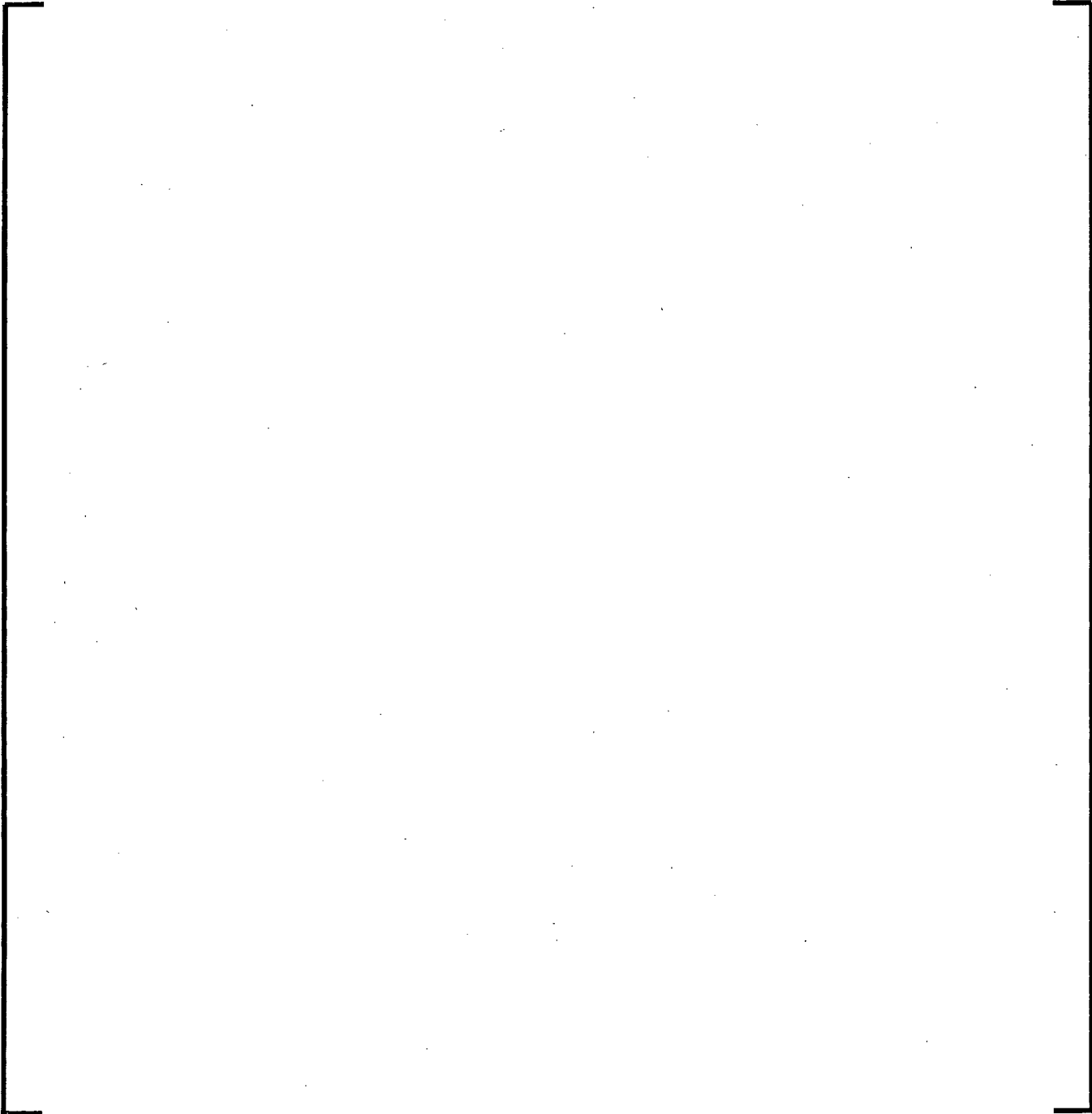


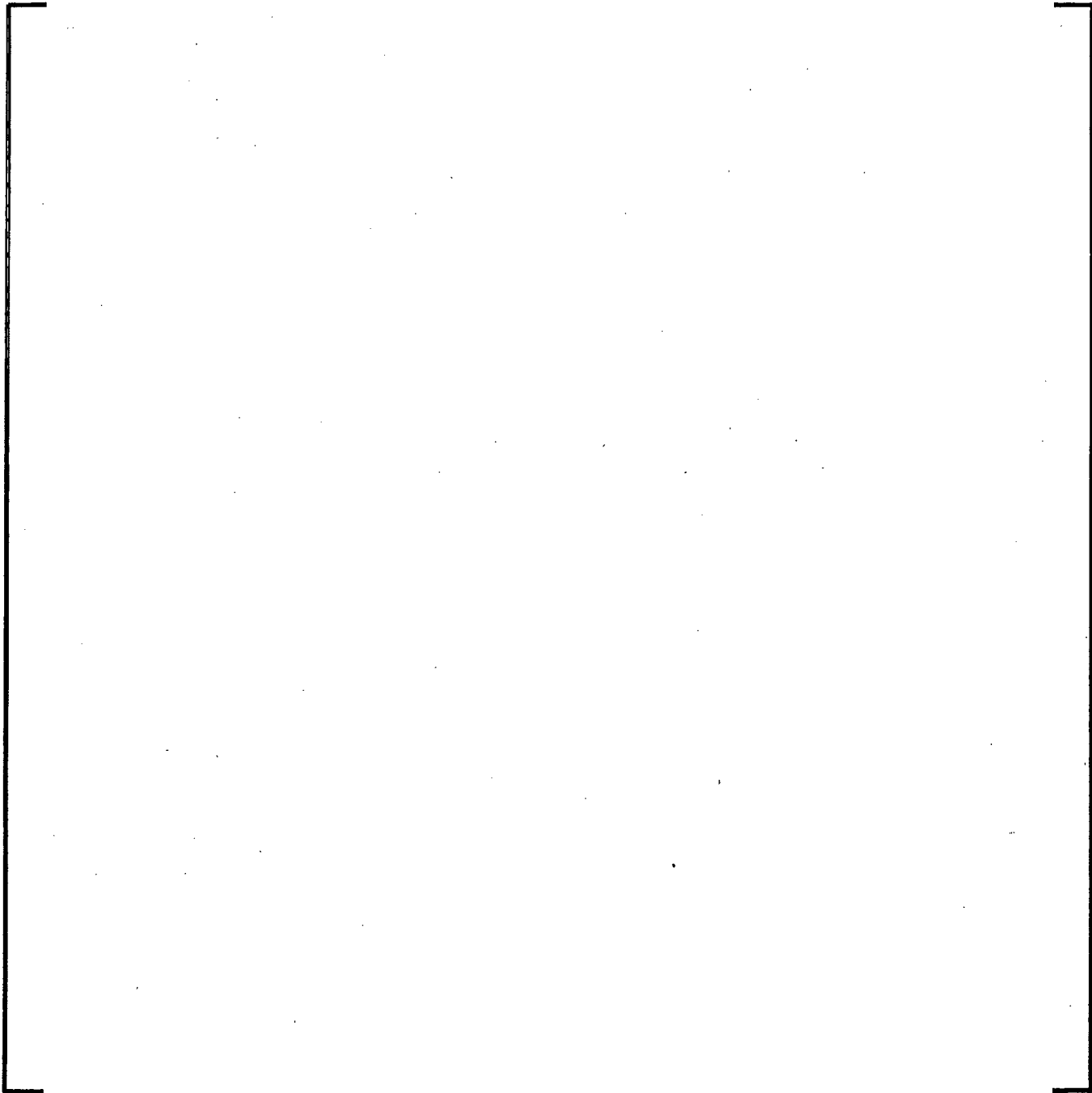
Figure 6-16 Mass Flow Vs. Time 100% x/L - Depleted Voids



Figure 6-17 CPR Vs. Time Depleted Voids



**Figure 6-18 RODEX Evolution of the
Doppler Effective Fuel Temperature for
SPC Fuel at Constant Power**



**Figure 6-19 RODEX Evolution of the
Doppler Effective Fuel Temperature for
SPC Fuel Vs. LHGR and Burnup**



**Figure 6-20 MICROBURN-B2 Correlation Evolution of the
Doppler Effective Fuel Temperature for
SPC Fuel Vs. LHGR and Burnup**



**Figure 6-21 BFN 2D TIP Statistic Comparison for
Variations of the Void Quality Correlation**



**Figure 6-22 BFN 3D TIP Statistic Comparison for
Variations of the Void Quality Correlation**

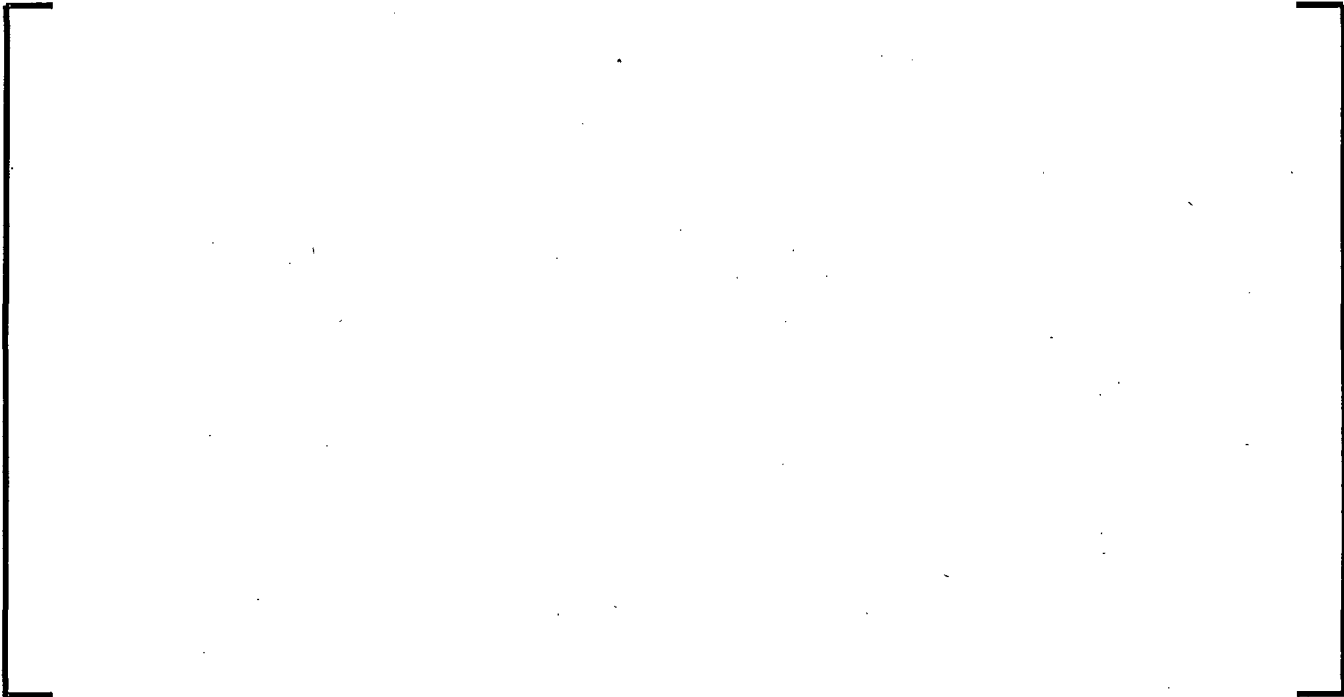


**Figure 6-23 BFN Core Average Axial TIP Comparison at
9026 MWd/MTU for Variations of the Void Quality Correlation**



**Figure 6-24 BFN Core Average Axial TIP Comparison at
1755 MWd/MTU for Variations of the Void Quality Correlation**



**Figure 6-25 BFN Core Average Axial TIP Comparison at
9197 MWd/MTU for Variations of the Void Quality Correlation**



**Figure 6-26 BFN Core Average Axial TIP Comparison at
1340 MWd/MTU for Variations of the Void Quality Correlation**



**Figure 6-27 A BWR/4 at EPU 2D TIP Statistic Comparison for
Variations of the Void Quality Correlation**



**Figure 6-28 A BWR/4 at EPU 3D TIP Statistic Comparison for
Variations of the Void Quality Correlation**



**Figure 6-29 A BWR/4 at EPU Core Average Axial TIP Comparison at
2127 MWd/MTU for Variations of the Void Quality**



**Figure 6-30 A BWR/4 at EPU Core Average Axial TIP Comparison at
10621 MWd/MTU for Variations of the Void Quality Correlation**



**Figure 6-31 A BWR/4 at EPU Core Average Axial TIP Comparison at
18459 MWd/MTU for Variations of the Void Quality Correlation**



**Figure 6-32 A BWR/4 at EPU Core Average Axial TIP Comparison at
2054 MWd/MTU for Variations of the Void Quality Correlation**

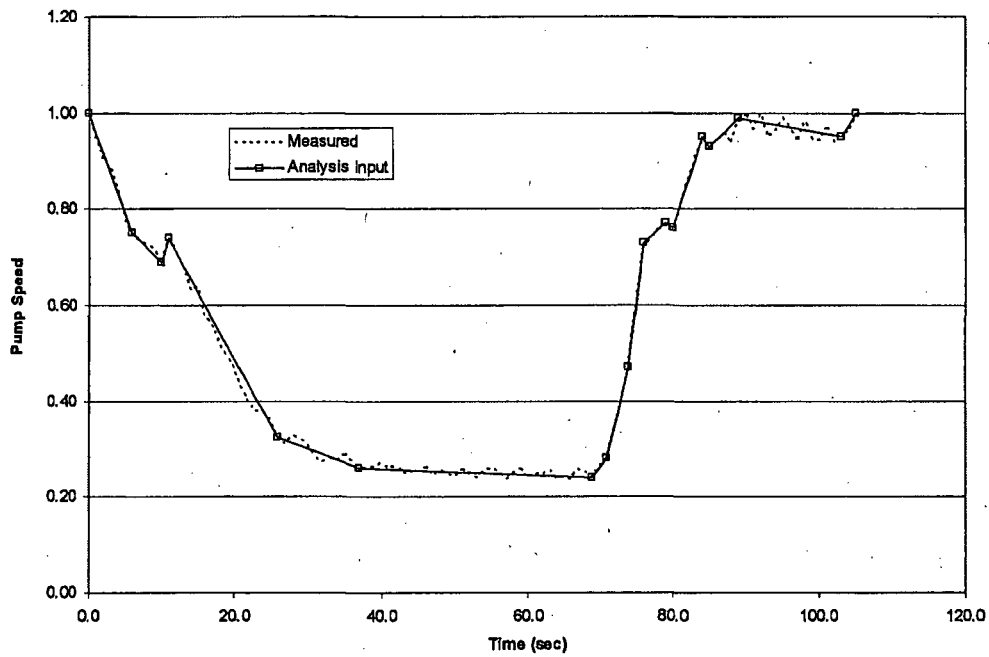


Figure 6-33 Pump Speed

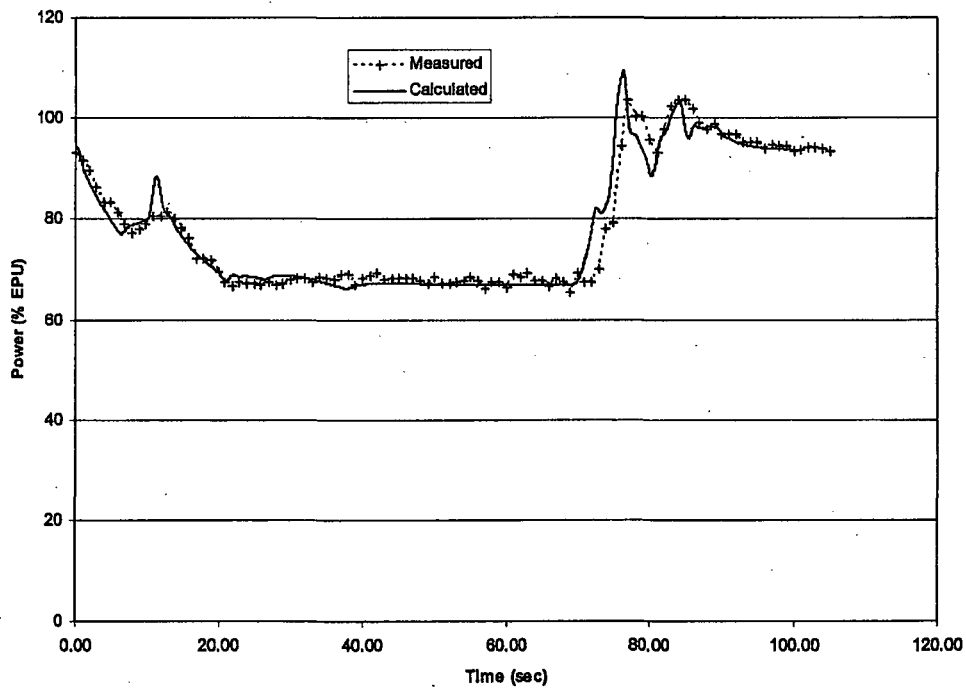


Figure 6-34 Core Power

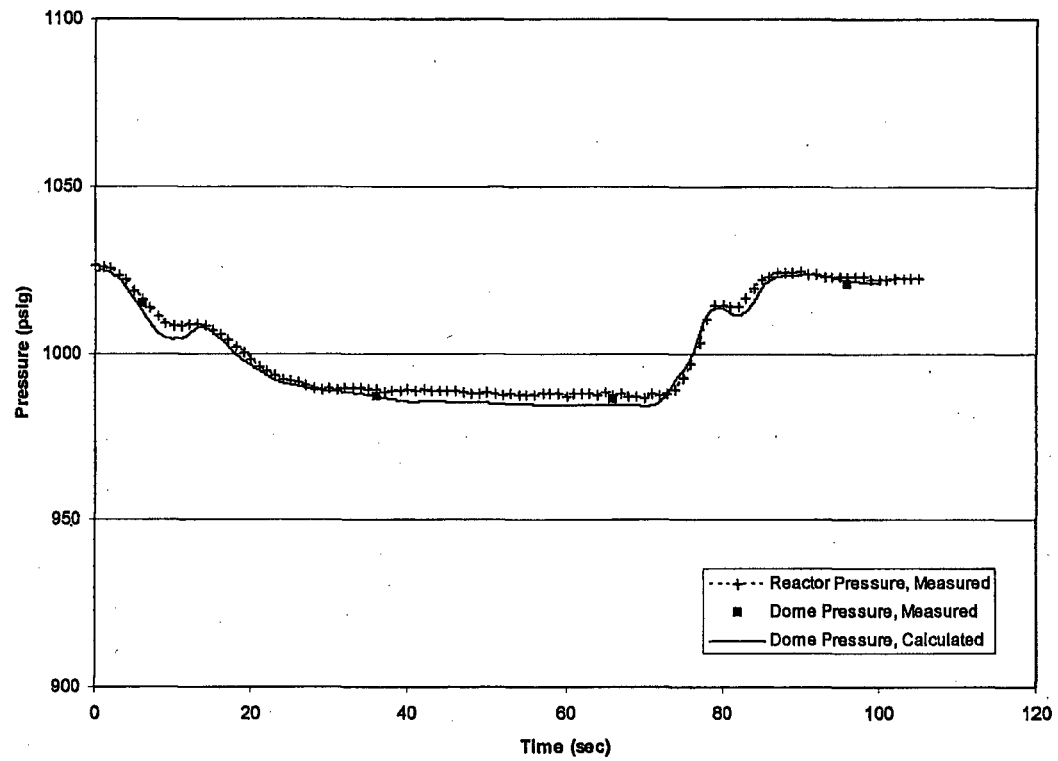


Figure 6-35 Reactor Pressure

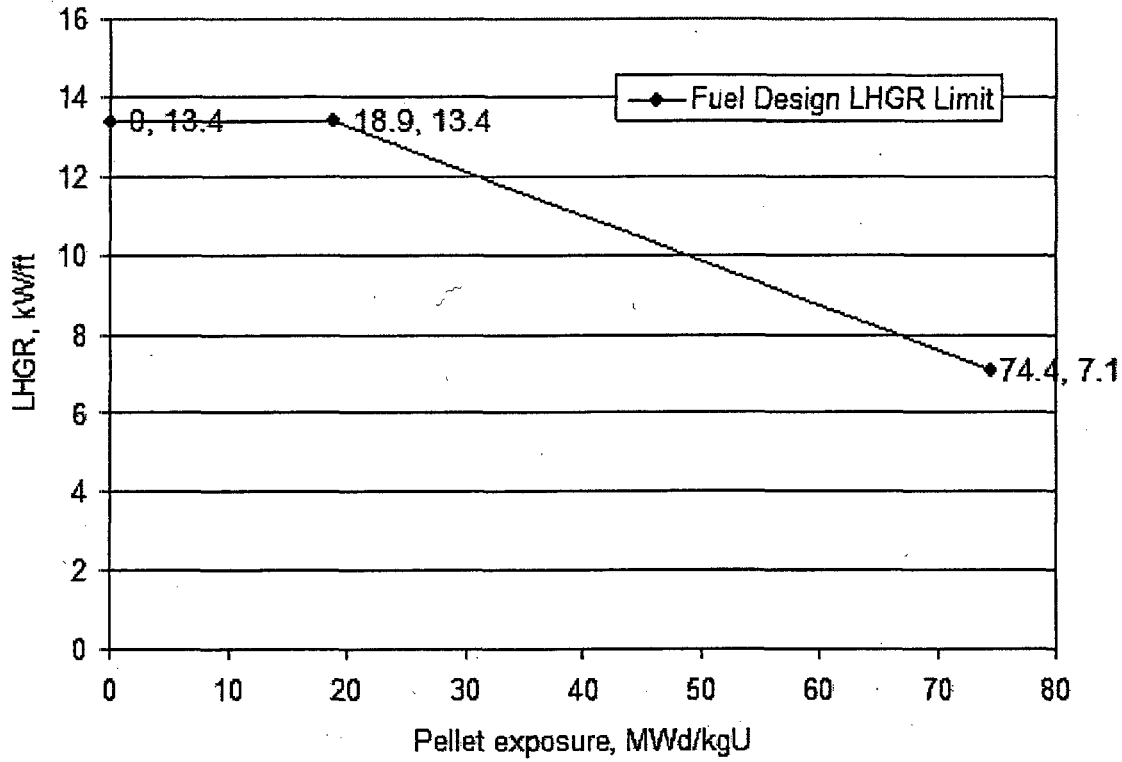


Figure 6-36 ATRIUM-10 LHGR Limit



Figure 6-37 ATRIUM-10 Void Data

NOTE:

[]

7.0 Neutronics

7.1 *Shutdown Margin*

In order to accurately determine shutdown margins during transition cycles, AREVA NP typically performs detailed benchmarking analyses of the three to five cycles previous to insertion of AREVA NP fuel in that reactor. This benchmarking is performed with the CASMO-4/MICROBURN-B2 3-D core simulator code system. Hot depletions are performed using actually operated state conditions including as-loaded core configurations, as-operated control rod patterns, and operating power, pressure, flow, and inlet subcooling. To confirm the validity of the hot depletions, comparison of eigenvalue trends and predicted versus measured TIP distributions for the benchmark cycles are performed. These results are used to establish the hot-operating target k -eff for design of the first transition cycle. All cold critical measurements taken during the benchmarking cycles are also modeled in MICROBURN-B2 by restarting from the hot cycle depletions discussed above. The results from the cold critical benchmarks are used to define a cold critical k -eff target. Once the cold target is determined based on the benchmarking, a statistically based design shutdown margin limit is chosen to bound the uncertainty observed by comparing the critical k -effs computed with MICROBURN-B2 to the target selected from the benchmarking. A typical design target is 1% $\Delta k/k$. This ensures that the transition loading fuel design will support the 0.38% $\Delta k/k$ technical specification cold shutdown margin requirement with additional margin to cover the uncertainty in the design target chosen based on the benchmarking results. Past AREVA NP experience indicates that the variation in the target cold critical k -eff when transitioning from GE14 to ATRIUM-10 is small (≤ 0.001).

During the design of each transition cycle, shutdown margin is computed by performing restart solutions based on a shuffled core from a short window previous cycle condition. This means that the previous cycle is assumed to shutdown earlier than the nominal planned shutdown for the cycle. The short window shutdown of the previous cycle results in additional carryover reactivity for the shutdown margin analysis of the cycle being designed. Setting the gadolinia design of the fresh fuel and the loading plan to meet the design shutdown margin based on the assumed short window shutdown of the previous cycle assures that adequate shutdown margin exists for the entire cycle at the design stage. The shutdown margin is also checked at the nominal previous cycle condition. Prior to actual startup of the cycle, shutdown margin is

recomputed based on the actual previous cycle shutdown exposure. At startup, when each designed cycle reaches cold critical conditions, comparison to the predicted point of criticality to the actual point of criticality is made. High accuracy of the predicted versus actual critical eigenvalue demonstrates the validity of the shutdown margin design for that cycle.

The initial critical and any subsequent cold critical data points achieved in each transition and follow-on cycle are fed back into the cold critical eigenvalue database for the reactor unit, and the target is revised as needed for the design of the subsequent cycle. This method assures continued accuracy in predicting the cold shutdown margin as new fuel is transitioned into the reactor core during the first and second transition cycles and all subsequent cycles.

As part of the design process for developing the fuel/core design for Browns Ferry Unit 1 Cycle 9 it is necessary to establish a target cold critical eigenvalue. The approach taken to determine the target cold critical eigenvalue for Browns Ferry Unit 1 is more conservative than that described above due to the extended shutdown of the unit. Information from Browns Ferry Units 2 and 3, as well as Unit 1, have been used to determine the target cold critical eigenvalue. A summary of the calculated cold critical for the three Browns Ferry Units is presented in Figure 7-1. This figure includes cold critical data from any Browns Ferry cycle that contained GNF fuel. The target cold critical eigenvalue used for Unit 1 Cycle 9 design is shown in Figure 7-1. The target was conservatively set to bound all the measured cold criticals for the three units. This conservative determination of the target, together with the conservatively determined design goal of $1\% \Delta k/k$, ensures conservative determination of shutdown margin for the Unit 1 Cycle 9 design.

The bounding curve is summarized below.

Cycle Exposure (MWd/MTU)	k-eff
0.0	0.9930
2,000.0	0.9910
20,000.0	0.9910

7.2 *Monitoring*

The explicit LPRM model is used in the core monitoring, hence LPRM rod power biases are accounted for in the monitoring of LHGR limits.

Monitoring for conformance with the operating limit MLHGR is not performed accounting for the fission gas plena, because sensitivity studies show the plena has negligible effect on LHGR.

Lattices occupying the node directly above the top of the PLFR active fuel length were evaluated in a 3-D full core equilibrium cycle model to determine the impact of modeling the PLFR upper plena regions as coolant versus modeling the plena explicitly. The difference in core limiting margin to the LHGR thermal limit due to the modeling of the PLFR varies throughout the cycle. The largest decrease in LHGR margin (conservative) due to modeling the PLFR upper plena as coolant is 0.019. The largest increase in LHGR margin (nonconservative) due to modeling the PLFR upper plena as coolant is 0.003. The changes in LHGR margin due to using the coolant model for the PLFR upper plena are small.

7.3 *Power Distribution Uncertainty*

7.3.1 Radial Bundle Power Uncertainty

The Reference 44 methodology calculates radial bundle power uncertainty ($\delta P'_{ij}$) from separately determined uncertainty components. Three uncertainty components used to calculate $\delta P'_{ij}$ are:

- the deviation between the CASMO-4/MICROBURN-B2 (C4/MB2) calculated radial TIP response and the measured radial TIP response ($\delta T'_{ij}$),
- radial TIP measurement uncertainty (δT^m_{ij}), and
- radial synthesis uncertainty (δS_{ij}).

These uncertainty components are determined using traversing incore probe (TIP) measurements, which are taken at or near full power conditions for Local Power Range Monitor (LPRM) calibration.

The BFN specific value of $\delta T'_{ij}$ was calculated in accordance with the Reference 44 methodology using BFN gamma TIP measurements and is []. BFN is a D-Lattice plant. For comparison, Reference 44 reports a $\delta T'_{ij}$ of [] for D-Lattice plants.

The BFN specific $\delta T'_{ij}$ database is shown versus cycle number in Figure 7-2, versus power to flow ratio in Figure 7-3, versus core void in Figure 7-4, and versus core power in Figure 7-5. Figure 7-2, Figure 7-3 and Figure 7-5 represent the same data. The database includes 112 full core gamma TIP measurements: 14 for Unit 1 Cycles 7 and 8, 46 for Unit 2 Cycles 13, through 15 (through February 2008), and 52 for Unit 3 Cycles 11 through 13 (to September 2007). Figure 7-4 represents the database consisting of Unit 1 Cycles 7 and 8, Unit 2 Cycles 14 and 15, and Unit 3, Cycles 12 and 13. Void fraction data for Unit 2 Cycle 13 and Unit 3 Cycle 11 was not readily available.

Figure 7-2 through Figure 7-5 clearly demonstrate that the D-lattice radial TIP uncertainty reported in the Reference 44 topical report is very conservative for BFN. Figure 7-2 through Figure 7-5 also clearly demonstrate there is no correlation in the BFN specific uncertainty component due to the core power to flow ratio, core power or core average void fraction. Operation at the maximum core power and minimum core flow conditions allowed for EPU operations corresponds to a power to flow ratio of 39.92 MW-th/Mlb/hr which is within the range of the data already taken.

The δT^m_{ij} is comprised of random instrument error and geometric measurement uncertainty caused by variations in the physical TIP location. A BFN specific radial TIP measurement uncertainty (δT^m_{ij}) was calculated in accordance with the Reference 44 methodology using BFN gamma TIP measurements and is []. For comparison, Reference 44 reports a δT^m_{ij} of [] for D-Lattice plants. The BFN gamma TIP system is far less sensitive than neutron TIP systems to variations in TIP location within the corner water gap between fuel assemblies. Because δT^m_{ij} is determined by comparing TIP measurements in symmetrically operated core locations, it is independent of the C4/MB2 core model and core operating conditions.

The δS_{ij} is the uncertainty associated with update of calculated power by the core monitoring system to more closely match in-core instrumentation. A BFN specific radial synthesis uncertainty (δS_{ij}) was calculated in accordance with the Reference 44 methodology using BFN gamma TIP measurements and is []. For comparison, Reference 44 reports a δS_{ij} of

[] for D-Lattice plants. δS_{ij} is a function of the core monitoring system update algorithm and is independent of core operating conditions. [

] a comparison of δS_{ij} to core operating conditions is not provided.

Utilizing the BFN specific values of δT^i_{ij} , δT^m_{ij} and δS_{ij} results in a measured assembly power distribution uncertainty of []. BFN Safety Limit Minimum Critical Power Ratio (SLMCPR) analyses are based on the radial bundle power uncertainty value of [] reported in the Reference 44 topical report rather than the BFN specific value of []. The BFN specific value is conservative relative to the topical report value by [] due primarily to BFN implementation of gamma TIPs for LPRM calibration. Both the BFN specific and topical report bundle power uncertainty values are additionally very conservative relative to their respective TIP measurement databases due to the use of a correlation coefficient to increase calculated power uncertainty above calculated TIP uncertainty, contrary to measured data that support decreasing calculated power uncertainty below calculated TIP uncertainty. Even if a 50% reduction was assumed in the correlation coefficient, the BFN specific evaluation of the power uncertainty would be conservative relative to the value used in the SLMCPR analysis. Therefore, increasing the power distribution uncertainty is not necessary for the SLMCPR analysis of BFN.

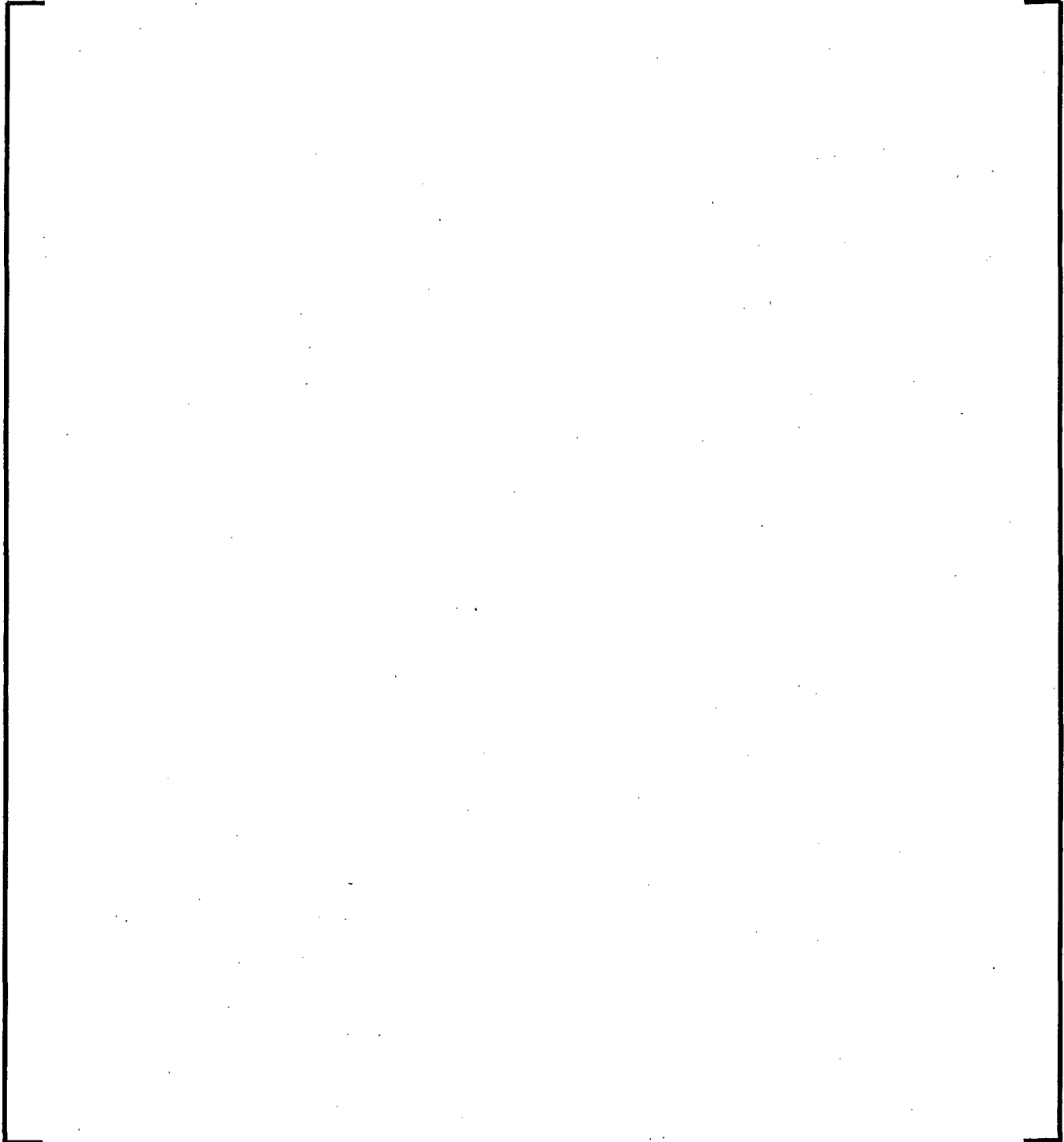
The Reference 44 topical report database includes TIP measurements of cores containing many different fuel designs and identifies no correlation between C4/MB2 uncertainty and fuel design. Figure 7-2 demonstrates there is no significant variation in uncertainty determined from the BFN gamma TIP measurements for various mixes of fuel types. These measurements include mixed GE13 and GE14 cores operated in Unit 1 Cycles 7 and 8, Unit 2 Cycle 11 and Unit 3 Cycle 13. Mixed cores of GE14 and ATRIUM™-10^{tt} fuel were operated in Unit 2 Cycles 14 and 15 as well as Unit 3 Cycles 12 and 13.

In addition to the calculated TIP uncertainty, the measured TIP uncertainty is a significant component of the measured power distribution uncertainty. The uncertainty in the measured assembly power is defined in Reference 44 as:

^{tt} ATRIUM is a trademark of AREVA NP.



The corresponding uncertainty in the measured 3D nodal power is defined in Reference 44 as:



The uncertainty in measured axial power is then defined as:

[]

The value of these parameters for the Browns Ferry specific analysis are compared to the topical report values for D-lattice plants in the following table.



The lack of assembly gamma scan data for ATRIUM-10 fuel at extended power uprate (EPU) conditions does not have any impact on the overall uncertainty. One could conservatively

assume a 50% reduction to the correlation coefficient in order to bound the impact of a minimal plant specific database. Applying this assumption would result in a Browns Ferry specific measured power distribution uncertainty value of [].

If only the TIP measurement uncertainty reduction is credited due to the implementation of gamma TIPs at Browns Ferry and using the values reported in Reference 44 for all other components except the correlation coefficient, the measured power distribution uncertainty value is [], which is still less than the EMF-2158(P)(A) value of [].

7.3.2 Local Power Uncertainty

C4/MB2 local power distributions are compared to bundle gamma scan data as reported in Tables 8.3, 8.4, and 8.5 of Reference 44 for 10x10 and other orthogonal lattice designs. These results indicate that there is no degradation in the uncertainty for 10x10 fuel relative to the other designs.

Also, SLMCPR has been shown to be very insensitive to the local power distribution uncertainty within an assembly as defined in EMF-2158(P)(A). A 50% increase in the local power distribution uncertainty from [] resulted in a change in the SLMCPR of [].

7.4 ***Gamma Scans***

The gamma scanning process for irradiated fuel uses germanium semi-conductor detectors for gamma radiation energy spectral analysis. Gamma rays deposit their energy in the germanium and produce free electrons and holes (vacancies where the electrons were located in the crystalline germanium). The amount of charge collected is correlated with the amount of energy deposited in the detector and therefore with the energy of the gamma ray that caused it. The detectors are used with single channel analyzers to sort the pulses according to pulse height. This means that if multiple gamma-ray energies are being analyzed simultaneously, the germanium detector will separate them cleanly. A single-channel analyzer (SCA) uses two discriminators. The discriminators are called upper and lower level discriminators. Pulses from the amplifier are fed to the analyzer, and if the pulse height falls between the lower and upper discriminators the usual logic is to allow such a pulse to be recorded (counted). The voltage levels of the two discriminators are adjustable so that the gap between them corresponds to a

group of pulse heights within a fixed energy interval. Even though the gamma rays from a specific decay transition are of a discrete energy, there is a statistical spread of pulses coming from the detector and associated electronics so that the gap between the discriminators must be large enough to include most of such pulses. By varying the voltage levels of each of the discriminators, it is possible to measure gamma rays of different energies.

Power measurements for irradiated fuel target the gamma spectrum associated with Lanthanum (La) 140. La140 is a decay product of Barium (Ba) 140 which is a direct fission product. The half life of Ba140 is 12.8 days and the half life of La140 is 40 hours. La140 activity is, therefore, directly related to the density of Ba140. The Ba140 density is representative of the integrated fissions over the last 25 days due to its short half life. Gamma scan measurements are taken shortly after reactor shutdown (within 25 days) before the Ba140 decays to undetectable levels. Gamma scan measurements may be performed on individual fuel rods removed from assemblies using a high-purity germanium (HPGe) detector and an underwater collimator assembly or on entire fuel assemblies where the collimator has a broad opening to capture the gamma radiation from all of the pins in the assembly.

Gamma scanning provides data on the relative gamma flux from the particular spectrum associated with La140 gamma activity. The relative gamma flux corresponds to the relative La140 concentration. Based upon the time of shutdown and the time of the gamma scan the Ba140 relative distribution at the time of shutdown is determined. This Ba140 relative distribution is thus correlated to the pin or assembly power during the last few weeks of operation. The data presented in the topical report, EMF-2158(P)(A), includes both pin and assembly Ba140 relative density data. The assembly gamma scan data was taken at Quad Cities after the operation of cycles 2, 3 and 4. Some of this data also included individual pin data. This data was from 7X7 and 8X8 fuel types. Additional fuel pin gamma scan data was taken at the Gundremingen plant for ATRIUM-9 and ATRIUM-10 fuel. This data is also presented in the topical report.

To compare core physics models to the gamma scan results, the calculated pin power distribution is converted into a Ba140 density distribution. A rigorous mathematical process using CASMO-4 pin nuclide inventory and MICROBURN-B2 nodal nuclide inventory is used.

7.5 *Bypass Modeling*

The core bypass water is modeled in the AREVA NP steady-state core simulator, transient simulator, LOCA and stability codes as [].

The steady-state core simulator, MICROBURN-B2, explicitly models the assembly specific flow paths through the lower tie-plate flow holes and the channel seals in addition to a [] [] through the core support plate. The numerical solution for the individual flow paths is computed based on a general parallel channel hydraulic solution that imposes a constant pressure drop across the core fuel assemblies and the bypass region. This solution scheme incorporates [] that is dependent on the [].

The MICROBURN-B2 state-point specific solution for bypass flow rate and [] is then used as initial conditions in the transient and LOCA analyses. When the reactor operates on high rod-lines at low flow conditions, the in-channel pressure drop decreases to a point where a solid column of water cannot be supported in the bypass region, and voiding occurs in the core bypass. For these conditions (in the region of core stability concerns) the neutronic feedback of bypass voiding []

[

]

The level of bypass boiling for a given state-point is a direct result of the hydraulic solution. The potential for boiling increases as the power/flow ratio increases or the inlet sub-cooling decreases. While the licensing methodology utilizes a lumped core bypass model, the MICROBURN-B2 core simulator does have a conservative multi-channel model to estimate the potential for localized bypass boiling. This multi-channel model uses one bypass channel per fuel assembly to specifically determine a bounding local void distribution in the core. The model is conservative in that it assumes that there is no cross-flow between bypass channels. Thus, the direct bypass energy from the hottest assembly is deposited in the surrounding $\frac{1}{2}$ width water gaps and there is no mixing with the adjacent $\frac{1}{2}$ width water gaps from its neighbors. The capability of this model to predict localized bypass boiling is demonstrated in Figure 7-6 for a hypothetical case where the inlet sub-cooling was artificially decreased to induce bypass boiling.

Bypass voiding is of greatest concern for stability analysis due to its direct impact on the fuel channel flow rates and the axial power distributions. The reduced density head in the core bypass due to boiling results in a higher bypass flow rate and consequently a lower hot channel flow rate. This lower hot channel flow rate and a more bottom-peaked power distribution (due to lower reactivity in the top of the core due to boiling in the bypass region) destabilize the core through higher channel decay ratios. AREVA NP stability methods directly model these phenomena to assure that the core stability is accurately predicted.

The expanded operating domain on the power/flow map associated with Extended Power Uprate was examined with respect to bypass modeling. For Browns Ferry, the entire 100% power boundary (120% of the original licensed thermal power) was assessed. Even with the conservative multi-channel model discussed above, there was no localized bypass boiling at the EPU power level. While this may not have been anticipated, the increased power/flow ratio of the core bypass was more than compensated by the increased inlet sub-cooling associated with the uprated operating conditions. When the core power is uprated the steam and feedwater flows increase and the internal recirculation ratio decreases. With a larger fraction of the core flow coming from the feedwater, the inlet subcooling increases. This assessment assures that the limiting transients at the uprated thermal power are not adversely affected by bypass boiling.

As the flow is reduced along the highest rod line in the operating domain, the propensity for bypass boiling increases and becomes significant for two-pump trip events.

Two pump trip transients are analyzed as part of the long-term stability solutions as they result in operation at high rod lines and natural recirculation flow. For stability analysis, the impact of bypass boiling is directly accounted for in the active channel flow rates, axial power distributions and dynamic reactivity changes during the oscillations. While these calculations use a [] bypass model, and may under-predict localized bypass boiling, it is important to note that the methodology was benchmarked to global and regional oscillations for internal pump plants that exhibit much higher levels of bypass boiling than jet pump plants for MELLLA operation due to the extremely low natural recirculation flow rates (~15% for internal pump plants compared to ~30% for jet pump plants). Uncertainties associated with localized bypass boiling are captured in the decay ratio uncertainties in the MICROBURN-B2/STAIF stability methodology.



Figure 7-1 Browns Ferry Cold Criticals



Figure 7-2 BFN δT_{ij} Gamma TIP Response vs. Cycle Number



Figure 7-3 FN δT_{ij} Gamma TIP Response vs. Power/Flow Ratio

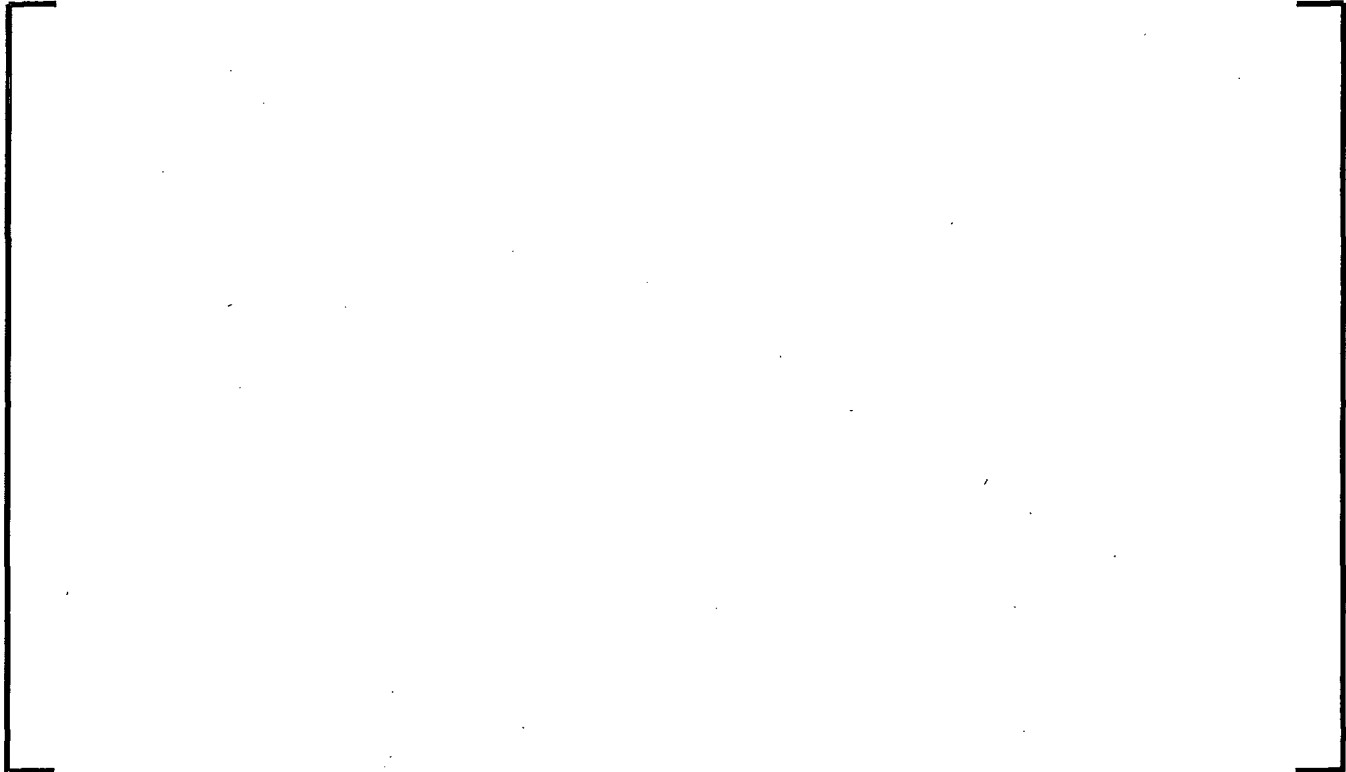


Figure 7-4 BFN $\delta T'_{ij}$ Gamma TIP Response vs. Core Average Void Fraction



Figure 7-5 BFN $\delta T'_{ij}$ Gamma TIP Response vs. Core Power



Figure 7-6 Hypothetical MICROBURN-B2 Multi-Channel Average Bypass Void Distribution

8.0 ATWS

8.1 *ATWS General*

The COTRANSA2 computer code is the primary code used for the ATWS overpressurization analysis. The XCOBRA-T computer code is not used in the ATWS overpressurization analysis. The ATWS overpressurization event is not used to establish operating limits for critical power; therefore, the SPCB critical power correlation pressure limit is not a factor in the analysis.

Dryout conditions are not expected to occur for the core average channel that is modeled in COTRANSA2 for the ATWS overpressurization analysis. Dryout might occur in the limiting (high power) channels of the core during the ATWS event; however, these channels are not modeled in COTRANSA2 analyses. For the ATWS overpressurization analysis, ignoring dryout for the hot channels is conservative in that it maximizes the heat transferred to the coolant and results in a higher calculated pressure.

The ATWS event is not limiting relative to acceptance criteria identified in 10 CFR 50.46. The core remains covered and adequately cooled during the event. Following the initial power increase during the pressurization phase, the core returns to natural circulation conditions after the recirculation pumps trip and fuel cladding temperatures are maintained at acceptably low levels. The ATWS event is significantly less limiting than the loss of coolant accident relative to 10 CFR 50.46 acceptance criteria.

8.2 *Void Quality Correlation Bias*

AREVA NP performs cycle-specific ATWS analyses of the short-term reactor vessel peak pressure using the COTRANSA2 computer code. The ATWS peak pressure calculation is a core-wide pressurization event that is sensitive to similar phenomenon as other pressurization transients. Bundle design is included in the development of input for the coupled neutronic and thermal-hydraulic COTRANSA2 core model. Important inputs to the COTRANSA2 system model are biased in a conservative direction.

The AREVA NP analysis methods and the correlations used by the methods are applicable for both pre-EPU and EPU conditions. The transient analysis methodology is a deterministic,

bounding approach that contains sufficient conservatism to offset biases and uncertainties in individual phenomena. For bundle designs other than ATRIUM-10, the void-quality correlation is robust as discussed in Section 5.1 for past and present fuel designs. For future fuel designs the void-quality correlation would be reviewed for applicability, which may involve additional verification and validation.

A sensitivity study was performed for the limiting ATWS pressurization event for a proposed BFN cycle with EPU to assess the bias between the ATRIUM-10 test data and the void-quality correlation. The event was a pressure regulator failure-open (PRFO), which is a depressurization event, followed by pressurization due to main steam line isolation valve (MSIV) closure. The neutronics input included the impact of the fuel depleted with the changes in the void-quality correlation. To remove the bias in the MICROBURN-B2 neutronics input, the [] void-quality correlation was modified. To address the bias in the Ohkawa-Lahey void-quality correlation for the COTRANSA2 code, the void-quality relationship was changed to a []. Additionally, the sensitivity study was repeated without depleting the fuel with the changes in the void-quality correlation (the change in the void-quality correlation was instantaneous at the exposure of interest).

The reference ATWS case had a peak vessel pressure of 1477 psig. The change in the void-quality correlations resulted in a 10-psi increase in the peak vessel pressure. The results for an instantaneous change in the void-quality correlation showed the same impact.

A study was also performed for the ASME overpressure event for the same BFN cycle with EPU. The event was the MSIV closure. The change in the void-quality correlations resulted in a 7-psi increase in the peak vessel pressure.

The impact of a change in the bias of the void-quality correlations on peak pressure is expected to be more than offset by the model conservatisms. Until quantitative values of the conservatisms can be demonstrated, AREVA NP has imposed that a 10-psi increase to the peak vessel pressure for the ATWS overpressure analysis and a 7-psi increase to the peak vessel pressure for the ASME overpressure analysis be included in analyses results.

8.3 *ATWS Containment Heatup*

The higher initial steam flow at EPU conditions will result in a slightly higher power pulse during the initial, relatively short pressurization phase of the ATWS event. However, the total energy released to the suppression pool is dominated by the later, much longer phase of the event where power is reduced after the recirculation pumps trip and the core power is slowly reduced as boron injection occurs. The ATWS analyses performed for BFN Units 2 and 3 included the Unit 1 applicability impact of the higher initial steam flow at EPU conditions. As shown in Table 9-4 of Reference 41, the impact of EPU operation on the maximum suppression pool temperature is not significant ($<1^{\circ}\text{F}$). This supports the conclusion that the initial power pulse, which is higher for EPU operation, is not significant relative to the total energy transferred to the suppression pool.

Suppression pool temperature analyses were performed for BFN with GNF fuel. An evaluation was performed to compare fuel neutronic parameters important for the ATWS analysis (void coefficient, boron worth) for ATRIUM-10 and GNF fuel. The boron worth characteristics of ATRIUM-10 were slightly better while the void reactivity characteristics were slightly worse relative to the impact on the ATWS suppression pool temperature analysis.

Additional analyses were performed to assess the impact of the difference in fuel assembly reactivity characteristics on the suppression pool temperature during an ATWS. [

]

All fuel types in the core designs including the GNF fuel were explicitly modeled in the above analyses consistent with the approved methodology. The GNF fuel was modeled with a level of detail equivalent to that used for the ATRIUM-10 fuel. CASMO-4 analyses explicitly modeled the water rod configuration of the GNF fuel. MICROBURN-B2 was used to calculate the core reactivity characteristics provided to the COTRANSA2 analysis. The GNF fuel assembly geometric and nuclear characteristics (enrichment and gadolinia distribution) were based on design data provided to AREVA NP by TVA. The hydraulic characteristics for the GNF fuel assemblies were based on GNF fuel assembly pressure drop tests performed by AREVA.

The BFN ATWS analyses described above were performed for cycles operating at pre-EPU power levels. As shown in Table 9-4 of Reference 41, the impact of EPU operation on the maximum suppression pool temperature is not significant. Therefore, the trends observed for ATRIUM-10 fuel in the above analyses are equally applicable for EPU operation.

The analyses described above confirm that the suppression pool temperature analysis documented in Reference 41 is slightly conservative for ATRIUM-10 fuel. In addition, the analyses show that the difference in reactivity characteristics between ATRIUM-10 and GNF fuel do not have a significant impact relative to the large margin to the suppression pool temperature limit shown in Reference 41.

The conclusions of the Reference 41 suppression pool temperature analysis are applicable for ATRIUM-10 fuel and the acceptance criteria will be met for BFN Units 2 and 3 EPU operation with ATRIUM-10 fuel.

The BFN Units 2 and 3 EPU containment heatup analysis is the same for Unit 1:

- Containment parameters are identical (suppression pool volume, maximum initial temperature).
- Same SRV capacities.
- Same SRV lift setpoints.

Therefore the conclusions for Units 2 and 3 are equally valid for Unit 1. The transition for Unit 1 will be very similar to the transition that has already occurred for Units 2 and 3, i.e., a transition from GE14 fuel to ATRIUM-10 fuel.

8.4 *Bypass Flow*

During the short-term ATWS analysis for peak pressure, the entering bypass flow remains strongly upwards due to the normal pressure gradients across the core. There are no inherent constraints on COTRANSA2 for upward bypass flow.

The results from the COTRANSA2 ATWS analyses supporting the Browns Ferry EPU submittal were reviewed and it was confirmed that the bypass inlet flow remained positive throughout the analyses.

8.5 *Safety Relief Value Flow*

A plot of total SRV flow during an ATWS overpressurization is provided in Figure 8-1 for EPU and non-EPU operation of a Browns Ferry Unit 3 Cycle 14 design.

8.6 *Time Steps*

Time step studies are performed for fast pressurization events to determine a converged solution. The parameter studied is []. Converging on [] also ensures that other parameters including peak pressure are converged. The converged time step used for Browns Ferry is [] for the system and a steam line time step that is [] finer. Specifically to demonstrate the time step for the ATWS event, results are provided below for the Browns Ferry Unit 3 Cycle 14 EPU limiting ATWS analysis. The steam line nodalization is consistent with the Peach Bottom benchmark of Reference 23 and consists of [] nodes from the dome to the MSIVs. The time step study and the consistent nodalization of steam line from the original benchmark model are sufficient to preclude numerical errors in the calculation of the pressure wave propagation to the reactor core from the MSIVs.

**Table 8-1 Energy Release to
Suppression Pool**

--

Table 8-2 ATWS Time Step Study

Parameter	TS = []			
Peak vessel pressure, # psig	1477	1478	1478	1477

Results do not contain the adder discussed in Section 8.2.

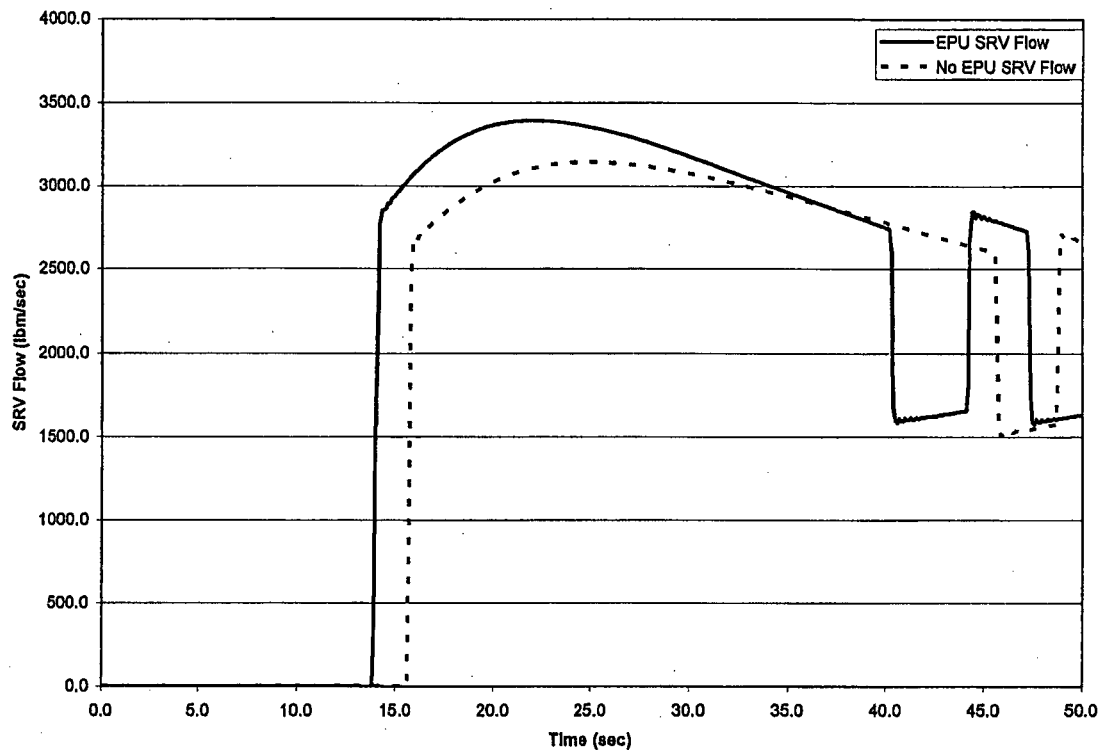


Figure 8-1 SRV Flow During ATWS Overpressurization

9.0 References

1. B.T. McKinney (PPL), Letter to NRC, "Supplement to Proposed License Amendment Numbers 285 for Unit 1 Operating License No. NPF-14 and 253 for Unit 2 License NPF-22 Constant Pressure Power Uprate," PLA -6306, November 30, 2007.
2. B. Waldrep (Progress Energy), Letter to NRC, "Brunswick Steam Electric Plant, Unit Nos. 1 and 2, Docket Nos. 50-325 and 50-324/License Nos. DPR-71 and DPR-62, Additional Information in Support for License Amendments Regarding Linear Heat Generation Rate and Core Operating Limits Report References for AREVA NP Fuel (NRC TAC Nos. MD4063 and MD4064)," January 24, 2008.
3. ANP-2638(P), Revision 2, "Applicability of AREVA NP BWR Methods to Extended Power Uprate Conditions," AREVA NP Inc., October 2009.
4. ANP-2637, Revision 2, "Boiling Water Reactor Licensing Methodology Compendium," AREVA NP Inc., December 2007.
5. J. C. Roberts (Entergy), Letter to NRC, "License Amendment Request, Main Turbine Bypass System, River Bend Station, Unit 1 – Docket No. 50-458, License No. NPF-47," April 14, 2009.
6. TVA Letter, D. Langley to NRC, "Browns Ferry Nuclear Plant (BFN) – Units 2 and 3 – Technical Specifications (TS) Change TS-418 – Extended Power Uprate (EPU) – Supplemental Response to Request for Additional Information (RAI) Rounds 3 and 18 and Response to Round 20 Fuels Methods RAIs (TAC Nos. MD5263 and MD5264)," September 19, 2008.
7. TVA letter, D. Langley to NRC, "Browns Ferry Nuclear Plant (BFN) - Units 2 and 3 – Technical Specification (TS) Change TS-418 – Extended Power Uprate (EPU) – Supplemental Response to NRC Round 16 Request for Additional Information (RAI) – SRXB-87 and SRXB-89 (TAC Nos. MD5263 and MD5264)," May 1, 2008.
8. TVA letter, D. Langley to NRC, "Browns Ferry Nuclear Plant (BFN) - Units 2 and 3 – Technical Specification (TS) Change TS-418 – Extended Power Uprate (EPU) – Supplemental Response to NRC Round 16 Request for Additional Information (RAI) – SRXB-88 (TAC Nos. MD5263 and MD5264)," June 3, 2008,
9. TVA letter, J. Emens to NRC, "Browns Ferry Nuclear Plant (BFN) - Units 2 and 3 – Technical Specification (TS) Change TS-418 – Extended Power Uprate (EPU) – Partial Response to NRC Round 18 Request for Additional Information (RAI) (TAC Nos. MD5263 and MD5264)," August 15, 2008.
10. TVA Letter, M. Brandon to NRC, "Browns Ferry Nuclear Plant (BFN) – Units 2 and 3 – Technical Specifications (TS) Change TS-418 –Extended Power Uprate (EPU) – Response to Round 21 Request for Additional Information (RAI) on Channel Bow (TAC Nos. MD5263 and MD5264)," October 17, 2008.

11. TVA letter, S. Douglas to NRC, "Browns Ferry Nuclear Plant (BFN) – Units 1, 2, and 3 – Technical Specifications (TS) Change TS-418 and TS-431 – Extended Power Uprate (EPU) – Response to Round 16 Request For Additional Information (RAI) – SRXB-74/86 and SRXB-87 Through SRXB-90 (TAC Nos. MD5262, MD5263, and MD5264)," March 6, 2008.
12. TVA letter, W. Crouch to NRC, "Browns Ferry Nuclear Plant (BFN) – Units 2, and 3 – Response to NRC Round 3 Requests for Additional Information Related to Technical Specifications (TS) Change No. TS-418 – Request for Extended Power Uprate Operation (TAC NOS. MC3743 and MC3744)," March 7, 2006.
13. TVA letter, W. Crouch to NRC, "Browns Ferry, Units 2 and 3 – Supplemental Response to NRC Round 3 Request for Additional Information Related to Technical Specifications Change No. TS-418 – Extended Power Uprate Operation (EPU) (TAC Nos. MC3743 and MC3744)," May 11, 2006.
14. *Poolside Measurement of AREVA BWR Fuel Channels*, EPRI, Palo Alto, CA: 2004. 1008097.
15. XN-NF-81-58(P)(A) Revision 2 and Supplements 1 and 2, *RODEX2 Fuel Rod Thermal-Mechanical Response Evaluation Model*, Exxon Nuclear Company, March 1984.
16. XN-NF-85-74(P)(A) Revision 0, *RODEX2A (BWR) Fuel Rod Thermal-Mechanical Evaluation Model*, Exxon Nuclear Company, August 1986.
17. XN-NF-85-92(P)(A), *Exxon Nuclear Uranium Dioxide/Gadolinia Irradiation Examination and Thermal Conductivity Results*, Exxon Nuclear Company, November 1986.
18. March-Leuba, J., D.G. Cacuci, and R.B. Perez, "Nonlinear Dynamics and Stability of Boiling Water Reactors: Part I – Qualitative Analysis," *Nuclear Science and Engineering*: 93, 111-123 (1986).
19. XN-NF-80-19(P)(A) Volume 3 Revision 2, *Exxon Nuclear Methodology for Boiling Water Reactors THERMEX: Thermal Limits Methodology Summary Description*, Exxon Nuclear Company, January 1987.
20. XN-NF-84-105(P)(A) Volume 1 and Volume 1 Supplements 1 and 2, *XCOBRA-T: A Computer Code for BWR Transient Thermal-Hydraulic Core Analysis*, Exxon Nuclear Company, February 1987.
21. XN-NF-84-105(P)(A) Volume 1 Supplement 4, *XCOBRA-T: A Computer Code for BWR Transient Thermal-Hydraulic Core Analysis - Void Fraction Model Comparison to Experimental Data*, Advanced Nuclear Fuels Corporation, June 1988.
22. ANF-81-58(P)(A) Revision 2, Supplements 3 and 4, *RODEX2 Fuel Rod Thermal Mechanical Response Evaluation Model*, Advanced Nuclear Fuels Corporation, June 1990.

23. ANF-913(P)(A) Volume 1 Revision 1 and Volume 1 Supplements 2, 3 and 4, *COTRANSA2: A Computer Program for Boiling Water Reactor Transient Analyses*, Advanced Nuclear Fuels Corporation, August 1990.
24. ANF-524(P)(A) Revision 2 and Supplements 1 and 2, *ANF Critical Power Methodology for Boiling Water Reactors*, Advanced Nuclear Fuels Corporation, November 1990.
25. R.T. Lahey Jr. and F.J. Moody, *The Thermal-Hydraulics of a Boiling Water Nuclear Reactor, Second Edition*, American Nuclear Society, Hinsdale, IL, 1993.
26. Correspondence, R.A. Copeland (Siemens) to R.C. Jones (NRC), "ATRIUM-10 Presentations," RAC:95:080, May 4, 1995 (38-9091703-000).
27. EMF-85-74(P) Revision 0 Supplement 1(P)(A) and Supplement 2(P)(A), *RODEX2A (BWR) Fuel Rod Thermal-Mechanical Evaluation Model*, Siemens Power Corporation, February 1998.
28. Correspondence, J.F. Mallay (Framatome) to U.S. Nuclear Regulatory Commission, "RODEX2 - Additional V&V and Consolidation of Approved Versions," NRC:01:025, September 10, 2001. (ADAMS Accession No. ML012610568)
29. I.K. Madni, et al., "Development of Correlations For Pressure Loss/Drop Coefficients Obtained From Flow Testing of Fuel Assemblies In Framatome ANP'S PHTF," Paper Number 22428, Proceedings of ICONE10, Arlington, VA, April 14-18, 2002.
30. EMF-2209(P)(A) Revision 2, *SPCB Critical Power Correlation*, Framatome ANP, September 2003.
31. EMF-2982(P) Revision 0, *Browns Ferry Units 2 and 3 Safety Analysis Report for Extended Power Uprate ATRIUM™-10 Fuel Supplement*, Framatome ANP, June 2004.
32. Y. Aounallah, "Boiling Suppression in Convective Flow," Proceedings of ICAPP '04, Pittsburgh, PA, June 13-17, 2004, Paper 4251.
33. BAW-10247PA Revision 0, *Realistic Thermal-Mechanical Fuel Rod Methodology for Boiling Water Reactors*, AREVA NP Inc., April 2008.
34. March-Leuba, J., "Density-Wave Instabilities in Boiling Water Reactors," NUREG/CR-6003, September 1992.
35. Wulff, W., H. S. Cheng, A.N. Mallen, and U.S. Rohatgi, "BWR Stability Analysis with the BNL Engineering Plant Analyzer," NUREG/CR-5816, October 1992.
36. NEDO-32164 Revision 0, "Mitigation of BWR Core Thermal-Hydraulic Instabilities in ATWS," December 1992.
37. ANF-89-98(P)(A) Revision 1 and Supplement 1, "Generic Mechanical Design Criteria for BWR Fuel Designs," Advanced Nuclear Fuels Corporation, May 1995.

38. NEDO-32047-A, "ATWS Rule Issues Relative to BWR Core Thermal-Hydraulic Stability," June 1995.
39. NEDO-32465-A, Reactor Stability Detect and Suppress Solutions Licensing Basis Methodology for Reload Applications, August 1996.
40. Services Information Letter, *Mitigation of the Effects of Peripheral Core Location on Fuel Channel Bowing*, SIL No. 320 Supplement 3, GE Nuclear Energy, April 2003.
41. NEDC-33047P Revision 2, Browns Ferry Units 2 and 3 Safety Analysis Report for Extended Power Uprate, GE Nuclear Energy, June 2004.
42. Farawila, Y.M., and D.W. Pruitt, "A Study of Nonlinear Oscillation and Limit Cycles in Boiling Water Reactors – I: The Global Mode," *Nuclear Science and Engineering*: 154, 302-315 (2006).
43. Farawila, Y.M., and D.W. Pruitt, "A Study of Nonlinear Oscillation and Limit Cycles in Boiling Water Reactors – II: The Regional Mode," *Nuclear Science and Engineering*: 154, 316-327 (2006).
44. EMF-2158(P)(A), "Siemens Power Corporation Methodology for Boiling Water Reactors: Evaluations and Violation of CASMO-4/MICROBURN-B2," Siemens Power Corporation, October 1999.

Appendix A Channel Bow

Effect of EPU Neutron Spectrum on Channel Bow

EPU operation will [

] To assess the impact of this difference on channel bow, a detailed channel bow model that calculates the bow effect due to [

] This bow model is described in the RODEX4 topical report (Reference 33) and it is included as an option in MICROBURN-B2. Channel bow is a function of [

[

]

Channel Bow Statistics

Channel bow statistics used for the SLMCPR analysis (Safety Limit Minimum Critical Power Ratio) are derived from channel bow measurements. Measurement data are [

] measurement data are used.

Figure A-2 displays existing D-lattice bow measurement data from [

]

Figure A-3 shows the same bow data except the absolute value is taken of the bow measurements. The SLMCPR analysis makes use of the statistics derived from the absolute values of bow measurement data.

More recent measurements have been obtained for comparison. The EPRI Fuel Reliability Program included an initiative to obtain a more modern characterization of fuel vendor channel performance (Reference 14). As part of this program, AREVA NP acquired data on [

]. A statistically relevant

sample of [] fuel channels ([] bow measurements) was measured by selecting assemblies over a range of operating conditions with exposures from [

] No special design guidelines to mitigate channel

bow were used for the core design during the time the measured fuel channels resided in []. The fuel operated in 24-month cycles.

The [] data are shown overlaid in Figure A-3. In the plot, lines showing the mean bow and the mean plus two times the standard deviation bow are shown on the plot for comparison purposes. Data are grouped in exposure "bins" for calculating the mean bow and sample standard deviation as a function of exposure. The more recent bow data fall well within the bounds of the existing data and there is no significant difference in bow between the [].

The bow statistics are applicable to the BFN units at EPU because:

- The data were obtained from plants with the same D-lattice core geometry as the BFN units.
- A sufficient quantity of data are available that extend to the licensed discharge exposure limit.
- The measurements are on channels from the same vendor.

[

]

Susceptibility of Browns Ferry Units to Abnormal Channel Bow

Over the past several years, the majority of industry channel bow problems have occurred primarily in BWR reactors with C/S-lattice cores. Less severe and less frequent operating events with cell friction have been reported in three D-lattice plants – Monticello, Brunswick Unit 2 and Peach Bottom Unit 3. In addition, the incidence of shadow corrosion bow appears to vary from plant-to-plant. The BFN units have not encountered any signs of cell friction as evidenced by normal control rod maneuvers, during the Technical Specification control rod operability surveillance and testing, and during additional cell friction testing. If shadow corrosion bow is present, operating experience indicates that the abnormal bow is significantly lower compared to bow in C/S-lattice plants.

A control rod that experienced friction at Monticello was confirmed to have been caused by channel bow. However, the operation of the fuel in the cell was atypical. Three of the four fuel assemblies in the cell were in the fourth cycle of operation. The other fuel assembly was in the third cycle. The cycle lengths underwent a transition to two-year cycles during this time. The overall residence time for the three assemblies was equivalent to approximately 3-1/3 cycles (where each cycle is 2 years). Prior operation involved some level of control (i.e., exposure to an inserted control rod) and operation in one of the outer three rows of the core.

Although AREVA NP does not possess detailed information on the Monticello event, the abnormal bow primarily was attributed to shadow corrosion bow caused by early control. The operating condition of the fuel bears some resemblance to the conditions that caused recent problems with AREVA NP fuel in core peripheral locations in C-lattice plants. That is, the operation included higher exposure (greater fast fluence), high residence time, and peripheral cell operation (higher fluence gradient). [

]

Similarly, the Brunswick Unit 2 event is attributed to a combination of high early control and higher exposure fuel in core peripheral locations (outer three rows). Two adjacent assemblies in a problem cell had been subject to power suppression in the first cycle. Thus the earlier power suppression and the decision to load the two assemblies in the same cell contributed to control rod interference.

While the two preceding events at Monticello and Brunswick were a result of exceptions to typical operation, the event at Peach Bottom Unit 3 represents the first case where shadow corrosion bow occurred in a D-lattice plant under typical operating conditions. However, the severity of interference and the quantity of affected cells are still significantly less compared to the general operating experience in C-lattice plants.

For discussion purposes, abnormal bow observed in C/S-lattice cores is divided into two categories as outlined below. Note that expected or "normal" behavior is considered to be predictable bow arising from fast fluence gradients.

[

]

As evidenced by a lack of reported control rod friction issues, there is an extensive amount of industry operating experience demonstrating that abnormal bow due to early control (shadow corrosion) is much less prevalent in D-lattice plants. The reason for the lack of shadow corrosion bow is [

] is a likely contributor to the lack of cell friction problems relative to C/S-lattice plants.

[

]

[] Still,
the events described earlier point to a much lower incidence of abnormal bow in D-lattice plants.

To further evaluate recent operation at the BFN units with AREVA NP fuel, the amount of early control and exposures of the AREVA NP channels were examined. The amount of early control is characterized as the [

] Yet, Unit 3 Cycle 13 operated to the end of the cycle and shutdown with no control rod friction issues and no indications of slow-to-settle rods. Unit 2 Cycle 15 also ended with no detection of cell friction. As of August 2009, Unit 3 has completed 15 months of operation in Cycle 14 with a full core of AREVA NP fuel. In Cycle 14, the fuel channels in [] There is no evidence of cell friction due to channel bow in Unit 3 to date as evidenced by normal control rod movement, control rod insertion during scrams, and additional cell friction tests (described below). The evaluation of the [

] in C/S-lattice plants provides additional assurance that abnormal bow will not be a problem in future cycles in the BFN units.

Note that the foregoing discussion is not dependent on EPU. [

]

Channel Bow Monitoring Methods at Browns Ferry

Based on the industry experience, TVA implemented a testing procedure in Unit 3 Cycle 14 specifically to detect cell friction due to abnormal bow. However, formalized testing or surveillance programs, in general, are not currently planned for the other BFN cores. The Unit 3 testing, as described earlier, is focused on a significant sample of the most susceptible cells among the two units. If significant shadow corrosion bow exists, then it is believed that the testing will reveal the problem.

Routine plant surveillance tests can also serve to detect excessive friction. Among these are the periodic scram time test and the control rod exercise surveillance test, both of which are required by Technical Specifications. One of the rod exercise tests specifically targets partially inserted rods; this test provides an opportunity to detect abnormal friction in cells where the blade would have significant contact area with the surrounding channels. In this test, a partially inserted rod is moved in one notch and is then withdrawn back to the original position. Since the BFN cores are designed with a conventional core design (all four control rod sequences are utilized), a significant number of the interior core cells would be sampled during the cycle by the partially inserted rod exercise test.

Abnormal cell friction also can be detected by periodic scram time testing. In this test, a sample of rods is individually scrambled in one at a time throughout the cycle from the fully withdrawn position to measure the insertion times to various specified positions. If sufficient control rod interference is present due to channel bow, the test will reveal a slower scram time compared to the average of the rods tested.

Most of the control rods in the core (including the edge and near edge rods) are withdrawn during startup. There are a significant number of rod movements each time a control rod

sequence exchange is performed that occur every few months during the cycle. These rod movements provide additional opportunities to detect any developing channel bow issues that could be creating excessive interference. If a control rod failed to properly settle during any rod movement, the operators will receive a rod drift alarm which will prompt documentation and investigation.

Hence, it is very unlikely that a systematic issue with abnormal channel bow can occur without indications of control rod friction. [

] Thus, the observation of control rod operation during testing and routine operation should be effective in identifying the onset of a channel bow problem.

Conservatism in Treatment of Channel Bow in Regard to Thermal Margins

Conservatism are discussed throughout the AREVA NP topical report on critical power methodology (Reference 24). In summary the conservatisms are:

[

]

[

]

Use of Services Information Letter 320 and Plans to Manage Greater Than Expected Bow

Core designs for the BFN units have followed SIL-320 Supplement 3 (Reference 40). The core design guide avoids an unfavorable combination of fluence gradient bow in core peripheral locations. There are options in the guide for C/S-lattice and D-lattice cores. The requirements are less restrictive in the case of a D-lattice core. For recent core designs, TVA [

] At a minimum, the BFN units will continue to use SIL-320 Supplement 3 or future improved means to limit the impact of fluence gradients on cell friction.

As noted above, industry operating experience indicates abnormal bow is much less extensive for D-lattice plants. And, no evidence of abnormal bow has been detected at the Browns Ferry

units. However, in the event unexpected bow is encountered; a similar process currently used for C-lattice plants would be used. An outline of the steps is provided below.

1. Following the identification of cell friction, perform settle time tests to determine the extent of cell friction in the core. Perform additional testing if necessary to narrow the cause to channel bow.
2. For cells that fail the settle time testing, subject the control rod to a scram time insertion test. Evaluate the control rod(s) for continued surveillance and operability based on the test results and establish the status (inoperable or continued surveillance frequency).
3. An evaluation would be performed to determine the impact of channel bow on thermal limits. Based on current experience, the evaluation would investigate the need to increase the channel bow assumed in the SLMCPR analysis beyond the standard values, and if needed, derive an administrative CPR penalty based on a revised analysis.
4. Implement periodic surveillance of susceptible cells. Depending on the outcome of the settle tests, it might be necessary to identify susceptible cells by application of more conservative C/S-lattice surveillance criteria.
5. It is likely that channel bow measurements would be made following the conclusion of the cycle. The measurements would be used to []

Channel Bow for Co-resident GE14 Fuel

For the legacy GE14 fuel at Browns Ferry Unit 1, the legacy fuel vendor confirmed that the channel bow data (mean and standard deviation) []

]



**Figure A-1 Average and Maximum Channel Bow for CLTP and EPU
Equilibrium Cycle Designs (Excluding the Peripheral Assemblies)**



Figure A-2 AREVA NP D-Lattice Channel Bow Measurement Data (Signed Values)



**Figure A-3 AREVA NP D-Lattice Channel Bow Measurement Data
(Absolute Values)**

ATTACHMENT 27

PART 3

**Response to Previous NRC Requests for Supplemental Information Regarding
Utilization of AREVA Fuel and Associated Analysis Methodologies**

(Non-proprietary Version)

Question 1.

Licensing topical report (LTR) ANP-2638P "Applicability of AREVA NP BWR [boiling water reactor] Methods to Extended Power Uprate Conditions," states that loss-of-coolant accident (LOCA) results are only weakly dependent on core average power. However, for the small break LOCA (SBLOCA) the analysis results are highly sensitive to the core average power level.

Since depressurization occurs through the automatic depressurization system (ADS) for SBLOCAs, the timing when low pressure injection systems reach rated flow is extended when the core steam generation rate is higher – as would be the case for EPU conditions. Based on the plant-specific power uprate and the ADS capacity, the limiting break for an EPU plant may be a SBLOCA. This was shown for Browns Ferry Unit 1 in the power uprate safety analysis report.

The EXEM BWR-2000 LOCA analysis methodology is described by LTR EMF-2361(P)(A), "EXEM BWR-2000 ECCS [emergency core cooling system] Evaluation Model." This LTR states:

SBLOCA PCTs [peak cladding temperatures] are bound when the conservatism included in the EM methodology is applied. This result is acceptable because small break events are not limiting in BWRs and the test evaluated simulated an extremely small break in which core uncover and the resulting heat-up is minor such that the conservatism (Appendix K coefficients) are not allowed to raise fuel temperature to values of concern.

When the LTR language is considered in the context of the Unit 1 LOCA analyses at EPU conditions, EXEM BWR-2000 does not appear to be applicable. First, for Unit 1 at EPU conditions, the limiting break is a small break. This appears contrary to the basis for the staff approval of EXEM BWR-2000.

Second, at EPU conditions the core heat-up is not rapidly terminated because blowdown times are prolonged for SBLOCA. Therefore, the core uncover persists for a longer duration and the Appendix K assumptions (e.g., the 20 percent increase in decay heat) will contribute to significant heatup and high fuel temperatures. This appears to conflict with the disposition of the SBLOCA qualification results in the LTR.

Therefore, it does not appear that EXEM BWR-2000 is applicable to analyze the limiting LOCA event for Unit 1. Provide the SBLOCA analyses for Unit 1 using acceptable methods.

Response 1.

For a Pressurized Water Reactor, SBLOCA results may be highly sensitive to core average power. However, for a BWR, SBLOCA results are not nearly as sensitive to initial core power primarily due to the mitigating effects of the

Automatic Depressurization System (ADS). The ADS essentially turns a SBLOCA into a large break steam line LOCA. If the ADS is significantly degraded (or not available), the sensitivity of a SBLOCA to initial power level would be more significant.

As indicated in the NRC request, the rate of depressurization and timing when low pressure injection systems reach rated flow is affected by initial power level. The core steam generation rate (i.e., the steam generated by decay heat) is higher at Extended Power Uprate (EPU) than at pre-EPU conditions. The higher steam generation rate will slow down the depressurization rate slightly; however, the depressurization rate is determined by the net inventory loss rate, that is, the difference between the steam generation rate and the sum of inventory loss out the ADS valves and the break. Because ADS flow rate is much larger than the steam generation rate, the change in depressurization rate is much less than the change in steam generation rate (power level) on a relative basis. For the 0.05 ft² recirculation line break (discharge side, top peaked) at EPU conditions, the steam generation rate is 13.8% of the combined ADS and break flow at the time of ADS initiation. A 15% change in the steam generation rate would change the net inventory loss by only 2.3%. This change would not significantly impact the depressurization rate or Low Pressure Core Spray (LPCS) initiation times following ADS actuation.

The impact of initial power level (steam generation rate) on depressurization rate and LPCS initiation times was further assessed by repeating the 0.05 ft² recirculation line break at pre-EPU conditions. Relative to pre-EPU, increasing to EPU initial core power delayed the start of LPCS flow after ADS initiation by 0.8 seconds (0.5% of the blowdown time) and delayed reaching rated LPCS flow by 10.7 seconds (3.4% of the blowdown time). The PCT increase for EPU conditions was not significant (25°F). Note, the higher EPU power level also results in an earlier initiation of ADS and LPCS due to a reduced initial liquid inventory and a higher steam generation rate.

The above sensitivities are dependent on the ADS characteristics assumed in the analyses. Degraded ADS performance may increase the sensitivity of a SBLOCA to initial core power level. The EXEM BWR-2000 evaluation model adequately models the important phenomena for SBLOCA analyses and would correctly reflect degraded PCT performance if the ADS system performance is degraded from that assumed in the Browns Ferry Nuclear Plant (BFN) LOCA analyses. Further discussion of SBLOCA analysis results with degraded ADS performance is provided in the response to NRC Question 4.

The statement referred to by the NRC question from the EXEM BWR-2000 LTR (EMF-2361(P)(A), "EXEM BWR-2000 ECCS Evaluation Model") was intended to indicate that the SBLOCA test resulted in relatively low peak cladding temperatures and therefore it was not surprising that a large amount of conservatism was not predicted in the analysis without the Appendix K model conservatisms included. The discussion in the LTR goes on to demonstrate that with Appendix K model conservatisms included in the analyses of the test, the AREVA methodology produced conservative results

as compared to test data. The statement referred to from the LTR was not intended to imply any restriction on the applicability of the methodology for SBLOCA analyses.

The AREVA LTR clearly indicates that the EXEM BWR-2000 methodology is conservative and applicable for SBLOCA analyses. The NRC specifically approved the method to be applicable and sufficiently conservative for analysis of SBLOCA events, as quoted in Section 4 of the Safety Evaluation for the EMF-2361:

“The test results for small breaks show low temperatures, and the EXEM BWR-2000 model using evaluation model options bounds the temperature data. Furthermore, the EXEM BWR-2000 model adequately predicts the important LOCA phenomena...”

The staff, therefore, concludes that the proposed EXEM BWR-2000 ECCS EM, as documented in References 1, 2, 4, and 5, is acceptable for referencing in BWR LOCA analyses, with the limitation that application of the revised evaluation model will be limited to jet pump plant applications..”

The EXEM BWR-2000 methodology conservatively predicts the important phenomena that occur during a SBLOCA. The EXEM BWR-2000 methodology has been used for complete LOCA break spectrum analyses submitted and approved by the NRC for two other US BWRs operating at EPU conditions. The LOCA analyses supporting the BFN Unit 1 submittal were performed consistent with the NRC approval of the EXEM BWR-2000 methodology. Therefore, the BFN SBLOCA analyses provided to the NRC were performed using acceptable methods.

Question 2.

Provide the LOCA results for hydrogen generation/core wide oxidation.

Response 2.

The AREVA methodology for core wide metal water reaction (CMWR) analysis calculates CMWR as a function of planar power, axial power shape, and radial power distribution. All assemblies in the core are considered which includes all axial planes. CMWR is calculated as a function of exposure.

The CMWR analysis for BFN was based on a limiting metal water reaction (MWR) LOCA case with a Planar Average MWR (at the peak PCT plane) of 0.4%. The results gave a limiting CMWR and hydrogen generation of 0.05% at a cycle exposure of 18994.7 MWd/MTU.

[

]

After the CMWR analysis was completed, the BFN break spectrum was reanalyzed in 2004 primarily because of a change in the ADS delay time. In the revised break spectrum (documented in Revision 1 of EMF-2950(P)), the limiting MWR LOCA case was more severe due to the additional ADS delay. The planar average MWR was 0.8%. The CMWR analysis results were reviewed to determine if a reanalysis was required with the revised break spectrum results. A reanalysis was not needed because the CMWR results did not challenge the 10 CFR 50.46 acceptance criteria of < 1% total hydrogen generation. [

] Since a new analysis was not performed, the CMWR results were reported as "< 1% hydrogen generation".

Figures 2.1 and 2.2 provide additional information on planar average MWR. The figures are based on the analysis with a PCT planar average MWR of 0.8%. [

] Figure 2.2 shows MWR vs. time at the PCT plane for the limiting LOCA case.

[

Figure 2.1 Metal Water Reaction vs. Elevation Above the Bottom of the Active Fuel Browns Ferry Nuclear Plant Limiting LOCA]

[

Figure 2.2 Metal Water Reaction vs. Time at the PCT Axial Location
Browns Ferry Nuclear Plant Limiting LOCA

]

Question 3.

The statements regarding the transition core effects on the LOCA analyses (EMF-2950(P), "Browns Ferry Units 1, 2, and 3 Extended Power Update LOCA Break Spectrum Analysis," Section 2), would inherently impose similar performance conclusions on the legacy fuel. By this logic, the current licensing basis analysis should demonstrate similar performance to the fuel transition analysis. Provide the report describing the previous licensing basis (in this case, the previous licensing basis is at EPU conditions) LOCA analysis and supplement the analysis by accounting for model differences that cause the results in break spectrum, location, geometry, and results to differ.

Response 3.

As discussed in the response to Question 4, TVA has worked with GE Hitachi (GEH) and AREVA to obtain additional LOCA analyses to address the ADS single failure issue (see Attachments 16, 17, 20, and 21). The new reports are based on current licensed thermal power (CLTP), as opposed to EPU. TVA is utilizing these reports to establish a new LOCA licensing basis at current licensed power. The new analyses address the effects of 250 VDC battery failure on both RMOV Board A (fails HPCI but leaves automatic ADS) and RMOV Board B (leaves HPCI operable but fails automatic ADS). The response below is focused on the differences observed in cases run for RMOV Board A. The GEH and AREVA analyses for RMOV Board B produced very similar results both in terms of limiting break size and peak clad temperature.

The trends observed in the EPU break spectrum (which had only considered battery failure affecting RMOV Board A) tend to also be observed in the new CLTP break spectrum. In order to better understand the differences in the break spectrum results, each vendor was asked to run additional cases beyond those required by their processes and procedures. TVA had both vendors run the same analysis cases, using the same input assumptions, for the same break sizes, to the extent practicable. For example, each vendor was asked to run a case for the limiting recirculation break size of the other vendor (at the smaller break end of the spectrum). The double ended guillotine (DEG) break of a recirculation suction line was also run by both vendors and compared. Comparable plots of key results were included in both vendor reports for these breaks to facilitate comparison. In addition, tables of key event times for each break were included in both vendor reports.

An assessment of differences was performed by comparing the following analysis cases from each of the two vendors.

- Large DBA Break LOCA Analysis for Battery A Failure (i.e., DEG break of recirculation suction line)
- Limiting Recirculation Discharge Line Break Analysis for Battery B Failure
- Small Recirculation Discharge Line Break Analysis for Battery A Failure (limiting small breaks for GEH and AREVA)

- Feedwater Line Break Analysis

Based on a review of both vendors' documentation, TVA was able to identify several differences in vendor input assumptions which appear to explain a significant amount of the observed differences. These differences involve:

- Assumptions regarding the timing of the closure of the main steam isolation and turbine control valves, which affects the vessel depressurization and influences break flow due to timing of depressurization.
- Assumptions regarding the low pressure ECCS system flow versus injection valve position.
- Assumptions related to core spray system cooling.
- Assumptions related to the initial vessel water level assumed by each vendor.
- Assumptions related to modeling of flow between the bypass region and the bundle.

The impact of these differences in vendor input assumptions were assessed by performing sensitivity studies.

A detailed discussion of the comparisons for each of the analysis cases, including an explanation of differences between the two vendors' results, is included in an assessment report prepared by TVA. Based on the results of the comparisons, it is concluded that many of the overall differences in results obtained from the two vendors can be explained in terms of differences in input assumptions. The sensitivity studies showed that for some of the cases, eliminating these differences results in reasonably comparable peak clad temperature results. Of course, the underlying differences in vendor analytical models would still produce some differences in peak clad temperature, even if all input differences were eliminated.

The report also offers insights and observations on the clad temperature behavior differences based on the event timing differences, comparing plots of key results, and by information obtained from each vendor about their cases.

In the assessment report, TVA utilized and compared information and results from the proprietary version of both vendors' LOCA reports. In order to perform a meaningful comparison, proprietary information from each of the two vendors was combined such that extracting the information to allow the development of separate proprietary documents by each of the vendors (i.e., the owners of the information) and the associated applications for withholding the document(s) from public disclosure in accordance with 10 CFR 2.390 for the assessment report was not possible. As a result, this assessment report is available for NRC review in TVA offices.

Question 4.

Single failure analyses do not account for the ADS unavailability. Please provide the failure modes and effects analysis for the ADS with respect to the limiting postulated SBLOCA, and for the postulated high pressure coolant injection (HPCI) line break. Justify not analyzing the failure of the ADS system in toto, or even a single ADS valve.

Response 4.

Background

For BFN, Unit 1, background information regarding the ADS and HPCI System is provided as follows.

The ADS consists of 6 of the 13 Safety/Relief Valves (S/RVs). BFN Unit 1 Technical Specifications (TS) Limiting Condition for Operation (LCO) 3.5.1, "ECCS-Operating," requires the ADS function of six S/RVs to be operable in Mode 1 and in Modes 2 and 3, except when reactor steam dome pressure is ≤ 150 psig. The ADS is designed to provide depressurization of the Reactor Coolant System during a small break Loss of Coolant Accident (SBLOCA) if the HPCI System fails or is unable to maintain required water level in the reactor pressure vessel (RPV). ADS operation reduces the RPV pressure to within the operating pressure range of the low pressure Emergency Core Cooling System (ECCS) subsystems (Core Spray (CS) and Low Pressure Coolant Injection (LPCI)), so that these subsystems can provide coolant inventory makeup. Therefore, the ADS provides the backup for the HPCI System. The ADS and HPCI System instrumentation and controls are designed such that no single failure can disable both the ADS and HPCI System functions.

Each of the six S/RVs used for automatic depressurization (i.e., ADS valves) is equipped with an air accumulator and associated inlet check valves. The accumulators provide the pneumatic power to actuate the valves.

Each of the six ADS valves is also provided with a direct current (DC) powered solenoid-operated pilot valve which controls the pneumatic pressure applied to a diaphragm actuator to actuate the ADS valve. The DC power for each of the six ADS solenoid valves is from the 250 VDC Unit Batteries. The normal power for the six ADS solenoid valves are evenly distributed across the three 250 VDC Unit Batteries (i.e., solenoid valves for ADS valves PCV-1-30 and PCV-1-22 are powered from Unit Battery # 1 (through 250 VDC RMOV Board 1A), solenoid valves for ADS valves PCV-1-34 and PCV-1-5 are powered from Unit Battery # 2 (through 250 VDC RMOV Board 1C), and solenoid valves for ADS valves PCV-1-31 and PCV-1-19 are powered from Unit Battery # 3 (through 250 VDC RMOV Board 1B)). In addition, the power for solenoid valves for two of the six ADS valves (i.e., PCV-1-30 and PCV-1-22) transfers to an alternate DC source in the event of the loss of the normal DC source.

The logic to initiate ADS includes two trip systems. BFN Unit 1 TS LCO 3.3.5.1, "Emergency Core Cooling System (ECCS) Instrumentation," requires the ADS trip systems A and B to be operable in Mode 1 and in Modes 2 and 3 with reactor steam dome pressure > 150 psig. The ADS logic in each trip system is arranged in two strings. Each string has a contact from each of the following variables: Reactor Vessel Water Level - Low Low Low, Level 1; Drywell Pressure - High; High Drywell Pressure Bypass Timer; and Pump Discharge Pressure - High. One of the two strings in each trip system must also have a confirmed Reactor Vessel Water Level - Low, Level 3 (confirmatory). Either the Drywell Pressure - High or the Drywell Pressure Bypass Timer contacts and all remaining contacts in both logic strings must close and the ADS initiation timer must time out to initiate an ADS trip system. Either the A or B trip system will cause all the ADS valves to open. Sufficiently redundant instrumentation components are provided such that no single instrument failure will preclude initiation of all ADS (e.g., four channels of Reactor Vessel Water Level - Low Low Low, Level 1 are provided; two channels input to ADS trip system A and the other two channels input to ADS trip system B). However, the logic for ADS trip system A and ADS trip system B are powered from the same DC source (i.e., 250 VDC RMOV Board 1B which is powered by Unit Battery # 3). As such, the ADS is not single failure proof, but the design is such that no single failure shall prevent the integrated operations of the ECCS from providing adequate core cooling (e.g., a single failure shall not result in the failure of both the ADS and the HPCI System functions).

For the HPCI System, the controls for the HPCI components (e.g., HPCI pump discharge valve) are powered from the 250 VDC RMOV Board 1A (which is powered by Unit Battery # 1). BFN Unit 1 TS LCO 3.5.1, "ECCS-Operating," requires the HPCI System to be operable in Mode 1 and in Modes 2 and 3, except when reactor steam dome pressure is \leq 150 psig. The HPCI initiation logic is arranged such with Division II is powered by 250 VDC RMOV Board 1A (which is powered by Unit Battery # 1) and Division I is powered from 250 VDC RMOV Board 1B (which is powered by Unit Battery # 3). The arrangement is such that a loss of power to 250 VDC RMOV Board 1B does not result in loss of HPCI System initiation capability. However, loss of power to 250 VDC RMOV Board 1A does result in loss of HPCI System initiation capability. BFN Unit 1 TS LCO 3.3.5.1, "Emergency Core Cooling System (ECCS) Instrumentation," requires the HPCI System initiation instrumentation functions to be operable in Mode 1 and in Modes 2 and 3 with reactor steam dome pressure > 150 psig.

LOCA Analyses with Single Failure of ADS Automatic Actuation

The original LOCA analysis supporting use of AREVA fuel for BFN Unit 1 is documented in Reference 1. This LOCA analysis was based on the plant parameters and potentially limiting ECCS single failures reflected in Reference 1 and Updated Final Safety Analysis Report (UFSAR) Table 6.5-3, "Single Failure Evaluation Used for LOCA Analysis." The Reference 1 analysis was based on EPU power conditions, with a limited number of cases at the current

licensed power of 3458 MWt. The Reference 9 analysis, while EPU based, did include a reasonable number of current licensed power based cases.

In defining the plant characteristics for the LOCA analysis, it had been previously identified that the ADS could not be disabled by a single failure. Therefore, it was not identified as a potentially limiting single failure that needed to be considered in the LOCA analyses. Subsequent investigation of the issue by TVA has concluded that the previous position was incorrect; a failure of the battery powering RMOV Board B can disable automatic initiation of the ADS (all valves). In addition, TVA determined that the potential failure of automatic initiation of the ADS had been considered in previous LOCA analyses and a requirement for operator action to initiate ADS (4 valves) within 10 minutes had been identified and was included in the analyses. Current BFN emergency operating procedures are consistent with this requirement.

New LOCA analyses from both AREVA and GE Hitachi have been provided to address the issue of the battery failure which disables RMOV Board B (which disables the automatic ADS initiation). Both analyses are based on current licensed thermal power. With the submittal of these reports, the LOCA analyses of record will transition from an EPU basis to a current licensed power basis.

The consideration of failure of the battery powering RMOV Board B results in a reduced availability of ECCS equipment. The specific equipment remaining is as follows.

- For recirculation discharge line breaks: HPCI and 1 LPCS
- For recirculation suction line breaks: HPCI, 1 LPCS, and 2 LPCI (one loop)
- For feedwater line or HPCI injection line breaks: 1 LPCS and 2 LPCI (one loop)
- For LPCS line breaks: HPCI and 2 LPCI (one loop)
- For all cases with loss of automatic ADS: Manual initiation of 4 ADS valves 10 minutes after event initiation

AREVA Analysis

The new AREVA LOCA analysis (Reference 11) evaluates the break spectrum at current licensed power for a variety of breaks, including recirculation line breaks, feedwater line breaks, steam line breaks, and core spray line breaks. The analysis considered the failure of the battery powering RMOV Board A, as well as failure of the battery that powers RMOV Board B. The report includes the detailed results of several RMOV Board A cases run to support the vendor comparisons discussed in Question 3 of this enclosure. The report includes an expanded single failure table, and lists the systems remaining for each single failure.

HPCI injection line breaks are covered by the feedwater line break analysis, which assumed no HPCI is injected into the feedwater line. The analysis

assumes the worst case situation of the feedwater line breaking downstream of the point where the HPCI injection line attaches to the feedwater piping. Therefore, any HPCI flow entering the feedwater line is assumed to be diverted out the break (regardless of the break size) and never reaches the vessel. The evaluated case is more limiting than a break in the HPCI injection line itself, since that piping is located outside of containment, and the break would be isolated by a check valve in the feedwater line located between the HPCI injection line connection and the vessel. The evaluated case represents a non isolable feedwater line break that effectively disables the HPCI system.

Breaks in the HPCI turbine steam supply line are covered by the main steam line break analysis. The main steam line break cases conservatively assume that for all break sizes, the steam to the HPCI turbine is cutoff, disabling the HPCI system.

The Reference 11 analysis utilizes the same inputs as the Reference 1 analysis, with the exception of the heat balance parameters (related to the power changing from EPU to current licensed power), and three other inputs. The HPCI capacity was modified to be consistent with the design and testing requirements. The assumed HPCI system startup time was reduced to be consistent with realistic, measured values. Finally, the core spray flow versus pressure characteristic was modified to remove unnecessary conservatism.

The analysis concluded that the most limiting single failure and break was a 0.25 ft² recirculation line break on the discharge side of the pump, with single failure of the battery powering RMOV Board B. This case produced a PCT (peak clad temperature) of 1973°F. By comparison, the limiting PCT for the battery powering RMOV Board A was 1809°F for a 0.5 ft² recirculation discharge break.

The non recirculation line breaks were shown to be much less limiting than the recirculation line breaks, both for battery failures impacting RMOV Board A and Board B. The feedwater line break analysis for battery failure associated with RMOV Board B (which bounds the HPCI injection line break by assuming no HPCI) yielded a PCT of approximately 1100°F. The steam line break analysis (which bounds the HPCI steam supply line break by assuming no HPCI) showed a minimal PCT increase.

Analysis of the LPCS line breaks were performed for battery failures affecting both RMOV Board A and RMOV Board B. This break is very mild for the RMOV Board B scenario, since HPCI is able to inject. The LPCS line break for the RMOV Board A scenario showed a PCT near 1500°F, due to the loss of HPCI.

The MAPLHGR analysis indicates that one of the BFN ATRIUM-10 bundle types is slightly more limiting than the reference bundle type used in the break spectrum analysis. Heatup analysis of this bundle produced a peak clad temperature of 1990 °F for the 0.25 ft² recirculation line with battery failure affecting RMOV Board B. This PCT value is the new licensing basis PCT for ATRIUM-10 fuel for BFN unit 1.

GE Hitachi (GEH) Analysis

The new GEH LOCA analysis (Reference 10) also evaluated the break spectrum at current licensed power for a variety of breaks, including recirculation line breaks, feedwater line breaks, steam line breaks, and core spray line breaks. The report is a supplement to Reference 9, and is focused primarily on the single failure of the battery that powers RMOV Board B. The single failure of the battery powering RMOV Board A is covered primarily from existing current licensed power cases presented in Reference 9. The Reference 10 report includes additional RMOV Board A cases run to support the vendor comparisons discussed in Question 3 of this enclosure. The report also includes an expanded single failure table.

HPCI injection line breaks are covered by the feedwater line break analysis. The GEH analysis allows the HPCI to run, and considers a range of feedwater line break sizes occurring downstream of the point where the HPCI injection line joins the feedwater line. The most limiting case was found to be the feedwater line break size which is just large enough to pass all of the HPCI flow out of the break. This limiting case covers the HPCI injection line break scenario, since it does not allow any HPCI flow to reach the vessel. This limiting case bounds a break in the actual HPCI injection line, since that piping is located outside of containment, and the break would be isolated by a check valve in the feedwater line located between the HPCI injection line connection and the vessel. The evaluated case represents a non isolable feedwater line break that effectively disables the HPCI system.

Breaks in the HPCI turbine steam supply line are covered by the main steam line break analysis. The main steam line break cases conservatively assume that for all break sizes, the steam to the HPCI turbine is cutoff, disabling the HPCI system.

The Reference 10 analysis utilizes the same inputs as the Reference 9 analysis, with the exception of the heat balance parameters (related to the power changing from EPU to current licensed power), and two other inputs. The HPCI capacity was modified to be consistent with the design and testing requirements. The assumed HPCI system startup time was reduced to be consistent with realistic, measured values. While the Reference 9 analysis had different values for these two HPCI parameters, the differences are of no consequence. The Reference 9 report is only relied upon for current licensed power based cases with battery failure impacting RMOV Board A; this single failure disables the HPCI logic, and therefore the assumed HPCI parameters do not affect the results.

The analysis concluded that the most limiting single failure and break was a 0.24 ft² recirculation line break on the discharge side of the pump, with single failure of the battery powering RMOV Board B. This case produced an Appendix K PCT (peak clad temperature) of 1828°F. By comparison, the limiting Appendix K PCT for the battery powering RMOV Board A was 1748 °F for the DBA recirculation suction break.

The non recirculation line breaks were shown to be much less limiting than the recirculation line breaks, both for battery failures impacting RMOV Board A and Board B. The feedwater line break analysis for battery failure associated with RMOV Board B (which bounds the HPCI injection line break by allowing all of the injected HPCI flow to be diverted out of the break) yielded a PCT of just under 1100°F. The steam line break analysis (which bounds the HPCI steam supply line break by assuming no HPCI) showed a minimal PCT increase.

Analysis of the LPCS line breaks were performed for battery failures affecting both RMOV Board A and RMOV Board B. As shown in Reference 10, this break is very mild for the RMOV Board B scenario, since HPCI is able to inject. While the Reference 10 analysis did not include a specific calculation of the LPCS line break for the RMOV Board A scenario, it had been previously evaluated in Reference 9. The LPCS line break for the RMOV Board A scenario was demonstrated in Reference 9 to be non limiting relative to recirculation line breaks.

The results using the GEH nominal model show a PCT of 1263°F for a break size of 0.41 ft² in the recirculation discharge piping, with battery failure impacting RMOV Board B. The limiting case for the failure of the power supplying RMOV Board A was still the DBA recirculation suction line break, with a PCT of 1176°F.

In the GEH method, additional uncertainties are applied to the Appendix K results to derive a Licensing Basis PCT. For the GE14 fuel type, the Licensing Basis PCT was determined to be 1920 °F. The Reference 10 report did not specifically calculate a Licensing Basis PCT for the GE13 fuel type. The report concludes that the GE13 Licensing Basis PCT provided in Reference 9 (1810°F) is valid, provided the LHGR and MAPLHGR limits for this fuel type are restricted to 75% of the values established in the Reference 9 analysis. As the GE13 fuel in Unit 1 Cycle 8 is on or near the core periphery, the fuel will not challenge this restricted limit. Note that all of the GE13 fuel is scheduled to be discharged from the Unit 1 core at the end of Cycle 8 in October 2010.

The Reference 10 analysis also provides an updated Upper Bound PCT value for the GE14 fuel. The updated Upper Bound PCT value of 1480°F is less than the Licensing Basis PCT value of 1920°F as required.

Operator Actions for Manual ADS

The LOCA analyses in References 10 and 11 assume that for battery failure affecting RMOV Board B, the operators will take manual action 10 minutes after the break to open a minimum of 4 ADS valves. The crediting of manual operator action is being used as a temporary measure until such time as the ADS can be modified at BFN to ensure automatic functioning for single failures. As a result, the guidance provided in Section C.5, "Use of Temporary Manual Action in Place of Automatic Action in Support of Operability," of NRC Inspection Manual Part 9900: "Technical Guidance, Operability Determination and Functionality Assessments for Resolution of Degraded or Nonconforming

Conditions Adverse to Quality or Safety," has been utilized. The following discussion provides the background and justification for making this assumption in the LOCA analyses.

Introduction

During a meeting between TVA and the NRC on February 17, 2010, NRC staff requested TVA provide additional information regarding ADS manual operation credit in certain portions of the LOCA reanalysis done for BFN. The additional information provided here, with respect to ADS manual operation credit, is consistent with the information provided by Detroit Edison Company for Fermi 2 in a letter to the NRC dated June 10, 2009 (Reference 12). NRC approval of Fermi 2 credit for ADS manual operation is documented in the NRC letter and associated Safety Evaluation dated June 30, 2009 (Reference 13). The LOCA reanalysis for BFN was performed to address a single failure disabling the automatic functioning of ADS. The single failure involves a loss of the 250 volt DC battery supplying power to RMOV Board B. Both logic trains of automatic ADS initiation instrumentation are powered from RMOV Board B; consequently, loss of power to the board results in the loss of automatic ADS function. For this single failure scenario, operators would still be able to manually open four ADS valves.

The RMOV Board B loss of DC power analysis assumes operators manually open four ADS valves 10 minutes after the break occurs. This is required because automatic ADS initiation logic is disabled in this scenario. The 10 minute assumption, although shorter than the 20 minute time period provided in the guidance in Section 6.3 of NUREG-0800 (Reference 14), is consistent with the earliest post accident delay after which credit for manual operator actions (such as initiation of suppression pool cooling) is considered for licensing and design basis analyses at BFN and has been demonstrated, as reflected below, to be conservative relative to the timing of the actual operator action.

The NRC requested TVA provide information to demonstrate BFN operators have appropriate procedures, training, control room indications, and time to ensure this manual action can be reliably performed as assumed in the LOCA analysis with RMOV Board B loss of DC power.

Procedures

In the event of a small break where the high pressure makeup cannot maintain water level, BFN Emergency Operating Instruction u-C-1 (Level Control) contains a step directing the operator to Emergency Operating Instruction u-C-2 (Emergency Depressurization). Note: here and in the discussion of control room indications to follow, "u" represents the reactor unit number.

The BFN Emergency Operating Instructions (EOIs) are based on the NRC approved BWR Owners Group Emergency Procedure Guidelines (EPGs), and Severe Accident Guidelines (SAGs). BFN EOIs require operators begin depressurization prior to reactor water level reaching a value of -180 inches

on the narrow range instruments, which corresponds to the EPG Minimum Steam Cooling Reactor Water Level (MSCRWL). The MSCRWL is defined as the lowest reactor water level at which the covered portion of the core will generate sufficient steam to prevent any clad temperature in the uncovered portion of the core from exceeding 1500 degrees Fahrenheit assuming the most limiting top peaked power shape prior to the event. For BFN, the MSCRWL is 18 inches below the top of the active fuel. Water levels between the top of active fuel and the MSCRWL represent the range in which the operator must recognize manual depressurization is required. The procedure also requires depressurization to begin prior to water level reaching -200 inches. This level corresponds to the Minimum Zero Injection Water Level defined in the EPGs, and ensures the clad temperature does not exceed 1800 degrees Fahrenheit, with no injection.

In addition, consistent with the NRC approved Revision 4 of the EPGs (Reference 15), manual inhibition of the ADS system is required to allow time for the high pressure ECCS systems to restore water level and avoid unnecessary core uncover. This action effectively makes reactor vessel depressurization a manual action regardless of the particular LOCA event.

The key steps in BFN depressurization instruction EOI u-C-2 are:

- Attempt to manually open all 6 ADS valves (minimum of four valves are required for depressurization)
- If the minimum number of four cannot be achieved with ADS only, manually open other non-ADS safety relief valves with the goal of opening a total of six valves (minimum of four total is still required)
- Bypass and restore drywell pneumatics as necessary.
- Actions are provided once depressurization is complete to establish shutdown cooling, or pursue alternate emergency depressurization systems if the minimum four relief valves cannot be opened.

Training

The BFN licensed operator training program utilizes a simulator facility in accordance with 10CFR55.46(c), "Plant-referenced simulators." Shift crews are typically evaluated in the simulator during each training cycle. Each simulator evaluation includes performance of Critical Tasks, which must be accomplished in order to pass the simulator evaluation. For all simulator scenarios involving small breaks requiring depressurization, one Critical Task includes commencing emergency depressurization after level drops below top of active fuel, but before reaching -200 inches. Another Critical Task of interest is for the crew to restore and maintain water level above the top of active fuel after depressurization is complete. If an operator fails to meet a Critical Task, he is removed from shift and a remediation plan is determined. The remediation plan typically requires additional training time in the simulator, and a retest involving a scenario similar to the one the operator failed.

During 2009, a total of sixteen BFN operator crews were presented with at least one simulator scenario requiring emergency depressurization based on water level indications. Operator lesson plan OPL177.078 was the principle scenario presented to the crews in 2009. In this scenario, the reactor is operating at 100% power, when an earthquake occurs. The operators then shutdown the reactor using plant procedure 0-AOI-100-5. Aftershocks then cause a feedwater line break to occur resulting in all available HPCI flow being diverted through the feedwater line break. Reactor Core Isolation Cooling (RCIC) is also lost due to a break in the RCIC steam supply line. This leaves the operators with control rod drive flow and standby liquid control as the only sources of high pressure injection. Reactor water level will decrease to the point where the crew is expected to manually depressurize the reactor (the automatic ADS would have already been inhibited per the EOs) in accordance with EOI u-C-2. Following manual depressurization, low pressure ECCS subsystems then terminate the event. All sixteen crews successfully passed this scenario, and initiated manual depressurization in accordance with the Critical Task requirements mentioned earlier.

This training scenario is comparable to the feedwater line break cases included in the LOCA reanalyses performed by GE Hitachi and AREVA. In those analyses, the feedwater line break is assumed to be large enough to result in all of the HPCI flow being diverted out of the break, just as in the training scenario. A manual depressurization is required both in the training scenario, and in the LOCA analyses. The operators must manually initiate ADS in the training scenario, due to the ADS being inhibited early in the event. In the LOCA analysis, automatic ADS would not occur due to the RMOV Board B loss of DC power, and the operators are assumed to manually start depressurization at 10 minutes, rather than on indicated level. Low pressure ECCS subsystems are used to recover reactor water level back above the top of active fuel in both the training scenario, and the LOCA analyses.

In the LOCA analyses, the most limiting case for the RMOV Board B loss of DC power is the recirculation discharge line break, rather than the feedwater line break. While this is a different break from the simulator scenario described above, the differences in terms of operator action are not significant. In the recirculation line break with RMOV Board B loss of DC power, HPCI is still available, but is unable to maintain water level for the worst break size. The LOCA analysis does not credit the Reactor Core Isolation Cooling (RCIC) System, so operators would still be presented with a situation where the high pressure systems (i.e., HPCI and RCIC Systems) cannot maintain level above the top of active fuel, thereby requiring manual depressurization. Results of the training scenario evaluation indicate BFN operators would be capable of mitigating the limiting recirculation line break event presented in the revised LOCA analysis reports.

Control Room Indications

In the event manual depressurization is required, operators have several independent means to confirm a given ADS or safety relief valve is open. The hand switch for each valve has two lights next to it, one red and one green, tied to the position of the solenoid on the valve operator. A change from

green to red provides indication the solenoid has repositioned, and the valve has opened. The valve position indicator lights are powered from the same source as the valve itself. For the case of RMOV Board B loss of DC power, the four remaining ADS valves would be operable and have position indication.

Each valve also has an acoustic flow indicator located on panel u-FMT-1-4, above the valve hand switches. When a valve is opened, a set of Light Emitting Diode (LED) lights on this indicator will light up. Each valve has its own associated set of LED lights. The acoustic monitoring detects the sound made by the steam as it passes through the relief valve piping, and provides the operator with a positive indication the valve is passing steam. The acoustic flow indicator is powered by 120 volt AC power, and would be unaffected by failure of the battery powering RMOV Board B.

The operator also has the ability to look at the tail pipe temperatures for each ADS or relief valve discharge pipe. This temperature is available to be viewed as a display point on the control room computer monitors, or by looking at chart recorder u-TR-1-1, which is also in the control room. The observed elevated temperature readings would provide further independent confirmation the valves of interest are in fact open. The tailpipe temperature indicators are also powered by 120 volt AC power, and would be unaffected by failure of the battery powering RMOV Board B.

The operators would be able to determine depressurization is occurring by observing reactor pressure indicators in the control room. These instruments are safety related divisional Class 1E equipment. The operators would use the narrow range reactor level instrumentation in order to determine the need for the manual depressurization. Like the pressure instrumentation, the narrow range level instrumentation is safety related divisional Class 1E equipment.

As noted earlier, manual depressurization in the BFN LOCA analysis is only assumed for the single failure of the DC battery powering RMOV Board B. If this failure were to occur, the operator is provided with annunciators indicating the failure. Annunciator u-EA-57-100 illuminates when RMOV Board B loses power. The loss of RMOV Board B power disables the automatic ADS function, resulting in the annunciator in control room panel u-XA-55-3C window 32 becoming lit. This annunciator reads "ADS BLOWDOWN POWER FAILURE." This annunciator has an associated Annunciator Response Procedure (ARP-9-3C), highlighting automatic ADS logic has failed, and manual valve operation will be required to depressurize. These annunciators are powered by 48 volt DC power, and are unaffected by failure of the battery powering RMOV Board B.

In summary, operators are provided with adequate instrumentation and indicators to recognize the need for depressurization, and to successfully carry out the action.

Timing Aspects

The limiting LOCA event in both vendor analyses is a small break of the recirculation discharge line with single failure of the battery powering RMOV Board B. In this event, the LOCA analysis from both vendors shows reactor water level reaches the top of active fuel approximately three minutes into the event. This represents the time at which operators would be required to start manual depressurization per the EOLs. This time is much less than the 10 minute time assumed for the manual operator action in the LOCA analysis. In addition, the LOCA analyses from both GE Hitachi and AREVA show that for this limiting break, the clad temperature reaches the peak value before the 10 minute point is reached. This means the issue of operator timing with regard to manual depressurization is irrelevant for the limiting break, since natural depressurization allows the low pressure ECCS to act prior to the 10 minute manual ADS initiation point being reached.

For feedwater line breaks, HPCI injection line breaks, and steam line breaks (with single failure of the battery powering RMOV Board B), the PCT is not reached prior to the 10 minute point, and the results are dependent upon the manual ADS initiation. However, these events are non limiting in terms of peak clad temperature compared to the recirculation line breaks. For these breaks, the PCT is approximately 1100 degrees F or less for both vendors. Therefore, a brief delay in operator action (one to two minutes) beyond the 10 minute assumption would not challenge PCT limits for these breaks.

For core spray line breaks with the RMOV Board B failure, the HPCI would be available, and the analyses by both vendors show that the RMOV Board A failure (which disables HPCI but leaves automatic ADS function) is much more limiting. In the GE analysis of RMOV Board B failure, the water level never reaches a point where manual ADS would be required, so the assumption of manual ADS at 10 minutes becomes an arbitrary assumption that does not affect the results. The AREVA analysis of the event with RMOV Board B failure shows the PCT remains below 1000 degrees F. A delay in operator action beyond 10 minutes for this break is either non consequential, or would result in only a modest PCT increase that would not challenge the limiting PCT.

The action to manually depressurize would only require a few minutes or less to perform, including any restoration of drywell pneumatics. The 10 minute assumption used in the LOCA analyses is reasonable and conservative relative to the actual operator timing that would occur.

Summary

Based on the information presented above, it is clear the operators have the training, procedures, instrumentation, control room indicators, and adequate time to complete the critical task of performing emergency manual depressurization of the reactor in response to a small break LOCA.

ADS System Modifications

TVA has investigated the feasibility of modifying the ADS system such that a single battery failure will not result in the total loss of ADS function. The modification would provide a single failure proof automatic initiation capability of 4 ADS valves, regardless of which 250 VDC battery fails. This modification is viable, and is expected to be made to Unit 3 during the Unit 3 outage in the Spring of 2012, to Unit 1 during the Unit 1 outage in the Fall of 2012, and to Unit 2 during the Unit 2 outage in the Spring of 2013.

An additional modification being considered is to alter the ADS timer start logic. Currently, the ADS timer requires a low pressure system to be running (in addition to having both low water level and high drywell pressure) in order to start. The more typical logic configuration in the industry uses the low pressure system operating check only as a final permission to open the ADS valves, rather than as part of the logic to start the ADS timer. TVA is evaluating a potential change to the timer initiation logic to remove the low pressure system check as a required input, and only use the check as a confirmation for valve opening permissive. This modification is not required to resolve any issues associated with crediting manual operator actions, but it would provide enhanced ECCS system response, and provide improved peak clad temperatures.

Conclusions

The ADS actuation single failure will increase the licensing PCT values relative to the prior values shown in References 1 and 9. The LOCA analysis of record for both vendors will be based on the current licensed power of 3458 MWt.

The revised LOCA analyses demonstrate that the LOCA MAPLHGR limits remain applicable for BFN operation and ensure 10 CFR 50.46 acceptance criteria continue to be met with consideration for a single failure of the automatic actuation of the ADS.

TVA will rely on crediting manual operator action to open ADS valves at 10 minutes, until such time as modifications can be made to the system to provide a single failure proof automatic initiation capability. The LOCA analyses in References 9, 10, and 11 will remain valid after the modifications are made, since the automatic initiation of ADS for a battery failure affecting RMOV Board B will occur sooner than the manual initiation assumed in those analyses. Battery failure affecting RMOV Board A with the current plant configuration results in a six valve automatic ADS capability; this will still be the case after the system modification is complete.

Question 4 (from NRC to TVA Letter dated February 25, 2010)

In question 4, the staff asked TVA to address failure modes and effects for the automatic depressurization system (ADS) during postulated loss-of-coolant accidents (LOCAs), including high pressure coolant injection (HPCI) line

breaks. TVA's January 15, 2010, supplement was not fully responsive to the staff's request. TVA identified that the ADS automatic actuation could be disabled by a single failure, and that a failure of the ADS could yield more limiting LOCA analysis results than those included in the license amendment request. TVA stated that additional analysis would be performed, taking credit operator action to initiate ADS, and the LOCA analyses would be supplemented in March 2010. Therefore, the January 15, 2010, supplement did not contain sufficient information on the LOCA analysis.

TVA's supplement also provided an evaluation of the high pressure coolant injection line break that is based on other injection line breaks, but a HPCI line break LOCA with a signal failure of the ADS would result in a total loss of high pressure emergency core cooling system. The staff believes that this postulated LOCA and single failure combination needs to be explicitly analyzed to demonstrate compliance with Title 10 of the Code of Federal Regulations (10 CFR) 50.46(a)(i).

Response

As discussed above, the LOCA analyses have been revised/supplemented to address the failure of ADS. The References 10 and 11 LOCA analyses are provided in Attachments 20 and 16, respectively.

As discussed above, the HPCI line break LOCA with a single failure of the ADS that results in a total loss of high pressure emergency core cooling system was analyzed and addressed in References 10 and 11 (Attachments 20 and 16, respectively).

Question 5.

Table 2.3, Cycle Specific Reload Evaluation Methodologies, of the Reload Safety Analysis Report (RSAR, ANP-2864(P), "Browns Ferry Unit 1 Cycle 9 Reload Safety Analysis") lists more transients than Table 2.1 indicates are analyzed on a cycle-specific basis. Provide an explanation for the discrepancy.

Response 5.

Table 2.1 of the RSAR (ANP-2864(P)) provides a disposition summary of BFN FSAR events and analyses. The summary provides the disposition status and applicable comments associated with the event/analysis. The basis of the disposition status is categorized as:

- FSAR analysis.
- Generic analysis. A bounding analysis that is independent of plant type.
- Plant specific analyses. The analysis is based on BFN (independent of unit) and is bounding for cycle-to-cycle variations.
- Cycle specific analysis. The analysis is specific to the Unit and Cycle.

Increased Core Flow (ICF) and Maximum Extended Load Line Limit Analysis (MELLLA) operating regions of the power/flow map are included in the disposition results presented in Table 2.1.

Table 2.3 provides a listing of FSAR events, identified in Table 2.1, that require analyses performed on a cycle specific basis and specifically addressed in the RSAR. The table includes the approved evaluation model and applicable methodology reference for each event/analysis. The table further provides applicable acceptance criteria and comments associated with each event/analysis.

The following event/analysis identified in Table 2.1 as being “addressed each cycle” or “address initial reload” are not included in Table 2.3, based on the following:

- FSAR Section 3.2. The analysis, acceptance criteria, methodology, and evaluation model are provided in Reference 2 of the RSAR.
- FSAR Section 3.6. The analysis, acceptance criteria, methodology, and evaluation model are provided in Reference 1 of the RSAR.
- FSAR Section 10.2. The analysis, acceptance criteria, methodology, and evaluation model are provided in Reference 24 of the RSAR.
- FSAR Section 10.3. The analysis, acceptance criteria, methodology, and evaluation model are provided in Reference 25 of the RSAR.
- FSAR Section 10.11. This item is addressed in Reference 37 of the RSAR.
- FSAR Section 14.5.5.1. Table 2.1 dispositions the event as a potentially limiting Anticipated Transient Without Scram (ATWS) pressurization event. Therefore the cycle-specific analysis becomes ATWS-Pressure Regulator Failure Open (PRFO), considered under Table 2.3, FSAR 7.19.
- FSAR Section 14.6.4. The analysis, acceptance criteria, methodology, and evaluation model are provided in Reference 27 of the RSAR.

Question 6.

The approved AREVA nuclear design method topical reports do not appear to describe a method for calculating the standby liquid control system (SLCS) cold shutdown margin (CSDM).

Provide a description of the SLCS CSDM calculation method. The methodology description should include:

- a. A discussion of the codes used;
- b. A discussion of the nuclear data that must be generated (e.g. lattice parameters for given boron concentrations);
- c. A list of pertinent analysis assumptions (e.g. active core averaged boron weight),
- d. A justification of the method accuracy;
- e. A discussion on the treatment of short-lived highly absorbing nuclides (e.g. xenon and samarium); and,

- f. A discussion of the assumed core thermal-hydraulic conditions (e.g. temperature of 68 degrees F).

This description should address the application of the method to the co-resident GE14 fuel.

Response 6.

AREVA performs a cycle specific SLCS shutdown margin calculation as part of the plant reload analyses as specified on page 19 of Reference 2. The result for BFN Unit 1 Cycle 9 is reported in Section 7.3 of Reference 3. The SLCS shutdown margin analysis is performed using the NRC approved AREVA neutronics analysis methodology (i.e., CASMO-4/MICROBURN-B2) documented in EMF-2158(P)(A) (Reference 4).

The approval of this neutronics methodology was in part based upon benchmarks for a number of reactors and fuel types as evaluated in Reference 4. This included a series of both borated and non-borated CASMO-4 criticality benchmarks based upon KRITZ and Babcock and Wilcox experimental data. These critical experiments include both PWR and BWR fuel assembly designs covering a range of fuel rod diameters and water to fuel ratios. Uniform arrays of rods as well as rod arrays with large gaps are included. The Reference 4 validation includes benchmarks to commercial reactors for hot and cold conditions. It also includes gamma traversing incore probe (TIP) and isotopic data measurement comparisons. Comparisons of fission rate distributions were also made to MCNP as part of the original Reference 4 validation that included lattices from modern AREVA and GE 10x10 fuel designs. BFN Unit 1 and the fuel types contained within the Cycle 9 core are consistent with the benchmarks provided in Reference 4. Furthermore, the results of benchmarking for BFN Unit 1 completed in support of the fuel transition meet the requirements of Reference 4 and include cores with the GE14 fuel that will be co-resident in the Cycle 9 reload design.

Recent comparisons between CASMO-4 and MCNP have been performed for GE-11 and ATRIUM-10 fuel designs with boron in the coolant. The standard deviation of these results, covering moderator temperatures at 300 K (80.3° F) and 600 K (620.3° F) and boron concentrations between 0 and 1016 ppm, was []. Standard deviations for both fuel types were nearly identical indicating no fuel type dependency.

The fuel assembly cold and warm lattice nuclear data with boron in the coolant is generated with the CASMO-4 computer code as a function of lattice type, exposure, void history, boron concentration, temperature, and control. The SLCS shutdown margin is calculated with the MICROBURN-B2 reactor simulator code using nuclear data for the lattices generated by CASMO-4 calculations. Additional borated branch cases are performed with CASMO-4 to support the SLCS calculation. These CASMO-4 borated branches are performed for cold, intermediate, and warm temperatures with boron concentrations that correspond to the cold and warm temperature conditions. This additional data is used by MICROBURN-B2 in the same manner as the unborated data except that the code is capable of interpolating or extrapolating

to boron concentrations other than those included in the lattice cross section library with high accuracy over a reasonable range. Even so, the amount of interpolation/extrapolation is typically minimized by choosing a warm temperature, usually 360°F, that is near the limiting temperature used for the calculation.

Cold conditions are not limiting for a SLCS calculation. For BFN Unit 1 Cycle 9, the SLCS calculation is performed at the temperature associated with RHR shutdown cooling initiation (i.e., it is based upon the saturation temperature corresponding with the shutdown cooling system initiation pressure). For SLCS conditions, higher temperatures are more reactive since B-10 exhibits a $1/v$ absorption cross-section (i.e., becomes a less efficient absorber with decreased moderation). The shutdown cooling initiation becomes the most reactive condition due to the dilution impact of adding the Residual Heat Removal (RHR) shutdown cooling volume as described in the BFN UFSAR section 3.8.4.1. The limiting nature of this higher temperature statepoint is illustrated in the answer to Question 7 below, where a direct comparison is made to a cold condition calculation.

The amount of boron assumed in the SLCS analysis is referenced to a natural Boron equivalent at cold conditions. For BFN Unit 1 Cycle 9 this concentration is 720 ppm natural boron equivalent at 70°F. The AREVA standard process is to use 68°F as the reference temperature which is consistent with Improved Standard Technical Specifications (e.g., definition of Shutdown Margin included in Section 1.1, "Definitions," of NUREG-1433). As mentioned in Section 7.3 of Reference 3, the AREVA cold analysis basis of 68°F represents a negligible difference and the results are adequate to protect the 70°F licensing basis of BFN Unit 1. This is further illustrated in the answer to question 7 below, where a comparison is provided between calculations assuming both 68°F and 70°F as the reference temperature.

For BFN Unit 1 Cycle 9, a series of SLCS shutdown margin restart calculations were performed at the desired cycle exposure points throughout the cycle. The MICROBURN-B2 control rod step out restart file used for the SLCS calculation was based upon the short previous cycle energy. In certain cases, such as performing a SLCS analysis after the previous cycle has shutdown, or when performing a SLCS analysis after the previous cycle has exceeded the short energy window, the restart file may be based on the actual (or expected) previous cycle energy.

The SLCS shutdown margin calculations for BFN Unit 1 Cycle 9 assume a conservative all control rods out (ARO) condition. In some cases, SLCS shutdown margin calculations may be performed with some control rods in the core, as allowed by the licensing basis of the event (i.e., use of the rated power rod pattern is allowed by NUREG-0800, Section 9.3.5). If a rodged calculation is performed then the CASMO-4 calculations will include controlled borated branches. The SLCS shutdown margin is based upon the core k -eff at the required boron concentration and warm moderator temperature with no xenon. The samarium concentration is obtained from the restart file (operating samarium, except at Beginning of Cycle (BOC) which uses shutdown samarium).

Based on uncertainty analysis for the CASMO-4/MICROBURN-B2 methodology, AREVA has determined that the minimum calculated SLCS shutdown margin at the limiting temperature must be greater than [] $\Delta k/k$. The uncertainties evaluated are generic to the Reference 4 methodology and are applicable to BFN Unit 1. Although not applied to BFN Unit 1 Cycle 9, a higher acceptance criterion is available for plants that desire to have this calculation performed at cold conditions. The higher acceptance criterion is provided to compensate for performance of the calculation at a non-limiting temperature. For BFN Unit 1 Cycle 9, the result is reported in Section 7.3 of Reference 3 and is conservatively well within the applicable [] $\Delta k/k$ criterion.

The pertinent analysis assumptions applied in the BFN Unit 1 Cycle 9 SLCS shutdown margin calculation are the following:

- The cold critical target k-eff values as a function of exposure, based on measured cold critical data, are applicable. It is noted that the use of cold target is conservative since the values are lower than the corresponding hot operating target.
- The reactor is xenon free and has operating samarium (with shutdown samarium at BOC). The most significant of the isotopes is xenon and the assumption of no xenon is conservative for a shutdown margin calculation. The less significant samarium isotope is modeled to be consistent with expected conditions.
- The weight of boron assumed in the calculation at 366° F is referenced to the weight that corresponds to 720 ppm at cold conditions. This ensures that the calculation remains consistent with the Technical Specification bases.
- The saturation temperature consistent with the RHR initiation pressure (366° F) is the appropriate temperature for the analysis. This is shown to be the limiting temperature in the discussion above and demonstrated in the answer to question 7 below.
- The all-rods-out condition was assumed. This is conservative since the licensing basis allows credit for the rated conditions rod patterns.

Question 6 (from NRC to TVA Letter dated February 25, 2010)

In question 6, the staff asked TVA to describe the method of determining the cold shutdown margin of the standby liquid control system. TVA's response provided much of the requested information; however, it was unresponsive to Item (d) and was incomplete in terms of addressing the applicability to GE14 fuel.

The response did not provide justification of the standby liquid control system shutdown margin accuracy. To initiate its review, the staff requires information justifying of the acceptance criterion. The January 15, 2010, supplement did not address the following sources of uncertainty:

- operation of the plant that is different than projected
- fuel manufacturing tolerances
- methodology approximations
- inexact tracking of the actual plant parameters
- depletion of absorber material in control blades

The uncertainty for the control blade depletion is relevant because the generic analysis method may be applied for conditions where control blades are partially inserted, in accordance with the description provided in the January 15, 2010, supplement.

The supplement also did not provide or justify any assumptions regarding GE14 manufacturing tolerances, and did not describe how the Technical Specification (TS) limit and the associated method uncertainties are incorporated in the acceptance criterion.

Response

Operation of the Plant that is Different than Projected

At the time of the licensing analysis of a particular cycle, the actual operation of the previous cycle is not completely known and is projected based on plans at the plant. Projection of plant operation will differ from actual operation relative to the cycle length of the previous operating cycle, the control rod patterns, and the corresponding core flow. These differences will result in variations in the control rod pattern and core flow for the actual hot operating conditions. The degree of variation is limited by controls on the end of cycle (EOC) projected axial power distribution. Reactor engineers at the plants are required to monitor actual plant operations and periodically project to the EOC state to ensure actual operations are not leading to an EOC axial power shape that is inconsistent with the licensing basis. This monitoring of actual operations is in place to ensure the continued applicability of the licensing analysis for MCPR limits but is also applicable to ensuring the continued applicability of the standby liquid control system (SLCS) analysis. Should actual plant operations deviate from that projected in the licensing basis, such that the criterion is not met, licensing analyses are revisited and dispositioned. AREVA has not quantified variation magnitude since there has always been large conservative margin to the SLCS criterion. AREVA has performed a sensitivity study by comparing the SLCS results for Browns Ferry Unit 2 Cycle 15 with the actual cycle 14 history (2.25% Δk) and the licensing projection for cycle 14 (2.17% Δk). Results showed the licensing analysis was conservative by 0.08% Δk . This difference is small relative to the other uncertainties described here, and therefore has not been explicitly accounted for in defining the acceptance criterion.

Fuel Manufacturing Tolerances

Fuel manufacturing tolerances are accounted for in the cold critical benchmarking. In the case of Browns Ferry, the cold critical benchmarking

includes data for all three units, all of which include cold critical data with GE-14 fuel.

An evaluation of the measured cold critical results that were presented in Reference 4 was performed to determine the uncertainty associated with the MICROBURN-B2 calculation relative to actual operating measurements. The results, by their very nature, include uncertainties in manufacturing tolerance and absorber depletion in the control blades, since the calculations were performed assuming original equipment control blades without accounting for depletion. The root mean square (RMS) deviation for 34 follow-on cycles was [] Δk (i.e., cold critical uncertainty, σ_{cold}).

An evaluation of the benchmarking calculations for all three Browns Ferry units was also performed. The evaluation included operating cycles with all GE fuel (including GE-14), mixed core with AREVA (commercial grade Uranium and BLEU) and GE fuel as well as cores with all AREVA (commercial grade Uranium and BLEU) fuel. There was no noticeable trend in critical measurements. The standard deviation of all of the beginning of cycle (BOC) cold critical data for the three Browns Ferry units is [] Δk . This is consistent with the σ_{cold} values. By including non BOC exposure statepoints, the standard deviation increases to [] Δk . This difference is accounted for in the SLCS analysis by using an exposure dependent target k-effective curve as presented in Figure 6.1.

Methodology Approximations

Since no experimental data for BWR fuel in borated conditions are available, an estimate of the uncertainty in the calculated results considers the primary methodology approximations. These approximations consist of the following.

- Standard measured cold critical statepoints for commercial reactors
- CASMO-4 calculation uncertainty as compared to MCNP
- Uncertainty in the computed eigenvalue due to cross section interpolation in MICROBURN-B2

Combining these components utilizes standard statistical methods assuming normal distribution for each of the independent components.

MCNP-4 B2 calculations were performed with history sizes of 4000 and calculated 550 cycles skipping over the first 50 cycles before accumulating k-effective values and statistics. With these parameters the one sigma uncertainty in k-effective was less than or equal to [] mk.

Calculations were performed for the three temperatures (293, 300 and 600 °K) and temperature corrected boron concentration equivalent to three boron concentrations (0, 660 and 849 ppm) at 68 °F for ATRIUM-10 and GE-11 fuel lattices. The RMS difference for 9 calculations of the ATRIUM-10 lattice between MCNP and CASMO-4 was [] Δk , and the RMS difference for 9 calculations of the GE-11 lattice was [] Δk , resulting in a combined RMS

value of [] Δk (i.e., Casmo-4 vs. MCNP uncertainty, σ_{code}). Since the values for the two different lattices are very similar, one can conclude the uncertainty is not fuel type dependent.

BLEU fuel differs from commercial fuel due to concentrations of U234 and U236. These isotopes add a fixed amount of absorption compensated for by the use of slightly more enriched U235. The presence of U234 and U236 would not be expected to change the uncertainty since it has an equal contribution to reactivity, independent of boron concentration and temperature; they are specifically accounted for in the model. The spectral effects are adequately handled by CASMO-4.

MICROBURN-B2 can perform calculations with libraries containing only one moderator temperature and boron concentration or with libraries containing two moderator temperatures and boron concentrations. Results of MICROBURN-B2 calculations, utilizing a number of individual libraries with a single moderator temperature and boron concentration, have been compared to MICROBURN-B2 calculations performed at specific moderator temperature and boron concentration, utilizing a library containing two moderator temperatures, and boron concentrations, such that interpolation to those specific conditions was required. The results provide information about the uncertainty associated with the cross section interpolation method employed in MICROBURN-B2. The standard deviation of the difference between the explicit calculation and the interpolated calculation was [] Δk (i.e., x-sec interpolation uncertainty, σ_{interp}). The interpolation uncertainties are not impacted by BLEU fuel for the same reasons as mentioned above.

Inexact Tracking of the Actual Plant Parameters

Uncertainty in the plant instrumentation for determining the core statepoint at which the cycle depletion is performed is included in the comparison between the plant measured critical configurations and the calculated results utilizing the core statepoint parameters determined from the plant instrumentation. Thus, the effects of inexact tracking are included in the cold critical benchmarking results.

Depletion of Absorber Material in Control Blades

Normally, analysis of the SLCS shutdown capability does not include the reactivity of the control blade inventory at hot full power operating conditions, so the issue of control blade depletion is not a factor. In the event SLCS shutdown capability is not sufficient without taking credit for the presence of control blades, AREVA will reduce the calculated control rod worth by 10%, consistent with the control blade replacement criteria. This is a conservative measure since not all of the control blades will be at the replacement criteria. The SLCS is normally limiting at or near BOC so the degree of reactivity loss is well below the replacement criteria since the replacement criteria is applied to the worst condition at EOC.

Combination of Uncertainties

The primary sources of uncertainty have been quantified by comparisons of measured and calculated cold critical configurations. Since the calculation utilizes design values for the fuel parameters and non-depleted control blades with nominal design parameters, this difference includes the manufacturing and control blade depletion effects. This uncertainty value was determined to be $\sigma_{cold} = [\quad] \Delta k$.

Additional uncertainty for the borated conditions was quantified by comparisons to MCNP with a value of $\sigma_{code} = [\quad] \Delta k$. Since the borated calculations are performed at higher temperatures and may be based upon interpolated values an additional interpolation uncertainty was determined to be $\sigma_{interp} = [\quad] \Delta k$. Using standard statistical techniques of combining independent uncertainties one obtains a combined uncertainty of $[\quad] \Delta k$.

The Technical Specification criterion for the cold shutdown margin for specific cycle measurements has traditionally been set to 0.38% Δk . This uncertainty can be divided into the primary components:

$$\sigma_{total} = \left(\sigma_{calc}^2 + \sigma_{manu}^2 \right)^{1/2}$$

Where:

σ_{calc} = Uncertainty in calculated k-eff under the same core depletion conditions.

σ_{manu} = k-effective uncertainty due to manufacturing tolerances.

In order to determine σ_{calc} , several cold critical calculations under the same core depletion conditions must be evaluated. AREVA has identified 7 separate criticality measurements (Teollisuuden Voima Oy (TVO) cycle 18, Susquehanna Unit 1 (SQA) cycle 3, Kuosheng Unit 1 (KS1) cycle 6, KS1 cycle 7, Kuosheng Unit 2 (KS2) cycle 6, Chinshan Unit 1 (CS1) cycle 9 and Chinshan Unit 2 (CS2) cycle 8) where as many as 24 different control rod patterns were in a critical condition. Combining these 86 statepoints results in a standard deviation of $[\quad] \Delta k$.

In order to evaluate the quantification of σ_{manu} , AREVA has performed a specific analysis of the uncertainty associated with manufacturing tolerances for ATRIUM-10 fuel. Variations in enrichment, pellet diameters, pellet densities, cladding diameters and Gadolinia concentrations are considered for the fuel assembly manufacturing uncertainties. In addition one needs to account for the control blade manufacturing uncertainties. The primary parameters of interest are the theoretical density of B4C and the tube diameter. Applying the calculated partial derivatives, as calculated by CASMO-4, to the associated parameter uncertainties resulted in a controlled manufacturing uncertainty of $[\quad] \Delta k$ and an uncontrolled manufacturing uncertainty of $[\quad] \Delta k$. The effective manufacturing uncertainty for the strongest control blade withdrawn is thus $[\quad] \Delta k$.

Combining the σ_{manu} and the σ_{calc} results in a total uncertainty of $\sigma_{sdm} = [\quad] \Delta k$. The value used for shutdown demonstrations in most plant technical specifications is a 95/95 bounding value of 0.38% Δk which corresponds to a standard deviation of $[\quad] \Delta k$. This value has been used for all fuel types including GE-14 and will be used as a conservative addition to the SLCS shutdown margin criterion. As discussed in the first paragraph of this response, the uncertainty due to manufacturing variations have already been accounted for in the cold critical benchmarking, which for the Browns Ferry plant includes data for all three units including reloads with GE-14 fuel. Hence by including the effect of manufacturing variations (σ_{manu}) in the total uncertainty (σ_{sdm}), σ_{manu} is accounted for twice, which is conservative.

In order to obtain a more conservative criterion the standard shutdown margin criterion has been combined together with the identified uncertainties using standard statistical methods to determine an overall uncertainty for all of the various components including BLEU fuel and modern fuel designs such as ATRIUM-10 and GE-14. These results are presented in Table 6.1, which shows that the overall uncertainty is $[\quad] \Delta k$. This criterion can be applied when the calculation is performed at the most limiting moderator temperature and is the standard criterion for AREVA analysis of SLCS.

Consequently, the Technical Specification requirement for the SLCS to be capable of bringing the reactor from full power to a subcritical condition is conservatively met by applying the $[\quad] \Delta k$ criterion.

Table 6.1 Summary of the Uncertainties Included in the Acceptance Criterion

[

]

Browns Ferry Cold Criticals

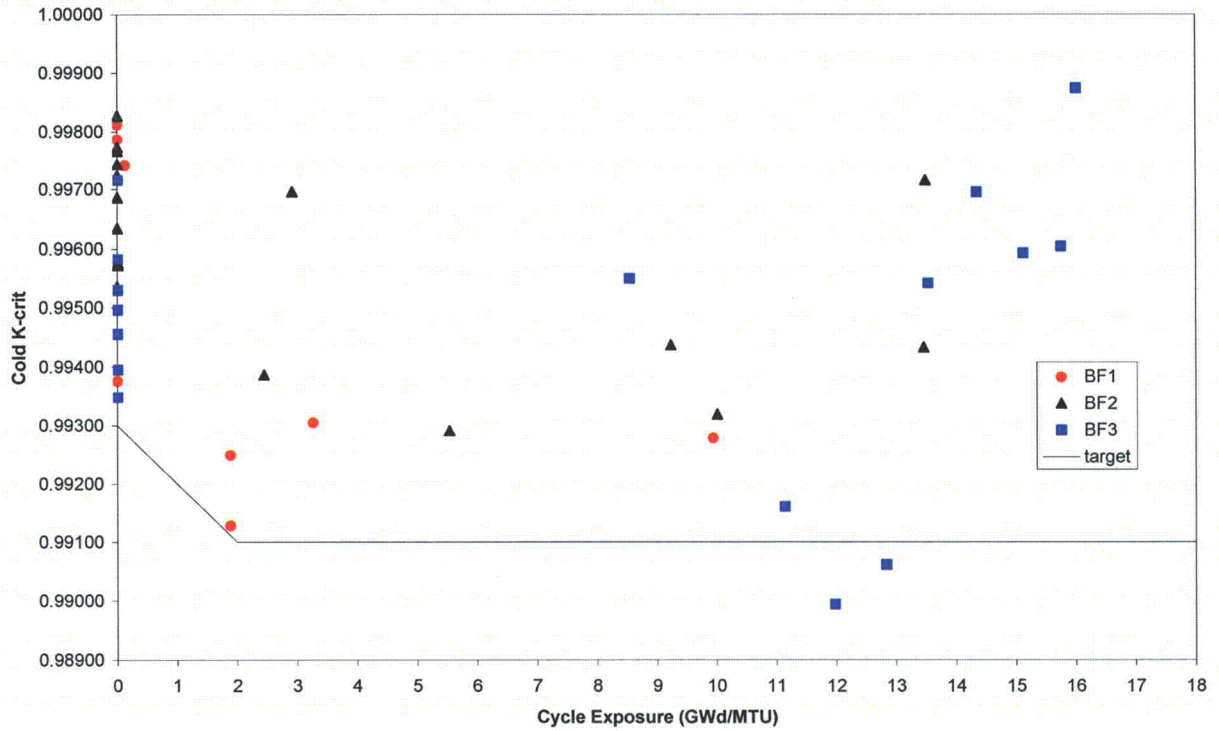


Figure 6.1 Browns Ferry Cold Critical Benchmark Results

Question 7.

Provide an analysis of SLCS shutdown margin at 68 degrees F, consistent with definition of rodged shutdown margin appearing in Unit 1 Technical Specifications (TSs). Demonstrate the capability to maintain subcritical configuration in cold conditions.

Response 7.

The SLCS analysis for BFN Unit 1 Cycle 9 was performed at 366°F, which is the reactor water temperature associated with RHR shutdown cooling initiation (i.e., the saturation temperature corresponding to the initiation pressure). As discussed in the answer to question 6, this temperature represents a more limiting condition than cold conditions. AREVA has performed a SLCS calculation at cold conditions (68°F) for the BFN Unit 1 Cycle 9 reload design. Results summarized in the table below confirm that the higher temperature is limiting and therefore provides a bounding result. Additionally, AREVA has performed a SLCS calculation at conditions defined in the BFN SLCS licensing basis documents (720 ppm boron at a cold temperature of 70°F). Results summarized in the table below confirm that the AREVA cold analysis basis of 68°F represents a negligible difference and the results are adequate to protect the 70°F licensing basis of BFN Unit 1.

Warm (366° F), Boron equivalent to 720 ppm @ 68°F	Warm (366° F), Boron equivalent to 720 ppm @ 70°F	Cold (68°F) 720 ppm
2.98% Δk/k	2.98% Δk/k	3.81% Δk/k

Question 8.

Clarify the following language in the TS: "...latest approved versions applicable to BFN." Several of the references listed have supplements and addenda. Address why the supplements and addenda were not included and provide a listing of the latest approved version as well as the latest approved supplements and/or addenda to the listed topical reports.

Also, clarify the process that is followed when a new version, supplement, or addendum is approved by the NRC in the midst of the generation of the cycle operating limits report for the next cycle.

Response 8.

The term "... latest approved versions applicable to BFN" is a qualifier meaning TVA must review a new version, supplement, or addenda to make sure it is actually applicable to BFN (for example, maybe the vendor revises a report to include language specific to a BWR 6. In this case, the new revision would not be applicable to BFN because it is not a BWR 6. Or perhaps a change is being made relative to a fuel product not actually used by BFN, in which case the new revision supplement, or addenda is not applicable).

Proposed changes to Technical Specification 5.6.5 (provided Attachments 2 and 3 of Technical Specification Change TS-467) are the same as those already approved for BFN Units 2 and 3. This minimizes differences between the three units. Full listings of applicable revisions, supplements, or addenda and dates are provided in the Core Operating Limits Report (COLR), based on actual BFN applicability. An itemized listing of supplements applicable for inclusion in the COLR are shown in Technical Specification Change TS-467 Attachment 17 (ANP-2637, Revision 2, Boiling Water Reactor Licensing Methodology Compendium, Table 1-2, Reference No. column items: 2-3, 2-10, 2-12, 3-1, 4-3, 5-6, and 5-7).

The process that is used when a new version, supplement, or addendum is approved by the NRC in the midst of the generation of the COLR for the next cycle is as follows.

The vendor uses computer code versions corresponding with specific, approved methodologies applicable to BFN. At the beginning of the design process, the vendor is aware of methodology related issues which may be applicable to the design and licensing process. Computer code versions (i.e., approved methodologies) are specified at the beginning of the cycle design process, independent of potential future revisions.

Results of licensing basis analyses are compiled in the Reload Safety Analysis, Maximum Average Planar Linear Heat Generation Rate (MAPLHGR), Fuel Cycle Design, and Mechanical Design Reports. The COLR is based on these reports. The COLR lists all approved methodologies utilized in the licensing basis analyses. At any point in the design and licensing process, the vendor may implement conservative changes to account for known methodology discrepancies and/or errors. Any methods changes used to develop COLR input are processed in accordance with the 10 CFR 50.59 process.

Development of the COLR proceeds through different stages. TVA Nuclear Fuels Engineering performs a technical review of vendor analyses and reports. The COLR and supporting information are assessed in accordance with the 10 CFR 50.59 screening and safety evaluation process. Finally, the COLR must be approved by the plant operations review committee (PORC) prior to inclusion in the Technical Requirements Manual (TRM). The approved COLR is sent to the NRC in accordance with the requirements of Technical Specification 5.6.5.d.

When a topical report revision, supplement, or addendum change is approved prior to the vendor analyses being completed and documented, it may be possible to incorporate the update during the normal COLR development process.

If the approved change constitutes an enhancement or relaxation, not involving a known discrepancy or error, then it would be processed by

a future COLR revision based on revised vendor analyses, or wait until the next cycle design and licensing process.

If an approved change involves resolution of a known discrepancy or error, conservative updates to the methodology will have already been included in vendor analyses, and addressed via the 10 CFR 50.59 process, (the vendor is aware of pending NRC reviews, and the potential time line for approval, as well as necessary compensatory action, as discussed up front during the initial design phase). For the special case where the NRC has issued a new Safety Evaluation Report (SER) to close a 10 CFR 21 issue, the new SER can also be noted in the COLR in accordance with the 10 CFR 50.59 process, until such time as the vendor officially issues a revision to the approved methodology report.

Question 9.

Explain why the following topical reports are not included in TS 5.6.5:

- EMF-2209(P), Rev. 2, Addendum 1(P)(A), "SPCB Additive Constants for ATRIUM-10 Fuel," May 1, 2008;
- EMF-CC-074(P)(A), "BWR Stability Analysis: Assessment of STAIF with Input from MICROBURN-B2," Vol. 4; Siemens Power Corporation, August 2000;
- EMF-85-74(P), Supplement 1(P)(A) and Supplement 2 (P)(A), "RODEX2A (BWR) Fuel Rod Thermal-Mechanical Evaluation Model," Siemens Power Corporation, February 1998;
- BAW-10255(P)(A), Revision 2, "Cycle-Specific DIVOM Methodology Using the RAMONA5-FA Code," Framatome ANP, May 2008; and
- BAW-10247(P)(A), Revision 0, "Realistic Thermal-Mechanical Fuel Rod Methodology for Boiling Water Reactors," AREVA, May 2008.

Response 9.

As reflected in reviewer's notes associated with Technical Specification 5.6.5, "Core Operating Limits Report (COLR)," of NUREG-1433, "Standard Technical Specifications General Electric Plants, BWR/4," Revision 3.0, the individual specifications that address core operating limits are to be referenced in Technical Specification 5.6.5.a and the topical reports that reflect the analytical methods used to determine these core operating limits are to be included in Technical Specification 5.6.5.b by number and title. The reviewer's note to Technical Specification 5.6.5.b also indicates that COLR will contain the complete identification for each of the Technical Specification referenced topical reports used to prepare the COLR (i.e., report number, title, revision, date, and any supplements).

The current BFN Unit 1 Technical Specification 5.6.5.a lists the following individual specifications

- (1) The Average Planar Linear Heat Generation Rates (APLHGRs) for Specification 3.2.1;
- (2) The Linear Heat Generation Rate (LHGR) for Specification 3.2.3;
- (3) The Minimum Critical Power Ratio (MCPR) Operating Limits for Specification 3.2.2; and
- (4) The Rod Block Monitor (RBM) setpoints and applicable reactor thermal power ranges for each of the setpoints for Specification 3.3.2.1, Table 3.3.2.1-1.

The Limiting Conditions for Operation (LCOs) for these Technical Specifications state that the associated limits are specified in the COLR.

- Consistent with the reviewer's note associated with NUREG-1433 Technical Specification 5.6.5.b, EMF-2209 (P)(A) and its title are included in the proposed BFN Unit 1 Technical Specification 5.6.5.b. On page 4 of the Enclosure to Technical Specification Change TS-467, in paragraph 4, the status of the EMF-2209 addendum is discussed (the SER is identified as Reference 13 of the Enclosure). Section 4 of the SER relevant to the Addendum 1 of EMF-2209 Revision 2 states"

"The NRC staff acknowledges that AREVA will combine this safety evaluation with the previously approved TRs, to issue Revision 3 of TR EMF-2209, and Revision 1 of TR ANP-10249. All parts of the latest revisions have been approved by the NRC staff. Therefore, Revision 3 of TR EMF-2209, and Revision 1 of TR ANP-10249, can be submitted as the approved versions of the TRs. This will allow use of current plant technical specification (TS) references without modifications to the standard TSs."

Therefore, the EMF-2209 Rev. 2 Addendum information was incorporated into EMF-2209 Rev. 2 to create the approved topical report EMF-2209PA Rev. 3 dated December 2009. The BFN Unit 1 COLR will incorporate EMF-2209PA Revision 3, consistent with the requirements of proposed Technical Specification 5.6.5.b (i.e., the latest approved versions applicable to BFN).

- The list of specifications, included in current BFN Unit 1 Technical Specification 5.6.5.a, for which core operating limits have been relocated to the COLR does not include limits associated with thermal hydraulic stability. As such, Technical Specification 5.6.5.b does not include a reference to EMF-CC-074(P)(A) since the analytical methods described in EMF-CC-074(P)(A) are associated with stability analysis.
- Consistent with the reviewer's note associated with NUREG-1433 Technical Specification 5.6.5.b, EMF-85-74 (P)(A) and its title are included in the proposed BFN Unit 1 Technical Specification 5.6.5.b. The BFN Unit 1 COLR will incorporate "EMF-85-74(P), Supplement 1(P)(A) and Supplement 2 (P)(A), "RODEX2A (BWR) Fuel Rod Thermal-Mechanical Evaluation Model," Siemens Power Corporation, February 1998," consistent with the requirements of proposed Technical Specification

5.6.5.b (i.e., the latest approved versions applicable to BFN) and the COLR will contain the complete identification for each of the Technical Specification referenced topical reports used to prepare the COLR (i.e., report number, title, revision, date and any supplements).

- As previously stated, the list of specifications, included in current BFN Unit 1 Technical Specification 5.6.5.a, for which core operating limits have been relocated to the COLR does not include limits associated with thermal hydraulic stability. As such, Technical Specification 5.6.5.b does not include a reference to BAW-10255(P)(A) since the analytical methods described in BAW-10255(P)(A) are associated with stability analysis.
- BAW-10247(P)(A) is not listed in proposed Technical Specification 5.6.5.b because the analytical methods described in BAW-10247(P)(A) are not used for the development of core operating limits for BFN Unit 1.

Question 9 (from NRC to TVA Letter dated February 25, 2010)

In question 9, the staff requested supplemental information on the Core Operating Limits Report (COLR) Reference Section of the TSs. Specifically, the staff asked about several AREVA licensing topical reports that the staff expected to be listed in this section. TVA's supplement was generally responsive; however, the absence of the stability analysis methods (i.e., STAIF and RAMONA5-FA) does not appear to be consistent with the reload licensing analysis process at Browns Ferry Unit 1.

The Boiling Water Reactor Owners' Group long term stability (LTS) detect and suppress solution (DSS) at Browns Ferry Unit 1 is based on Option III. This LTS DSS requires the specification of cycle-specific oscillation power range monitor (OPRM) setpoints. The Period Based Detector Algorithm setpoints and the Delta per Initial Critical Power Ratio versus Oscillation Magnitude slope are generally determined using cycle-specific analyses. Additionally, the Option III Backup Stability Protection generally requires the calculation of an exclusion region based on the STAIF code. This approach appears inconsistent with the proposed TS revision.

The OPRM setpoints are directly tied to the safety limits because the OPRM provides automatic protective action, during instabilities, to assure that the safety limit minimum critical power ratio is not exceeded. Thus, the OPRM setpoints are limiting safety system settings subject to 10 CFR 50.36(c)(1)(ii)(A). Therefore, cycle-specific parameter limits are within the scope of Generic Letter 88-16 and need to be included in the TSs and COLR, accordingly.

The supplementary information was unresponsive to the staff concern. The supplement confirms that the regulatory basis for the proposed change does not appropriately treat 10 CFR 50.36 requirements.

Response

As discussed previously, the current BFN Unit 1 Technical Specification 5.6.5.a, which lists core operating limits that have been relocated to the COLR, does not include limits associated with thermal hydraulic stability. The BFN Unit 1 Technical Specifications were revised to include Oscillation Power Range Monitor (OPRM) requirements in Amendment No. 266, dated December 29, 2008. In the associated Safety Evaluation Report, the NRC concluded that the proposed changes were acceptable since the changes were consistent with the approved methodology NEDC-32410P-A, Supplement 1. NEDC-32410P-A, Supplement 1, included Technical Specification revisions for the Improved Standard Technical Specifications to reflect incorporation of the OPRM. These Technical Specification revisions did not include changes to reflect relocation of limits associated with thermal hydraulic stability to the COLR.

However, revisions to TS 3.3.1.1, Reactor Protection Systems Instrumentation, for the OPRM Upscale Function, i.e., Function 2.f, are proposed in Attachments 2 and 3 to indicate that OPRM period based detection algorithm setpoint limits are included in Core Operating Limits Report (COLR) since these limits are evaluated each reload using analytical methodologies included in the COLR. Corresponding revisions are also proposed to TS 5.6.5.a to include the OPRM setpoint as a COLR item. In addition, revisions to TS 5.6.5.b are proposed to include the following stability related Topical Reports which describe the analytical methods used for determining the OPRM period based detection algorithm setpoint limits.

- EMF-CC-074(P)(A) Volume 4, BWR Stability Analysis: Assessment of STAIF with Input from MICROBURN-B2
- BAW-10255(P)(A), Cycle-Specific DIVOM Methodology Using the RAMONA5-FA Code

These revisions will also be proposed for BFN Units 2 and 3 in future Technical Specification Change Request(s).

Question 10.

Section 4.8.1 of ANP-2860P, "Browns Ferry Unit 1 Summary of Responses to Requests for Additional Information" states that for fast pressurization transients surface heat flux calculations are provided to the licensee and that appropriate linear heat generation rate factor (LHGRFAC) values are developed based on Global Nuclear Fuel (GNF) thermal-mechanical analyses. Provide a description of the analysis procedures that are used to demonstrate that the GNF fuel meets applicable thermal-mechanical licensing limits. Describe the number of cases that were benchmarked in the safety analysis. This description should address both fast and slow transients.

Response 10.

AREVA Thermal Overpower (TOP)/Mechanical Overpower (MOP)
Benchmarking Process

[

]

GNF takes the information provided by AREVA and applies it to the process described in Attachment 5 to produce bounding TOP/MOP limits for application with AREVA's methods. These limits are then provided to AREVA.

Application of GNF Methods

[

]

For analysis of transients, both with or without an early/direct scram, the appropriate GNF supplied TOP/MOP criteria and setdown procedure are implemented. This evaluation is performed for every event and state point analyzed to determine thermal margin.

Question 11.

Provide the results of the Thermal Mechanical Analyses for GE14 fuel, which are not contained in the Reload Safety Analysis Report.

Response 11.

The following table presents the event and state point specific limiting GE14 TOP/MOP results used to develop the GE14 Linear Heat Generation Rate Factor (LHGRFAC) multipliers for EPU conditions, defined by the following events and equipment out of service:

- LRNB: All LRNB events, including Power Load Unbalance Out of Service (PLUOOS), for all combinations of Feedwater Heater Out of Service (FHOOS), and Recirculation Pump Trip Out of Service (RPTOOS).
- FWCF Turbine Bypass Valve in Service (TBVIS): All FWCF events for all combinations of FHOOS, and RPTOOS.
- FWCF Turbine Bypass Valve Out of Service (TBVOOS): All FWCF events for all combinations of FHOOS, RPTOOS, and TBVOOS.

The base case load rejection event already assumes the turbine bypass system inoperable. Separate TBVOOS multipliers are only needed for the FWCF event.

Power (% Rated)	LRNB MOP/TOP	FWCF TBVIS MOP/TOP	FWCF TBVOOS MOP/TOP
<i>Technical Specification Scram Speed (TSSS) Insertion Times</i>			
100	49 / 49	52 / 50	57 / 57
90	46 / 46	58 / 56	63 / 61
77.6	45 / 45	63 / 63	68 / 68
60	46 / 46	70 / 69	75 / 74
55	75 / 75	74 / 72	78 / 77
50	79 / 79	77 / 77	81 / 81
40	86 / 86	94 / 94	98 / 98
26	101 / 101	128 / 125	136 / 136
26 at > 50%F below P _{bypass}	---	165 / 164	219 / 217
26 at ≤ 50%F below P _{bypass}	---	161 / 151	175 / 174
23 at > 50%F below P _{bypass}	102 / 102	174 / 170	237 / 234
23 at ≤ 50%F below P _{bypass}	75 / 75	171 / 155	194 / 190
<i>Nominal Scram Speed (NSS) Insertion Times</i>			
100	42 / 42	49 / 47	54 / 52
90	44 / 44	57 / 54	62 / 59
77.6	43 / 43	61 / 61	66 / 66
60	42 / 42	68 / 67	74 / 72
55	74 / 74	72 / 71	76 / 75
50	78 / 78	76 / 75	80 / 80
40	85 / 85	93 / 93	97 / 97

	Power (% Rated)	LRNB MOP/TOP	FWCF TBVIS MOP/TOP	FWCF TBVOOS MOP/TOP
26		100 / 100	124 / 124	133 / 133

Using calculated TOP/MOP data and the process described previously in the response to Question 10, required LHGRFAC multipliers are developed for all the transient events and state points used to determine thermal margin. Two sets of GE14 LHGRFACp multipliers are developed for plant operation, shown in Table 8.10 and Figures A.162 and A.164 of the RSAR. The multipliers are developed to support operation at all cycle exposures, both NSS and TSSS insertion times, and the EOOS conditions identified in Table 1.1 with and without TBVOOS. GE14 LHGRFAC multipliers further take into consideration the previous cycle limits developed by GNF (Cycle 8 was the final cycle prepared by GNF). Cycle 9 multipliers are the most restrictive value of Cycle 9 calculations and Cycle 8 existing limits.

Question 12.

Provide the reference, Mneimneh, GNF, letter to McNelley, TVA, "Revised LHGR Limits for BF1 Transition," MJM-TVA-ER1-09-39.

Response 12.

GNF has generated a document which summarizes the thermal mechanical information they provided to support the transition (Attachments 5 and 6). Sections 2-1 and 2-2 of Attachments 5 and 6 contain all of the technical information from the referenced GNF letter.

Question 13.

Provide additional details regarding the control rod drop accident (CRDA) analysis. Results of the CRDA analysis appear inconsistent with the methodology. Provide an updated description of the analytic method that explains how the maximum number of rods exceeding 170 cal/g is determined, and what assumptions are used to make this determination.

Response 13.

The NRC-approved CRDA analysis method employed by AREVA is described in Section 4.1 and Section 7.1 of Reference 5. The Reference 5 parameterized methodology is used to determine the maximum enthalpy deposited in fuel rods. For each rod drop case with the maximum enthalpy exceeding 170 cal/gm, the minimum four-bundle local peaking factor (a combination of assembly radial peaking and lattice local peaking with pin power reconstruction effects incorporated) required to achieve a deposited enthalpy at the 170 cal/gm limit can be determined. Any assemblies that

experience the combination of radial peaking factor and local peaking factor such that the minimum four-bundle local peaking factor is exceeded are counted as having failed rods. For BFN Unit 1 Cycle 9, the resulting number of assemblies exceeding 170 cal/gm was four (two ATRIUM-10 and two GE14). All rods in those four assemblies were conservatively assumed to be failed, resulting in 366 failed rods, which is well below the number of 850 assumed in the UFSAR. In some other cases where the result of assuming all rods in assemblies that exceed 170 cal/gm are failed is excessively conservative, the number of rods with a local peaking factor equal to or higher than that required to exceed the minimum four-bundle local peaking factor are counted. This less conservative approach of counting individual failed rods was not used in the BFN Unit 1 Cycle 9 analysis. For BFN Unit 1 Cycle 9, the result is reported in Section 6.2 of Reference 3.

The assumptions applied in determining the number of failed rods in the BFN Unit 1 Cycle 9 CRDA calculation are the following:

- All rods are assumed to be failed in any assembly that is determined to deposited enthalpy of 170 cal/gm or greater.
- Pin power reconstruction is assumed in the local peaking factor applied to determine the four-bundle local peaking factor.

Question 14.

The approved methodology relies on parameterization of generic analysis results. Provide the parameterized function. Given the application to GE14, justify the applicability of the generic analyses to modern fuel bundle designs; in particular describe how the differences in bundle fuel mass are accounted for in the parameterized function.

Response 14.

The NRC-approved CRDA parameterized function employed by AREVA is described in Section 7.1 of Reference 5. AREVA has performed analyses to justify the continued applicability of the existing Reference 5 parameterized function to evolutions in fuel design (8X8, 9X9, and 10X10 lattices), core design, and AREVA neutronics methodology through the years since Reference 5 was approved.

As documented in Section 7.1 of Reference 5, the AREVA method for CRDA analysis [

]. For BFN Unit 1 Cycle 9, the analysis was completed at BOC and at the high reactivity point in the cycle (peak hot excess reactivity), and at end-of-full power (EOFP).

The NRC approved Reference 5 parameterized analysis incorporates additional conservatism by assuming adiabatic conditions during the power excursion (i.e., no direct moderator heating is credited during the analysis), and that the reactor remains at hot zero power conditions for the entire Banked Position Withdrawal Sequence (BPWS). As reported to the NRC in Reference 6, the adiabatic assumption has been evaluated to be conservative by approximately a factor of 2.

The factor in the parameterization most affected by bundle fuel mass is the Doppler coefficient. AREVA evaluates the Doppler coefficient for each fuel type with CASMO-4 calculations and has conservatively determined applicable Doppler coefficients for different fuel designs with different fuel masses, including all of the fuel types resident in the BFN Unit 1 Cycle 9 core design.

Question 14 (from NRC to TVA letter dated February 25, 2010)

The supplemental response to request Question 14 did not address the staff's question.

The staff asked TVA to specifically describe how differences in bundle fuel mass are accounted for in the parameterized function. The response does not provide details as to how gross changes in bundle fuel mass are taken into account or how modern fuel geometries (e.g., GE14) are taken into account. The figure of merit in the analysis is the enthalpy change as measured in units of calories per gram. The response references studies performed by AREVA to demonstrate the conservatism in the application of the parameterized function to newer fuel designs (e.g., 8X8, 9X9, and 10X10 designs); however, these studies have not been provided to the staff.

Response

There are three ways in which differences in fuel geometries and bundle mass are accounted for in the CRDA analysis:

1. The Doppler coefficient used in the cycle specific CRDA analysis is fuel geometry specific.
2. Each fuel assembly and lattice is explicitly modeled in the MICROBURN-B2 3-D core simulator model used to calculate the Control Rod Worth and Four-Bundle-Local-Peaking factor (P4BL) local parameters for the CRDA analysis.
3. As described in more detail below, the Reference 5 parameterized method has been shown to be applicable to a variety of different fuel designs and lattice dimensions (8x8, 9x9, 10x10, etc).

It is noteworthy that the fuel rod (or lattice) weight is not a parameter in the Reference 5 generic parameterized analysis. The characterization by control rod worth and Doppler coefficient are the critical parameters in determining the transient neutron flux. The associated energy production is a product of this flux and the fission cross-section and thus the fuel rod (or lattice) weight is

accounted for directly. Since the criterion is in terms of cal/gm and calories generated is directly proportional to the weight, the fuel rod (or lattice) weight cancels out so that the reactivity characteristics can be correlated to the criterion without direct parameterization to lattice weight.

A summary of the studies performed by AREVA to demonstrate the conservatism in the application of the parameterized function to newer fuel designs follows.

Analysis of CRDA for GE-11 Fuel

The CRDA calculation has been performed with the COTRAN code (Reference 7) using input generated from cycle step out of Grand Gulf Cycle 11 with MICROBURN-B2. This cycle design is representative for the purpose of calculating the CRDA for the GE-11 and AREVA 9X9 fuel designs. Figure 14.1 shows the adiabatic hot standby calculated deposited enthalpy as a function of rod worth for the Grand Gulf cycle 11 core loaded with GE-11 fuel. The calculations were performed with banked rods as required by the plant rod withdrawal procedures to meet BPWS requirements (Reference 8). The results presented represent middle of cycle conditions. The NRC approved generic deposited enthalpy results from page 7-18 of Reference 5 are also shown on the plot (identified as Generic). The generic results utilize the parameters determined for the Grand Gulf Cycle 11 middle of cycle (MOC) conditions, where the Doppler coefficient is $-10.0E-6 \Delta k/k\Delta^{\circ}F$ (interpolated from the $-10.5E-6 \Delta k/k\Delta^{\circ}F$ and the $-9.5 E-6 \Delta k/k\Delta^{\circ}F$ results shown in Reference 5, page 7-18), and a Beta of 0.0055. Results for the GE-11 specific analysis are conservatively bounded by those from the generic parametric analysis as shown in Figure 14.1.

Analysis of CRDA for ATRIUM-10 Fuel

The CRDA calculation has been performed with the COTRAN code (Reference 7) using input generated from an equilibrium cycle step out of Grand Gulf with MICROBURN-B2. This cycle design is representative for the purpose of calculating the CRDA for the AREVA ATRIUM-10 fuel design. Figure 14.2 shows the adiabatic hot standby calculated deposited enthalpy as a function of rod worth for the Grand Gulf equilibrium cycle core loaded with ATRIUM-10 fuel. The calculations were performed with banked rods as required by the plant rod withdrawal procedures to meet BPWS requirements (Reference 8). The results presented represent beginning, middle and end of cycle conditions. The NRC approved generic deposited enthalpy results from Reference 5, page 7-18 are also shown on the plot (identified as Generic). The generic results utilize the parameters determined for the Grand Gulf equilibrium cycle EOC conditions where the Doppler coefficient is $-11.2E-6 \Delta k/k\Delta^{\circ}F$ (interpolated from the $-10.5E-6 \Delta k/k\Delta^{\circ}F$ and the $-11.5 E-6 \Delta k/k\Delta^{\circ}F$ results shown in Reference 5, page 7-18), and a Beta of 0.00537. The generic results for a rod worth of 16 mk are extrapolated from the 8 and 12 mk results. Figure 14.2 shows that the results for the ATRIUM-10 specific analysis are conservatively bounded by those from the generic parametric analysis.

Analysis of CRDA for ATRIUM 10XM Fuel

The CRDA calculation has been performed with the COTRAN code (Reference 7) using input generated from an equilibrium cycle step out of Brunswick with MICROBURN-B2. This cycle design is representative for the purpose of calculating the CRDA for the AREVA ATRIUM-10XM fuel design. Figure 14.3, Figure 14.4, and Figure 14.5 show the adiabatic hot standby calculated deposited enthalpy as a function of rod worth for the Brunswick equilibrium cycle core loaded with ATRIUM-10XM fuel at BOC, MOC and EOC, respectively. The calculations were performed with banked rods as required by the plant rod withdrawal procedures to meet BPWS requirements (Reference 8). The NRC approved generic deposited enthalpy results from Reference 5, page 7-18 are also shown on the plot (identified as Generic). The generic results utilize a Doppler coefficient of $-10.0E-6 \Delta k/k \Delta^{\circ}F$ and the Beta value determined for the Brunswick equilibrium cycle exposure conditions BOC (0.0063), MOC (0.0058) and EOC (0.0055). The generic results for a rod worth of 16 mk are extrapolated from the 8 and 12 mk results. Figure 14.3, Figure 14.4, and Figure 14.5 show the results for the ATRIUM 10XM specific analyses are conservatively bounded by those from the generic parametric analysis.

Evaluation of Doppler Coefficient

The Doppler coefficient is an important parameter in the evaluation of the deposited enthalpy. A study of the Doppler coefficient for various fuel designs has been performed with CASMO-4 calculations. The conditions of interest for the CRDA represent the top of the core without any voids. This is best represented by a 40 void or 80 void depletion with instantaneous branch calculations at 0 void. Results for both void histories are similar. In order to make a comparison on an equivalent basis, the Doppler coefficient calculated at a lattice exposure of 20 GWd/MTU, for a variety of fuel designs is presented in Figure 14.6. These results show a general trend that lower lattice weight results in a less negative Doppler coefficient. It should be noted that the GE-14 lattice weight (upper zone [] kg/cm) is the lightest weight lattice in Figure 14.6. Other variations occur due to Gadolinia concentration and the water to fuel ratio. A conservative value for the Doppler coefficient is determined from the core composition for the evaluation of the deposited enthalpy on a cycle specific basis. The cycle-specific analyses for BFN assume the ATRIUM-10 (non-BLEU) Doppler, which is smaller (less negative) than the actual Doppler for BLEU ATRIUM-10 fuel and hence is conservative (the AREVA fuel results in Figure 14.6 that are as negative as the BLEU result are not ATRIUM-10 fuel).

Conclusions

The specific analyses for GE-11, ATRIUM-10, and ATRIUM 10XM confirm the generic parametric analysis applies conservatively to a variety of modern fuel designs. Control Rod worths, Doppler coefficient values, delayed neutron fraction and the P4BL used in the cycle-specific evaluation of CRDA are conservatively determined for each fuel design in the core, including GE-14 fuel.

The U234 and U236 isotopes are specifically modeled in the CASMO-4/MICROBURN-B2 core simulator model used to calculate the Dropped Control Rod Worth and Four-Bundle-Local-Peaking factor (P4BL) local parameters for the cycle-specific BFN CRDA analyses. Also, the cycle-specific analyses assume the ATRIUM-10 (non-BLEU) Doppler, which is smaller (less negative) than the actual Doppler for BLEU ATRIUM-10 fuel and hence is conservative.

[

]

Figure 14.1 Deposited Enthalpy Results for GE-11 Fuel

[

Figure 14.2 Deposited Enthalpy Results for ATRIUM-10 Fuel

]

[

Figure 14.3 Deposited Enthalpy Results for ATRIUM-10XM Fuel at BOC

]

[

Figure 14.4 Deposited Enthalpy Results for ATRIUM-10XM Fuel at MOC

]

[

]

Figure 14.5 Deposited Enthalpy Results for ATRIUM-10XM Fuel at EOC

[

Figure 14.6 Doppler Coefficient for Various Fuel Designs

]

Question 15.

Describe the core conditions that are evaluated to determine the limiting values for the following parameters: (1) control blade worth, (2) four bundle local peaking factor, (3) Doppler coefficient, and (4) delayed neutron fraction.

Response 15.

The maximum dropped rod worth is determined assuming core conditions of no xenon and at hot standby conditions (i.e., $T_{\text{fuel}} = T_{\text{mod}} = \text{hot operating temperature, zero void}$). Rod drop calculations are completed for as many rods in each group as required, based on symmetry, to determine the limiting dropped rod. For rod pull sequences that are quarter-core symmetric, rod drop calculations can be completed for rods in one quarter of the core, and for half-core symmetric situations only rods in half the core can be analyzed. Control rods from each of the planned operating sequences are included in the analysis. For BFN Unit 1 Cycle 9, the determination of maximum dropped rod worth incorporated the effect of inoperable rods, which has the effect of making the maximum dropped rod worth more conservative. As shown in Section 6.2 of Reference 3, the maximum dropped rod worth for BFN Unit 1 Cycle 9 was 11.17 mk.

As shown on page 159 in Section 4.1 of Reference 5, the four bundle local peaking factor consists of the radial peaking factors for the four bundles in the control cell and the local peaking factors associated with those same four fuel assemblies. Both the radial peaking factors and the local peaking factors are taken from MICROBURN-B2 calculations with pin power reconstruction under the same conditions as the dropped rod worth, i.e., no xenon and hot standby conditions (i.e., $T_{\text{fuel}} = T_{\text{mod}} = \text{hot operating temperature, zero void}$). As shown in Section 6.2 of Reference 3, the four bundle local peaking factor applied in the BFN Unit 1 Cycle 9 limiting case was 1.382.

The Doppler cross-section input used in the parameterized CRDA analysis reported in Reference 5 is correlated to a core average Doppler reactivity coefficient which can be determined for a specific cycle. AREVA has determined conservative generic Doppler coefficients specific to different fuel designs (ATRIUM-10, GE-13, GE-14, etc) for use in applying the CRDA parameterization on the cycle-specific analysis basis. For mixed cores, the core average Doppler coefficient is obtained by volume weighting the values for each fuel type. Alternatively, if additional conservatism is tolerable, the least negative coefficient for the fuel in the core can be used. For new fuel designs and special conditions not covered by the conservative generic Doppler coefficients, CASMO-4 can be used to generate the CRDA Doppler coefficient. Any such CASMO-4 calculations would be done assuming the same conditions assumed in the generation of the generic Doppler coefficients, which is no xenon, 40% void history, and 0% instantaneous voids. As shown in Section 6.2 of Reference 3, the core average Doppler coefficient applicable to BFN Unit 1 Cycle 9 was -10.51×10^{-6} .

For BFN Unit 1 Cycle 9, the End of Cycle (EOC) delayed neutron fraction that is calculated for the plant transient analysis was used for the rod drop

calculation. The plant transient value was calculated with an exposure window added to the EOC exposure resulting in additional conservatism. The value is calculated using MICROBURN-B2 and assuming at-power conditions with equilibrium xenon. If plant transient results from MICROBURN-B2 are not available, the core average delayed neutron fraction can be calculated by using CASMO-4 results. For each fuel type at EOC conditions, the CASMO-4 delayed neutron fraction data for the dominant lattice of each fuel type must be determined using interpolation on exposure and void history. Once the individual fuel type β_{eff} values have been determined for the batch average exposure and void history, the core average β_{eff} can then be determined by volume weighting the fuel type β_{eff} values. As shown in Section 6.2 of Reference 3, the effective delayed neutron fraction for BFN Unit 1 Cycle 9 was 0.0052.

Question 16.

Discuss the relationship between the maximum dropped rod reactivity worth and the cycle analyses provided in the fuel cycle design report. This documentation should specify the limiting rod, the method used to identify the limiting rod, the limiting point in exposure, and any consideration given for operational flexibilities (e.g., suppressing power in a leaking fuel bundle).

Response 16.

The rod drop calculations for BFN Unit 1 Cycle 9 were completed at BOC, at the peak reactivity point in the cycle, and at EOF, based on the cycle analysis provided in the fuel cycle design report. Rod drop calculations were completed for as many rods in each group as required, based on symmetry, to determine the limiting dropped rod. For rod pull sequences that are quarter-core symmetric, rod drop calculations can be completed for rods in one quarter of the core, and for half-core symmetric situations only rods in half the core can be analyzed. Control rods from each of the planned operating sequences were included in the analysis. For BFN Unit 1 Cycle 9, the limiting rod was found to be rod 18-47 in BPWS group 2 of sequence A at the peak hot excess reactivity point in the cycle.

The CRDA licensing basis of most plants allows some number of inoperable rods. For these plants, the rod drop calculations are completed for rods on the side of the core opposite the location of the assumed inoperable rods. The location and separation of the assumed inoperable rods is chosen to maximize the worth of the remaining rods while maintaining Technical Specification spacing requirements between inoperable control cells. For the BFN Unit 1 Cycle 9 CRDA, a maximum total of eight inoperable rods were assumed, with a maximum of three in any BPWS group.

AREVA has had experiences with plants inserting multiple suppression rods and has evaluated the CRDA, with the result being that the effect of the suppression rods is bound by the conservative treatment of the inoperable rods assumed in the CRDA analysis.

Question 17.

The American Society of Mechanical Engineers overpressure analysis using ATRIUM-10 fuel and AREVA methods credits the failure of a direct scram as the limiting single failure. NUREG-0800, "Standard Review Plan for the Review of Safety Analysis Reports for the Nuclear Power Plants", Chapter 5.2.2 assumes a reactor scram on the second safety-grade scram signal. This is a condition of the analysis, not an assumed failure. Identify the limiting single failure assumed in this analysis.

Response 17.

AREVA performs the American Society of Mechanical Engineers (ASME) overpressure analysis assuming the second safety grade signal from the reactor protection system, the high neutron flux trip signal, initiates the reactor scram. As noted in the question, this is consistent with NUREG-0800 Chapter 5.2.2, as a condition of the analysis.

Item C, page 5.2.2-6 of NUREG-0800 Chapter 5.2.2 states the following.

"A single malfunction or failure of an active component should not preclude safety-related portions of the system from functioning as required during normal operations, adverse environmental occurrences, and accident conditions, including loss of offsite power."

This is consistent with the AREVA ASME overpressurization analyses and Abnormal Operational Transient (AOT) analyses in general. The ASME overpressurization analysis does not credit systems if a single malfunction or failure of an active component precludes safety related portions of the system from functioning. No additional single failure considerations are included in the ASME overpressurization analysis.

Question 18.

The RSAR dispositions criticality for new and spent fuel storage based on previous analyses. Address why the use of previous analyses are acceptable.

Response 18.

The TVA requested NRC approval of AREVA ATRIUM-10 fuel design and storage for Units 1, 2, and 3 in a License Amendment Request dated February 13, 2003 (Letter from R. G. Jones (TVA) to NRC, "Browns Ferry Nuclear Plant (BFN) - Units 1, 2, and 3 - Technical Specifications (TS) Change 421 - Framatome Fuel Design and Storage," dated February 13, 2003, ADAMS Accession Number ML030560671). Supplemental information to support the request was provided to the NRC on April 14, 2003 (Letter from T. E. Abney (TVA) to NRC, "Browns Ferry Nuclear Plant (BFN) – Units 1, 2, and 3 – Technical Specifications (TS) Change 421 – Framatome Fuel Design and

Storage – Supplemental Information” dated April 14, 2003, ADAMS Accession Number ML031130549).

NRC subsequently issued the associated License Amendments for Units 1, 2, 3 on September 5, 2003. The NRC approval and associated safety evaluation report for ATRIUM-10 fuel design and storage at Units 1, 2, and 3 are included in the letter from K. N. Jabbour (NRC) to J. A. Scalice (NRC), “Browns Ferry Nuclear Plant, Units 1, 2, and 3, Re: Issuance of Amendments (TAC Nos. MB7743, MB7744, MB7745) (TS 421),” dated September 5, 2003, ADAMS Accession Number ML032520003.

Technical approval for the criticality basis of ATRIUM-10 fuel was determined by TVA in accordance with the 10 CFR 50.59 process. Explicit Unit 1, 2, and 3 spent fuel storage pool analyses were performed by AREVA in 2003 prior to the introduction of ATRIUM-10 fuel in 2004. These analyses explicitly evaluated the storage rack configuration for a bounding enrichment design.

Fuel reactivity is calculated in the spent fuel storage pool rack lattice to demonstrate that the k-effective (k-eff) is less than 0.95. The AREVA criticality analyses utilized an accepted computer code (KENO). The analyses concluded a reference lattice design does not exceed an array k-eff of 0.95 in the BFN spent fuel storage pool. Fuel with a lower enrichment and/or more gadolinia than the reference lattice will also not result in exceeding a k-eff of 0.95. The reference fuel design corresponds to a CASMO-4 cold k-eff reactivity of 0.872. Consequently, if the reference lattice conditions regarding enrichment and gadolinia are not met, cycle specific fuel designs can be verified to be in compliance by performance of criticality analyses with CASMO-4 to confirm the cold k-eff is less than 0.872.

Cycle specific fuel designs are verified to be within the bounding design basis prior fuel manufacture.

The Unit 1 spent fuel rack and fuel designs have been verified to remain within the design basis.

Question 19.

The RSAR dispositions Final Safety Analysis Report (FSAR) Section 14.5.2.8 - Pressure Regulator Failure Downscale - by stating that this event is eliminated as an Anticipated Operational Transient by installation of a digital fault-tolerant main turbine electro-hydraulic control (EHC) system. Address why this event was eliminated and whether the modification was made to support the transition to AREVA fuel.

Response 19.

Section 14.5.2.8 of the BFN UFSAR details the basis for this disposition. The modification was not made as part of the AREVA fuel transition. The modification was made to BFN Unit 1 prior to unit recovery. The UFSAR discussion is as follows.

14.5.2.8 Pressure Regulator Failure

Approval to remove the pressure regulator downscale failure event as an abnormal operational transient was approved by License Amendment Nos. 244, 281, and 239 to Facility Operating Licenses Nos. DPR-33, DPR-52, and DPR-68 by NRC on April 4, 2003, based on the installation of a fault-tolerant electro-hydraulic turbine control system on Units 2 and 3, and a commitment to similarly modify Unit 1 prior to return to power operation. The reliability of the upgraded electro-hydraulic control system is such that a system failure that results in the simultaneous closure of all turbine control valves is not an anticipated failure and, hence, the Pressure Regulator Downscale Failure (PRDF) transient no longer merits evaluation as an AOT.

Question 20.

The RSAR dispositions FSAR Chapter 14.5.6.4 – RCP [Reactor Coolant Pump] Rotor Seizure Accident - based on the fact that its consequences are bounded by the LOCA accident; however, the acceptance criteria are listed in terms of minimum critical power ratio (MCPR) and peak pressure. Provide an explanation for the discrepancy.

Response 20.

UFSAR 14.5.6.4 addresses the one recirculation pump seizure AOT event. The physical phenomena of this event are driven by the core response to the pump seizure. Flow through the affected loop is rapidly reduced due to the large hydraulic resistance introduced by the stopped rotor. This causes the core thermal power to decrease and reactor water level to swell. The sudden decrease in core coolant flow while the reactor is at power results in a degradation of core heat transfer.

The pump seizure analysis in UFSAR 14.5.6.4.3 shows that the peak neutron and heat fluxes did not increase above the initial conditions, nor the peak vessel pressure challenge the nuclear system process barriers. The calculated Δ CPR was well below that for other types of transients analyzed. Therefore, no impact on fuel integrity occurs and no nuclear system process barrier damage results from the pump seizure event. Since there is no release of radioactive material beyond that of normal operation, the acceptance criteria of 10 CFR 50.67, "Accident source term," are met.

The core response during this event is not significantly affected by fuel design. ATRIUM-10 and GE14 fuel are both 10X10 fuel types designed with similar core hydraulics. While differences in the fuel neutronic design will have some impact on the transient response, the affect of any difference will be small compared with the margin to the thermal limits. Since the differences in the ATRIUM-10 and GE14 fuel designs will not significantly affect the transient response, no damage to either fuel type will occur and no nuclear system process barrier damage will result from the pump seizure event. Since there is

no release of radioactive material beyond that of normal operation, the acceptance criteria of 10 CFR 50.67 are met.

The pump seizure event has been reclassified as an accident as noted in the footnote in UFSAR 14.5.6.4. The pump seizure event is a very mild accident in relation to LOCA. This is easily verified qualitatively by consideration of the two events. In both accidents, the recirculation driving loop flow is lost extremely rapidly. In the case of the seizure, stoppage of the pump occurs; for the LOCA, the severance of the line has a similar, but more rapid and severe influence. Following a pump seizure event, flow continues, water level is maintained, the core remains submerged and this provides a continuous core cooling mechanism. However, for the LOCA, complete flow stoppage occurs and the water level decreases due to loss of coolant, resulting in uncovering of the reactor core and subsequent overheating of the fuel rod cladding. In addition, for the pump seizure accident the reactor pressure does not significantly decrease, whereas complete depressurization occurs for the LOCA. The increased temperature of the cladding and reduced reactor pressure for the LOCA combine to yield a much more severe stress and potential for cladding perforation for the LOCA than for the pump seizure. Therefore, it can be concluded that the potential effects of the hypothetical pump seizure accident are conservatively bounded by the effects of a LOCA and specific analyses of the pump seizure accident are not required.

The pump seizure event, as described above, meets the acceptance criteria of minimum critical power ratio, peak pressure, and radioactive material release of 10 CFR 50.67.

References

1. EMF-2950(P) Revision 1, Browns Ferry Units 1, 2, and 3 Extended Power Uprate LOCA Break Spectrum Analysis, AREVA NP, April 2004.
2. XN-NF-80-19(P)(A) Volume 4 Revision 1, Exxon Nuclear Methodology for Boiling Water Reactors: Application of the ENC Methodology to BWR Reloads, Exxon Nuclear Company, June 1986.
3. ANP-2864(P) Revision 1, Browns Ferry Unit 1 Cycle 9 Reload Safety Analysis, AREVA NP, October 2009.
4. EMF-2158(P)(A) Revision 0, Siemens Power Corporation Methodology for Boiling Water Reactors: Evaluation and Validation of CASMO-4/MICROBURN-B2, Siemens Power Corporation, October 1999.
5. XN-NF-80-19(P)(A) Volume 1 and Supplements 1 and 2, Exxon Nuclear Methodology for Boiling Water Reactors - Neutronic Methods for Design and Analysis, Exxon Nuclear Company, March 1983.

6. Letter from R. A. Copeland (Siemens Power Corporation) to R. C. Jones (U.S. NRC Reactor Systems Branch), "Additional Information on SPC Topical Reports," RAC:95:143, November 2, 1995.
7. XN-NF-661, COTRAN: A Two Dimensional Reactor Kinetics Program with Reactivity Feedback for BWR Core Analysis, Exxon Nuclear Company, December 1982.
8. NEDO-21231, Banked Position Withdrawal Sequence, GE Nuclear Energy, January 1977.
9. NEDC-32484P "Browns Ferry Nuclear Plant Units 1, 2, and 3 SAFER/GESTR LOCA Loss of Coolant Accident Analysis", Revision 7, January 2010.
10. GEH Report 0000-0115-3713-R0, "Browns Ferry Nuclear Plant Unit 1, Supplementary Report of ECCS-LOCA Additional Single Failure Evaluation at Current Licensed Thermal Power (CLTP)", March 2010.
11. ANP-2908(P) Revision 0, Browns Ferry Units 1, 2, and 3 105% OLTP LOCA Break Spectrum Analysis, March 2010.
12. Letter from J. H. Plona (DTE Energy) to NRC, "Additional Information to Support Review of Plant Specific Emergency Core Cooling System Evaluation Model Reanalysis," dated June 10, 2009.
13. Letter from M. L. Chawla (NRC) to J. M. Davis (Detroit Edison Company), "Fermi 2 - Approval of Plant Specific Emergency Core Cooling System (ECCS) Evaluation Model Reanalysis (TAC No. MD9169)," dated June 30, 2009.
14. NUREG-0800, "Standard Review Plan for the Review of Safety Analysis Reports for Nuclear Power Plants: LWR Edition," Section 6.3, "Emergency Core Cooling System," Revision 3, March 2007.
15. Letter from USNRC, Ashok C. Thadani to BWROG Chairman Donald Grace, "Safety Evaluation of "BWR Owners Group – Emergency Procedure Guidelines, Revision 4," NEDO-31331, March 1987," dated September 12, 1988.